Characterization of the role of Hydroxyprostaglandin dehydrogenase 15-(NAD) in human regulatory T cells

Dissertation

zur

Erlangung des Doktorgrades (Dr. rer. nat.)

der

Mathematisch-Naturwissenschaftlichen Fakultät

der

Rheinischen Friedrich-Wilhelms-Universität Bonn

vorgelegt von

Eva Alexandra Schönfeld

aus

Ulm

Bonn, Oktober 2011

Angefertigt mit Genehmigung der Mathematisch-Naturwissenschaftlichen Fakultät der
Rheinischen Friedrich-Wilhelms-Universität Bonn

1.Gutachter: Prof. Dr. Joachim L. Schultze

2.Gutachter: Prof. Dr. Waldemar Kolanus

Tag der Promotion: 22.05.2012

Erscheinungsjahr: 2012

Eidesstattliche Erklärung

Hiermit versichere ich, dass die vorliegende Arbeit ohne unzulässige Hilfe Dritter und ohne die Benutzung anderer als der angegebenen Quellen und Hilfsmittel angefertigt wurde. Die aus fremden Quellen direkt oder indirekt übernommenen Gedanken sind gemäß §6 der Promotionsordnung vom 07.01.2004 als solche kenntlich gemacht.

Die in der vorliegenden Arbeit angegebenen Genexpressions Daten wurden von Frau Dr. Susanne V. Schmidt und Herrn Dr. Michael Mallmann, sowie den früheren Labormitgliedern Frau Dr. Sabine Claßen und Frau Dr. Daniela Eggle generiert.

Ferner wurde die angegebene Bestimmung der enzymatischen Aktivität von HPGD von Herrn Prof. Dr. Andrew J. Dannenberg und Dr. Kotha Subbaramaiah vom Department of Medicine and Weill Cornell Cancer Center (Cornell University), 525 East 68th St., Rm.F-206, New York, NY 10065 (USA) durchgeführt.

Des Weiteren wurden die in der vorliegenden Arbeit angegebenen FOXP3-knockdown Daten in humanen regulatorischen T-Zellen in Zusammenarbeit mit Frau Anne-Christine Flach erstellt und in Ihrer Diplomarbeit mit dem Titel „Characterization and cloning of novel FOXP3-dependent marker genes in human regulatory T cells (2009)“ veröffentlicht.

Die in der vorliegenden Arbeit angegebenen Promoter Tiling Array Daten wurden von Herrn Prof. Dr. Simon C. Barry und Kollegen am Women’s and Children’s Health Research Institute, 72 King William Road, North Adelaide, South Australia 5006 (Australia) generiert.

Bonn, den ….……

Eva Alexandra Schönfeld

Summary

The focus of the present study was the characterization of the hydroxyprostaglandin dehydrogenase 15-(NAD) (HPGD) in $CD4^+CD25^+$ regulatory T cells (T_{reg}) concerning its regulation and role for the development and suppressive function of T_{reg} cells. On the one hand, HPGD fulfills an important function in the metabolism of prostaglandins and is one of the major prostaglandin E_2 (PGE_2)-metabolizing enzymes. On the other hand, HPGD was reported to be a tumor suppressor. As enhanced numbers of T_{reg} cells can be found in tumor tissue and PGE_2 was shown to activate T_{reg} cells and contributes to carcinogenesis, the expression of HPGD in T_{reg} cells is of particular interest.

HPGD expression was shown to be significantly higher expressed in human T_{reg} cells compared to $CD4^+CD25^-$ T cells (T_{conv}). Notably, HPGD expression was specific for naturally occurring T_{reg} cells (nT_{reg}) as HPGD was not upregulated during $CD4^+$ T cell differentiation and even induced T_{reg} cells (iT_{reg}) do not show an enhanced HPGD expression. Furthermore, exclusively in nT_{reg} cells, HPGD expression could be specifically modulated by different extracellular stimuli. Even minuscule amounts of IL-2 were sufficient to strongly upregulate HPGD expression. These data further support that HPGD belongs to the nT_{reg} cell specific gene repertoire as low IL-2 receptor signaling also supports thymic development of T_{reg} cells. Thus HPGD might represent a novel nT_{reg} cell molecule that can be used to distinguish them from iT_{reg} cells. Besides that, the dependency of HPGD expression on the extracellular microenvironment also indicates a tissue-specific expression and potential function of HPGD in the T_{reg} cell.

Taken together, the present study demonstrates that HPGD represents a novel gene, which is specific for human naturally occurring T_{reg} cells. Although the relevance of HPGD for the T_{reg} cell function remains to be elucidated, the present study indicates a tissue-specific role of HPGD in T_{reg} cells and provides a basis for further research, to determine the role of T_{reg} cells in the tumor microenvironment.

Table of Contents

List of Figures

List of Tables

Abbreviations

ab	antibody
AP-1	activator protein1
APS	ammoniumperoxodisulfate
APC	antigen presenting cell
aAPC	artificial antigen presenting cell
BCA	bicinchoninic acid assay
BSA	bovine serum albumin
cAMP	cyclic adenosine monophosphate
CD	cluster of differentiation
CFA	complete freud's adjuvant
CFSE	carboxyfluorescein diacetate succinimidyl ester
COX	cyclooxygenase
CTLA-4	cytotoxic T-lymphocyte antigen 4
DC	dendritic cell
DMEM	Dulbecco's Modified Eagle Medium
DMSO	dimethyl sulfoxide
DNA	deoxyribonucleic acid
DTT	Dithiothreitol
EDTA	ethylenediaminetetraacetic acid
EMSA	Electrophoretic Mobility Shift Assay
EtBr	Ethidium bromide
FACS	Fluorescence activated cell sorting
FCS	Fetal calf serum
FITC	Fluorescein isothiocyanat
GFP	Green fluorescent protein & HEK293 cells transfected with pcDNA6/ GFP/V5-His vector
HPGD	Hydroxyprostaglandin dehydrogenase 15-(NAD)
HPGD-GFP	HEK293 cells transfected with pLenti6.2/V5-Dest EF1α/HPGD-GFP or

	with pcDNA6/HPGD-GFP/V5-His vector
HPGD-IRES-GFP	HEK293 cells transfected with HPGD-pIRES2-AcGFP1 vector
IC	inhibitory concentration
Ig	immunoglobulin
IFN	Interferon
IκB	inhibitor of nuclear factor κ light chain gene enhancer in B cells
IKK	inhibitor of NF-κB kinase
IL	interleukin
IL-2R	interleukin-2 receptor
iT_{reg}	induced regulatory T cells
JAK	janus kinase
mab	monoclonal antibody
MACS	magnetic activated cell sorting
MEKI	MEK kinase
MHC	Major Histocompatibility Complex
NFAT	nuclear factor of activated T cells
NF-κB	nuclear factor kappa-light-chain enhancer of activated T cells
nT_{reg}	naturally occurring regulatory T cells
PBMC	peripheral blood mononuclear cells
PBS	phosphate buffered saline
PE	phycoerythrin
PerCP	Peridinin Chlorophyll Protein Complex
PGE_2	prostaglandin E_2
PI	propidium iodide
PI3K	phosphoinosite 3-kinase
SAP	shrimp Alkaline Phosphatase
SDS	sodium dodecylsulfate
SDS-PAGE	sodium dodecylsulfate polyacrylamide gel electrophoresis
siRNA	small interfering RNA
STAT	signal transducer and activator of transcription

TBE	Tris/Borate/EDTA
T_{conv}	conventional T cells
TCR	T cell receptor
T_{eff}	effector T cells
TGF-β	transforming growth factor-β
T_H1/2/3/9/17	T helper cell 1/2/3/9/17
TNFα	tumor necrosis factor α
Tr1 cells	type-I regulatory T cells
T_{reg}	regulatory T cells
Tris	Tris-[hydroxymethyl]aminomethan
RNA	Ribonucleic acid
WT	wild-type

1 Introduction

1.1 Regulatory T cells

The mammalian immune system has many mechanisms to protect the body from external harmful pathogens such as bacteria, viruses and parasites. Moreover, the immune system regulates immunological homeostasis and protects the body from deleterious immune reactions against body-own tissue. The well-balanced regulation of immune responses results from interactions between the different immune cells in the body with T-lymphocytes playing a central role in the immune response. On the one hand, they can act as direct effector cells, on the other hand they can have regulatory functions to control and modulate the immune reactions and functions of numerous other cell types [1].

1.1.1 Discovery of T cells with regulatory characteristics

The first evidence for the existence of cells with immune regulatory features was provided by several studies in the seventies of last century. It was demonstrated that T cells could also depress immune responses and were required to induce tolerance. Tolerance could even be adoptively transferred to naïve recipients [2-6]. Following studies supplied further evidence for the existence of a specialized T cell subset and suppressor T cells were later defined by anti-Ly antisera, as $Ly23^+$ ($CD8^+$) T lymphocytes [7,8].

In the eighties, however, the research into suppressor T cells was discontinued because of different reasons. Among other things was the indication that no coding region corresponding to the I-J region was displayed in the murine MHC gene [9,10]. The I-J region was thought to encode the (soluble) I-J molecule, which was associated with the suppressive function of the T suppressor cells as a key suppressor molecule [11].

In the early nineties the interest in suppressive T cells was revitalized. It could be demonstrated that BALB/c athymic nude (nu/nu) mice, inoculated with $CD25^+$ depleted $CD4^+$ T cell suspensions ($CD4^+CD25^-$ T cells), developed severe autoimmune diseases such as thyroiditis, gastritis etc. The progression of the autoimmune disease could, however, be prevented by the reconstitution with $CD4^+CD25^+$ cells [12]. These suppressive $CD4^+CD25^+$ T cells were called “regulatory T cells” and represent approximately 5-10 % of the peripheral $CD4^+$ T cells in normal unimmunized adult mice [12].

1.1.2 Development of naturally occurring $CD4^+CD25^+FOXP3^+$ regulatory T cells

1.1.2.1 Development in the thymus

Naturally occurring $CD4^+CD25^+FOXP3^+$ regulatory T cells (nT_{reg}) can be found in the thymus and the periphery of naïve mice [1,13] and have been isolated from peripheral blood, tonsils and thymus of healthy human [14,15]. They are generated in the thymus, as it was shown that neonatal thymectomy at day 3 after birth leads to transiently reduced numbers of T_{reg} cells and severe organ-specific autoimmune diseases in mice [1,16]. Despite the fact that regulatory T cells suppress self-reactive T cells and limit their reactivity to self-antigens, it is likely that T_{reg} cells display characteristics of self-specific cells and show elevated affinity for peripheral self-peptides [17-19]. The reason for this is that T_{reg} cells have been shown to require T cell receptor (TCR) stimulation to mediate their suppressive activities *in vitro* and to regulate organ-specific autoimmune diseases *in vivo* [18,19]. It is remarkable that self-reactive T_{reg} cell precursors are not depleted in the thymus, as is the rule with normal self-reactive T cells. Instead highly autoreactive T_{reg} cells seem to differentiate into mature T_{reg} cells. It has been demonstrated that $CD4^+CD25^+$ thymocytes with a high affinity TCR for self-peptide were more likely to develop into mature T_{reg} cells than thymocytes that bear TCRs with a low affinity for self-antigen [20,21]. Nonetheless the exact signaling events and genetic signatures that lead to the preference of T_{reg} cells with high avidity for self-peptides remain to be elucidated[22]. The increased specificity for self-peptide though seems not to be a requisite for T cells to develop into T_{reg} cells. This was demonstrated by means of a transgenic mouse model, in which the expression of a particular T cell epitope by the thymic stromal cells could be quantitatively and temporally controlled. The T_{reg} cell differentiation and cell number occurred to be independent of the dose of T cell epitope [23]. Instead $CD4^+CD25^+$ T_{reg} precursor cells were rather more resistant to clonal deletion than $CD4^+CD25^-$ T cells. This explains the enlarged amount of self-reactive cells within the $CD4^+CD25^+$ T_{reg} cell population [23]. Besides that additional molecules other than the TCR and other mechanisms may be involved in the development of T_{reg} cells in the thymus, since it has been reported that mice deficient in B7-1/ B7-2-($B7^{-/-}$) or CD28 show reduced frequencies of $CD4^+CD25^+$ thymocytes compared to mice sufficient for B7 or CD28 [24,25]. Moreover, IL-2 appears to play an important role in the development and maintenance of T_{reg}, as IL-2Rβ-deficient mice show a loss of functional T_{reg} cells [26]. Naturally occurring T_{reg} constitutively express CD25, the alpha chain of the IL-2 receptor, but are in contrast to conventional $CD4^+CD25^-$ T cells (T_{conv}) unable to secrete IL-2 [27].

1.1.2.2 Development of $CD4^+CD25^+$ regulatory T cells in the periphery and induced T_{reg} cells

The central role of the thymus in the development of $CD4^+CD25^+$ regulatory T cells is well established but it is not the only site for their formation. If the thymus was the only location for T_{reg} cell development, the number of T_{reg} cells in humans would due to thymic involution decrease with the advance of years. However, the T_{reg} number does not decline but even increases with aging [28]. Several studies with transgenic mice have demonstrated the peripheral generation of $CD4^+CD25^+$ T_{reg} cells. Mice that were thymectomized at day 3 after birth showed a transient absence of T_{reg} at first and later within 3 months the T_{reg} numbers increased again to normal amounts [1]. Another study used $CD4^+$ T cells from OVA-specific DO11.10 TCR transgenic mice on a Rag-2 deficient background. These cells were transferred into BALB/c receptor mice with following intravenous or oral administration of antigen to induce peripheral tolerance. After tolerance induction TCR-transgenic $CD4^+CD25^+$ T cells emerged in tolerized animals with phenotypic characteristics similar to T_{reg} cells [29,30]. Obviously the new T_{reg} cells were induced (iT_{reg}) from the $CD4^+CD25^-$ T cells pool towards a T_{reg} cell phenotype. Similar results were obtained when mice were tolerized with antigen that was coupled to the monoclonal antibody (mab) against DEC205, which is an endocytic receptor highly expressed by dendritic cells (DCs) [31-33]. The regulatory T cells generated in the periphery were termed 'adaptive' or 'induced' T_{reg} cells (iT_{reg}) and different subpopulations of these cells have been described by now.

$CD4^+$ T helper-3 T cells (T_H3) can be induced by TGF-β *in vitro* or by antigen feeding in rodents *in vivo*. They lack FOXP3 expression but express TGF-β and suppress via TGF-β secretion [34]. Besides that, CD4 positive type 1 regulatory T cells (Tr1) exist. They can be generated *in vitro* and *in vivo* in the presence of IL-10. Tr1 cells lack FOXP3 expression and mediate suppression via IL-10 secretion and TGF-β [35]. Recently, it was shown that naïve human or mouse T cells can be induced *in vitro* towards the regulatory 'iT_R35' cells by IL-35 treatment. Their generation *in vivo* was induced under inflammatory conditions in the intestines of mice infected with *Trichuris muris*. These iT_R35 cells did not express FOXP3 and mediated suppression via IL-35 [36].

Furthermore, additional subpopulations of T cells with regulatory activities have been described like $CD4^+LAP^+$ T cells, that lack FOXP3 expression but express TGF-β receptor type II and the activation marker CD69, are hypoproliferative and exhibit IL-10 and TGF-β-dependent suppressive activity *in vitro* [37]. Moreover, there are different CD4 negative subpopulations with regulatory capacities including $CD8^+$, $CD4^-CD8^-$ (double negative

$CD3^+$), γδ T cells and natural killer T (NKT) cells [38-41] . A summary of thymic and peripheral formation of T_{reg} cells is given in Figure 1.

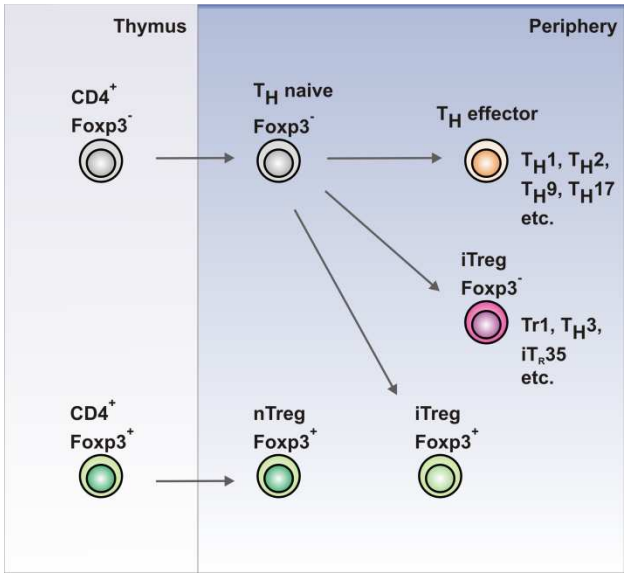

Figure 1: Generation of $FOXP3^+$ T_{reg} cells in the thymus and in the periphery.
Natural $FOXP3^+$ T_{reg} cells (nT_{reg}) differentiate in the thymus and migrate to peripheral tissue. The differentiation of adaptive $FOXP3^+$ T_{reg} (iT_{reg}) cells as well as $FOXP3^-$ iT_{reg} (Tr1, T_H3 and iT_R35 cells) occurs in the periphery. Also T_H effector cells such as T_H1, T_H2, T_H9, T_H17 etc. differentiate in secondary lymphoid tissue. The graphic was modified from Curotto de Lafaille et al. 2009 [42].

1.1.3 Immunological phenotype and features of regulatory T cells

1.1.3.1 Surface molecules specifically expressed on naturally occurring regulatory T cells

Naturally occurring $CD4^+CD25^+FOXP3^+$ regulatory T cells (nT_{reg}) are described as a subset of $CD4^+$ T cells that show constitutively expression of CD25, the alpha chain of the IL-2 receptor (IL-2R) [12]. The IL-2R consists of three subunits, the α- (CD25, IL-2Rα), β- (CD122, IL-2Rβ) and γ-chain (CD132, IL-2Rγ). The β- and γ-chain are constitutively expressed on the cell surface. Upon antigen activation also the α-subunit is expressed and transported to the cell membrane. All three subunits need to be present so that the receptor gains a sufficient affinity of IL-2 [43]. In non-immunized, healthy mice CD25 expression can be used as a good marker for nT_{reg} cells. However, CD25 is frequently found on all T cells upon activation [44].

For this reason several studies were made to find other surface markers suitable for the characterization of nT_{reg}. Different surface molecules have been proposed to be associated with the function, development or generation of $CD4^+CD25^+FOXP3^+$ regulatory T cells. In addition to CD25 the most commonly used surface markers for nT_{reg} are the cytotoxic T lymphocyte-associated antigen 4 (CTLA-4) [18,45], the interleukin-7 receptor-α-chain (CD127)

[46,47], the glucocorticoid-induced TNF receptor (GITR) [48,49] and lymphocyte activation gene-3 (LAG-3) [50]. But also other surface molecules like the nucleoside triphosphate diphosphohydrolase-1 (NTPDase 1; CD39) have been shown to be primarily expressed by immune-suppressive FOXP3$^+$ regulatory T cells [51]. The TGF-β latency-associated peptide (LAP) is expressed on the surface of activated mouse and human FOXP3$^+$ T_{reg} and it was shown that immunosuppression by cell-cell interactions is mediated via cell-surface bound TGF-β [52-54]. The TNFR family members OX40 (CD134) and 4-1BB (CD137) have also been suggested to play a role in controlling the generation and activity of T_{reg} cell, although they do not have a major role in homeostasis of nT_{reg} *in vivo* [55-57]. Recent studies have shown that GARP (or LRRC32), an orphan toll-like receptor composed of leucine-rich repeats, is highly expressed on activated nT_{reg} in comparison to non-activated and activated non-T_{reg} cells [52,58].

However, these surface molecules can also be found on CD4$^+$ T cells in different activation, differentiation and developmental states and up to now no specific surface molecule was identified to be unique for naturally occurring CD4$^+$CD25$^+$FOXP3$^+$ T_{reg} cells.

1.1.3.2 The transcription factor FOXP3 – a master switch for development and function of T_{reg} cells

In 2003 the transcription factor FOXP3 (forkhead box P3), a member of the forkhead/winged-helix family of transcription factors was described to be expressed in naturally occurring regulatory T cells and identified as lineage marker for nT_{reg} [59-62]. Previous studies initially described *Foxp3* as the defective gene in the Scurfy mutant mouse. This mouse strain is an X-linked recessive mutant that is lethal in hemizygous males within a month after birth. Scurfy mice exhibit fatal X-linked lymphoproliferation that is characterized by hyperactivation of CD4$^+$ T cells, overproduction of proinflammatory cytokines and a multiorgan immunopathology [63]. The immunodysregulation, polyendocrinopathy, enteropathy, X-linked (IPEX) syndrome is the corresponding disease in humans and is caused by a mutation within the FOXP3 gene. The IPEX syndrome is an X-linked recessive disorder that is caused by mutations in the FOXP3 gene located at Xq11.23-Xq13.3 of the X chromosome. Human individuals that suffer from IPEX develop various symptoms and diseases. These can be eczema, watery diarrhea, type I diabetes mellitus, excessive cytokine production and chronic inflammation, which lead to an early death [64-66].

Though FOXP3 is not exclusively expressed in human nT_{reg}, as recent works identified a transient expression of FOXP3 in activated human T_{conv} cells, which however does not

necessarily confer suppressive activity [67-69] as these FOXP3-expressing T cells did either exert suppressive activities [70,71] or not [68,69].

In fact a high and stable expression of FOXP3 is required for the induction of suppressive activity in T_{conv} cells. This was demonstrated with the retroviral transduction of FOXP3 into $FOXP3^-$ non-regulatory $CD4^+$ cells. They gained a fully functional T_{reg} cell like phenotype; they became anergic, expressed T_{reg} typical surface markers and showed suppression *in vitro* and *in vivo.* These observations demonstrate that FOXP3 is a highly specific marker for T_{reg} cells and that it plays a role as master regulator because its expression is sufficient and necessary for the development of T_{reg} [59-61].

1.1.3.3 Anergy of regulatory T cells

Naturally occurring T_{reg} cells display specific characteristics and functions by which they can be characterized. On the one hand, nT_{reg} cells can be identified by the expression of T_{reg}-associated surface molecules (see 1.3.1) and the expression of FOXP3 (see 1.3.2). On the other hand, although T_{reg} cells require TCR activation for their functional activation, they possess an anergic phenotype and stay hypoproliferative towards CD3/CD28 engagement. Upon TCR stimulation T_{reg} will not proliferate or produce IL-2 as for instance T_{conv} cells (effector T cells) [19,72,73]. However, protocols have been developed for their *in vitro* expansion. The expansion is thereby performed via TCR/CD28 engagement in the presence of very high concentrations of IL-2 [74]. Furthermore, T_{reg} cells were found to proliferate extensively *in vivo* in response to immunization, without losing their suppressive function *in vivo,* and they accumulated locally in response to transgenically expressed tissue antigen [75,76].

The relationship between anergy and suppressive capacity needs to be further investigated. The anergic state in T_{reg} can be abrogated by TCR stimulation *in vitro* combined with high-dose costimulation of IL-2 or CD28 and leads to a loss of the suppressive activity [77]. Once IL-2 and CD28 costimulation are removed, T_{reg} cells regain their anergic state and suppressive activity [78]. This was also observed *in vivo* [76].

1.1.3.4 Suppressive activity of regulatory T cells

Another feature is their suppressive capacity *in vitro* and *in vivo*. nT_{reg} show suppression of the proliferation and cytokine production of activated T_{conv} cells and of $CD8^+$ T cells. But they can also suppress dendritic cells (DC), natural killer (NK) cells, natural killer T cells and B cells [18,78-80]. Various potential suppression mechanisms and molecules that are used by T_{reg} cells have been described.

1.1.4 Different suppression mechanisms used by regulatory T cells

Different suppression mechanisms have been demonstrated to be used by T_{reg} cells to suppress the proliferation of T_{conv} cells and their effector cell functions. These mechanisms were shown to be cell-contact-dependent on the one hand. T_{reg} cells were not able to suppress proliferation of T_{conv} cells when they were separated by a semi-permeable membrane from the T_{conv} [19,72]. Further evidence for a cell-contact dependency proved that T_{reg} failed to suppress B7-deficient T cells [81]. On the other hand, also various cell contact-independent mechanisms have been described. Concerning the mode of action the suppression mechanisms can be divided into four main groups:

a. Suppression by cytolysis
b. Suppression by inhibitory cytokines
c. Suppression by metabolic disruption
d. Suppression by modulation of dendritic-cell (DC) maturation and function.

1.1.4.1 Suppression by cytolysis

T_{reg} were shown to exhibit cytolytic activity to kill T_{conv} cells in a granzyme- or perforin-dependent manner [82,83] Also B cells, NK cells and cytotoxic T lymphocytes have been shown to be killed in a granzyme-B-dependent and perforin-dependent manner by T_{reg} cells [84,85]. Furthermore, it was suggested that activated T_{reg} induce apoptosis of T_{conv} cells through a TRAIL-DR5 (tumor-necrosis-factor-related apoptosis-inducing ligand-death receptor 5) pathway [86]. Another study has shown that human and murine T_{reg} upregulated galectin-1 (LGALS1), which can induce T cell apoptosis and that galectin-1-deficient T_{reg} had reduced regulatory activity *in vitro* [87].

1.1.4.2 Suppression by inhibitory cytokines

Besides cell-contact dependent suppression also cytokines like IL-10 or TGF-β seem to play an important role, as these cytokines possess immunosuppressive characteristics. However, *in vitro* studies with neutralizing antibodies against IL-10 and TGF-β revealed that IL-10 and TGF-β are not essential for the T_{reg} cell function [18,19]. Contrary to that these cytokines contribute to suppression *in vivo*, because IL-10 deficient T_{reg} were unable to suppress inflammatory bowel disease (IBD) in a mouse model [88]. Furthermore, blockade of the IL-10 receptor (IL-10R) and neutralization of TGF-β did abolish T_{reg}-mediated inhibition of the disease [45]. Other studies suggest a crucial role for membrane-bound TGF-β. Membrane-tethered TGF-β on T_{reg} cells was shown to participate in a cell-cell contact-dependent suppression [54,89].

Recent studies have identified IL-35 as another immunosuppressive cytokine. IL-35 is a novel member of the IL-12 heterodimeric cytokine family and is formed by pairing of the Epstein-Barr virus-induced gene 3 (*Ebi3*) with p35 (*Il12a*). Natural $FOXP3^+$ T_{reg} cells were shown to produce predominantly immunosuppressive IL-35 and IL-35-deficient T_{reg} were less suppressive *in vivo* (in controlling IBD) and *in vitro* (in a suppression assay) [90].

1.1.4.3 Suppression by metabolic disruption

The high expression of CD25 on nT_{reg} and their inability to produce IL-2 themselves gave rise to the studies whether T_{reg} cells 'consume' IL-2 in order to inhibit effector T cell responses. Cytokine deprivation led to apoptosis of dividing T_{conv} cells that need IL-2 to survive and was therefore proposed to be a prominent suppression mechanism used by T_{reg} cells [19,91,92]. However, other studies suggested that cytokine depletion is not a fundamental suppression mechanism of T_{reg}. The relevance of IL-2 for immunosuppression was challenged by a study that used human T_{reg} cells. It was demonstrated that IL-2 deprivation alone was not required for suppression of effector T cells [93]. Therefore, the role of IL-2 deprivation as a suppression mechanism used by T_{reg} needs to be further investigated.

Besides IL-2 depletion, T_{reg} cells have been reported to directly transfer cyclic adenosine monophosphate (cAMP) through membrane gap junctions into T_{conv} cells. Thereby intracellular cAMP levels in T_{conv} are upregulated, which finally lead to inhibition of T cell proliferation and IL-2 formation [94].

Furthermore, T_{reg} express the ectoenzymes CD39 (ectonucleoside triphosphate diphosphohydrolase 1) and CD73 (ecto-5'-nucleotidase). These ectoenzymes catalyze the generation of pericellular adenosine, which also suppresses effector T cell function through activation of the adenosine receptor 2A ($A_{2a}R$) [51,95].

1.1.4.4 Suppression by modulation of dendritic-cell (DC) maturation and function

T_{reg} cells have been shown to suppress effector T cell function by directly affecting these cells via cell-contact-dependent and -independent mechanisms. In addition, intravital microscopy revealed that T_{reg} cells interact with dendritic cells (DCs) *in vivo* [96,97]. T_{reg} cells have been reported to modify the function of APCs especially DCs, that in turn leads to suppression of effector T cell functions [96,97]. T_{reg} may for example induce the down-modulation of CD80 and CD86 on DCs [98]. Thereby the co-stimulatory molecule cytotoxic T-lymphocyte antigen 4 (CTLA-4) plays an important role that is constitutively expressed on T_{reg} cells [45]. This was demonstrated by use of CTLA-4-specific blocking antibodies or CTLA-4-deficient T_{reg} that suppression mediated via DCs was reduced [98,99]. Moreover, T_{reg} cells can induce the expression of immunosuppressive molecules like the tryptophan-degrading enzyme indoleamine 2,3-dioxygenase (IDO) in DCs. IDO is known to induce production of pro-apoptotic metabolites from the catabolism of tryptophan. This leads to the suppression of effector T cells through a mechanism dependent on interactions between CTLA-4 and CD80 and/or CD86 [100,101]. Other studies have reported that T_{reg} can modulate and even block the maturation of DCs via a lymphocyte-activating gene 3 (LAG-3; CD223) mediated mechanism [50,102]. Moreover, the molecule neuropilin-1 was found to prolong interactions with T_{reg} cells and immature DCs [103].

It has been suggested that the nT_{reg} cell population maintains immunological tolerance and amplifies their suppressive function by the *in vivo* conversion of non-T_{reg} into induced T_{reg} cells (see also chapter 1.1.2.2). This induction process is also called 'infectious tolerance' and is shown to be cytokine-mediated, for instance by IL-10 or TGF-β [35,36,104,105] (see also chapter 1.1.2.2). Natural T_{reg} cells were shown to secrete IL-35 [90]. A recent study has shown that T_{conv} cells can be induced towards a T cell subset with regulatory activities called 'iT_R35' cells by incubation with IL-35 *in vitro* [36]. This conversion was also observed *in vivo* under inflammatory conditions in intestines infected with *Trichuris muris* and within the tumor

microenvironment. Thereby it was shown that approximately half of the regulatory microenvironment in the tumor consisted of 'iT$_R$35' cells [36].

In view of the plethora of suppressive mechanisms the question arises whether all these different molecules and mechanisms together are crucial for the T$_{reg}$-cell function or whether single mechanisms exist that are used by all T$_{reg}$-cells. The dependency on some single suppressive mechanism used by all T$_{reg}$, is rather unlikely. So it was demonstrated that the abrogation of one suppression mechanism leads to a substantial but not a complete loss of the regulatory T$_{reg}$-cell function. Otherwise the lack of a single molecule, for instance IL-10, would result in a scurfy-like phenotype. It is rather more presumable that T$_{reg}$ cells use different mechanisms of suppression depending on the type of target cell. Furthermore, different mechanisms may be required or may be more effective in different tissues compartments or for different diseases. Thereby, the mechanisms could also act in concert to enhance the suppressive efficacy. However, the exact interaction of the different mechanisms needs to be further investigated.

1.1.5 Regulatory T cells in the tumor microenvironment

Various studies have demonstrated the presence of regulatory T cells in tumor tissues as well as tumor-draining lymph nodes in rodents and also in cancer patients suffering from tumors in head and neck [106], lung [107], liver [108], in the gastrointestinal tracts [109], pancreas [110], breast tissue [111] and ovary tissue [112]. Thereby increased numbers of T$_{reg}$ cells can be observed within the tumor tissue, which correlates with poor prognosis in patients with breast cancer [113], gastric cancer [109] and ovarian cancer [109,112].

The question of how and why T$_{reg}$ cells are recruited to the tumor and are found in increased numbers in the tumor tissue is the focus of several studies. It is proposed that the proliferating and dying tumor cells provide large amounts of self-antigens that may attract and recruit T$_{reg}$ cells. Furthermore the inflammatory environment can also attract T$_{reg}$ to migrate to the tumor site [114]. Besides that the tumor cells and tumor infiltrating macrophages produce chemokines like CCL22 that can recruit CCR4-expressing T$_{reg}$ cells [112,115]. Finally it is proposed that FOXP3$^+$ T$_{reg}$ cells are induced from non-T$_{reg}$ cells in the tumor microenvironment as a result of the high concentrations of tumor-derived TGF-β [116,117].

1.2 Interleukin-2 receptor signaling pathways

Interleukin-2 is important for T cell proliferation, survival and programmed cell death and is primarily produced by activated T cells, which also represent the main target of IL-2 [118-121]. Besides, IL-2 is also important for other biological processes, like growth and differentiation of B cells [122], generation of lymphokine-activated killer cells [123], augmentation of natural killer cells [124] and proliferation and maturation of oligodendroglial cells [125]. IL-2 consists of 133 amino acids with a molecular mass of 15-18 kDa and mediates signaling via a multichain receptor complex [43]. This interleukin-2 receptor (IL-2R) belongs to the type I cytokine receptor superfamily [118,119]. It is composed of three subunits: the affinity-modulating subunit IL-2Rα (CD25) and the two signaling subunits IL-2Rβ (CD122) and IL-2Rγ (CD132) [126]. Thereby the β- and γ-chain are constitutively expressed on the cell surface. Upon antigen activation also the α-subunit is expressed and transported to the cell membrane. All three subunits need to be present so that the receptor gains a sufficient affinity for IL-2 [43]. The binding of IL-2 to the IL-2R can activate a variety of different signaling cascades, which are depicted in a generalized overview in Figure 2. IL-2 can activate for instance the JAK/STAT-signaling pathway. Phosphorylation of the cytoplasmic β- and γ-chain of the IL-2R provide docking sites for the janus kinases-1 and -3 (JAK1 and JAK3) [127,128], which are in turn autophosphorylated and thus provide docking sites for Signal Transducer and Activator of Transcription-5 (STAT-5). STAT5 is phosphorylated, which leads to dimerisation and nuclear translocation of STAT5 complexes, where they initiate transcription of target genes [129]. Moreover, IL-2 can activate the PI3K/Akt-signaling pathway. Binding of IL-2 leads to activation of Phosphatidylinositol 3-kinase (PI3K). This leads to production of inositol phospholipids PtdIns (3,4,5)P3 and PtdIns(3,4)P2, which attract Akt (also known as Protein Kinase B, PKB) to the plasma membrane, where it is phosphorylated[130]. Akt in turn phosphorylates and thus activates IκB kinase (IKK), which is comprised of the catalytic subunits IKK-α and IKK-β and the regulatory subunit IKK-γ (NEMO)[131-133]. IKK phosphorylates the inhibitor of κBα protein (IκBα), which leads to ubiquitination of IκBα, its dissociation from nuclear factor κB (NF-κB, subunits p50 and p65) and eventual degradation of IκBα by the proteasome. The release of NF-κB allows its translocation to the nucleus where it initializes transcription[132-134]. The IL-2R can also activate the MAPK-signaling pathway as it binds spleen tyrosine kinase (Syk) and lymphocyte-specific protein tyrosine kinase (Lck), which are activated downstream of JAK1 and JAK3 [135]. This stimulates association of SHC (Src homology 2 domain containing) transforming protein 1(Shc), GRB2 (Growth factor receptor-bound protein 2) and SOS (Son of sevenless homologs), which

further activate signaling via Ras (v-Ha-ras Harvey rat sarcoma viral oncogene homolog), Raf (v-Raf-1 murine leukemia viral oncogene homolog 1), MEK1/2 (Mitogen-activated protein kinase 1 and ; MEKs2) and ERK1/2 (Extracellular signal-regulated kinase 1 and 2; ERKs). This pathway leads to activation of the transcription factors such as Elk-1, c-Myc, c-Fos or c-Jun/c-Fos (AP-1) [136-139].

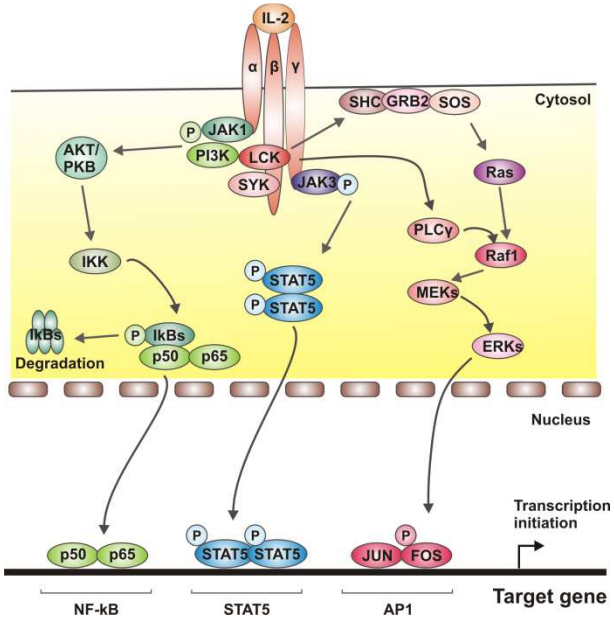

Figure 2: Generalized overview of different IL-2 signaling pathways.
Binding of IL-2 to the IL-2R (subunits α, β and γ in orange) can activate different signaling cascades. IL-2 can activate the JAK/STAT-signaling pathway by activation of JAK1 and JAK3, resulting in the activation of STAT-5, its dimerisation and translocation to the nucleus where STAT5 initiates transcription of target genes. IL-2R signaling can also activate PI3K/Akt-signaling cascade, which leads to activation of Akt. Akt in turn activates IKK that phosphorylates IκBα. This results into the degradation of IκBα and the release of NF-κB, which can now translocate to the nucleus and initialize transcription. Phosphorylation of JAK1/JAK3 can also activate the MAPK-signaling pathways. SYK and LCK are activated, which leads to association of SHC, GRB2 and SOS that further activate signaling via Ras, Raf, MEK1/2 (MEKs) and ERK1/2 (ERKs). This pathway leads to activation of the transcription factors such as Elk-1, c-Myc, c-Fos or c-Jun/c-Fos (AP-1).The graphic was modified from www.proteinlounge.com/Pathway/Default.aspx (01.05.2011).

1.3 The hydroxyprostaglandin dehydrogenase 15-(NAD)

1.3.1 Identification of HPGD as a prostaglandin metabolizing enzyme

The NAD^+-dependent 15-hydroxyprostaglandin dehydrogenase type-I (HPGD or 15-PGDH) maintains a crucial role in the metabolism of prostaglandins as it is considered as key catabolic enzyme, which controls their biological activity [140,141]. The first evidence for the existence of a prostaglandin metabolizing enzyme was brought by Änggård and Samuelsson in 1964. They observed that lung homogenates from guinea-pigs converted prostaglandin E_1

(PGE_1) into the metabolites 13,14-dihydro-prostaglandin E_1 and 13,14-dihydro-15-keto-prostaglandin E_1. The occurrence of metabolites was thereby not due to a non-enzymatic conversion, as boiled homogenates did not convert PGE_1 into its metabolites [140]. Two years later the same group reported the 11-fold purification of a specific prostaglandin dehydrogenase from swine lung [142]. Since then HPGD was successful isolated from different tissues and organisms like human placenta [143,144], rabbit lung [145], rat kidney [146] and chicken heart [147]. HPGD is ubiquitously expressed in mammalian tissues with the highest activities for HPGD detected in lung, kidney and placenta [141].

1.3.2 Genomic location

The HPGD gene encodes the NAD^+-dependent 15-hydroxyprostaglandin dehydrogenase (15-PGDH; HPGD; EC 1.1.1.141), an enzyme that belongs to the short-chain nonmetalloenzyme alcohol dehydrogenase protein family [148]. Chromosomal localization of the human HPGD gene revealed that it maps to chromosome 4 with further location to the bands 4q34-q35[149]. The HPGD gene contains 7 exons and 6 introns and is approximately 31 kb long [150]. The primary structure of the human HPGD was elucidated by peptide sequencing [148] and cDNA cloning [151]. The open reading frame of the human enzyme type I codes for a protein of 266 amino acids with a molecular weight (M.W.) of 28,975 Da [148,151].

Initial studies on the gene transcription revealed two different mRNA species in human placenta, with 2.0 kb and 3.4 kb in length, indicating the existence of spliced variants or an alternative gene [152]. Further investigation identified two truncated forms of the human HPGD variant 1 in HL-60 and TT cells [153,154]. Variant 2 lacks thereby an alternate exon (the sixth exon) in the 3' coding region. This smaller sequence codes for a predicted C-terminal-truncated form of HPGD of 178 amino acids (19,28kDa) and has approximately 64 % identity with HPGD variant 1 [153]. The third variant is missing the fifth and sixth exon [154]. The truncated variants seemed to be splicing isoforms of HPGD variant 1, because both showed N-terminal protein sequence homology but differed in the C-termini. However, both truncated variants are not likely to display enzymatic activity because they lack the catalytically essential amino acid residues Tyr 151 and Lys 155 [155,156]. The cDNAs for HPGD were also cloned from other species like mouse [157], rat [145] or guinea pig [158]. The murine HPGD gene is approximately 11.3 kb in length and contains like the human gene seven exons and six introns and maps to chromosome 8 (8 B3.2;8) [157].

1.3.3 Protein structure and enzymatic activity

Sequence alignments indicated that HPGD belongs to the short chain dehydrogenase/reductase (SDR) family [148,159]. HPGD shows approximately 20 % homology compared to other short-chain dehydrogenases (SDRs) [159]. The amino acid residues Tyr151, Lys155 and Ser138 have been demonstrated to be essential for the catalytic activity, because site-directed mutagenesis leads to a loss of enzymatic activity [155,156]. Moreover, the residues Thr11 and Thr188 were found to be important for the interaction with NAD^+ [160,161]. The primary structures of HPGD from various species are largely homologous except for two regions, the C-terminal domain and the region from residue 205 to 224. HPGD forms a homodimeric protein to mediate its enzymatic function although it is also thought to be active as a monomer [162].

HPGD plays a crucial role in the metabolism of prostaglandins (PGs), because it represents a major enzyme in the degradation of prostaglandins. Prostaglandins are rapidly inactivated *in vivo* by the β-oxidation of their 15-hydroxyl group into a 15-keto group, catalyzed by HPGD. The 15-keto-metabolite thereby represents the first step in the biological inactivation of PGs [141,163]. The prostaglandins are then further metabolized by the 15-ketoprostaglandin Δ^{13}-reductase (15-13PGR), resulting in 13,14-dihydro-15-keto-prostaglandins the so called PG(A, D, F, E, M) [164].The 13,14-dihydro-15-keto-prostaglandins finally undergo β- and ω-oxidation to form a variety of metabolites that are excreted in the urine [163]. Two different types of enzymes have been identified in human tissue that catalyze the oxidation of the 15-hydroxy group of prostaglandins: HPGD type I is described to be NAD^+-dependent and uses basically prostaglandins and related eicosanoids as substrates [165]. HPGD type II is $NADP^+$-dependent but can also use NAD^+ as cofactor. HPGD type II has a broader substrate specificity and approximately 20 % homology with the HPGD type I [165,166]. This enzyme has also a much higher K_m value for prostaglandins than the HPGD type I enzyme and does therefore not appear to contribute significantly to the catabolism of prostaglandins. HPGD type I is also believed to be the enzyme primarily involved in controlling the biological activities of prostaglandins and related eicosanoids [141,167]. For this reason, only HPGD type I was considered in the present study and will be referred to as HPGD in the following. HPGD can use a variety of different prostaglandins as substrate, such as PGE_1, PGE_2, $PGF_{1\alpha}$, $PGF_{2\alpha}$, PGI_2 and 6-keto-$PGF_{1\alpha}$. PGB2, PGD_2 and TXB_2, however, are poor substrates. Besides prostaglandins also the unsatureated fatty acids that contain a hydroxyl group at their ω-6 position like 12-L-hydroxy-5,6,10-heptadecatrienoic acid (12-HHT); 15-

hydroxyeicosatetraenoic acid (15-HETE); 5,15-dihydroxy-6,8,11,13-eicosatetraenoic acid (5,15-diHETE); 8,15-Dihydroxy-5,9,11,13-eicosatetraenoic acid (8,15-diHETE) and lipoxin A_4 were reported to serve as substrates for HPGD [168-170] .

1.3.4 Regulation of the HPGD gene expression

The regulation of HPGD has been investigated by various studies in whole animals and also in isolated cells [163,167]. The induction of HPGD expression and activity was first reported in dimethyl formamide treated HL-60 cells [171]. Subsequently the induction of HPGD was also achieved by 1,25-dihydroxyvitamin D_3 in human neonatal monocytes [149] and by treatment of humanerythroleukemia (HEL) cells with phorbol 12-myristate 13-acetate (PMA) [172]. Also dimethyl sulfoxide (DMSO) could stimulate the enzyme activity [173]. Besides that, also indomethacin increased HPGD mRNA expression in HL-60 cells [174]. In contrast, HPGD expression and activity was sustained by glucocorticoids such as cortisol and dexamethasone [172,175] and treatment with IL-1β [176] or TNF-α. The effect of IL-1β could be reversed by the concurrent addition of the immunosuppressive cytokine IL-10 [176]. Similarly, the anti-inflammatory cytokine IL-4 was also shown to stimulate HPGD activity in the human lung cancer cell lines A549, H358, H1435 and H460 [177]. Bile acids were also shown to inhibit HPGD transcription in human colon cancer cell lines [178].

Besides that, several potential regulatory elements have been identified. The human promoter regions exhibit key regulatory elements such as Ets, CREB, AP-1, AP-2, GRE and Sp1, which may provide potential binding sites for these agents to initiate gene transcription [179,180]. Recently, the forkhead transcription factor hepatocyte nuclear factor 3β (HNF3β) was shown to regulate HPGD expression, as HNF3β showed direct binding to promoter elements of HPGD in lung cancer cells [181].

1.3.5 The role of HPGD in perinatal development and in cancer

In addition to the role of HPGD in inflammation this protein maintains a crucial role in perinatal development. HPGD-deficient mice ($Pgdh^{-/-}$) die shortly after birth because of the defective remodeling of the ductus arteriosus. Under normal conditions PGE_2 levels are significantly reduced due to enhanced pulmonary HPGD activity in late gestation. This results in the closure of the ductus arteriosus [182].

Furthermore, HPGD seems to play an important role in cancer. This was demonstrated in a study that compared the protein expression profiles of normal bladder urothelium with that of 63 transitional cell carcinomas of various histopathological grades and tumor stages. Among other protein biomarkers a loss of HPGD expression was associated with the progression of human bladder transitional cell carcinomas [183]. Also in colon tumor samples, the median HPGD expression was at least 17-fold below the median HPGD expression of normal colon tissue [184]. Similar results were found in primary breast tumors where HPGD was shown to be under-expressed [185] and in lung tumors where HPGD gene expression was found to be under-presented [186]. Moreover, experiments with a xenograft model where stable HPGD-transfected H358 lung cancer cells were injected into athymic mice, showed that tumor formation was markedly suppressed in mice injected with HPGD-transfected cells compared to empty-vector-transfected cells. The suppression was thereby mediated by an antiangiogenic mechanism [181]. In addition, an *in vitro* study with SW480 colorectal cells demonstrated that HPGD over-expression in these cells resulted in a decreased cell motility and invasive activity [187]. These observations indicate a potential role for HPGD as tumor suppressor.

1.4 Different methods of antibody generation

The immune system produces antibodies with high specificity to their antigen by well-directed selection processes. To mimic the processes of antibody generation *in vivo*, different methods were developed. One method to produce antibodies is performed by the repeated immunization of animals, for instance mice, rabbits, goats, horses etc. The animals are injected with an antigenic substance, for example (recombinant) protein or peptide together with a booster substance such as CFA (Complete Freud's Adjuvant). The serum is isolated from these immunized animals and contains polyclonal antibodies specific for the antigenic substance [188,189]. Antibodies obtained from serum can be produced relatively fast and with low costs. Disadvantageous of polyclonal antibodies is that they may contain large amounts of non specific and unspecific antibodies. Besides that, the products are highly dependable on donor blood availability, both in terms of quantity and suitability, resulting in considerable variation between batches. With the generation of hybridoma cells, which are produced by the fusion of murine B lymphocytes with myeloma cells, presented by Köhler and Milstein in 1975 [190], a method to produce monoclonal antibodies was invented. The hybridoma technique can be expensive and time consuming because of screening for the right hybridoma clones. However, monoclonal antibodies from hybridoma clones have a high specific antigen recognition [190].

Moreover, an unlimited supply of a monoclonal antibody with defined and reproducible affinity and specificity is permitted once an appropriate hybridoma clone is identified [190]. Besides that, other methods like the phage display technology have been developed. The phage display technology was invented when first murine antibody fragments from lymphocytes of immunized animals were obtained and expressed in *E.coli*, whereby either the variable region of the light (vL) or the heavy chain (vH) were used [191]. Later on the display of peptides on filamentous phage was demonstrated by fusing the peptide of interest on to gene3 of filamentous phage [192-194]. The phage display technology is a relatively fast and simple method and less cost intensive to produce antibody fragments [192-194].

1.5 Objectives

The characteristics and functions of $CD4^+CD25^+$ regulatory T cells (T_{reg}) have been extensively studied – yet further investigation is required to completely resolve how T_{reg} cells mediate their suppressive activity especially *in vivo* and which molecules are actually involved in their development and function. Various molecules have been identified, such as the lineage specific transcription factor FOXP3, which regulates the transcription of many target genes in T_{reg}. However, there are still unknown genes that are required for a complete regulatory phenotype of T_{reg} cells.

In order to identify novel target molecules involved in the development and function of T_{reg} cells, global gene expression profiling was carried out to designate genes that are specifically expressed in T_{reg} cells in comparison to $CD4^+CD25^-$ T cells (T_{conv}) cells under different activation states. Thereby the NAD^+-dependent 15-hydroxyprostaglandin dehydrogenase type-I (HPGD), the major Prostaglandin E_2 (PGE_2)-metabolizing enzyme, was identified as one of the differentially expressed transcripts. The objective of the present study was the characterization of the role of HPGD in human T_{reg} cells concerning its regulation and role for the development and suppressive function of T_{reg} cells. Therefore, it should be investigated whether HPGD expression is specific for naturally occurring T_{reg} cells or whether it can be also upregulated during T cell differentiation or the induction of adaptive T_{reg} cells (iT_{reg}). Moreover, the enzymatic activity of HPGD in T_{reg} cells and its contribution to the T_{reg} cell function should be examined. Besides, it was tested whether HPGD is a target gene of FOXP3. In addition, this study aimed at characterizing the influence of extracellular stimuli on the HPGD expression. Depending on these results, the underlying downstream signaling

pathways were further analyzed. Finally, it was investigated whether the observations made in the human could be transferred to the murine system.

In conclusion the results of the present study could help to better understand the regulatory phenotype of T_{reg} cells and provide a basis for future experiments to determine tissue-specific functions of T_{reg} cells and their function in the tumor microenvironment.

2 Material and Methods

2.1 Materials

2.1.1 Chemicals and reagents

Name	Manufacturer
30 % Acrylamide/bis Solution 29:1 (3,3%)	Bio-Rad Laboratories, München (DE)
Agar	Applichem, Darmstadt (DE)
Agarose	Applichem, Darmstadt (DE)
Ammoniumacetate	Merck, Darmstadt (DE)
Ammonium persulfate (APS)	Sigma-Aldrich, St Louis (USA)
Ampicillin	Applichem, Darmstadt (DE)
Bovine serum albumin (BSA)	Sigma-Aldrich, St Louis (USA)
β-Mercaptoethanol	Applichem, Darmstadt (DE)
Boric acid	Sigma-Aldrich, St Louis (USA)
Bromophenole blue	Roth, Karlsruhe (DE)
Calcium chloride-Dihydrat ($CaCl_2 \cdot 2H_2O$)	Merck, Darmstadt (DE)
5,6-Carboxyfluorescein diacetate succinimidyl ester (CFSE)	Sigma-Aldrich, München (DE)
$CD25^+$ Microbeads II	Miltenyi Biotec GmbH, Bergisch-Gladbach (DE)
$CD45^+$ Microbeads	Miltenyi Biotec GmbH, Bergisch-Gladbach (DE)
CellFix™	BD Biosciences, Heidelberg (DE)
Chloroform p.a.	Applichem, Darmstadt (DE)
Complete mini (Protease Inhibitor cocktail tablets)	Roche Diagnostics, Basel (CH)
1,4-Diazabicyclo[2.2.2]octan (Dabco)	Sigma-Aldrich, St Louis (USA)
Disodiumhydrogenphosphate-Dihydrate (Na_2HPO_4 $2H_2O$)	Merck, Darmstadt (DE)
Dulbecco's Modified Eagle Medium (D-MEM) (High	PAA Laboratories GmbH, Pasching

Glucose with L-Glutamine)	(AT)
Dimethyl sulfoxide (DMSO)	Sigma-Aldrich, Müchen (DE)
Dithiothreitol (DTT)	Fermentas GmbH, St. Leon-Rot, (DE)
Dynabeads® M-450 Tosylactivated	Invitrogen Life Technologies, Karlsruhe (DE)
Ethylendiamintetraacetate (EDTA)	Sigma-Aldrich, St Louis (USA)
Ethanol	Roth, Karlsruhe (DE)
Ethidiumbromide	Applichem, Darmstadt (DE)
Fc receptor blocking reagent	Miltenyi Biotec GmbH, Bergisch-Gladbach (DE)
Fetal calf serum (FCS)	PAA Laboratories GmbH, Pasching (AT)
Fluoromount-G	Southern Biotech, Birmingham (US)
Formaldehyde solution (37 %)	Sigma-Aldrich, St Louis (USA)
Gelatin from bovine skin	Sigma-Aldrich, St Louis (USA)
Gelatin from cold water fish skin	Sigma-Aldrich, St Louis (USA)
Gibco distilled water (RNase/ DNase free)	Invitrogen Life Technologies, Karlsruhe (DE)
Glacial acetic acid	Roth, Karlsruhe (DE)
D (+) Glucose	Merck, Darmstadt (DE)
Glutamax™ (100 x)	Invitrogen Life Technologies, Karlsruhe (DE)
Glycine	Applichem, Darmstadt (DE)
Glycerol (87 %) p.a.	Applichem, Darmstadt (DE)
Goat serum (normal)	DakoCytomation, Glostrup (DK)
HEPES	Applichem, Darmstadt (DE)
Isopropanol for the molecular biology	Applichem, Darmstadt (DE)
Isopropanol p.A.	Roth, Karlsruhe (DE)

Kanamycin	Applichem, Darmstadt (DE)
Laemmli buffer for SDS-PAGE (10 x)	Serva Electrophoresis GmbH, Heidelberg (DE)
Magnesiumchloride-Hexahydrate ($MgCl_2 \cdot 6H_2O$)	Applichem, Darmstadt (DE)
Magnesium ($MgSO_4*7H_2O$)	Merck, Darmstadt (DE)
Methanol p.a.	Roth, Karlsruhe (DE)
Milk powder	Roth, Karlsruhe (DE)
MOPS	Acros Organics, New Jersey (USA)
N,N,N',N'-Tetramethylethylenediamine (TEMED)	Applichem, Darmstadt (DE)
NuPAGE® Transfer Buffer 20x	Invitrogen Life Technologies, Karlsruhe (DE)
Odyssey® Blocking Buffer	Licor Biosciences, Bad Homburg (DE)
Odyssey® Two-Color Molecular Weight Marker (10 – 250 kDa)	Licor Biosciences, Bad Homburg (DE)
O'Range Ruler™ 100+500 bp DNA-Ladder	Fermentas GmbH, St. Leon-Rot, (DE)
O'GeneRuler™ 1 kb Plus DNA-Ladder	Fermentas GmbH, St. Leon-Rot, (DE)
6x O'Range DNA loading dye	Fermentas GmbH, St. Leon-Rot, (DE)
Pancoll human (density 1.077 g/l)	PAN Biotech GmbH, Aidenbach (DE)
Paraformaldehyde	Sigma-Aldrich, St Louis (USA)
Penicillin/ Streptomycin	Invitrogen Life Technologies, Karlsruhe (DE)
Phosphate buffered saline (PBS)	PAA Laboratories GmbH, Pasching (AT)
Potassium chloride (KCl)	Merck, Darmstadt (DE)
Potassium dihydrogenphosphat (KH_2PO_4)	Merck, Darmstadt (DE)
Potassium hydrogen carbonate ($KHCO_3$)	Merck, Darmstadt (DE)

Potassium hydroxide (KOH)	Merck, Darmstadt (DE)
Prostaglandin E_2 (PGE_2)	Sigma-Aldrich, St Louis (USA)
Propidium Iodide (PI)	Sigma-Aldrich, St Louis (USA)
Re-Blot plus mild solution (Chemicon)	Millipore GmbH, Schwalbach/Ts. (DE)
Rosette Sep $CD4^+$ T cell enrichment cocktail	Stem Cell Technologies, London (GB)
RPMI cell culture medium (1640)	PAA Laboratories GmbH, Pasching (AT)
Sandoglobulin	ZLB GmbH, Springe (DE)
Saponine powder	Sigma-Aldrich, St Louis (USA)
Sodium acetate	Applichem, Darmstadt (DE)
Sodium azide (NaN_3)	Roth, Karlsruhe (DE)
Sodium dodecylsulfate (SDS) 10% solution	Applichem, Darmstadt (DE)
Sodium dodecylsulfate (SDS) powder	Roth, Karlsruhe (DE)
Sodium chloride (NaCl)	Applichem, Darmstadt (DE)
Sodium dihydrogenephosphate-monohydrate ($NaH_2PO_4 \cdot H_2O$)	Merck, Darmstadt (DE)
Sodium hydroxide (NaOH)	Merck, Darmstadt (DE)
Trichloroacetic acid	Merck, Darmstadt (DE)
Tris	Applichem, Darmstadt (DE)
Tris-HCl	Applichem, Darmstadt (DE)
Triton X-100	Applichem, Darmstadt (DE)
Trizol® Reagent	Invitrogen Life Technologies, Karlsruhe (DE)
Tryptone	Roth, Karlsruhe (DE)
Trypan blue solution (0,4 %)	Sigma-Aldrich, St Louis (USA)
Trypsin/ EDTA 10x (0,05 %/ 0,02 %)	Invitrogen Life Technologies, Karlsruhe (DE)

Turbofect™ in vitro Transfection Reagent	Fermentas GmbH, St. Leon-Rot, (DE)
Tween 20	Applichem, Darmstadt (DE)
Yeast extract	Applichem, Darmstadt (DE)
X-vivo 15 cell culture medium	Lonza, Verviers (B)

2.1.2 Kits

Name	**Manufacturer**
Amaxa Human T Cell Nucleofector® Kit	Lonza Cologne AG, Köln (DE)
BCA protein assay kit	Thermo Scientific, Rockford (US)
Cytofix/ Cytoperm™	BD Biosciences, Heidelberg (DE)
$CD4^+CD25^+$ Regulatory T Cell Isolation Kit mouse	Miltenyi Biotec GmbH, Bergisch-Gladbach (DE)
FOXP3 Fix/Perm Buffer Set	BioLegend, San Diego (USA)
FOXP3 staining buffer set	eBioscience, San Diego (USA)
Gateway® LR Clonase™ Enzyme Mix	Invitrogen Life Technologies, Karlsruhe (DE)
GeneJet Plasmid Miniprep kit	Fermentas GmbH, St. Leon-Rot, (DE)
LightCycler 480 Probes Master	Roche Diagnostics, Basel (CH)
Midi Plasmid HiSpeed Prep	Qiagen, Hilden (DE)
PKH-26 Red Fluorescent Cell Linker Kit	Sigma-Aldrich, St Louis (USA)
Prostaglandin E_2 EIA Kit monoclonal	Cayman Chemicals, Ann Arbor (USA)
Prostaglandin E_2 metabolite EIA Kit	Cayman Chemicals, Ann Arbor (USA)
Qia Quick Gel extraction kit	Qiagen, Hilden (DE)
Qia Quick PCR purification kit	Qiagen, Hilden (DE)
5x siRNA annealing buffer	Dharmacon, Lafayette (USA)
Transcriptor First Strand cDNA synthesis kit	Roche Diagnostics, Basel (CH)
Universal Probe Library Set Human	Roche Diagnostics, Basel (CH)

2.1.3 Cytokines

Name	**Manufacturer**
Interleukin 1β, human recombinant (rhIL-1 β)	Immunotools, Friesoythe (DE)
Interleukin 2, human recombinant (rhIL-2)	Chiron, Emeryville (USA)
Interleukin 4, human recombinant (rhIL-4)	Immunotools, Friesoythe (DE)
Interleukin 6, human recombinant (rhIL-6)	Immunotools, Friesoythe (DE)
Interleukin-10, human recombinant (rhIL-10)	Immunotools, Friesoythe (DE)
Interleukin 12, human recombinant (rhIL-12)	Immunotools, Friesoythe (DE)
Interleukin 21, human recombinant (rhIL-21)	Immunotools, Friesoythe (DE)
Transforming growth factor beta, human recombinant (rhTGF-β)	PeproTech EC Ltd., London (UK)

2.1.4 Enzymes

All enzymes were purchased from Fermentas GmbH, St. Leon-Rot, (DE). Enzymes that are a component of a kit are not mentioned here.

Enzyme name	Function
BamHI	Restriction enzyme
NotI	Restriction enzyme
NcoI	Restriction enzyme
XhoI	Restriction enzyme
BclI	Restriction enzyme
Pfu DNA Polymerase	DNA Polymerase
Shrimp alkaline phosphatase (SAP)	Alkaline Phosphatase
T4 DNA Ligase	DNA Ligase

2.1.5 Antibodies

2.1.5.1 Antibodies for flow cytometry

Antigen	Clone	Isotype	Fluorophore	Manufacturer
Anti-human-CD3	SK7	$IgG_1\kappa$	APC-Cy7	BD Biosciences, Heidelberg (DE)
Anti-human-CD3	SK7	$IgG_1\kappa$	FITC	BD Biosciences, Heidelberg (DE)
Anti-human-CD3	UCHT1	$IgG_1\kappa$	Pe	BD Biosciences, Heidelberg (DE)
Anti-human-CD4	SK3	$IgG_1\kappa$	FITC	BD Biosciences, Heidelberg (DE)
Anti-human-CD4	SK3	$IgG_1\kappa$	Pe	BD Biosciences, Heidelberg (DE)
Anti-human-CD4	SK3	$IgG_1\kappa$	Pe-Cy7	BD Biosciences, Heidelberg (DE)
Anti-human-CD4	L200	$IgG_1\kappa$	PerCp-Cy5.5	BD Biosciences, Heidelberg (DE)
Anti-human-CD8	SK1	$IgG_1\kappa$	APC	BD Biosciences, Heidelberg (DE)
Anti-human-CD8	SK1	$IgG_1\kappa$	PerCP	BD Biosciences, Heidelberg (DE)
Anti-human-CD8	SK1	$IgG_1\kappa$	Pe	BD Biosciences, Heidelberg (DE)
Anti-human-CD14	MφP9	$IgG_1\kappa$	FITC	BD Biosciences, Heidelberg (DE)
Anti-human-CD14	HCD14	$IgG_1\kappa$	Pe	BioLegend, San Diego (USA)
Anti-human-CD19	SJ25C1	$IgG_1\kappa$	APC	BD Biosciences, Heidelberg

				(DE)
Anti-human-CD19	SJ25C1	$IgG_1\kappa$	Pe	BD Biosciences, Heidelberg (DE)
Anti-human-CD25	M-A251	$IgG_1\kappa$	APC	BD Biosciences, Heidelberg (DE)
Anti-human-CD25	M-A251	$IgG_1\kappa$	FITC	BioLegend, San Diego (USA)
Anti-human-CD25	M-A251	$IgG_1\kappa$	Pe	BD Biosciences, Heidelberg (DE)
Anti-human-CD25	2A3	$IgG_1\kappa$	Pe-Cy7	BD Biosciences, Heidelberg (DE)
Anti-human-CD45RA	L48	$IgG_1\kappa$	FITC	BD Biosciences, Heidelberg (DE)
Anti-human-CD45RA	HI100	$IgG_{2b}\kappa$	Pe-Cy5	BioLegend, San Diego (USA)
Anti-human-CD45RO	UCHL1	$IgG_{2b}\kappa$	APC	BD Biosciences, Heidelberg (DE)
Anti-human-CD45RO	UCHL1	$IgG_{2b}\kappa$	Pe	BD Biosciences, Heidelberg (DE)
Anti-human-CD56	MY31	$IgG_1\kappa$	Pe	BD Biosciences, Heidelberg (DE)
Anti-human-CD127	hIL-7R-M21	$IgG_1\kappa$	Alexa Fluor 647	BD Biosciences, Heidelberg (DE)
FoxP3	206D	$IgG_1\kappa$	Pe	BioLegend, San Diego (USA)
Isotype Control	MOPC-21	$IgG_1\kappa$	Alexa Fluor 647	BD Biosciences, Heidelberg (DE)
Isotype Control	MOPC-21	$IgG_1\kappa$	Pe	BD Biosciences, Heidelberg (DE)
Isotype Control	MOPC-21	$IgG_1\kappa$	FITC	BD Biosciences, Heidelberg (DE)
Isotype Control	MOPC-21	$IgG_1\kappa$	PerCp-Cy5.5	BioLegend, San Diego (USA)
Anti-mouse IgG		$IgG_1\kappa$	Alexa Fluor 647	Invitrogen Life Technologies, Karlsruhe (DE)

2.1.5.2 Antibodies for Electrophoretic Mobility Shift Assay (EMSA)

Antigen	**Clone**	**Isotype**	**Manufacturer**
Anti-human-FOXP3	259D/C7	$IgG_1\kappa$	BD Biosciences, Heidelberg (DE)
Isotype control	MOPC-21	$IgG_1\kappa$	BD Biosciences, Heidelberg (DE)

2.1.5.3 Antibodies for Western blot analysis

Name	**Species**	**Manufacturer**
Anti-*β*-actin (primary antibody)	mouse	Chemicon, Temecula (US)
Anti-mouse IgG IRDye 680 (secondary antibody)	goat	Licor Biosciences, Bad Homburg (USA)
Anti-mouse IgG, IRDye 800CW	goat	Licor Biosciences, Bad Homburg (USA)

(secondary antibody)		

2.1.5.4 Antibodies for coating of cell culture plates and beads

Name	Clone	Manufacturer
CD3	OKT-3	Janssen-Cilag GmbH, Neuss (DE)
CD28	9.3	A kind gift of Dr. James L. Riley, University of Pennsylvania, Philadelphia (USA)
CD28	28.2	BD Biosciences, Heidelberg (DE)
MHC-I	W6/ 32	Lab-own hybridoma

2.1.6 Inhibitors

Name	Alternate name	Manufacturer
HPGD-Inhibitor	CK47A 5-[[4-(ethoxycarbonyl)phenyl]azo]- 2-hydroxy-benzeneacetic acid	Cayman Chemicals, Ann Arbor (USA)
NF-κB inhibitor BAY11-7082	BAY11-7082 3-[(4-methylphenyl)sulfonyl]-(2E)-propenenitrile	Cayman Chemicals, Ann Arbor (USA)
NF-κB activation inhibitor	6-Amino-4-(4-phenoxyphenylethylamino)quinazoline	Merck, Darmstadt (DE)
JAK3 inhibitor	Janex-1 4-[(6,7-dimethoxy-4-quinazolinyl)amino]-phenol	Cayman Chemicals, Ann Arbor (USA)
PI3K inhibitor	LY294002 2-(4-Morpholinyl)-8-phenyl-4H-1-benzopyran-4-one	Merck, Darmstadt (DE)
STAT5 inhibitor	STAT5 inhibitor N'-((4-Oxo-4H-chromen-3-yl)methylene) nicotinohydrazide	Merck, Darmstadt (DE)
MEK1 inhibitor	PD98059 2'-Amino-3'-methoxyflavone	Merck, Darmstadt (DE)

2.1.7 Oligonucleotides

Primers were purchased from the manufacturer Sigma-Aldrich (Taufkirchen, DE). The selection of primers and probes for qRT-PCR were made with the tool 'Universal Probe

Library Assay Design Center' offered by Roche Diagnostics (https://www.roche-applied-science.com/sis/ rtpcr/upl/index.jsp?id=UP030000; 07. October 2010). For Real-time PCR analysis probes were used from the Universal Probe Library Set Human provided (Roche Diagnostics, Basel, CH). Other oligonucleotides were purchased from Biomers.net GmbH (Ulm, DE).

2.1.7.1 Primer for qRT-PCR

Name	**Sequence**	**Probe**
Human Beta-2 microglobulin (B2M)	forward: 5'-TTC TGG CCT GGA GGC TAT-3' reverse: 5'-TCA GGA AAT TTG ACT TTC CAT TC-3'	(#42)
Murine Beta-actin (β-actin)	forward: 5'-CTA AGG CCA ACC GTG AAA AG-3' reverse: 5'-ACC AGA GGC ATA CAG GGA CA-3'	(#64)
Human cAMP response element-binding protein (CREB)	forward: 5'-CGG TGC CAA CTC CAA TTT AC-3' reverse: 5'-ATT GCT CCT CCC TGG GTA AT-3'	(#86)
Human CREB-Binding protein (CREBBP)	forward: 5'-TGA ACA GCA TGG GCT CAG T-3' reverse: 5'-CAT CAT GTT CGG AGG CTG A-3'	(#12)
Human cAMPCCAAT/enhancer-binding protein alpha (CEBPA)	forward: 5'-GCA AAT CGT GCC TTG TCA T-3' reverse: 5'-CTC ATG GGG GTC TGC TGT AG-3'	(#12)
Human proto-oncogene protein c-fos (FOS)	forward: 5'-AGG TCC GTG CAG AAG TCC T-3' reverse: 5'-CTA CCA CTC ACC CGC AGA CT-3'	(#67)
Human Forkhead box P3 (FOXP3)	forward: 5'-ACC TAC GCC ACG CTC ATC-3' reverse: 5'-TCA TTG AGT GTC CGC TGC T-3'	(#50)
Human GATA binding protein 3 (GATA-3)	forward: 5'- ACT ACG GAA ACT CGG TCA GG- 3' reverse: 5'-GGT AGG GAT CCA TGA AGC AG-3'	(#36)
Human Hydroxyprostaglandin dehydrogenase 15-(NAD)	forward: 5'-GGT TCC ACT GAT AAC AGA AAC CA-3' reverse: 5'-TTT GGT CAA TAA TGC TGG AGT G-3'	(#48)
Murine Hydroxyprostaglandin dehydrogenase 15-(NAD)	forward: 5'-ATC GGA TTC ACA CGC TCA G-3' reverse: 5'-TGG GCA AAT GAC ATT CAG TC-3'	(#46)
Murine Hydroxyprostaglandin dehydrogenase 15-(NAD)	forward: 5'-GCA GGC GTG AAC AAT GAG A-3' reverse: 5'-AAA CCA AGA TAG GTC CCA CTG A-3'	(#48)
Murine hypoxanthine-guanine phosphoribosyltransferase (mHRPT1)	forward: 5'-TGA TAG ATC CAT TCC TAT GAC TGT AGA-3' reverse: 5'-AAG ACA TTC TTT CCA GTT AAA GTT GAG-3'	(#22)
Human Interleukin) (IL-9)	forward: 5'-TGG ACA TCA ACT TCC TCA TCA-3' reverse: 5'-TGC CCA AAC AGA GAC AAC TG-3'	(#4)
Human RAR-related orphan receptor C	forward: 5'-AGA AGG ACA GGG AGC AAG-3' reverse: 5'-CAA GGG ACT ACT TCA ATT TGT G-3'	(#21)

(RORγt)		
Human T-box 21 (T-bet)	forward: 5'-GAC TCC CCC AAC ACA GGA G-3' reverse: 5'-GGG ACT GGA GCA CAA TCA TC-3'	(#72)

2.1.7.2 Primer for Cloning

Name	**Sequence**
HPGD forward (BclI)	5'-TAT GAT CAA CCA TGC ACG TGA ACG GCA AA-3'
HPGD 3'GFP reverse (XhoI)	5'-GCG GGG CTC GAG TTT ACT TGT ACA GCT CGT C-3'
HPGD reverse (NotI)	5'-TGC GCG GCC GCA TTG GGT TTT TGC TTG AAA TGG AGT-3'
HPGD forward (XhoI)	5'-ACT ACT CGA GAC CAT GCA CGT GAA CGG CAA AGT G-3'
HPGD reverse (BamHI)	5'-ATC AGG ATC CTC ATT GGG TTT TTG CTT GAA A-3'

2.1.7.3 Primer for Sequencing

Name	**Sequence**
pDest EF1alpha forward	5'-TTA TGC GAT GGA GTT TCC CC-3'
pDest V5 reverse	5'-ACC GAG GAG AGG GTT AGG GA-3'
T7 promoter forward	5'-TAA TAC GAC TCA CTA TAG GG-3'
Bovine growth hormone (BGH) reverse	5'-TAG AAG GCA CAG TCG AGG-3'
CMV forward	5'-CGC AAA TGG GCG GTA GGC GTG-3'
pIRES reverse	5'-TAT AGA CAA ACG CAC ACC G-3'

2.1.7.4 Oligonucleotides for Electrophoretic mobility shift assay

Name	**Sequence**	**5'-Modification: IRDye**
HPGD forward FOXP3 BS	5' – TTC TAT GGA TAT TAT CAC TAT TTG TTT ACC CAT TTA TCT GTT AG – 3'	DY-681
HPGD reverse FOXP3 BS	5' – CTA ACA GAT AAA TGG GTA AAC AAA TAG TGA TAA TAT CCA TAG AA – 3'	DY-681
HPGD forward mutated FOXP3 BS	5' – TTC TAT GGA TAT TAT CCC GGG GCC GCG GGC CAT TTA TCT GTT AG – 3'	DY-781
HPGD reverse mutated FOXP3 BS	5'- CTA ACA GAT AAA TGG CCC GCG GCC CCG GGA TAA TAT CCA TAG AA – 3'	DY-781
FKH forward	5' – TCA AAA ATA TTG AAG TGT TAT CAC ATA CAC - 3'	DY-781
FKH reverse	5' – GTG TAT GTG ATA ACA CTT CAA TAT TTT TGA – 3'	DY-781

2.1.8 siRNAs

SiRNAs were purchased from Biomers.net GmbH, (Ulm; DE).

Name	Target Gene	Sequence
HPGD sense	HPGD	5'-GCA CAG CAG CCG GUU UAU U-3'
HPGD antisense	HPGD	5'-AAU AAA CCG GCU GCU GUG C-3'
FOXP3 sense	FOXP3	5'-GCA CAU UCC CAG AGU UCC-3'
FOXP3 antisense	FOXP3	5'-AGG AAC UCU GGG AAU GUG C-3'
Control sense	Control siRNA	5'-UUC UCC GAA CGU GUC ACG U-3'
Control antisense	Control siRNA	5'-ACG UGA CAC GUU CGG AGA A-3'

2.1.9 Buffers and solutions

Name	Contents
ACK lysing buffer	0,15 M NH4Cl, 10,0 mM KHCO3, 0,1 mM Na2EDTA, pH=7,2-7,4 adjusted with 1 N HCl, solution was sterile filtered
Bead wash buffer	0.02 %w/v NaN3, 0,1 % w/v BSA in PBS, pH=7,4
EMSA10 x loading dye	65 % (w/v) Sucrose, 10 mM Tris-HCl (pH7.5), 10 mM EDTA
EMSA 10 x binding buffer	100 mM Tris, 500 mM NaCl, 10 mM DTT, pH=7,5
EMSA buffer 2	25 mM DTT, 2,5 % Tween-20
5 x Laemmli loading buffer	0,3 M Tris-HCl pH6,8; 50% glycerol, 25 % β-Mercaptoethanol, 2 % SDS, 0,01 % bromophenol blue
LB-medium	5 g yeast extract, 10 g trypton, 5 g NaCl, ad 1 l H_2O, pH=7,5
Lysis buffer	20 mM Tris-HCl pH=8, 10 % Triton X-100, 100 mM NaCl, 1 mM EDTA, 1 M DTT, a Complete Mini Protease inhibitor tablet
MACS buffer	1 x PBS supplemented with 0,5 % BSA, 2 mM EDTA, pH=7,2 sterile-filtered
Protein lysis buffer	1 % Triton-X 100, 0,1 NaCl, 1 mM EDTA, 1 mM DTT, 20 mM Tris-HCl pH=8
Saponine buffer	PBS supplemented with 0,5 % BSA, 0,01 % sodium azide solution and 200 mg saponine powder
10 % separating gel	2,01 ml H_2O_{dest}, 1,25 ml 1,5 M Tris-HCl (pH8,8), 50 µl 10x SDS, 1,67 ml 30 % polyacrylamide, 16,65 µl 10 % APS, 7 µl TEMED
4 % native polyacrylamide gel (for 20ml)	2.5 ml 40% polyacrylamide (Polyacrylamide-BIS ratio =29:1), 1 ml 1M Tris (pH=7,5), 3,8 ml 1 M Glycine, 80 µl 0.5M EDTA, 13 ml H2O, 100 µl 10 % APS, 15 µl TEMED
SOB-medium	5 g yeast extract, 20 g trypton, 0,6 g NaCl, 0,2 g KCl ad 1 l H_2O, Medium was autoclaved and before use further supplemented with 10 ml of a 1 M $MgCl_2$ solution and

	10 ml of a 1 M $MgSO_4$ solution
SOC-medium	SOB-medium was supplemented with sterile filtrated 1 M glucose solution to yield 20 mM glucose solution
4,5 % stacking gel	1,83 ml H_2O_{dest}, 0,83 ml 1M Tris-HCl (pH6,8), 25 µl 10 x SDS, 0,42 ml 30 % Acrylamide, 17 µl 10 % APS, 3,3 µl TEMED
50 x TAE buffer	242 g Tris, 57,1 ml glacial acetic acid, 100 ml 0,5 M EDTA pH=8, ad 1 l H_2O
1 x TBE buffer	89 mM Tris-base, 89 mM Boric acid, 2 mM EDTA-NA_2, pH=8,3
10 x TGE buffer (1 liter)	30,3 g Tris, 142 g glycine, 37,2 g EDTA, add 1 l H_2O
10 x Tris/ glycine buffer	25 mM Tris, 192 mM glycine, pH=8,3
TfB I solution	30 mM NaAc pH=6, 50 mM $MnCl_2x4H_2O$, 100 mM NaCl, 10 mM $CaCl_2$, 15% glycerol
TfB II solution	10 mM MOPS, 75 mM $CaCl_2$, 10 mM NaCl, 15% glycerol
Western blot transfer buffer (for semi dry blotting)	25 mM Tris, 192 mM glycine
Western blot transfer buffer (for wet blotting)	4,8 mM Tris-Base, 3,9 mM glycine, 20 % methanol

2.1.10 Peripheral blood samples

Human blood samples from healthy donors were obtained in form of buffy coats from the Institute for Experimental Hematology and Transfusion Medicine of the University hospital of Bonn (Germany). Isolation of primary cells was approved by the local Ethics Committee.

2.1.11 Eukaryotic cell lines

Human embryonic kidney cells (HEK293) (DSMZ no: ACC 305) were purchased from the "Deutsche Sammlung von Mikroorganismen und Zellkulturen GmbH" (DSMZ; Braunschweig, Germany).

2.1.12 Bacterial strains and genotype

Chemically competent *E.coli* strains were obtained from Invitrogen Life Technologies, Karlsruhe (DE).

***E.coli* strain**	**Genotype**
DH5α	F^- Φ80*lac*ZΔM15 Δ(*lac*ZYA-*arg*F)U169 *rec*A1 *end*A1 *hsd*R17(r_k-, m_k+) *pho*A *sup*E44 *thi*-1 *gyr*A96 *rel*A1λ^-
TOP10	F^- *mcr*A Δ(*mrr-hsd*RMS-*mcr*BC)

	*φ80lac*ZΔM15Δ*lac*X74*rec*A1*ara*D139Δ(*ara-leu*)7697 *gal*U *gal*K *rps*L *end*A1 *nup*G
Stbl3	F$^-$ *mcr*B *mrr hsd*S20(r_B-, m_B-) *rec*A13 *sup*E44 *ara*-14*gal*K2 *lac*Y1 *pro*A2 *rps*L20(Str^R) *xyl*-5 *–leu mtl*-1

2.1.13 Murine tissue samples

Murine spleens from C57BL/6 and BALB/c mice were a kind gift of Dr. Zeinab Abdullah and Dr. Li-Rung Huang respectively from the team of Professor Percy Knolle, Institutes of Molecular Medicine and Experimental Immunology (IMMEI) Bonn (DE).

2.1.14 Equipment

Name	**Manufacturer**
AutoMACS Pro Separator	Miltenyi Biotech, Bergisch-Gladbach (DE)
Centrifuge Rotina 420R	Hettich, Tuttlingen (DE)
Centrifuge Mikro-200R	Hettich, Tuttlingen (DE)
Centrifuge Avanti™ J-20 XP	Beckman Coulter, Brea (USA)
Centrifuge 5810R	Eppendorf GmbH, Hamburg (DE)
Centrifuge 5815R	Eppendorf GmbH, Hamburg (DE)
CO_2 Incubator	Heraeus Christ Instruments, Düsseldorf (DE)
Confocal Laser Scanning Biological FC1000	Olympus, Hamburg (DE)
Dynal magnet MPC-S	Dynal Biotech, Oslo (NO)
Flow cytometer FACS CANTO™	BD Biosciences, Heidelberg (DE)
Flow cytometer FACS LSR II Special Order System	BD Biosciences, Heidelberg (DE)
Flow cytometer / cell sorter FACS Aria	BD Biosciences, Heidelberg (DE)
Gene pulser XCell™	BioRad Laboratories, München (DE)
Electroporator	Amaxa, Köln (DE)
Heating magnetic stirrer ARE	Velp Scientifica, Usmate (I)
Light microscope Eclipse TS100	Nikon, Tokio (J)
Magnet MACS Multi Stand	Miltenyi Biotech, Bergisch-Gladbach (DE)
Mini-& MidiMACS™ Separation Units	Miltenyi Biotech, Bergisch-Gladbach (DE)
Microplate reader Infinite® M200	Tecan Austria GmbH, Grödig (AT)
Mini-Protean Electrophoresis System	Bio-Rad Laboratories, München (DE)
Multi-Detection Microplate Reader Synergy HT Sirius	BioTek Instruments, Bad Friedrichshall (DE)
Neubauer chamber	Roth, Karlsruhe (DE)
Odyssey® Infrared Imaging System	LI-COR Biosciences, Bad Homburg (DE)
pH-meter S20-SevenEasy™	Mettler Toledo, Giessen (DE)
Pipette Controller Accu Jet Plus	Brand GmbH, Wertheim (DE)
Pipette Multipette Plus	Eppendorf GmbH, Hamburg (DE)
Pipette Set Ergo One	Starlab, Ahrensburg (DE)
PowerPac HC Power Supply	Bio-Rad Laboratories, München (DE)
Real-time PCR system LightCycler 480	Roche Diagnostics, Basel (CH)

Roller Mixer SRT9D Stuart	Bibby Scientific, Staffordshire (UK)
Scale EL2001	Mettler Toledo, Giessen (DE)
Analysis Scale MS104S	Mettler Toledo, Giessen (DE)
Spectrophotometer NanoDrop 2000	Thermo Scientific, Waltham (USA)
Steril work bench	BDK, Sonnbuhl (DE)
Thermocycler T3000	Biometra GmbH, Göttingen (DE)
Thermomixer comfort	Eppendorf GmbH, Hamburg (DE)
Trans-Blot Semi-Dry Transfer Cell	Bio-Rad Laboratories, München (DE)
Vortexer	Velp Scientifica, Usmate (I)
Water bath	Memmert, Schwabach (DE)

2.1.15 Disposables

Name	**Manufacturer**
6-well tissue culture plates	Sarstedt, Nürnbrecht (DE)
12-well tissue culture plates	Sarstedt, Nürnbrecht (DE)
24-well tissue culture plates	Sarstedt, Nürnbrecht (DE)
48-well tissue culture plates	Sarstedt, Nürnbrecht (DE)
96-well tissue culture plates	Sarstedt, Nürnbrecht (DE)
10 cm plates	Sarstedt, Nürnbrecht (DE)
LightCycler 480 Multiwell Plate and sealing foil	Roche Diagnostics, Basel (CH)
0,5-2,0 ml reaction tubes	Eppendorf GmbH, Hamburg (DE)
0,2 ml PCR reaction tubes	Eppendorf GmbH, Hamburg (DE)
15 ml Falcon tubes	Sarstedt, Nürnbrecht (DE)
50 ml Falcon tubes	Sarstedt, Nürnbrecht (DE)
MACS LS columns (with plunger)	Miltenyi Biotech, Bergisch Gladbach (DE)
MACS LD columns (with plunger)	Miltenyi Biotech, Bergisch Gladbach (DE)
MACS MS columns (with plunger)	Miltenyi Biotech, Bergisch Gladbach (DE)
Nitrocellulose-membrane Hybond-C Extra	GE healthcare, Piscataway (US)
Parafilm	Pechiney, Chicago (US)
2, 5, 10 & 25 ml Pipettes	Sarstedt, Nürnbrecht (DE)
10, 200 & 1.000 µl Pipette tips	Sarstedt, Nürnbrecht (DE)
Pre-Separation Filters	Miltenyi Biotech, Bergisch Gladbach (DE)
10, 20, 100, 200 & 1.000 µl Filter Tips	Starlab, Ahrensburg (DE)
0,2 µm Sterile filter	Sartorius, Hannover (DE)
50 ml Syringe	Braun, Melsungen (DE)

2.1.16 Software

Name	**Manufacturer**
CorelDraw X3	Corel Corporation, CA
dChip	Free license, http://www.biostat.harvard.edu/complab/dchip/
FACSDiva™	BD Biosciences, Heidelberg (DE)
FlowJo 7.5 and later	Tree Star, Ashland (USA)
KC4 plate reader software	Biotek, Winooski (USA)
LightCycler 480 software	Roche Diagnostics, Basel (CH)
Mayday 2.0	Free license, http://www.zbit.uni-tuebingen.de/pas/mayday
Microsoft Office 2007	Microsoft Corporation, Redmond (USA)
Odyssey V3.0 software	Licor Biosciences, Bad Homburg (DE)

Statistical software package R (version 2.9.2)	Free license, http://www.r-project.org
Sigma Plot 10.0	Systat Software GmbH (DE)
Vector NTI	Invitrogen Life Technologies, Karlsruhe (DE)

2.2 Methods

Standard methods of the molecular biology were performed according to the guidelines and protocols of Current Protocols in Molecular Biology (Volume 3, 2000) if not otherwise stated.

2.2.1 Prokaryotic cell culture

2.2.1.1 Culture conditions and storage of E.coli

Bacteria colonies were grown on LB-agar plates (see 2.1.9) containing the appropriate antibiotic (e.g. 100 µg/ml ampicillin or 50 µg/ml kanamycin) overnight at 37°C in an incubator. For long-term storage of transformed bacteria, a single colony was grown in 4 ml overnight culture with the appropriate selectable antibiotic and frozen in liquid nitrogen in 1 ml LB-medium, supplemented with 0,5 ml 80 % sterile glycerol.

2.2.1.2 Generation of chemically competent E.coli

E.coli were made competent by means of the calcium chloride method. Therefore, 50 ml LB-Medium were inoculated with 500 µl of an overnight culture and grown to a cell density of OD_{550nm}=0,5-0,8. Bacteria were resuspended in 20 ml of sterile TfB I solution (see 2.1.9), incubated for 10 min on ice, centrifuged and resuspended in 10 ml of TfB II solution (see 2.1.9) and finally frozen as 100 µl aliquots in liquid nitrogen and stored at -80°C.

2.2.1.3 Transformation of E.coli

Chemically competent *E.coli* (strains TOP10, DH5α or Stbl 3) were transformed using the heat shock method. Therefore, bacteria were thawn on ice, mixed with 1 to 5 µl (10 pg to 100 ng) of vector DNA, incubated on ice for 30 min, subsequently heat-shocked at 42°C in a water bath for 90 sec (30 sec for TOP10) and incubated for another 2 min on ice. Afterwards bacteria were incubated for 60 min in 400 µl (250 µl for TOP10) pre-warmed SOC-medium

(see 2.1.9) at 37°C with shaking them at 300 rpm and then seeded agar plates containing the appropriate antibiotic.

2.2.1.4 Plasmid-DNA extraction

'Mini'-plasmid extractions were performed by means of the isolation kit of the GeneJET^{TM} Plasmid Miniprep Kit (Fermentas GmbH) according to the manufacturers' instructions. 'Midi'-plasmid extractions were performed using the Qiagen HiSpeed Plasmid Midi Kit (Qiagen GmbH) according to the manufacturers' instructions. 'Maxi'-plasmid extractions were performed using the isolation kit Qiagen Maxi Plasmid Prep Kit (Qiagen GmbH) according to the manufacturers' recommendations. The concentration of the isolated plasmids was measured with a spectrophotometer NanoDrop 2000.

2.2.1.5 General cloning procedure

For the present study different hydroxyprostaglandin dehydrogenase 15-NAD expression vectors were generated. The vector maps of plasmids used during the present study are listed in Appendix A.

2.2.1.5.1 Preparative polymerase chain reaction (PCR)

The HPGD gene was amplified in a polymerase chain reaction (PCR) with the reaction mix:

Table 1: Preparative PCR reaction mix

Reagent (stock concentration)	Amount
Template (cDNA)	0,25 µl (ca. 50pg – 500 ng)
dNTPS (2 mM)	3,75 µl
Primer forward (20 µM)	0,75 µl
Primer reverse (20 µM)	0,75 µl
10x PCR buffer (with $MgSO_4$)	2,5 µl
Pfu DNA Polymerase (2,5 u/µl)	0,25 µl
H_2O ultrapure	Ad 25µl

The PCR reaction was performed according to the following program:

Table 2: PCR reaction program

Incubation step	Temperature	Duration	Cycles
Initial denaturation	95°C	3 min	1 x
Denaturation	95°C	45 sec	35 x
Annealing	56-66°C, depending on the primer pair sequence	30 sec	
Elongation	72°C	1-2 min	
Cooling	72°C	10 min	1 x

The PCR products were loaded onto a 1,5 % agarose gel containing ethidium bromide (0,5 µg/ml), separated at constant 100 V for 1 h, the respective bands (at 800 bp) were excised and the PCR product was eluted with the Qiaquick gel extraction kit (Qiagen) according to the manufacturers' instructions.

2.2.1.5.2 Preparative restriction digest

A double digest was performed with the purified PCR product and the circular vector for 1 hour at 37°C with the respective restriction enzymes according to the manufacturers' instructions. The vector DNA was additionally dephosphorylized with shrimp alkaline phosphatase (SAP) to prevent re-ligation. Table 3 gives an overview of the restriction enzymes used for each plasmid and corresponding insert. The digested DNA fragments were purified with the PCR Purification Kit (Fermentas) according to the manufacturers' instructions and redissolved in a volume of 30 µl.

Table 3: Survey of restriction enzymes used for the different plasmids and inserts

Plasmid	Insert	Restriction enzymes for plasmid	Restriction enzymes for insert
pENTR4 GFP 3'	HPGD	BamHI & NotI	BclI & NotI
pcDNA6/V5-His B	HPGD	BamHI & NotI	BclI & NotI
pcDNA6/V5-His B	HPGD-GFP	BamHI & XhoI	BclI & XhoI
pIRES2-AcGFP1	HPGD	BamHI & XhoI	BamHI & XhoI

2.2.1.5.3 DNA ligation

Following the preparative digest and purification the digested DNA insert and the digested dephosphorylated plasmid were ligated at 22°C with T4 Ligase for 1 h. The reaction mix consisted of 2 µl vector DNA (~50 ng), 10 µl insert DNA (~500 ng), 2 µl 10x ligation buffer and 0,4 µl T4 ligase.

2.2.1.5.4 Transformation in *E.coli* and plasmid extraction

After ligation of insert and vector, 10 µl of the ligation approach were used for transformation in *E.coli* (strains TOP10 or DH5α) as described in 2.2.1.3 and plasmid extraction was prepared as described in 2.2.1.4.

2.2.1.5.5 Control digest and DNA sequencing

Purified plasmids were subjected to a control digest. The restriction enzymes were thereby chosen that specific fragments were created. The digested plasmid-bands were separated on a gel (see 2.2.1.5.1) and compared to a computer-simulated gel run with program Vector NTI (Invitrogen). Constructs that had performed positive restriction digest analysis were sequenced. Therefore 30 µl of plasmid solution (30-100 ng/µl) and 30 µl of forward and reverse primer (10 µM) were sent for sequencing to the company GATC biotech.

2.2.1.5.6 Recombination

pENTR4 constructs were used as entry clone for subsequent recombination reactions. Therefore, the Gateway® LR Clonase™ Enzyme Mix (Invitrogen) was used according to the manufacturers' recommendations. The reaction mix contained 100 ng/µl pENTR4 construct, 150 ng/µl pLenti6/V5-Dest EF1α lentivector, 1 µl 5xLR Clonase reaction buffer, 1 µl Clonase and filled up to 5 µl with TE-buffer (pH 8). The reaction was performed at 25°C for 1 h and terminated by adding of 1 µl proteinase K for 10 min at 37°C. The recombination samples were transformed into the *E.coli* strain Stbl3 (see 2.2.1.3), plasmid was prepared (see 2.2.1.4) and control double digest as well as sequencing were performed with the constructs.

2.2.2 Eukaryotic cell culture

2.2.2.1 Cell Culture

All cells were maintained in an incubator at 37°C in an atmosphere humidified with 5 % CO2. Human embryonic kidney cells (HEK293) were cultured in Dulbecco's Modified Eagle Medium (D-MEM), containing 4500 mg/L glucose and L-glutamine but no sodium pyruvate, supplemented with 10 % fetal calf serum, 5 % glutamax and 5 % penicillin/streptomycin. HEK293T cells were splitted every 2-3 as 1:5 or 1:6. Primary human lymphocytes were cultured in X-vivo 15 medium supplemented with 5 % glutamax. Cells were counted in a Neubauer-Counting chamber and were, therefore, diluted with trypan blue as 1:10 or 1:100, to distinguish dead from living cells. By means of the 4 engraved quadrates in each chamber the cell number per ml was calculated on the basis of the following formula:

Cells/ml=Viable cells x chamber factor (here: 10^4) x dilution factor (e.g. 10 for 1:10 dilution)

For cryoconservation cell lines were harvested when being 80 % confluent and frozen in the adequate cell culture medium supplemented with 10 % DMSO and 20 % FCS in a cell density of 3-10*10^6 cells per ml. Primary cells were frozen in FCS supplemented with 10 % DMSO. Frozen cells were thawn at 37°C in a water bath, washed with 20 ml normal cell culture and then used for normal cell culture.

2.2.2.2 Transfection of eukaryotic cells via Turbofect™ Reagent

HEK293 cells were transfected by using the Turbofect™ *in vitro* Transfection Reagent (Fermentas). The cells were seeded 24 h prior to transfection to yield 70 % confluency and were transfected according to the manufacturers' instructions. After 8 h the transfection was stopped by substitution of the culture medium. Transgene expression was analyzed 24-48 h later and transfection efficiency was assessed by flow cytometry.

2.2.2.3 Isolation of human Peripheral blood mononuclear cells

Peripheral blood mononuclear cells (PBMC) were isolated by density-gradient centrifugation. Therefore, human peripheral blood obtained from buffy coats was diluted 1:3 with 1xPBS and overlaid on Pancoll. The centrifugation was performed at 900 x g for 30 min at 20°C without

break. After centrifugation the interphase containing the PBMC was carefully extracted and cells were washed with 1xPBS and counted before further processing.

2.2.2.4 Isolation of human CD4$^+$ T cells

$CD4^+$ T cells were isolated by combining human RosetteSep $CD4^+$ enrichment cocktail and Pancoll density-gradient centrifugation. Human peripheral blood obtained from buffy coats was mixed with RosetteSep $CD4^+$ T Cell enrichment cocktail (45 µl/ml blood) and was incubated for 20 min at RT with mixing every 5 min. Following the incubation the blood was diluted 1:3 with 1xPBS, overlaid on Pancoll and centrifuged at 900 x g for 30 min at 20°C without break. After centrifugation the $CD4^+$ T cells containing interphase was carefully removed, cells were washed with 1xPBS and counted before further processing. The purity was checked by flow cytometric analysis and cells with 90 % purity were regularly obtained.

2.2.2.5 Isolation of human CD4$^+$ T cell populations

$CD4^+$ T cells were obtained as described in 2.2.2.4 Further separation into subpopulations was achieved by positive selection with magnetic activated cell sorting (MACS) using CD25 and CD45RA microbeads (Miltenyi Biotec, Bergisch Gladbach, DE). The cells were labeled with antibody-coupled microbeads (10 µl microbeads, 90 µl PBS per 10^7 cells) and separated on LS, MS or LD MACS columns in a magnetic field according to the manufacturers' instructions (Miltenyi Biotec, Bergisch Gladbach (DE)). The following subpopulations were purified: regulatory $CD4^+CD25^+$ T cells, conventional $CD4^+CD25^-$ T cells, naïve $CD4^+CD25^-CD45RA^+$ T cells and memory $CD4^+CD25^-CD45RA^-$T cells. After purification cells were washed with PBS, counted and checked for purity by flow cytometry. Purities of 80-90 % were regularly obtained.

2.2.2.6 Differentiation of primary human T cells

Naïve $CD4^+CD25^-CD45RA^+$ T cells (T_{naive}) were isolated as described under 2.2.2.5 and were differentiated into different T helper cell subsets (T_H1/2/9 or 17) or towards an induced T_{reg} cell (iT_{reg}) phenotype by incubation with CD3/CD28/MHC-I-coated beads (3 beads: 1 cell) together with an adequate cytokine mixture for 5 days. As controls untreated T cells (T_{unstim})

or T cells only stimulated with CD3/CD28/MHC-I-coated beads (T_H0) were used. Table 4 shows the different cytokines that were used for differentiation and the respective restimulation on day 3:

Table 4: Cytokines used for T cell differentiation

T cell subset	Cytokine mix after isolation	Restimulation (day 3)
T_H1	10 ng IL-12/ ml 10 U IL-2/ ml	10 ng IL-12/ ml & 10 U IL-2/ ml
T_H2	20 ng IL-4/ ml	20 ng IL-4/ ml
T_H9	20 ng IL-4/ ml 1,0 ng TGF-β/ ml	20 ng IL-4/ ml 1,0 ng TGF-β/ ml
T_H17	25 ng IL-21/ ml 5,0 ng TGF-β/ ml	25 ng IL-21/ ml 5,0 ng TGF-β/ ml
iT_{reg}	10,0 ng TGF-β/ ml 300 U IL-2/ml	10,0 ng TGF-β/ ml 300 U IL-2/ml

On day 5 cells were harvested and differentiation of the cells was controlled by qRT-PCR. Therefore, the upregulation of lineage specific transcription factors was controlled and compared to the expression of β_2 microglobulin (B2M). T_H1 cells were assessed for T-bet expression, T_H2 for GATA-3, T_H9 for Pu.1, T_H17 for RORγt and iT_{reg} cells for FOXP3 expression.

2.2.2.7 Isolation of murine $CD4^+$ T cell populations

Murine $CD4^+CD25^+$ regulatory T cells and conventional $CD4^+CD25^-$ T cells were isolated from murine spleens of C57BL/6 and BALB/c mice, using a protocol modified from a method published by Kruisbeek 2001 [195]. The freshly removed spleens were extruded through a 100 µm mesh to gain a single cell suspension. The cell suspension was further incubated for 5 min in 5 ml/spleen ACK lysing buffer (see 2.1.9) with occasional shaking, to remove remaining red blood cells, and then cells were washed twice with RPMI. Further separation into T_{reg} and T_{conv} cells was achieved by magnetic activated cell sorting (MACS) using the $CD4^+CD25^+$ Regulatory T Cell Isolation Kit mouse (Miltenyi Biotec, Bergisch Gladbach,

DE) according to the manufacturers' instructions. The principle of this kit is a two step procedure which first enriches $CD4^+$ T cells by depletion of unwanted cells and then positively selects $CD25^+$ from the enriched $CD4^+$ T cell fraction. Small aliquots of the purified cell populations were collected and purity was checked in flow cytometry. Purities of higher than 90 % were regularly obtained.

2.2.2.8 Generation of synthetic, artificial antigen-presenting cells (aAPCs)

An optimal activation of T cells requires the interaction of a specific antigen with the T cell receptor (signal 1) and concomitant costimulation (signal 2). These signals were mimicked *in vitro* by means of artificial antigen-presenting cells (aAPC), comprised of tosylactivated magnetic beads (Dynal Biotech, Oslo, Norway), which were coated with the following monoclonal antibodies: anti-CD3 (OKT3), anti-CD28 (9.3), anti-PD-1 (1-17), anti-CTLA4 (ER5.3D6) and anti-MHC-I (W6/32). Thereby, suboptimal levels of anti-CD3 antibody (5 %) and suboptimal levels of anti-CD28 antibody (14 %) were coated on the beads together with either anti-MHC-I antibody (CD3/CD28/MHC-I) or with anti-PD-1 antibody (CD3/CD28/PD-1) or with anti-CTLA4 antibody (CD3/CD28/CDTLA4), which constituted the remaining 81 % of coated protein. This should guarantee that the bead is not completely coated with anti-CD3 and anti-CD28 to achieve a more physiological T cell activation. Magnetic beads were mixed with the designated antibodies (150 µg antibodies per ml beads), diluted in 0.1 M boric acid and incubated at 4°C overnight under constant rotation. Afterwards beads were washed four times with bead wash buffer (see 2.1.9) for 10 min at 30°C and one time at 4°C overnight. The beads were then counted and stored in fresh bead wash buffer at 4°C. Before application in cell culture, aAPCs were washed three times with the appropriate culture medium to remove the sodium azide. The method was previously described by Chemnitz et al. [196].

2.2.2.9 Flow cytometry

Flow cytometry is a method to gain information about individual particles (e.g. cells) concerning size and granularity as well as qualitative and quantitative analysis of the expression of different surface markers. For routine surface staining, $2x10^5$ – $5x10^5$ T cells were stained in a volume of 100 µl PBS with 0.5 – 5 µl of each labeled antibody for 20 min at 4°C. Cells were washed with PBS and measured immediately on a flow cytometer FACS LSR

II (Becton Dickinson, USA) or were stored until measurement at 4°C in the dark to minimize cell modifications or dye degradation. For overnight storage, cells were resuspended in 1 x CellFix™. The antibodies with their respective conjugation that were used can be found in 2.1.5.1. Cell viability was determined by staining cells with 1 µl propidium iodide (PI) (2 mg/ml) immediately before analysis. PI is a fluorescent molecule that enters only dead or dying cells. Data were analyzed with the FlowJo Software.

2.2.2.10 Protocols for intracellular staining in flow cytometric analysis

2.2.2.10.1 Intracellular FOXP3 staining

Intracellular staining of FOXP3 in T lymphocytes was performed with the FOXP3 staining buffer set (eBioscience, USA) according to the manufacturers' instructions. Typically $1x10^6$ cells were stained. Blocking was performed with after permeabilization with 2 % (2 µl) normal mouse or rat serum and cells were stained with 15 µl FOXP3 antibody or with the respective isotype control.

2.2.2.10.2 Intracellular HPGD staining

Intracellular staining of HPGD was performed either with the eBioscience FOXP3 staining kit described above, using HPGD antibody instead of FOXP3 antibody. In addition, intracellular HPGD staining was performed with the Cytofix/Cytoperm™ kit (BD, USA) according to the manufacturers' instructions or with an approach based on a formaldehyde buffer for fixation and a saponine-based buffer for permeabilization modified from a method published by Assenmacher et al. 1994 [197].

For staining with the Cytofix/Cytoperm™ kit typically $5x10^5$ cells were stained. Blocking was performed before and after permeabilization for 10 min at 4°C with irrelevant Ig (sandoglobulin 20 µg/ml) and cells were stained after permeabilization for 30 min at 4°C with either the unconjugated or the directly labeled HPGD antibody. Different HPGD antibody concentrations were used, with an initial stock solution of 0,25 mg/ml. The staining with the Alexa Fluor 647-labeled secondary antibody was performed for 30 min at 4°C, cells were washed with 1 x Perm/ Wash buffer and then subjected to flow cytometry within the next 30 min.

For intracellular staining with the formaldehyde- and saponine-based buffers, $1x10^6$ cells were washed with PBS, stained for 30 min at 4°C with the desired surface marker, washed with PBS and fixated at RT with 400 µl 4 % formaldehyde in PBS. After 20 min of fixation cells were washed with PBS and incubated for 10 min at RT with 400 µl 0,1 M glycine solution. Following that cells were washed with PBS, incubated 10 min at RT with 400 µl of 0,5 %BSA/0,01 % sodium azide in PBS and then permeabilized for 30 min at RT in 100 µl saponine buffer (see 2.1.9), supplemented with additional 10 µl blocking serum (mouse or rat serum). Afterwards cells were stained for 20 min with HPGD antibody (unconjugated or labeled with Alexa Fluor 647) at RT. Then cells were washed with saponine buffer, incubated for 20 min at RT with the secondary antibody, washed again with saponine buffer and 0,5 %BSA/0,01 % sodium azide in PBS and were finally measured in flow cytometric analysis within the next 30 min.

2.2.2.11 Suppression assay

A suppression assay was performed in order to investigate the suppressive function of T_{reg} cells. Therefore, CFSE-labeled T_{conv} cells (see 2.2.2.11.1) were activated with CD3/CD28/MHC-I-coated beads (see 2.2.2.8) in a ratio of 1 cell: 3 beads. PKH-26-labeled T_{reg} cells (see 2.2.2.11.2) were titrated to the T_{conv} in different ratios. After 72-96 h proliferation of the CFSE-labeled T_{conv} cells was measured by flow cytometry.

2.2.2.11.1 CFSE staining of T_{conv} cells

T_{conv} were stained with 5,6-carboxyfluorescein diacetate succinimidyl ester (CFSE), a green fluorescent cytoplasmic dye that covalently binds to intracellular macromolecules. With each cell division the CFSE-labeled macromolecules are equally segregated in such a way that each daughter cell contains half of the CFSE amount of the parent cell. This principle can be used to visualize proliferation and can be analyzed by flow cytometry [198]. For CFSE staining $1x10^7$ cells/ ml were mixed with CFSE until a final concentration of 0,5 mM was reached and incubated for 8 min at RT by shaking it constantly. The reaction was stopped by adding 2 ml heat-inactivated FCS and 25 ml RPMI medium supplemented with 10 % FCS. Cells were washed again with 10 %FCS/RPMI, counted and resuspended in X-vivo 15 as $1x10^6$ cells/ ml for further application.

2.2.2.11.2 PKH-26 staining of T_{reg} cells

T_{reg} cells were stained with PKH-26, provided with the Red Fluorescent Cell Linker Kit (Sigma-Aldrich, USA) according to the manufacturers' protocol. PKH-26 is a red fluorescent cell dye with long aliphatic tails that can be stably incorporated into lipid regions of the cell membrane [199]. After staining, cells were washed with 10 %FCS/RPMI, counted and resuspended in X-vivo 15 as $1x10^6$ cells/ ml for further application.

2.2.2.12 siRNA knockdown

SiRNA-mediated gene silencing was used to downregulate the expression of HPGD or FOXP3 in human T_{reg} cells. Small interfering RNA duplexes (siRNA) are a class of double-stranded RNA molecules with a length of typically 20-25 nucleotides and a base-paired structure characterized by two-nucleotide 3'overhangs. siRNAs are involved in RNA interference (RNAi) a mechanism that causes sequence-specific mRNA degradation of single-stranded target RNAs without changing the transcription rate of the target gene [200,201]. Single-stranded siRNA was dissolved as 1.000 µM solution in sterile RNAse free water for storage at -80°C. For siRNA annealing 30 µl of each 500 µM single stranded siRNA were mixed together with 15 µl annealing buffer and was incubated for 1 min at 90°C, slowly cooled down to RT, heated again for 1 min at 90°C and then incubated of 1 hour at 37°C. The annealed siRNA was stored as 10 µl aliquots in -80°C. The knockdown of HPGD or FOXP3, respectively, was performed in freshly isolated $CD4^+CD25^+$ T_{reg} cells (see 2.2.2.5). Therefore $5\text{-}10x10^6$ cells were mixed with 100 µl of Human T cell Nucleofector Solution and 5 µl of annealed siRNA, and cells were electroporated with an AMAXA electroporator for 5 sec with the Nucleofector program U14. Immediately after nucleofection cells were transferred into fresh, pre-warmed culture medium. After 24-48 h knockdown efficiency was assessed by qRT-PCR or flow cytometric analysis. The FOXP3 knockdown data was generated in part by Anne-Christine Flach, a former diploma student.

2.2.2.13 Inhibitor assays

Chemical inhibition of HPGD and intracellular signaling molecules in $CD4^+CD25^+$ T cells (T_{reg}) was achieved by incubation for 24 h with specific inhibitors that target the respective molecule. All inhibitors were dissolved in DMSO according to the manufacturer's

instructions. For inhibitor experiments, freshly isolated T_{reg} (isolation see 2.2.2.5) were incubated as $1x10^6$ cells/ ml with varying concentrations of the different inhibitors. As a control, T_{reg} cells were incubated with DMSO alone. Notably, for experiments investigating the IL-2R signaling pathways, T_{reg} cells were pre-incubated with the inhibitors for 60 min before additional costimulation with IL-2 was initiated, to avoid activation of the IL-2 signaling pathway before the inhibitor achieves its complete effect. After 24 h of inhibitor treatment the cells were extensively washed with PBS and used for further applications in suppression assays, flow cytometry or qRT-PCR analysis.

2.2.2.14 Immunofluorescence staining

For immunofluorescence experiments 50.000 suspension cells were spun onto glass slides by centrifugation. Adherent cells were seeded into 8-well chamber slides as $3\text{-}4x10^4$ cells/ well, transfected on the next day and subjected to immunofluorescence staining 24 h later. In general cells were fixated for 10 min with 4 % paraformaldehyde at RT, washed with PBS and permeabilized for 10 min in 0,1 % Triton-X 100 at RT. Then glass slides were washed with PBS and unspecific binding sites were blocked for 60 min at RT, either with 3 % BSA in PBS or with 1 % cold fish gelatin and 10 % goat serum in PBS. Afterwards cells were stained in a dark and humidified atmosphere for 1 h at RT with directly-conjugated or unconjugated antibodies against HPGD or FOXP3. After incubation for 1 h the slides were washed extensively with PBS and if the antibodies were unconjugated, the cells were further stained for 1 h at RT with the secondary antibody. All antibodies were diluted in PBS with dilutions varying from 1:100-1:1.000. Finally the glass slides were washed and stained for 10 min at RT with DAPI (4'6-Diamidino-2-phenylindole), diluted 1:3.000 in PBS. DAPI is used to stain the nucleus as it forms fluorescent complexes with natural double-stranded DNA. The slides were extensively washed with PBS and one drop of mounting medium and a cover slip were applied. The mounting medium was supplemented with 50 µg Dabco (1,4-Diazabicyclo[2.2.2]octan) per ml mounting medium before usage, as additional bleaching protection. The glass slides were dried overnight in the dark at RT and analyzed on a confocal laser scanning microscope on the next day.

2.2.3 Molecular biological methods

2.2.3.1 RNA isolation

RNA was isolated with Trizol-Reagent® from Invitrogen Life Technologies according to the manufacturers' instructions. This single-step method is based on an acid guanidinium thiocyanate-phenol-chloroform extraction, described by Chomczynski and Sacchi [202]. The RNA quality and quantity were determined with a spectrophotometer Nano Drop 2000 (Thermo Scientific, Waltham (USA).

2.2.3.2 Quantitative real-time polymerase chain reaction (qRT-PCR)

Gene expression of selected genes was analyzed using quantitative real-time polymerase chain reaction (qRT-PCR). Therefore, 100 ng to 1 µg RNA were reverse transcribed using the 'Transcriptor First Strand cDNA Synthesis' kit (Roche) following the manufacturers' instructions. The qRT-PCR reaction approach consisted of:

- 4 µl template cDNA or water as control
- 5 µl ready-to use reaction mix 'LightCycler 480 Probes Master' containing FastStart *Taq* DNA polymerase, dNTP mix and $MgCl_2$ containing reaction buffer
- 0,1 µl forward primer (20 µM stock solution)
- 0,1 µl reverse primer (20 µM stock solution)
- 0,1 µl appropriate Universal ProbeLibrary probe
- 0,7 µl RNase/ DNase-free water

Each reaction was run in duplicate in 96 well plates on the Real-time PCR system LightCycler 480 with the program recommended by the manufacturer, see table 5.

Table 5: Standard program for qRT-PCRs

Program	Temperature	Acquisition mode	Duration	Ramp Rate	Cycles
Pre-incubation	95°C	None	5 min	4.4 (°C/s)	1 x
Amplification	95°C 60°C 72°C	none single none	10 sec 30 sec 1 sec	4.4 (°C/s) 2.2 (°C/s) 4.4 (°C/s)	45 x
Cooling	20°C	None	30 sec	2.2 (°C/s)	1 x

2.2.3.3 Cell lysates and protein concentration

Cells were harvested, washed with PBS and incubated for 30 min on ice with ice-cold lysis buffer (see 2.1.9) as 20 µl buffer/ $5x10^6$ for T cells and 40 µl buffer/ $1x10^6$ cells for cell lines. Cell debris were removed by centrifugation at 16.000 x g in a table centrifuge at 4°C and protein concentrations were determined, using the BCA protein assay kit (Thermo Scientific) according to the manufacturers' instructions. The absorbance was measured at 562 nm and the protein concentration was calculated by comparing it with the absorbance of a standard curve.

2.2.3.4 Sodium Dodecylsulfate-Polyacrylamid-Gelelektrophoresis of proteins (SDS-PAGE)

The SDS-PAGE is a procedure to separate proteins according to their electrophoretic mobility [203]. 15-50 µg of protein were mixed with laemmli loading buffer (5x) (see 2.1.9), incubated for 5 min at 95°C and then applied onto the electrophoresis gel, consisting of a 4,5 % stacking gel and a 10 % separating gel (see 2.1.9). The gel was run in Laemmli buffer for SDS-PAGE (1x) (see 2.1.1), protein bands were collected for 20 min at constant 100 V and separated for 1-1,5 h at constant 180 V. After the run, the gel was transferred onto a nitrocellulose membrane using a semi-dry blotting or a wet-blotting system.

2.2.3.5 Western Blot

Western blotting was used to transfer protein, previously separated by SDS-PAGE, onto nitro cellulose membranes. For semi-dry blotting the protein transfer was carried out at 20-25 V for 20-40 min. Wet-blotting was conducted at 100 V for 1.5 h. Membranes were blocked 1 h at RT in Licor blocking solution. For immunodetection the blot was incubated overnight at 4°C with the primary antibody, diluted in Licor blocking solution. Afterwards the blot was washed three times for 10 min with PBS + 0,1% Tween-20 (PBST) at RT and incubated for 1 h in the dark at RT with the secondary antibody that was diluted in Licor blocking solution at 1:5.000. The blot was washed three times with PBST, once with PBS and then the membrane was scanned on an Odyssey Imager. The secondary antibody was coupled to one of two different infrared dyes (IRdye), which allow near-infrared (NIR) fluorescence detection. The Odyssey Scanner images the membrane in two IR channels, with simultaneous laser excitation at 680 nm and 780 nm. Emitted light is detected at 720 nm and 820 nm by two avalanche photodiodes and images are generated for each fluorescence channel. The expression of β-

actin was analyzed to guarantee equal loading on the membrane and as a house-keeping protein, β-actin served to determine differences in protein expression. Membranes were stripped with Re-blot mild solution 1:10 diluted in PBS for 10 min at RT, blocked for 30 min at RT with Licor blocking solution and further proteins were detected. Membranes were stored at -20°C wrapped in an air-tight plastic foil.

2.2.3.6 Electrophoretic mobility shift assay (EMSA)

Protein-DNA-interactions were studied by electrophoretic mobility shift assay (EMSA). Synthetic oligonucleotides, labeled with infrared dyes, were diluted to a final concentration of 20 pmol/µl and 5 µl of reverse oligonucleotide and 5 µl forward oligonucleotide were mixed and then annealed by incubation at 100°C for 3 min, followed by slowly cooling it down to RT. Annealed oligonucleotides were diluted 1:200 with H_2O ('oligonucleotide working solution') and stored at -20°C for further application. For the binding reaction the following components were mixed together and incubated for 20 min at RT in the dark:

- 1 µl EMSA 10x binding buffer (see 2.1.9)
- 2 µl EMSA buffer 2 (see 2.1.9)
- 1 µl oligonucleotide working solution
- 5 µg FOXP3 recombinant protein
- Optional: 1 µl of competitor oligonucleotide working solution
- Optional: 1 µl of antibody for supershift reaction (FOXP3 or isotype control)
- Add sterile ddH_2O to 10 µl

Afterwards the samples were mixed with 1 µl EMSA 10x loading dye (see 2.1.9), loaded onto a 4% native separation gel (see 2.1.9) and run at 10 V/ cm for about 40 min in 1xTGE buffer (see 2.1.9).

2.2.3.7 Enzymatic activity assay of HPGD

The enzymatic activity of the NAD^+-dependent 15-hydroxyprostaglandin dehydrogenase was assessed in human T_{reg} and T_{conv} cells, which were stimulated for 24 h with IL-2. The enzymatic activity was determined by means of a radioactive assay that measures the transfer of tritium from 15(S)-[15-^{3}H]PGE_2 to glutamate by coupling HPGD with glutamate

dehydrogenase [178,204,205]. The assay was performed by Professor Andrew J. Dannenberg and Dr. Kotha Subbaramaiah, Department of Medicine and Weill Cornell Cancer Center (Cornell University), 525 East 68th St., Rm.F-206, New York, NY 10065 (USA).

2.2.3.8 Whole-genome gene expression of human T, B and NK cells as well as monocytes

For the present study the gene expression data from former projects was used. The microarray data can be accessed under GSE15390. Data generation and analysis was conducted by Dr. Susanne Schmidt and Dr. Michael Mallmann as well as by the former group members Dr. Sabine Claßen and Dr. Daniela Eggle. Details concerning sample processing, data collection, data assessment and statistical analysis can be obtained from the Ph.D. thesis of Dr. Sabine Claßen and Dr. Daniela Eggle. In brief PBMCs and $CD4^+$ T cell populations were isolated from human peripheral blood as described under 2.2.2.3 to 2.2.2.5. Human $CD19^+$ B lymphocytes, $CD3^+$ T lymphocytes and $CD14^+$ monocytes were isolated from PBMCs by positive selection with magnetic activated cell sorting (MACS), using CD19, CD3 or CD14 microbeads (Miltenyi Biotec, Bergisch Gladbach, DE) and NK cells with the human NK cell isolation kit (Miltenyi Biotec, Bergisch Gladbach, DE) according to the manufacturers' instructions. RNA isolation and quantification were performed as described in 2.2.3.1. The amplification, labeling and hybridization of the samples were performed on Illumina WG6 Sentrix Bead Chips V1 or V3, respectively, according to the manufacturers' instructions (Illumina) using an Illumina Bead Station. The data were analyzed with the Bioconductor for the statistical software R (http://www.r-project.org). Gene expression values were quantile normalized. In brief, differentially expressed genes in human $CD4^+$ T cell populations were identified by a combined t-test/fold change analysis with the following criteria: fold change $\geq$ 2, absolute difference in signal intensity between group means $\geq$ 100 and p-value $\leq$ 0.05. A detailed description can be found in the Ph.D. thesis of Dr. Daniela Eggle.

2.2.4 Statistics

Statistical analysis of the sample data was performed with the free software package R (version 2.12.1, www.r-project.org). Given that sample values belonging to one group are not inevitably distributed normally, sample data were tested beforehand for normal distribution using the Shapiro-Wilk test. Normally distributed sample values were subjected to the

student’s t-test. The Wilcoxon signed-rank test was applied to data showing no normal distribution. If not otherwise mentioned student’s t-test was used for analysis of statistical significance. Differences between sample groups were thereby assumed as statistically significant when the p-value was below 0.05 ($p < 0.05$). Analysis of variance between more than two sample groups was tested with a one-way ANOVA test. No variance between the sample groups was assumed when the p-value was above 0.05 ($p > 0.05$).

3 Results

3.1 Identification of HPGD as differentially expressed in human T_{reg} cells

In order to identify novel target molecules involved in the development and function of human regulatory T cells, global gene expression profiling was carried out. In contrast to previous approaches from other groups [206,207] the present study integrated T_{reg} and T_{conv} cells in the resting state as well as cells under activating or inhibiting conditions. Furthermore, T cells were used from healthy individuals as well as patients suffering from chronic lymphocytic leukemia (CLL). By the use of T_{conv} cells under different conditions, genes could be excluded that were unspecifically upregulated in T_{reg} cells. Thus it was assured to identify only genes being specifically expressed in T_{reg} cells in comparison to T_{conv} cells. Global gene expression profiling of human $CD4^+$ T cells, $CD4^+CD25^-$ T cells (T_{conv}), regulatory $CD4^+CD25^+$ T cells (T_{reg}) and expanded regulatory $CD4^+CD25^+FOXP3^+$ T cells (expanded T_{reg}), isolated from peripheral blood of healthy individuals or cancer patients (CLL) was performed as described in the methods section (see 2.2.3.8). The cells were either left untreated (resting) or incubated with different stimuli (activated). In total 34 different experimental conditions (summarized in Appendix B) with 2 – 4 replicates of each condition were assessed. In Figure 3, a generalized overview of the experimental setup for the gene expression profiling approach is given.

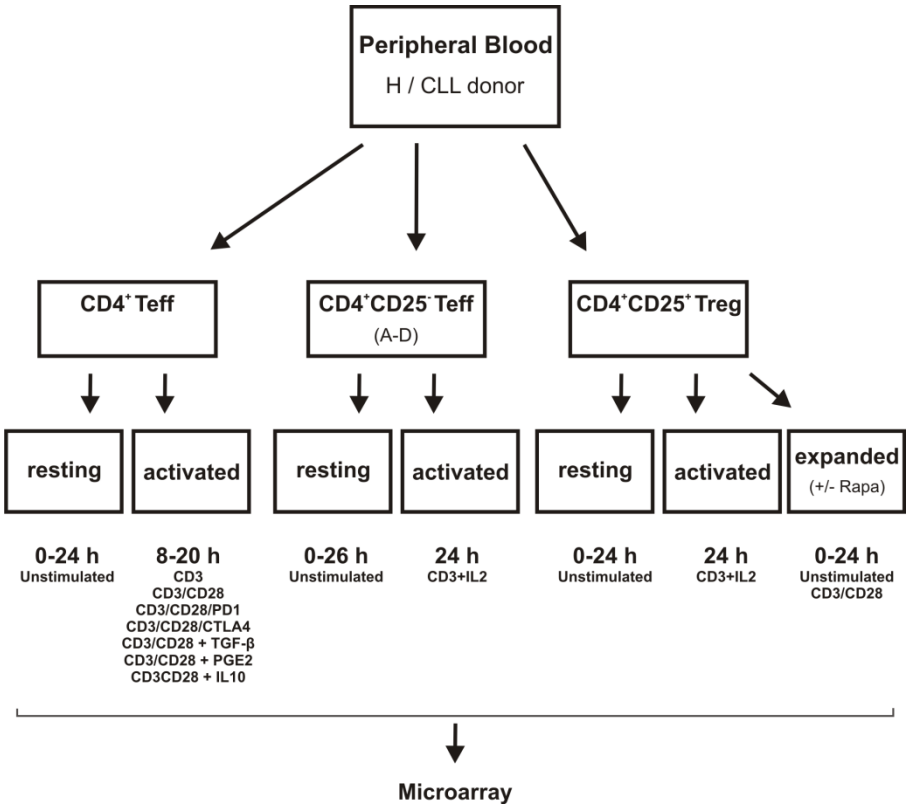

Figure 3: Generalized overview of the experimental setup for the global gene expression profiling.
Human $CD4^+$ T_{eff} cells (T_{eff}), $CD4^+CD25^-$ T_{eff} cells (T_{eff}) and $CD4^+CD25^+$ T_{reg} cells (T_{reg}) were isolated from peripheral blood of healthy (H) donors or cancer patients (CLL) in order to identify genes specifically expressed in T_{reg} cells. $CD4^+CD25^-$ T_{eff} cells (A-D) were either used directly as $CD4^+CD25^-$ T_{eff} cells (D) or were additionally further separated according to their expression of CD25 into $CD4^+CD25^{low}$ T_{eff} cells (A), $CD4^+CD25^{int.}$ T_{eff} cells (B), $CD4^+CD25^{low\text{-}int.}$ T_{eff} cells (C). $CD4^+CD25^+$ T_{reg} cells were either used directly for following stimulation experiments or were additionally expanded with rapamycin (exp-Rapa) or without (exp) before they were used for further treatment. All cells were either rested (unstimulated) for 0-26 h or were stimulated (activated) with different substances for up to 26 h (indicated as 0 h, 8 h, 12 h, 18 h, 19 h, 20 h, 24 h or 26 h). The cells were stimulated with 1 µg/ml anti-CD3 (CD3), 1 µg/ml anti-CD3 in the presence of 20 U IL-2/ml (CD3+IL-2), with beads coated with anti-CD3/MHC-I (CD3), anti-CD3/CD28/MHC-I (CD3/CD28), with beads coated with anti-CD3/CD28/PD1 (CD3/CD28/PD1), with beads coated with anti-CD3/CD28/CTLA4 (CD3/CD28/CTLA4), with beads coated with anti-CD3/CD28/MHC-I in the presence of 30 ng/ml TGF-β (CD3/CD28+TGF-β), with beads coated with anti-CD3/CD28/MHC-I in the presence of 1 µM PGE_2 (CD3/CD28+PGE_2) or with beads coated with anti-CD3/CD28/MHC-I in the presence of 50 ng IL-10/ml (CD3/CD28+IL-10). In total, 34 different experimental conditions were used, which are summarized in Appendix B. Gene expression was assessed using whole genome microarrays

The gene expression values were normalized with the quantile method and differentially expressed genes were identified as described in the Ph.D. thesis of Dr. Daniela Eggle, a former group member. A group of 41 genes could be identified that were significantly differentially expressed in T_{reg} compared to T_{conv} among all experimental conditions. One of the differentially expressed transcripts was the hydroxyprostaglandin dehydrogenase 15-(NAD) (HPGD or 15-PGDH). HPGD plays an important role in the metabolism of prostaglandins and is one of the major prostaglandin E_2 (PGE_2)-metabolizing enzymes [163,167]. In Figure 4, the average gene expression of these 41 differentially expressed genes across 34

experimental conditions (summarized in Appendix B) is visualized. The graphic was generated with pre-analyzed data that was normalized with the quantile method (therefore see also methods 2.2.3.8). Before visualization, the average gene expression was Z score transformed (mean=0, standard deviation=1). HPGD belongs to the group of genes that show a higher expression in T_{reg} cells but a lower expression in T_{conv} during all experimental conditions (Figure 4).

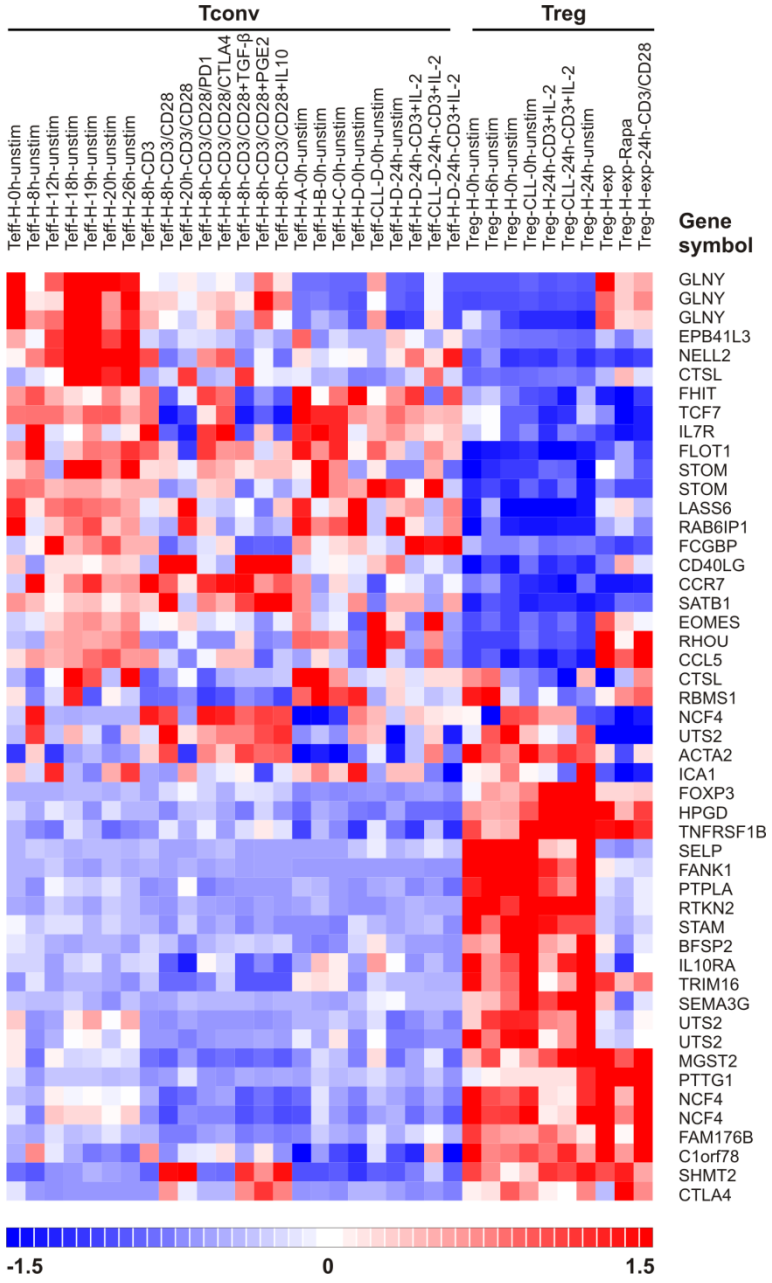

Figure 4: Differentially expressed genes in T_{reg} compared to T_{conv} cells.
Visualization of the average gene expression values of genes that were identified to be differentially expressed in T_{reg} cells compared with T_{conv}. Gene expression was assessed in 34 different experimental conditions (denoted on top of the diagram), which are summarized in Appendix B. The abbreviations for the different cell types and experimental conditions are consistent with Figure 3. The different genes are indicated by their gene symbol on the right side of the graphic. Pre-analyzed data, normalized by the quantile method, was used to create the graphic. The average gene expression values were further processed using Z score transformation. Expression values are color-coded. A high gene expression is depicted in red color, low expression in blue color, respectively. The microarray data can be accessed under GSE15390. The graphic was created with dChip software [208].

In addition to Figure 4, the HPGD expression is shown separately in Figure 5 A in comparison to FOXP3 expression across the 34 different experimental conditions (Figure 5 B). A high HPGD expression was detected in $CD4^+CD25^+$ T_{reg} cells, whereas a low

HPGD expression was observed in $CD4^+CD25^-$ T_{conv} cells. Notably, the expression pattern of HPGD was similar to the expression of FOXP3.

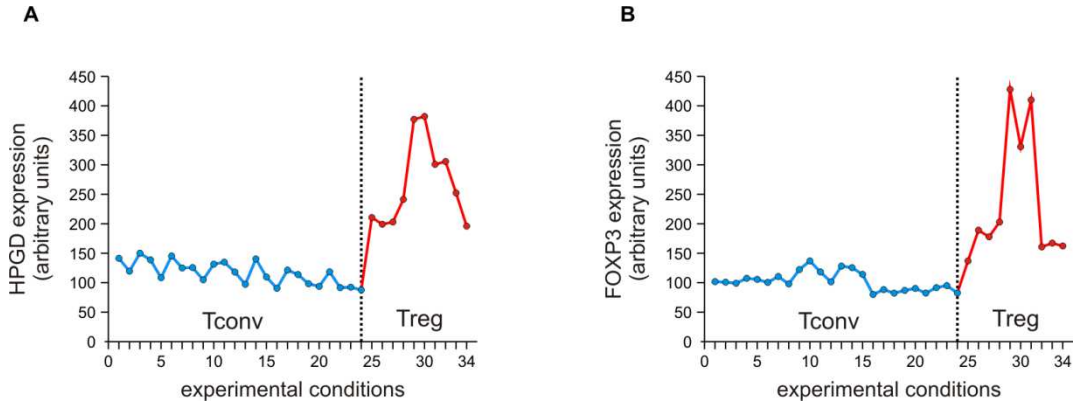

Figure 5: High expression of HPGD and FOXP3 in T_{reg} compared to T_{conv} cells.
The average gene expression of (**A**) HPGD or (**B**) FOXP3 respectively, was obtained by DNA microarray experiments. Human $CD4^+$ T cells, $CD4^+CD25^-$ T cells (T_{conv}), regulatory $CD4^+CD25^+$ T cells (T_{reg}) and expanded regulatory $CD4^+CD25^+$ T cells (expanded T_{reg}) were therefore isolated from human peripheral blood of healthy or cancer patients (CLL) and either left untreated or incubated up to 24 h with different stimuli. 34 different experimental conditions with 2-4 replicates of each condition were analyzed. The 34 conditions are consistent with those described in Figure 3 and are summarized in Appendix B. The graphic was created with pre-analyzed data, which was normalized with the quantile method. The layout was adapted from a graphic originally designed by Prof. Dr. J. L. Schultze.

Remarkably, the high HPGD expression in T_{reg} cells appears to be more T_{reg}-specific than for instance the expression of the molecules CTLA4 or CD127 (shown in Figure 6 A or Figure 6 B), which are commonly used as surface markers to characterize and discriminate T_{reg} cells.

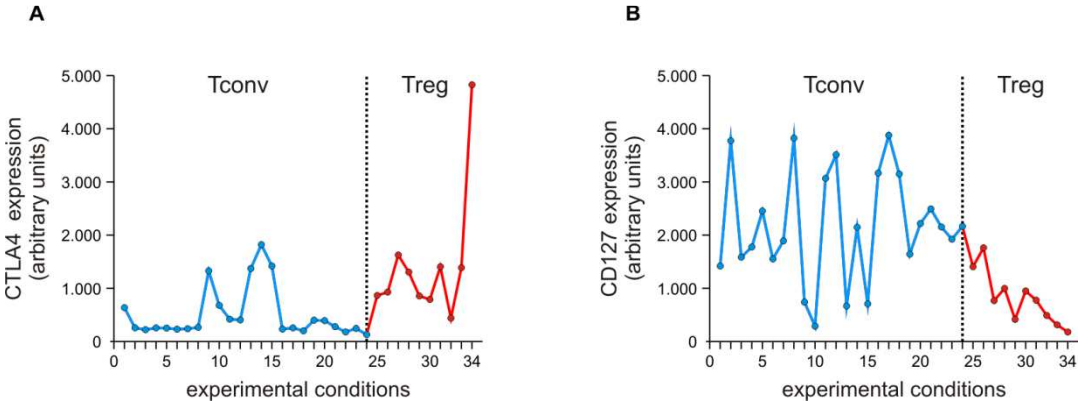

Figure 6: Differential gene expression of CTLA4 and CD127 in T_{reg} compared to T_{conv} cells.
The average gene expression of (**A**) CTLA4 or (**B**) CD127 respectively, was obtained by DNA microarray experiments. Data were analyzed and processed as in Figure 5. The layout was adapted from a graphic originally designed by Prof. Dr. J. L. Schultze.

Next, qRT-PCR of T_{reg} and T_{conv} cells purified from human peripheral blood was performed to assess the relative mRNA expression of HPGD in T_{reg} cells. Consistent with the microarray data, qRT-PCR revealed a significantly higher HPGD mRNA expression in T_{reg} cells compared to T_{conv} cells (Figure 7). HPGD expression in T_{conv} cells was reduced by a factor of eight compared to T_{reg} cells.

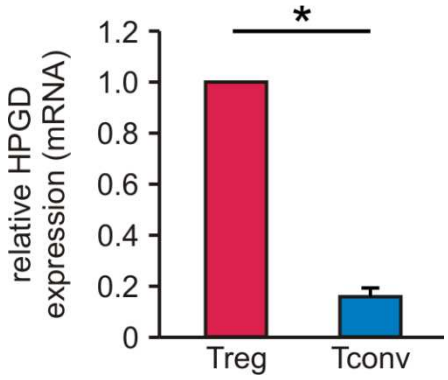

Figure 7: Differential expression of HPGD in human T_{reg} compared to T_{conv} cells.
Human $CD4^+CD25^+$ T_{reg} and $CD4^+CD25^-$ T_{conv} were purified from human peripheral blood and relative HPGD mRNA expression, compared to B2M expression was assessed by qRT-PCR. Samples are normalized to T_{reg} cells. Data represent mean values and standard deviations of ten independent experiments. Statistically significant differences are marked with an asterisk (* $p < 0.001$).

HPGD mRNA expression was furthermore analyzed in resting T_{reg} or T_{conv} cells over a period of 72 h to investigate possible variations in unstimulated cells. Therefore, T_{reg} or T_{conv} cells were purified from human peripheral blood, cultured *in vitro* without additional stimulus for 12 h, 24 h, 48 h and 72 h and HPGD mRNA expression was assessed by qRT-PCR (Figure 8). Although a strong decrease of HPGD mRNA expression was observed already after 12 h in untreated T_{reg} cells, HPGD mRNA expression in T_{reg} was significantly higher for all time points compared to T_{conv} cells. HPGD mRNA expression in T_{conv} cells remained relatively constant over 72 h. These data show that the HPGD expression is specific for T_{reg} cells, as HPGD expression remains constantly higher in T_{reg} compared to T_{conv} cells, although HPGD expression declines in resting T_{reg} cells over time.

Taken together, this indicates that there might be external influences that maintain high levels of HPGD expression in T_{reg} cells in peripheral blood that are not present in *in vitro* culture conditions.

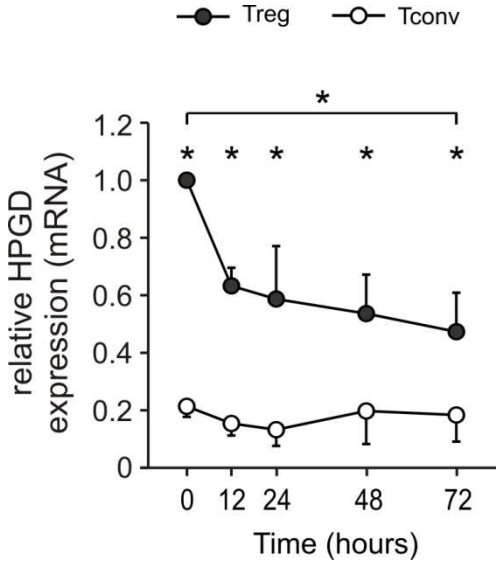

Figure 8: HPGD expression in T_{reg} and T_{conv} cells over time.
Human $CD4^+CD25^+$ T_{reg} and $CD4^+CD25^-$ T_{conv} were purified from human peripheral blood and relative HPGD mRNA expression, compared to B2M expression, was assessed by qRT-PCR at different time points (0 h, 12 h, 24 h, 48 h & 72 h). Samples are normalized to T_{reg} cells (0 h). Mean values and standard deviations of five independent experiments are shown. Statistically significant differences are marked with an asterisk (* $p < 0.05$).

3.2 Generation of an antibody specifically detecting HPGD

HPGD expression in T_{reg} cells should be also assessed on protein level by Western blot analysis, immunofluorescence as well as flow cytometry. However, since no monoclonal antibody (mab) suitable for the above mentioned approaches was commercially available, mabs specific for human HPGD were generated in cooperation with Ravi Hingorani and Robert Balderas, both Becton Dickinson Biosciences. Part of this thesis was the analysis of binding specificity of the HPGD antibodies in flow cytometry, Western blot analysis and immunofluorescence while the generation, purification and labeling of the monoclonal antibodies was carried out by Ravi Hingorani.

In the following paragraphs the transfection of HEK293 cells with HPGD will be described, which served for the subsequent analysis of binding specificity and application spectrum of the HPGD specific antibodies.

3.2.1 Transfection of HEK293 cells with HPGD-GFP for the screening of HPGD antibodies

Antibodies were produced using the classical approach of generating antibody-producing hybridomas after immunization of BALB/c mice with recombinant protein as antigen.
The murine sera and later on the generated hybridoma clones were tested by Ravi Hingorani for production of the desired antibodies and for recognition of HPGD *in vitro* by ELISA and Western blot analysis. For the purpose of ELISA and Western blot analysis, we provided human embryonic kidney (HEK) 293 cells, which were transfected with a pLenti 6.2/V5-Dest

EF1α/HPGD-GFP vector encoding a fusion protein of the hydroxyprostaglandin dehydrogenase 15-(NAD) and 3'-green-fluorescent protein (GFP). Transfections with different vectors, which encode a fusion protein, consisting of HPGD and GFP, are abbreviated with the acronym HPGD-GFP throughout this thesis. Transfections with a GFP encoding vector will be abbreviated with GFP. The expression of recombinant eukaryotic HPGD protein was carried out in mammalian cells to minimize differences in posttranslational modifications and processing between recombinant and wildtype HPGD. Transfection efficiency was determined by flow cytometry (see Figure 9) and only cells with transfection efficiencies of at least 50 % were used for further processing. As a positive control for the transfection, HEK293 cells were transfected with pcDNA6/V5-His B/GFP vector, encoding GFP (see Figure 9).

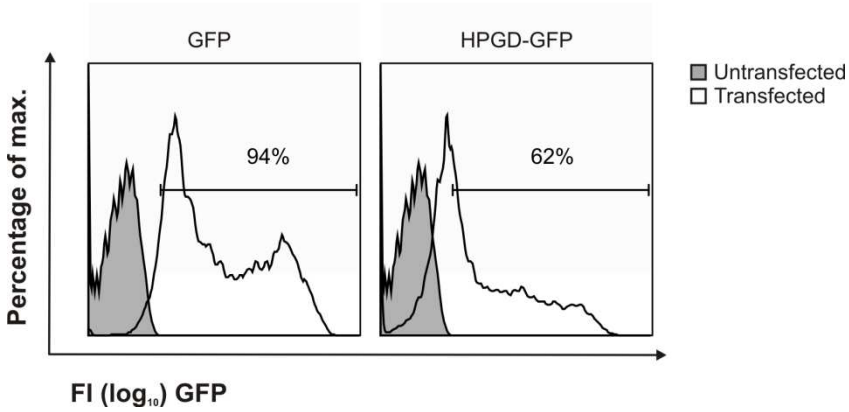

Figure 9: Control of transfection efficiency of HPGD-GFP or GFP transfected HEK293 cells
HEK293 cells were transfected either with pLenti 6.2/V5-Dest EF1α/HPGD-GFP vector encoding a HPGD-GFP fusion protein or with pcDNA6/V5-HisB/GFP vector encoding a GFP protein as positive control for transfection. Transfection efficiency was analyzed by flow cytometry and transfected HEK293 cells (open area) are depicted in a histogram in comparison to untransfected HEK293 cells (grey area). The numbers in the histograms indicate the percentage of transfected cells in the gate. One representative experiment out of three is shown.

In addition to flow cytometric analysis, the protein expression of positive HPGD-GFP-transfected HEK293 cells was assessed by Western blot analysis as a further quality control (Figure 10). The blot was incubated with an anti-GFP-antibody to determine the correct size of the over-expressed HPGD-GFP fusion protein in comparison to GFP-transfected cells. Untransfected cells served as negative control. The estimated band size of the HPGD-GFP fusion protein is 55.8 kDa (Figure 10) and only in HPGD-GFP transfected cells a respective band was detected. In contrast a band at 26.9 kDa was only detected in GFP-transfected HEK293 cells, indicating GFP protein expression.

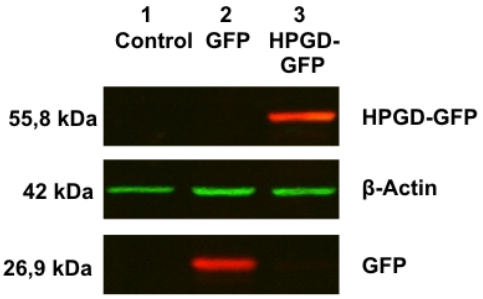

Figure 10: Analysis of HPGD-GFP protein expression in HPGD-GFP-transfected HEK293 cells
HEK293 cells were either left untransfected (Column 1: Control) or were transfected with GFP as control (Column 2: GFP) or with HPGD-GFP (Column 3: HPGD-GFP) respectively. The expression of the respective protein was detected with an anti-GFP antibody (red bands). The estimated band size of the fusion protein HPGD-GFP is 55.8 kDa and the band size of GFP is 26.9 kDa. β-actin (green bands; 42 k Da) was used as loading control. One representative experiment out of three is shown.

HEK293 cells being at least 50 % positively transfected with HPGD-GFP and exhibiting the right band size on Western Blot were sent either as cell pellet or alive for further processing and subsequent testing of polyclonal and monoclonal antibodies to BD. Different hybridoma clones were tested for production of the desired antibodies and for recognition of HPGD *in vitro* by ELISA and Western blot analysis. The pre-screened hyridoma supernatants that showed positive results in both assays were then sent back to us for further tests determining binding specificity.

3.2.2 Initial specificity tests on HPGD antibody containing hybridoma supernatants

Initial quality experiments performed by BD with crude hybridoma supernatants had shown positive results *in vitro* in ELISA tests and Western blot analysis concerning antibody production and specific binding of the antibodies to HPGD antigen. These pre-screened antibody-containing hybridoma supernatants were used for further binding specificity tests in flow cytometry. HEK293 cells were therefore left untreated or transfected with HPGD-GFP. After 24 h the transfected and untransfected cells were used for candidate clone screening via flow cytometric analysis. For this purpose, the cells were fixated and permeabilized and then stained with the respective antibody containing hybridoma supernatants. In total 16 different hybridoma supernatants were tested. In Figure 11, the results of the flow cytometric analysis are shown. The staining quality of each HPGD antibody clone was determined by HPGD- and GFP-signal intensity. HPGD-GFP-transfected HEK293 cells are GFP positive and should therefore ideally show a linear correlation between the HPGD staining, visualized as HPGD signal intensity, and the GFP signal intensity. The supernatants of clone 1, 2 and 3 showed the

best staining performance in intracellular flow cytometric staining and were consequently used for further antibody screening.

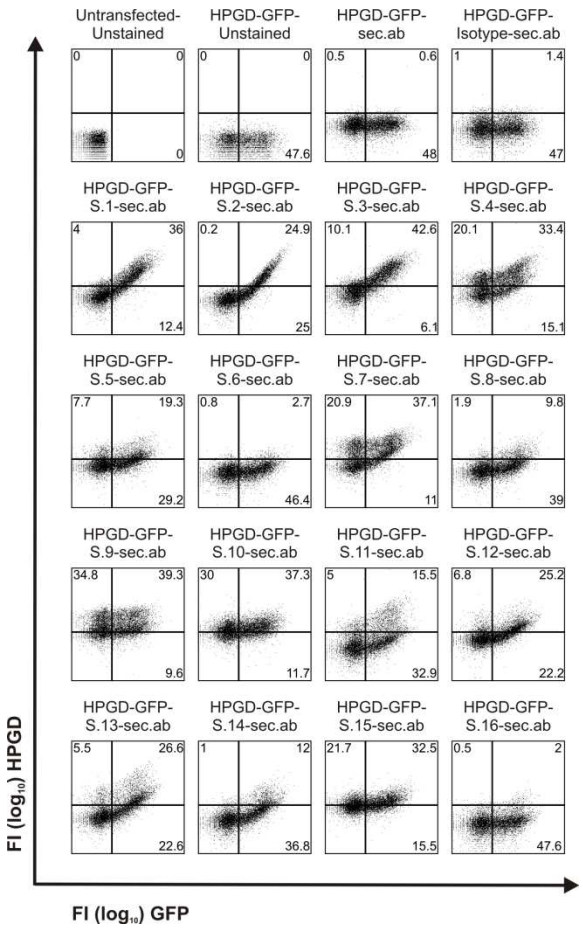

Figure 11: Binding specificity of HPGD antibodies on HPGD-GFP-transfected HEK293 cells
HEK293 cells were left untransfected (Untransfected) or transfected with HPGD-GFP. HEK293 cells were stained with one of the supernatants 1-16 (S.1 - S.16) together with the secondary antibody (sec. ab). As control, cells were left untreated (Unstained), stained with the secondary antibody (sec. ab) alone or in combination with the isotype control (Isotype). The x-axis represents the GFP fluorescence intensity and the y-axis shows the HPGD fluorescence intensity. The numbers in the quadrants represent the percentage of cells. One representative experiment is shown.

3.2.3 Optimization of the staining conditions for flow cytometric analysis

Initial intracellular flow cytometric staining was performed with fixation and permeabilization buffers from the BD Cytofix/Cytoperm^{TM} Fixation/Permeabilization kit. Most of the commercially available kits for intracellular flow cytometric stainings contain similar compounds, such as formaldehyde for fixation and saponine for permeabilization. However, differences in the concentrations of the chemicals can lead to varying staining results. Thus three different staining protocols were tested:

1. Protocol and staining buffers from the initially used BD Cytofix/Cytoperm™ Fixation/Permeabilization Kit
2. Standard staining protocol with saponine and formaldehyde – based buffer (see 2.2.3.7 Intracellular staining for FACS analysis and 2.1.8 Buffers and solutions – Saponine buffer)
3. Protocol and staining buffers from eBioscience FOXP3-Staining Kit.

HEK293 cells were transfected with HPGD-GFP and stained with the three supernatants (S.1, S.2 & S.3) that had performed best under 3.2.2. In Figure 12, it is shown that the initial conditions with the BD Cytofix/Cytoperm™ Fixation/Permeabilization kit performed best in intracellular HPGD staining. The standard protocol based on saponine and formaldehyde, however, showed poor staining results and the FOXP3 staining buffers from eBioscience even led to a loss of the HPGD signal. Therefore, the protocol and buffers from the BD Cytofix/Cytoperm™ Fixation/Permeabilization kit were used for subsequent intracellular flow cytometric stainings with the HPGD antibodies.

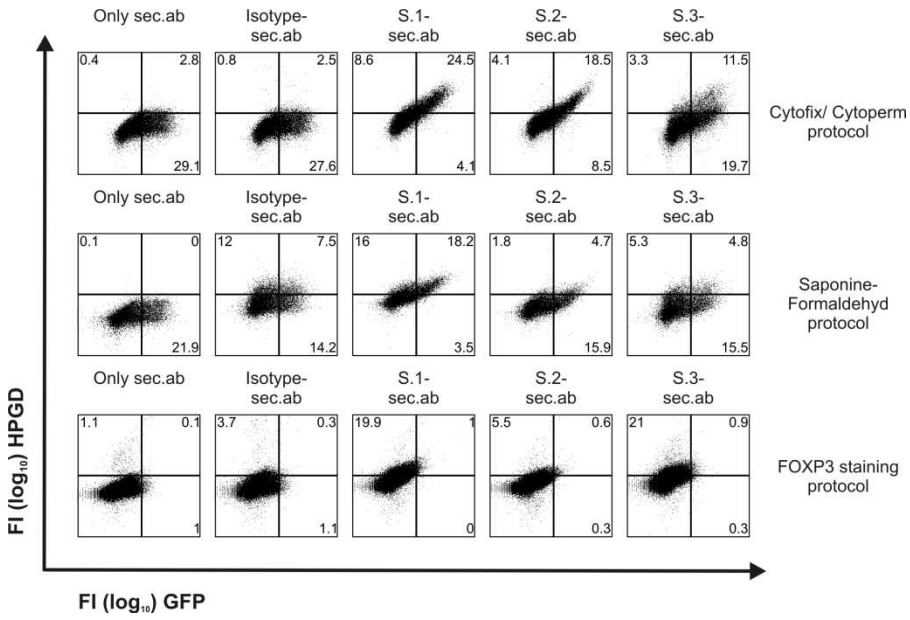

Figure 12: Optimization of staining conditions for intracellular staining with HPGD antibodies
HEK293 cells were transfected with HPGD-GFP and further processed with one of the following staining protocols: Cytofix/Cytoperm protocol, Saponine-Formaldehyd protocol or FOXP3 staining protocol. Cells were stained with one of three supernatants (S.1 - S.3) together with the secondary antibody (sec. ab). As control cells were stained with the secondary antibody (sec.ab) alone or in combination with the isotype control (Isotype). The x-axis represents the GFP fluorescence intensity. The y-axis shows the fluorescence intensity of the HPGD stained cells. The numbers in the quadrants represent the percentage of cells. One representative experiment is shown.

3.2.4 Specific binding of unlabeled HPGD antibodies

As the initial screening mentioned above had identified 3 clones producing HPGD antibodies as being appropriate for flow cytometric applications, these three hybridoma clones were subcloned and the resulting antibodies were purified and concentrated by Ravi Hingorani. Subsequently, these concentrated antibodies (clone 1, 2 and 3) were tested for their binding specificity in flow cytometric applications. For this purpose HEK293 cells were left untreated or were transfected with either HPGD-GFP or with GFP as a control. Afterwards, intracellular staining with one of the three antibodies in different dilutions (1:100, 1:300, 1:500, 1:1.000 & 1:3.000) was performed. In Figure 13, the staining with HPGD antibody clone 1 is shown, in Figure 14 the staining with HPGD antibody clone 2 and in Figure 15, the staining with HPGD antibody clone 3 is shown.

All three HPGD antibody clones showed a linear increase in HPGD signal intensity with increasing GFP signal intensity for HPGD-GFP-transfected cells. For untransfected or GFP-transfected cells, however, this was not observed, indicating good and specific staining of the HPGD antibodies and that the antibodies did not bind to the GFP part of the HPGD-GFP fusion protein. Appropriate staining results were obtained up to a dilution of 1:500 by all three clones and HPGD clone 2 even showed HPGD staining with a dilution of 1:1.000. With a dilution of 1:100, however, a high background staining and only a marginal increase in the HPGD staining were observed, compared to the staining results when a dilution of 1:300 was used. These results indicated an unspecific staining, which might be due to a highly concentrated antibody dilution. In contrast, good and specific HPGD staining results were obtained with a dilution of 1:300 and the background staining decreased to levels of the isotype control staining. Therefore, only dilutions below 1:100 were regarded as appropriate for further flow cytometric stainings.

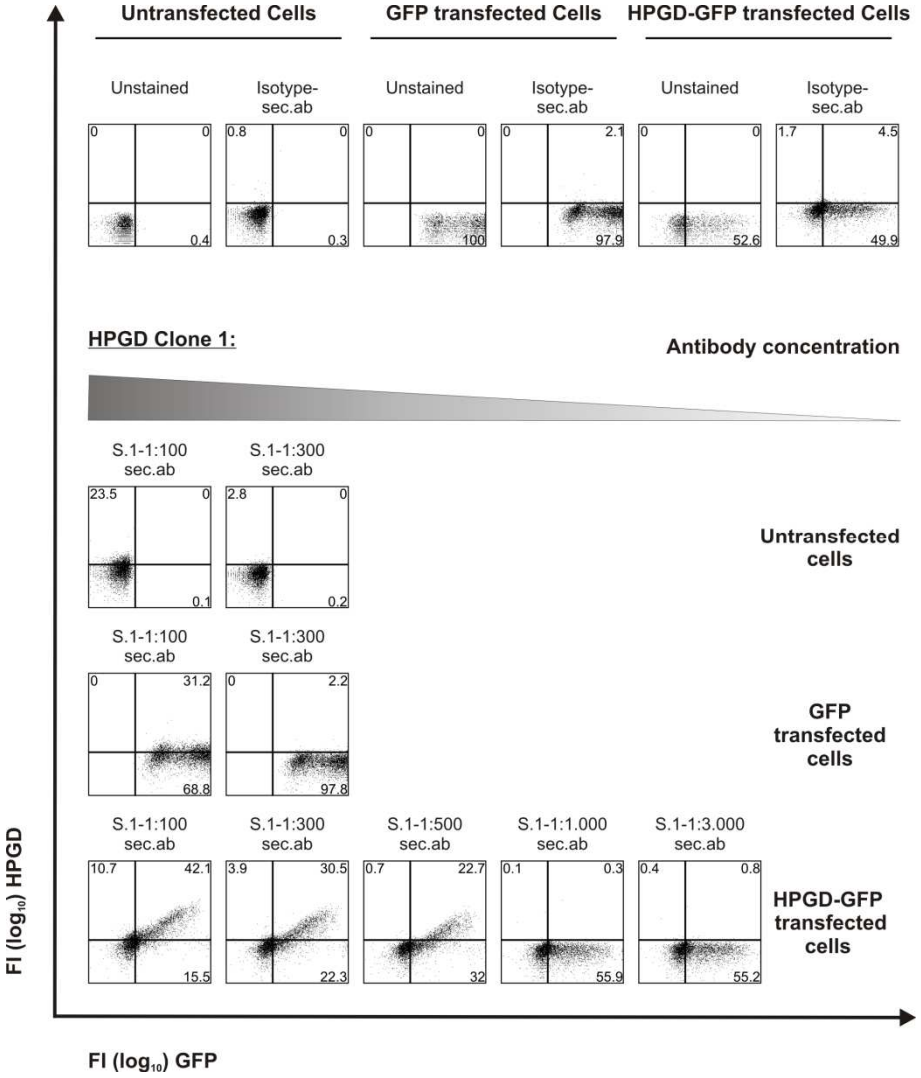

Figure 13: Binding specificity of unconjugated HPGD antibody clone 1 to HEK293 cells.
HEK293 cells were left untransfected (Untransfected cells) or were transfected with GFP (GFP transfected cells) or HPGD-GFP (HPGD-GFP transfected cells). Cells were stained with HPGD antibody clone 1 (S.1) in different dilutions (1:100, 1:300, 1:500, 1:1.000 & 1:3.000) and the secondary antibody (sec. ab). The stock solution was 0,25 mg/ml. As control, cells were left untreated (Unstained) or stained with the isotype control (Isotype) and the secondary antibody (sec.ab). FI (log_{10}) GFP indicates the fluorescence intensity of the GFP signal, FI (log_{10}) HPGD indicates the fluorescence intensity of the HPGD stained cells. The numbers in the quadrants represent the percentage of cells. One representative experiment out of three is shown.

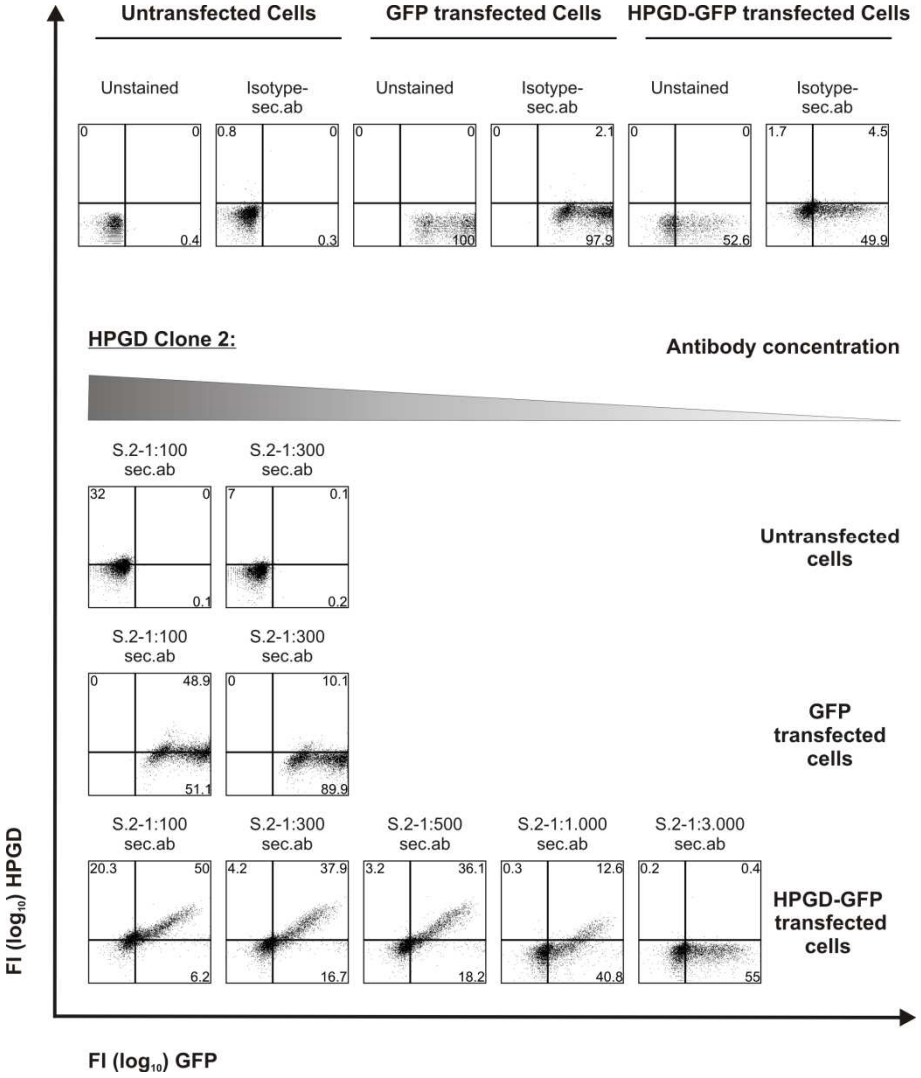

Figure 14: Binding specificity of unconjugated HPGD antibody clone 2 to HEK293 cells.
HEK293 cells were transfected, processed and analyzed as described in Figure 13. HPGD antibody clone 2 (S.2) was used instead of clone 1. The stock solution was 0,25 mg/ml. The axis annotation is consistent with Figure 13. The numbers in the quadrants represent the percentage of cells. One representative experiment out of three is shown.

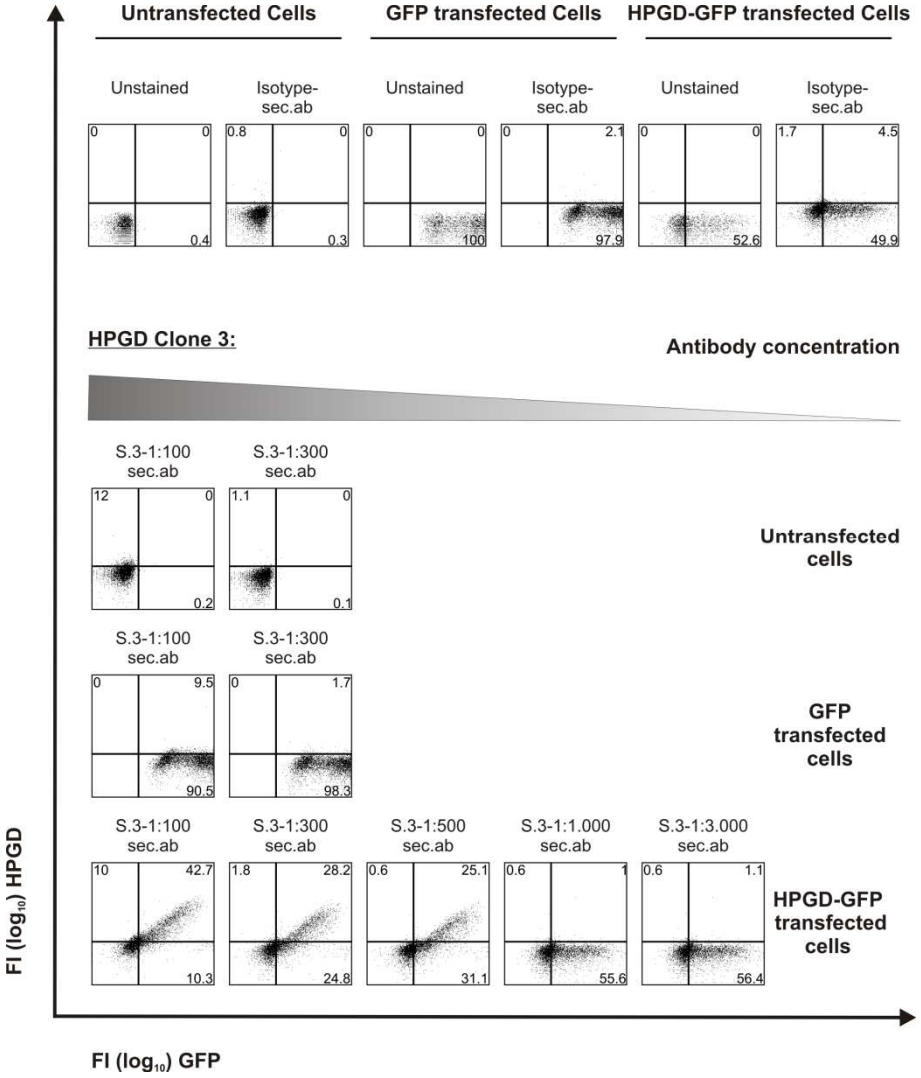

Figure 15: Binding specificity of unconjugated HPGD antibody clone 3 to HEK293 cells.
HEK293 cells were transfected, processed and analyzed as described in Figure 13. HPGD antibody clone 3 (S.3) was used instead of clone 1. The stock solution was 0,25 mg/ml. The axis annotation is consistent with Figure 13. The numbers in the quadrants represent the percentage of cells. One representative experiment out of three is shown.

3.2.5 Endogenous HPGD mRNA expression in HEK293 cells

HPGD expression can be found in various tissues and cell types [141]. Jurkat cells for instance express HPGD mRNA at a level comparable with that seen in placenta [180]. In the previous staining experiments a slight staining of untransfected, GFP- as well as HPGD-GFP-transfected cells was observed when concentrated antibody solutions were used. Although the observed effects could represent background staining that was caused by an over-saturated antibody staining solution, the slight staining could be also due to endogenous HPGD expression in HEK293 cells. To test this hypothesis, the relative expression levels of HPGD in HEK293 cells were examined as a control experiment. HEK293 cells were left untreated (Control) or were transfected with HPGD-GFP or with GFP as a control. In Figure 16, the

relative HPGD mRNA expression, assessed by qRT-PCR in untransfected, GFP- or HPGD-GFP-transfected cells is shown. Untransfected and GFP-transfected cells showed similar levels of endogenous HPGD expression, whereas HPGD-GFP-transfected cells demonstrated a strongly enhanced HPGD expression, that is over 100.000-fold higher compared to untransfected and GFP-transfected cells.

Although these results demonstrate that HEK293 cells show HPGD mRNA expression, the observed background staining of untransfected or GFP-transfected cells in flow cytometry is rather not due to staining of HPGD protein. As HPGD-GFP transfected cells show a much higher HPGD mRNA expression than untransfected of GFP-transfected cells, it is unlikely to observe these differences likewise on protein level. Thus, the observed staining of untransfected or GFP-transfected HEK293 cells in flow cytometry is unspecific and due to an oversaturated antibody solution.

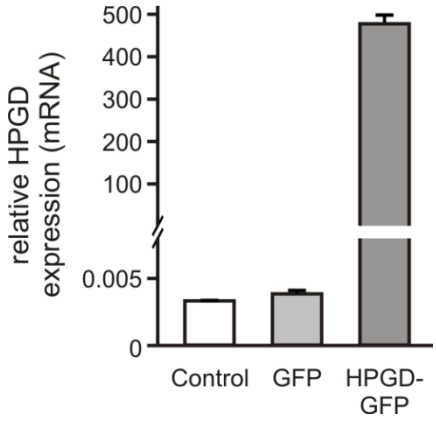

Figure 16: Endogenous HPGD mRNA expression in HEK293 cells
HEK293 cells were left untransfected (Control) or transfected either with GFP (GFP) or with HPGD-GFP- (HPGD-GFP). Relative HPGD mRNA expression was assessed by qRT-PCR 24 h after transfection and is plotted compared to B2M. Mean values and standard deviations of one representative experiment are shown.

3.2.6 Binding specificity of directly-conjugated HPGD antibodies

In addition to the unconjugated HPGD antibodies also HPGD antibodies directly labeled with Alexa Fluor 647 were obtained from Beckton Dickinson Biosciences. These conjugated HPGD antibodies were also used for intracellular flow cytometric stainings to determine their binding specificity. For this purpose HEK293 cells were left untreated or were transfected with pcDNA6/myc-HisB/HPGD-GFP (HPGD-GFP), a further HPGD-GFP encoding vector, which gave better transfection efficiencies due to its smaller size. Furthermore, as control, cells were transfected with GFP or as additional control with the vector pIRES2-AcGFP1/HPGD (HPGD-IRES-GFP), where HPGD is separated by an IRES-site (internal ribosome entry site) from AcGFP1 (a green fluorescent protein from *Aequorea coerulescens*).

This permits the simultaneous expression of the gene of interest (here: HPGD) and the fluorescent reporter gene (here: AcGFP1) from a single bicistronic mRNA. The control served to exclude unspecific binding of the HPGD antibody to an antigen specific for the HPGD-GFP fusion protein. Following transfection after 24 h, cells were stained intracellularly with the conjugated HPGD antibodies clones 1, 2 and 3 in different dilutions (1:1.000, 1:2.000, 1:5.000 and 1:10.000). In Figure 17, the staining for HPGD antibody clone 1 is shown, in Figure 18 the staining for HPGD antibody clone 2 and in Figure 19, the staining for HPGD antibody clone 3 is shown.

Similar to the unconjugated antibodies tested before, the directly-conjugated HPGD antibodies showed specific staining of HPGD-GFP-transfected cells, whereas untransfected or GFP-transfected cells remained unstained. Also HPGD-IRES-GFP transfected cells were specifically stained and the intensity of the HPGD staining increased with the amount of GFP-signal. However, the binding affinity of the three antibody clones strongly differed. With a dilution of 1:1.000 and 1:2.500 the HPGD antibodies clone 1 and clone 2 showed only a marginal staining for highly HPGD-GFP-transfected cells, which displayed a high GFP-signal. In contrast, HPGD antibody clone 3 exhibited good and specific staining of HPGD-GFP- and also HPGD-IRES-GFP-transfected cells, using these dilutions. Staining of HPGD-GFP- and also HPGD-IRES-GFP-transfected cells was even observed with clone 3 for the dilutions of 1:5.000 and 1:10.000, whereas this was not achieved with the other HPGD antibodies clone 1 and clone 2, using these concentrations. For these reasons only HPGD antibody clone 3 was further used for the following experiments.

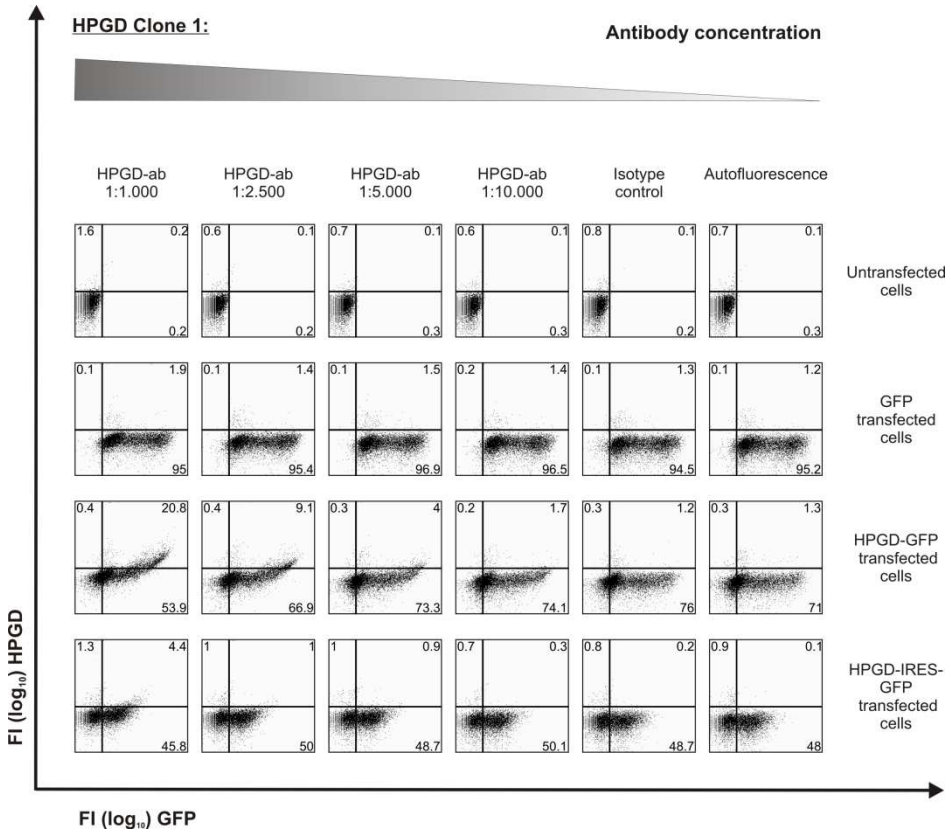

Figure 17: Binding specificity of directly-conjugated HPGD antibody clone 1 to HEK293 cells.
HEK293 cells were left untransfected (Untransfected cells) or were transfected with GFP (GFP transfected cells), pcDNA6/myc-HisB/HPGD-GFP (HPGD-GFP transfected cells) or pIRES2-AcGFP1/HPGD (HPGD-IRES-GFP transfected cells). Cells were stained with HPGD antibody clone 1 (HPGD-ab) in different dilutions (1:1.000, 1:2.500, 1:5.000 and 1:10.000, stock solution 0,25 mg/ml). As control, cells were left untreated (Autofluorescence) or stained with the isotype control (Isotype). FI (log_{10}) GFP indicates the fluorescence intensity of the GFP signal; FI (log_{10}) HPGD indicates the fluorescence intensity of the HPGD stained cells. The numbers in the quadrants represent the percentage of cells. One representative experiment out of three is shown.

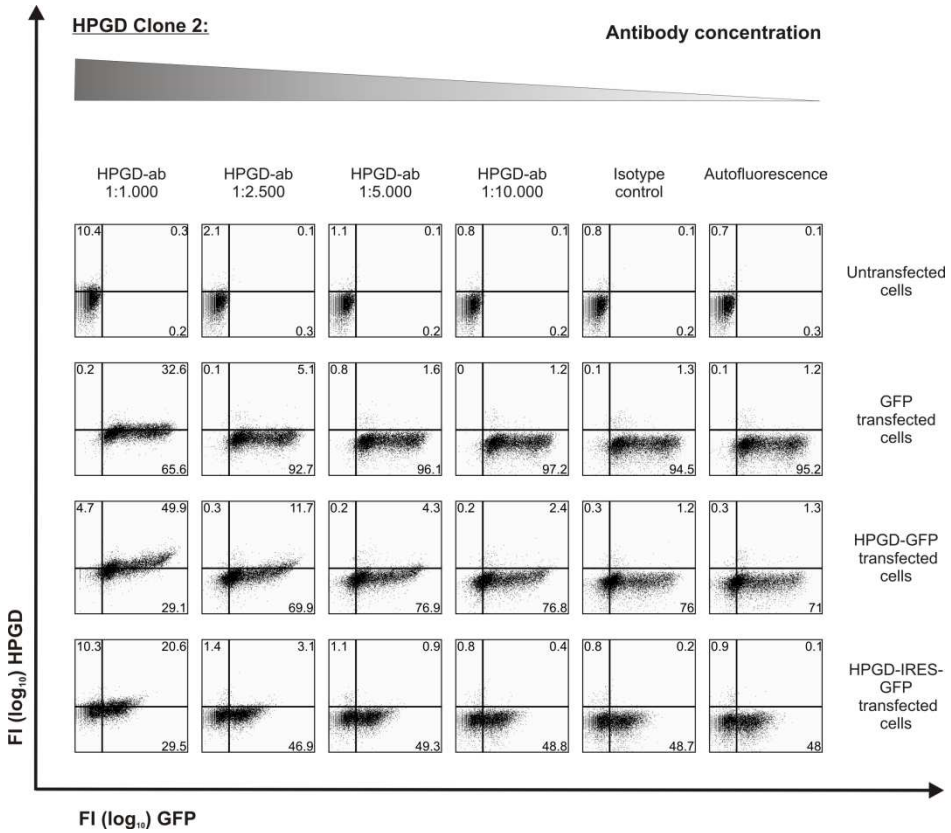

Figure 18: Binding specificity of directly-conjugated HPGD antibody clone 2 to HEK293 cells.
HEK293 cells were transfected, processed and analyzed as described in Figure 17. HPGD antibody clone 2 was used instead of clone 1. The antibody stock solution was 0,25 mg/ml. The axis annotation is consistent with Figure 17. The numbers in the quadrants represent the percentage of cells. One representative experiment out of three is shown.

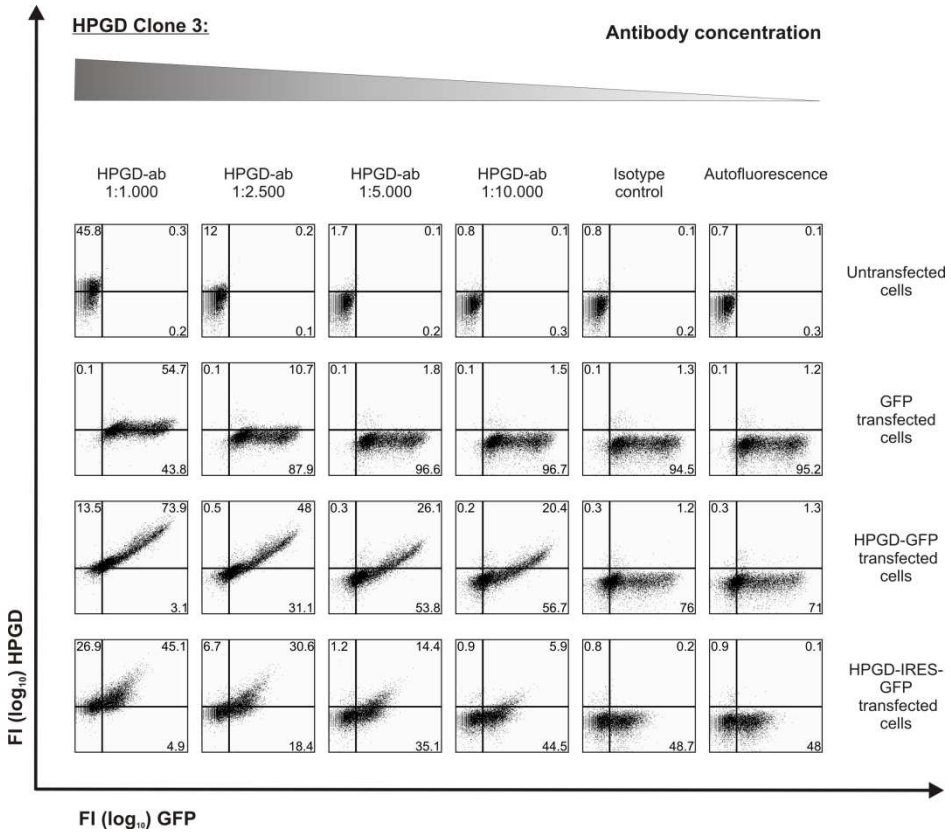

Figure 19: Binding specificity of directly-conjugated HPGD antibody clone 3 to HEK293 cells.
HEK293 cells were transfected, processed and analyzed as described in Figure 17. HPGD antibody clone 3 was used instead of clone 1. The antibody stock solution was 0,25 mg/ml. The axis annotation is consistent with Figure 17. The numbers in the quadrants represent the percentage of cells. One representative experiment out of three is shown.

3.2.7 HPGD staining of peripheral blood mononuclear cells

3.2.7.1 Staining of peripheral blood mononuclear cells with a HPGD specific antibody

HPGD antibody clone 3 had demonstrated specific and efficient staining of HEK293 cells, which were transfected with HPGD or HPGD-GFP, for flow cytometric experiments. In the following experiment, the binding of this antibody should be further tested in extracellular and intracellular staining of peripheral blood mononuclear cells (PBMC), to examine the binding intensity of the HPGD antibody towards different cell populations such as $CD4^+$ or $CD8^+$ T cells, B lymphocytes, natural killer (NK) cells or monocytes. Therefore, PBMC were isolated, pre-stained with different surface markers (CD3, CD4, CD8, CD14, CD16, CD19 and CD56) and stained extra- or intracellularly with HPGD antibody clone 3 in different concentrations according to the concentration used in previous experiments (1:500, 1:1.000, 1:2.500 and 1.5.000).

In Figure 20, the extracellular staining of $CD4^+$ and $CD8^+$ T cells, B lymphocytes, NK cells or monocytes with HPGD antibody is shown. 5 % of the monocytes were stained with HPGD

antibody (dilution: 1:500), while other cell populations displayed only marginal extracellular staining with the HPGD antibody. These data show that the HPGD antibody does not bind unspecifically to $CD4^+$ and $CD8^+$ T cells. The slight staining of B cells, NK cells and monocytes could be due to antibody binding to Fc receptors that were not efficiently blocked.

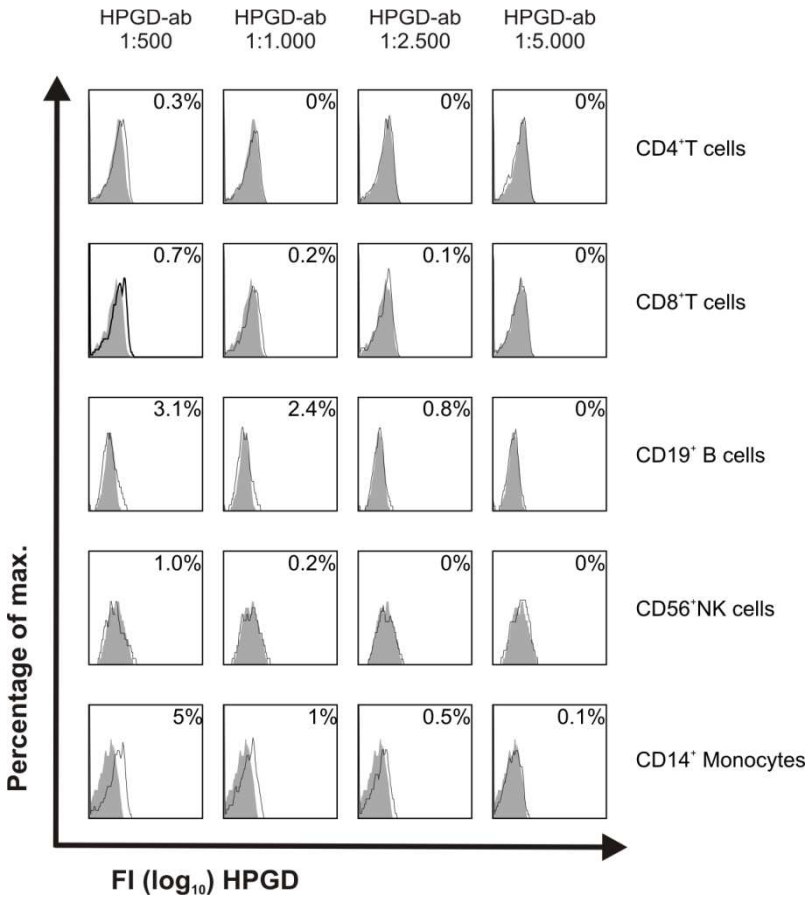

Figure 20: Extracellular HPGD staining of $CD4^+$ T cells, $CD8^+$ T cells, B cells, NK cells and monocytes. PBMC were isolated from human peripheral blood and stained with surface markers for CD3, CD4, CD8, CD14, CD16, CD19 and CD56 to distinguish between $CD4^+$ T cells, $CD8^+$ T cells, $CD19^+$ B cells, $CD56^+$ NK cells and $CD14^+$ monocytes. Cells were stained with HPGD antibody clone 3 in varying concentrations (1:500 – 1:5.000, stock solution 0,25 mg/ml). The staining with HPGD antibody is depicted in a histogram (open area) in comparison to the isotype control (grey area). The numbers in the histograms indicate the percentage of HPGD stained cells. FI (log_{10}) HPGD indicates the fluorescence intensity of the HPGD signal of HPGD stained cells. One representative experiment out of three is shown.

In Figure 21, the intracellular HPGD staining of $CD4^+$ and $CD8^+$ T cells, B lymphocytes, NK cells or monocytes is shown. 4,5 % of the $CD4^+$ T cells were positive for HPGD with an antibody dilution of 1:500. Also $CD8^+$ T cells (10.1 %), B cells (30.5 %), NK cells (9.7 %) and monocytes (53.4 %) were stained by the HPGD antibody using a dilution of 1:500. The number of positively stained cells decreased with the next antibody dilution and cells were only stained marginally or not with higher dilutions than 1:1.000.

In addition to the intracellular HPGD staining, HPGD gene expression in different PBMC subsets was examined (see Appendix C), to determine whether HPGD expression can be observed in these cell populations and thus the observed HPGD signal in flow cytometry could be due to intracellular staining of HPGD. HPGD expression levels were compared with those of T_{reg} cells, which show a high HPGD mRNA expression. It could be demonstrated that the mean HPGD expression values in the PBMC cell populations were below or near the background level compared to the high expression levels of T_{reg} cells. Only NK cells showed a slightly enhanced HPGD expression. Therefore, the above mentioned results indicate that the observed HPGD signals in flow cytometry were unspecific and could be due to a highly concentrated antibody solution or binding of the HPGD antibodies to unblocked Fc receptors in monocytes, B lymphocytes and NK cells.

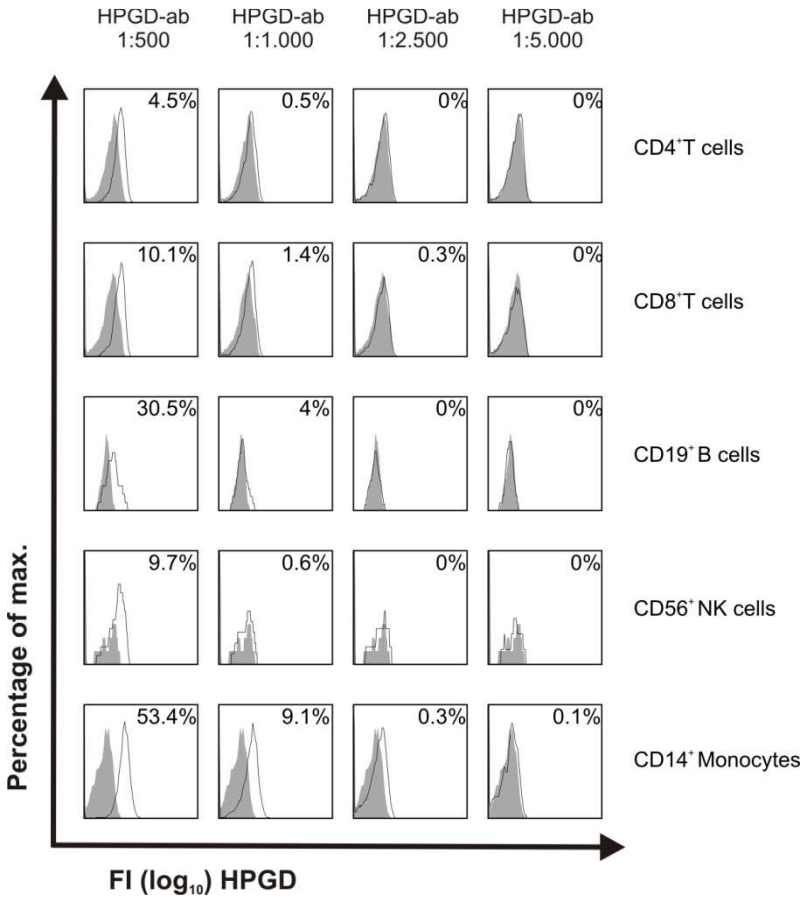

Figure 21: Intracellular HPGD staining of $CD4^+$ T cells, $CD8^+$ T cells, B cells, NK cells and monocytes. PBMC were isolated from peripheral blood as described in Figure 20. Cells were stained intracellularly with HPGD antibody clone 3 in varying concentrations (1:500 – 1:5.000, stock solution 0,25 mg/ml). The staining with HPGD antibody is depicted in a histogram (open area) in comparison to the isotype control (grey area). The numbers in the histograms indicate the percentage of HPGD stained cells. FI (log_{10}) HPGD indicates the fluorescence intensity of the HPGD signal of HPGD stained cells. One representative experiment out of three is shown.

3.2.7.2 T_{reg} and T_{conv} cells are not differentially stained by the HPGD antibody in flow cytometry

The previous results had demonstrated that HPGD antibody clone 3 specifically stains HPGD-GFP- and HPGD-IRES-GFP-transfected cells in flow cytometric experiments. However, HPGD staining of $CD4^+$ T cells was not observed, although differential HPGD expression in T_{reg} compared to T_{conv} had been observed on mRNA level. To answer the questions whether T_{reg} cells can be stained with the HPGD antibody and if this cell population was just missed among the $CD4^+$ T cells, it was tested whether the HPGD antibody would show differential staining of T_{reg} and T_{conv} cells. Therefore, $CD4^+$ T lymphocytes were isolated from human peripheral blood as described in 2.2.2.4 and pre-stained with different surface markers (CD3, CD4, CD8, CD25 and CD127). Furthermore, cells were stained extra- or intracellularly with HPGD antibody clone 3 in different concentrations (1:500, 1:1.000, 1:2.500 and 1.5.000). The flow cytometric analysis revealed only marginal extracellular staining of T_{reg} and T_{conv} cells with the HPGD antibody, as depicted in Figure 22. This result further demonstrates the specificity of the HPGD antibody, as surface molecules are not bound.

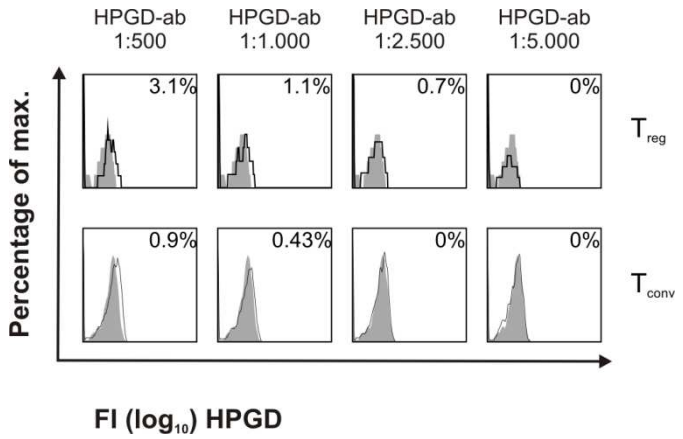

Figure 22: Extracellular staining of T_{reg} and T_{conv} cells with HPGD antibody clone 3
$CD4^+$ T lymphocytes were isolated from peripheral blood and stained with surface markers for CD3, CD4, CD8, CD25 and CD127 to distinguish between $CD4^+$ $CD25^+$ T_{reg} cells and $CD4^+CD25^-$ T_{conv} cells. Cells were stained with HPGD antibody clone 3 in varying concentrations (1:500 – 1:5.000, stock solution 0,25 mg/ml). The staining with HPGD antibody is depicted in a histogram (open area) in comparison to the isotype control (grey area). FI (log_{10}) HPGD indicates the fluorescence intensity of the HPGD signal of the HPGD stained cells. The numbers in the histograms indicate the percentage of HPGD stained cells. One representative experiment is shown.

The intracellular HPGD staining of T_{reg} and T_{conv} is displayed in Figure 23. 13.4 % of the T_{reg} cells were stained with HPGD antibody (dilution 1:500) compared to the isotype control, whereas only 3.4 % of the T_{conv} were stained. However, with increasing antibody dilution almost no HPGD stained cells were further detectable.

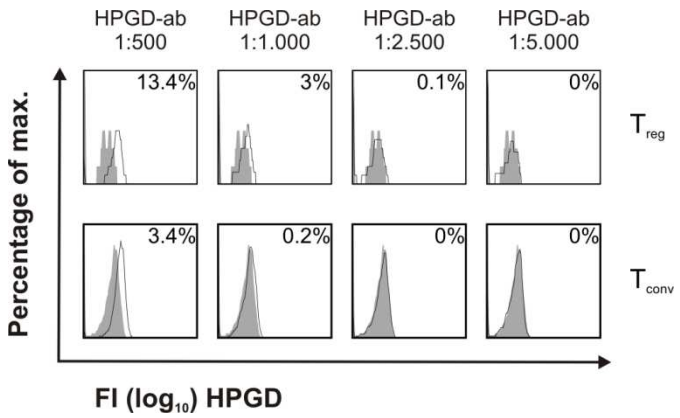

Figure 23: Intracellular HPGD staining of T_{reg} and T_{conv} cells with HPGD antibody clone 3
$CD4^+$ T lymphocytes were isolated and treated as described in Figure 22. Cells were stained intracellularly with HPGD antibody clone 3 in varying concentrations (1:500 – 1:5.000, stock solution 0,25 mg/ml). The staining with HPGD antibody is depicted in a histogram (open area) in comparison to the isotype control (grey area). FI (log_{10}) HPGD indicates the fluorescence intensity of the HPGD signal of the HPGD stained cells. The numbers in the histograms indicate the percentage of HPGD stained cells. One representative experiment is shown.

Next, the mean fluorescence intensity (MFI) of HPGD in T_{conv} and T_{reg} was assessed to determine whether the HPGD antibody staining would reflect the differences observed on mRNA level. However, no differences in the MFI between T_{reg} and T_{conv} cells could be observed (Figure 24). Although the staining of the HPGD antibody was shown to be specific using, transfected cells, the HPGD staining could not distinguish HPGD stained T_{reg} cells from T_{conv} cells. This suggests that the antibody probably has only a low affinity for the HPGD antigen and cannot be used to display differences when low protein amounts are present. Therefore, the HPGD antibody was not used for further flow cytometric staining of $CD4^+$ T cells.

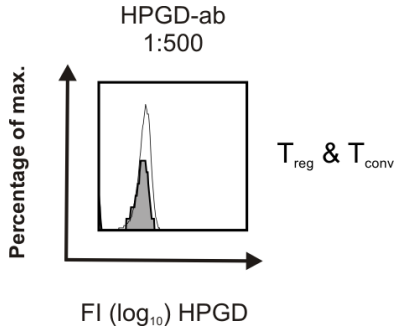

Figure 24: The MFI of HPGD in T_{reg} and T_{conv} cells is equal
$CD4^+$ T lymphocytes were isolated and further processed as described in Figure 23. Cells were stained with HPGD antibody clone 3 in a dilution of 1:500 (stock solution 0,25 mg/ml). Intracellular HPGD staining of T_{reg} (grey area) and T_{conv} (open area) was analyzed by flow cytometry and is depicted in a histogram. FI (log_{10}) HPGD indicates the fluorescence intensity of the HPGD signal of HPGD stained cells. One representative experiment is shown.

3.2.8 Application of the HPGD antibody for immunofluorescence staining

Although, HPGD antibody clone 3 had demonstrated good staining results in flow cytometry, using HPGD-GFP- and HPGD-IRES-GFP-transfected HEK293 cells, the antibody showed poor staining results for primary cells. Only high protein amounts in HPGD overexpressing cells were sufficiently stained, indicating a low affinity of the antibody for HPGD. Thus, the HPGD antibody could not be used for flow cytometric stainings of primary cells. Despite the negative results in flow cytometry, the antibody was also tested for immunofluorescence staining. Different fixation and permeabilization procedures are used for immunofluorescence staining, which might change the confirmation of the HPGD protein, thereby enhancing the accessibility of the epitope and thus the staining result.

HEK293 were therefore left untreated or transfected with HPGD-GFP or as control with GFP or HPGD-IRES-GFP, respectively. Cells were stained with the conjugated HPGD antibody clone 3 in different dilutions, decreasing from 1:50 to 1:1.000 (stock solution 0,25 mg/ml). Unstained cells served as autofluorescence control. Staining of HPGD-GFP transfected cells with the HPGD antibody is depicted in Figure 25. Only cells that displayed GFP fluorescence were also positive for HPGD staining and in addition the signal intensity for HPGD correlated with the GFP signal intensity. In contrast to flow cytometric staining, higher antibody dilutions were required for adequate immunofluorescence stainings of transfected HEK293 cells. With decreasing antibody concentration the HPGD staining attenuated and was almost undetectable using a dilution of 1:500.

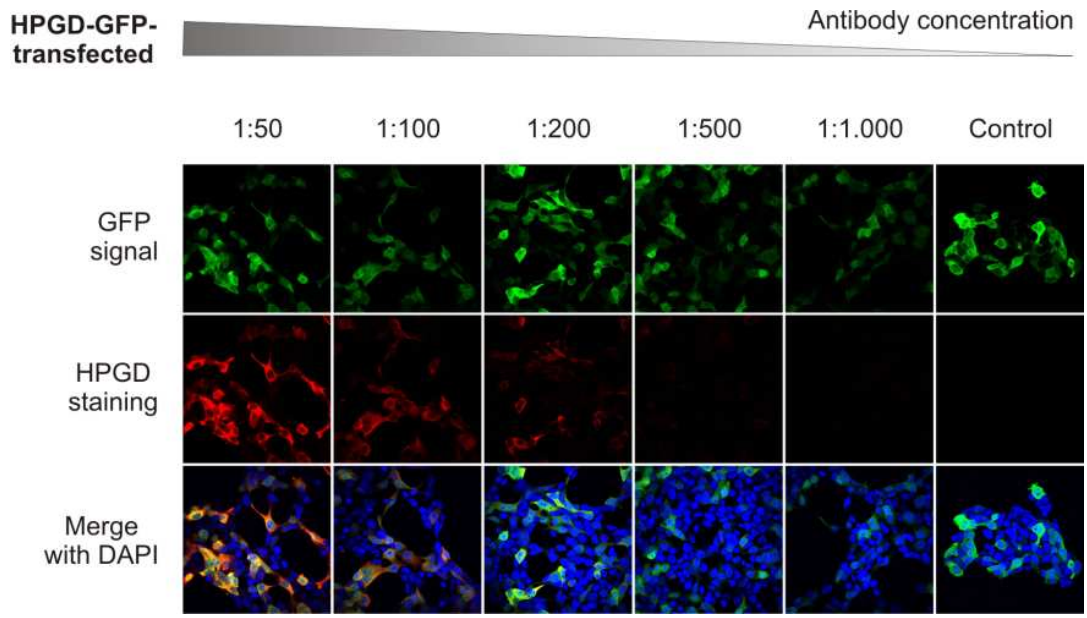

Figure 25: Immunofluorescence staining of HPGD-GFP transfected HEK293 cells with HPGD antibody clone 3.
HEK293 cells were transfected with pcDNA6/myc-HisB/HPGD-GFP (HPGD-GFP). Cells were left unstained (Control) or were stained with HPGD antibody clone 3 in different dilutions (1:1.50, 1:100, 1:200, 1:500 and 1:1.000, stock solution 0,25 mg/ml). The first row represents the GFP fluorescence, depicted in green for transfected cells (GFP signal). The middle row represents the HPGD fluorescence, depicted in red for HPGD stained cells (HPGD staining). The third row (Merge with DAPI) shows an overlay of both images together with DAPI, which visualizes the nucleus. Magnification for all pictures: 60x. One representative experiment out of two is shown.

The staining of HPGD-GFP-transfected cells seemed to be specific as untransfected and GFP-transfected HEK293 cells did not exhibit specific staining by the HPGD antibody even at high concentrations, as depicted in Figure 26 or Figure 27.

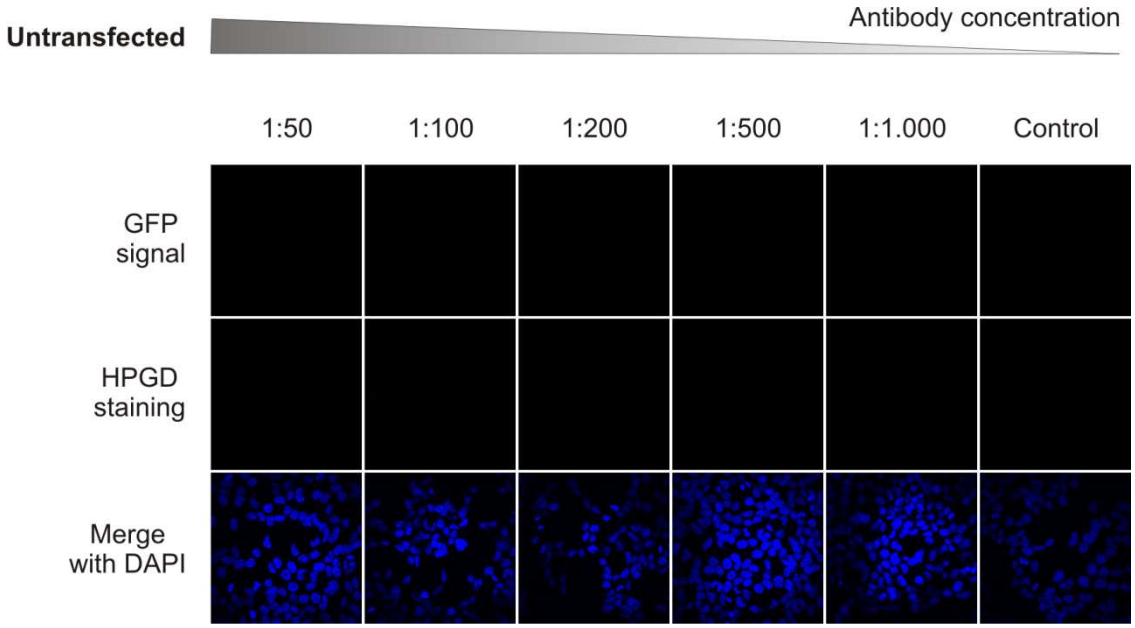

Figure 26: Immunofluorescence staining of untransfected HEK293 cells with HPGD antibody clone 3
Untransfected HEK293 cells were stained and analyzed as in Figure 25. The row annotation is consistent with Figure 25. Magnification for all pictures: 60x. One representative experiment out of two is shown.

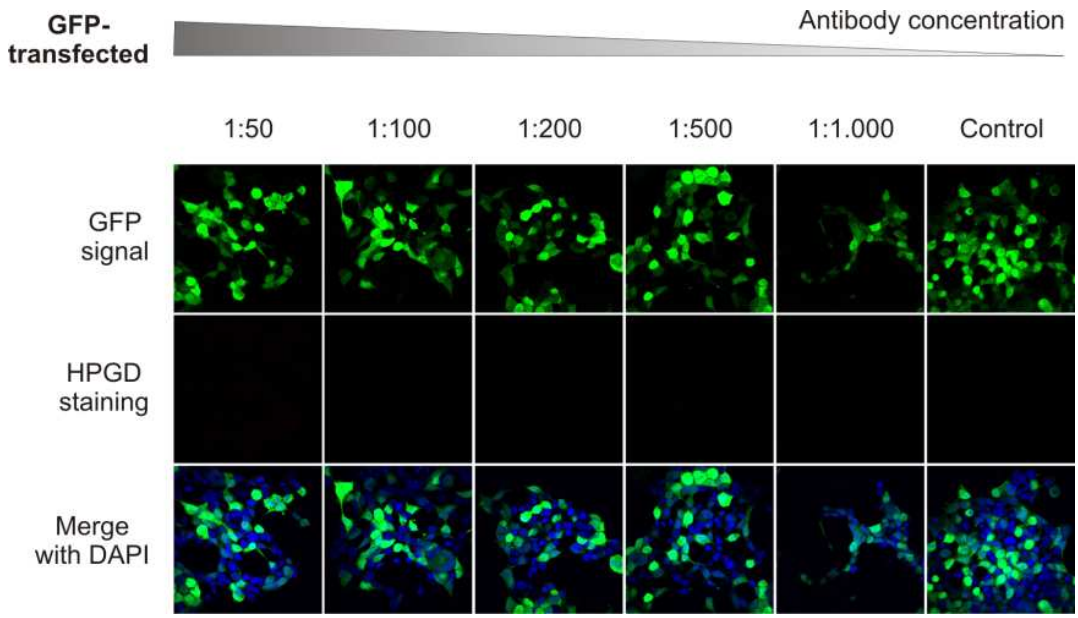

Figure 27: Immunofluorescence staining of GFP transfected HEK293 cells with HPGD antibody clone 3
HEK293 cells were transfected with GFP and stained and analyzed as in Figure 25. The row annotation is consistent with Figure 25. Magnification for all pictures: 60x. One representative experiment out of two is shown.

In addition, HPGD-IRES-GFP-transfected cells were used as further control for immunofluorescence staining, as depicted in Figure 28. This control allows the simultaneous expression of the two separate proteins HPGD and GFP. On the one hand this excludes that the antibody recognizes a HPGD-GFP fusion protein-specific epitope and thus leads to false positive binding results. On the other hand this rules out the possibility that the real epitope is hidden and not accessible due to a HPGD-GFP-specific protein confirmation. Besides that, the localization of HPGD protein in the cell can be examined, which may be different from that of the HPGD-GFP-protein. Similar to the observations made for HPGD-GFP-transfected cells, only HPGD-IRES-GFP-transfected cells that were GFP-positive cells were also stained for HPGD. The HPGD staining could thereby be merged with the GFP signal. With decreasing antibody concentration the HPGD staining attenuated and was almost undetectable at a dilution of 1:500. In comparison to HPGD-GFP-transfected cells the HPGD staining was weaker in HPGD-IRES-GFP-transfected cells, although cells were processed in parallel. An explanation for this phenomenon could be an enhanced degradation rate of HPGD compared to GFP. Moreover, the expression rates of the two genes might be different, as it was shown for example that the expression of the IRES-dependent second gene in a bicistronic vector can vary [209]. In conclusion, the results show that the HPGD antibody specifically binds to HPGD in HPGD-GFP- and HPGD-IRES-GFP-transfected cells in immunofluorescence staining.

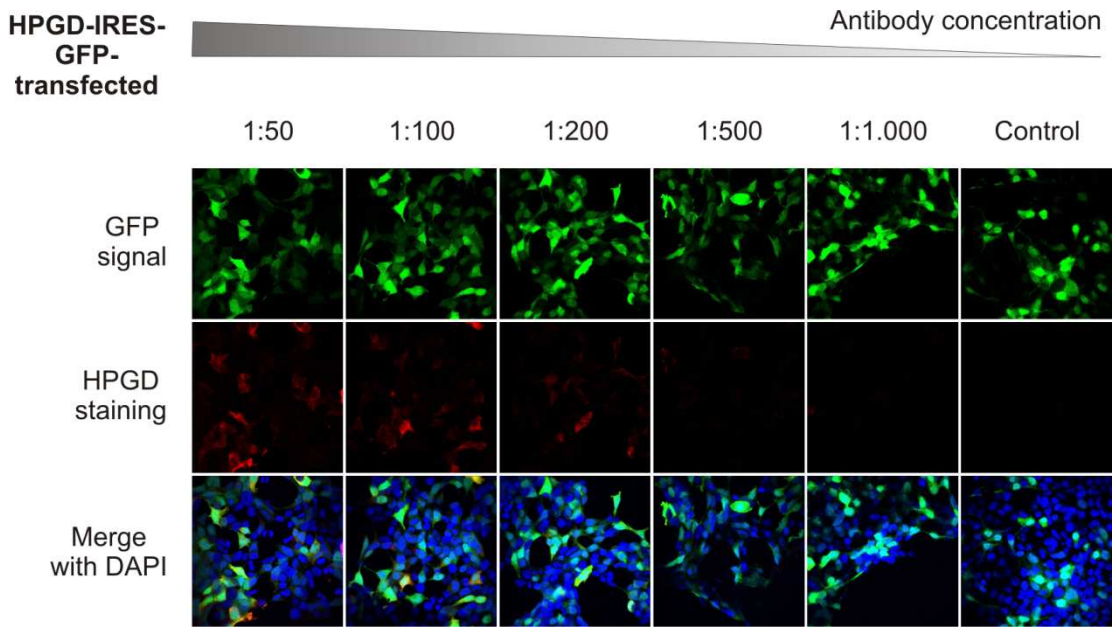

Figure 28: Immunofluorescence staining of HPGD-transfected HEK293 cells with HPGD antibody clone 3.
HEK293 cells were transfected with HPGD-IRES-GFP and stained and analyzed as in Figure 25. The row annotation is consistent with Figure 25. Magnification for all pictures: 60x. One representative experiment out of two is shown.

Finally it was tested whether the differences in HPGD mRNA expression between T_{reg} and T_{conv} could be also observed on protein level, using the HPGD antibody for immunofluorescence staining. Therefore, $CD4^+$ T lymphocytes were isolated and stained intracellularly with FOXP3 antibody to distinguish T_{reg} from T_{conv} cells. Furthermore, cells were stained with the HPGD antibody in two different concentrations (1:50 and 1:100) or left untreated (Control). In Figure 29, it is shown that both, T_{reg} and T_{conv} cells were marginally stained with the HPGD antibody but no differences in the staining intensity between T_{reg} and T_{conv} cells could be observed.

This result indicates that the affinity of the HPGD antibody is too low for appropriate intracellular staining of HPGD in primary cells. Only high protein amounts in HPGD-overexpressing cells, such as HPGD-GFP- or HPGD-IRES-GFP-transfected cells, were sufficiently stained. Therefore, the HPGD antibody was not used for immunofluorescence staining.

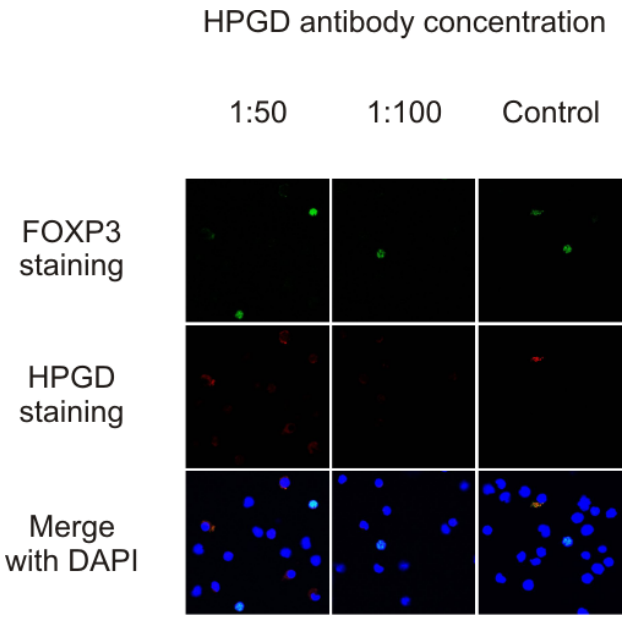

Figure 29: Similar staining of T_{reg} and T_{conv} cells by the HPGD antibody in immunofluorescence.
$CD4^+$ T cells were isolated from human peripheral blood and stained intracellularly with HPGD antibody clone 3 in different dilutions (1:1.50, 1:100, stock solution 0,25 mg/ml) and with FOXP3 antibody (Fitc-conjugated) to locate $FOXP3^+$ T_{reg} cells. As control, cells were stained with all antibodies except the HPGD antibody (Control). The first row (FOXP3 staining) shows the FOXP3 stained T_{reg} cells displayed in green. The middle row (HPGD staining) displays the HPGD stained cells in red. The third row (Merge with DAPI) shows an overlay of both images together with DAPI, which visualizes the nucleus. Magnification for all pictures: 60x. One representative experiment out of two is shown.

3.2.9 Application of the HPGD antibody for Western blot analysis

3.2.9.1 Detection of HPGD in HPGD-transfected HEK293 cells

Despite the poor staining results for T_{reg} and T_{conv} cells in flow cytometry and immunofluorescence, HPGD antibody clone 3 should be also tested for Western blot analysis, to answer the question whether the differences of HPGD mRNA expression in T_{reg} and T_{conv} cells would be also observed on protein level. In contrast to the previous methods, the protein is highly and irreversibly denaturated for Western blot analysis by the treatment with sodium dodecylsulfate (SDS). The epitope and its ability to interact with the HPGD antibody can be altered by this treatment and consequently change the staining result. Furthermore, additional epitopes may be uncovered, which can then be bound by the HPGD antibody.

Therefore, HEK293 cells were left untransfected or were transfected with HPGD-GFP or with GFP as control. Protein lysates were prepared from cells showing a transfection rate above 50 % as determined by flow cytometry. Subsequently, different HPGD antibody dilutions were tested in Western blot analysis with HPGD-GFP-transfected cells to determine the concentration range for specific binding of the HPGD antibody and define an optimal working concentration. The relative binding affinity for HPGD, normalized to β-actin is depicted in

Figure 30 and demonstrates a concentration dependent decrease in the detection of HPGD. Nevertheless, even minuscule amounts of antibody resulted in a clear signal. Taken together these results suggest that a dilution of 1:1.000 represents a convenient working concentration for the HPGD antibody.

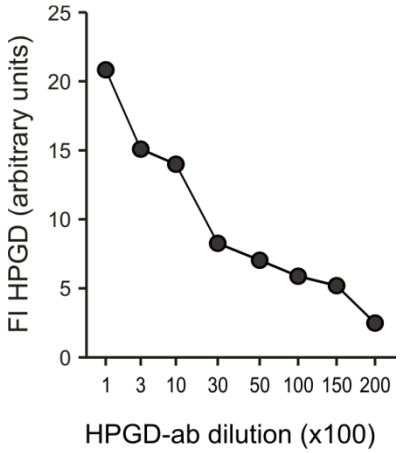

Figure 30: Low HPGD antibody concentrations detect HPGD-GFP protein by Western blotting.
HEK293 cells were transfected with HPGD-GFP (vector pcDNA6/myc-HisB/HPGD-GFP) and equal amounts of protein were blotted on several blots. Different HPGD antibody dilutions were then tested for the detection of HPGD-GFP protein on Western Blot. Antibody dilutions of 1:100 - 1:20.000 (stock solution 0,25 mg/ml) were applied. The fluorescence intensity (FI) is shown for each HPGD antibody dilution. Samples were normalized to the FI of the loading control β-actin. One representative experiment of two is shown.

In addition, also HPGD-IRES-GFP-transfected cells were used as control on Western Blot. This control should proof specific binding to an HPGD-specific epitope and exclude that the antibody unspecifically binds to an epitope specific for the HPGD-GFP fusion protein or GFP. Thus HEK239 cells were left untreated or were transfected either with HPGD-GFP, HPGD-IRES-GFP or GFP. HPGD antibody clone 3 was used in a dilution of 1:1.000, as this dilution had proven to be a convenient working solution for Western blot analysis for HPGD-transfected cells. The HPGD antibody detected the expected size of HPGD (28,9 kDa) in HPGD-IRES-GFP-transfected cells as well as the HPGD-GFP fusion protein (55,8 kDa) in HPGD-GFP-transfected cells, but did not bind to GFP (26,9 kDa) in GFP-transfected cells as shown in Figure 31 A. Additionally, the Western Blot was incubated with an anti-GFP antibody to control the size of the HPGD-GFP fusion protein and display the GFP protein expressed by HPGD-IRES-GFP or GFP-transfected cells. The expected size of HPGD-GFP (55,8 kDa) in HPGD-GFP-transfected cells and GFP (26,9 kDa) in GFP- and HPGD-IRES-GFP-transfected cells were detected by the anti-GFP antibody, as shown in Figure 31 B.

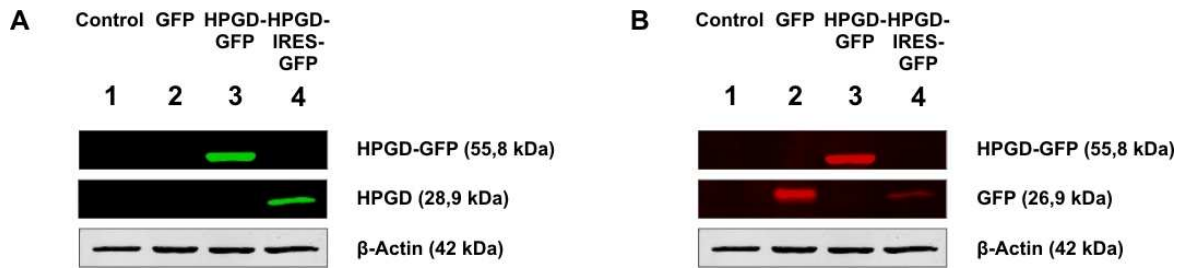

Figure 31: Detection of HPGD expression using the HPGD antibody clone 3 by Western blotting
HEK293 cells were either left untransfected (Column 1: Control) or were transfected with pcDNA6/myc-His B/GFP as transfection efficiency control (Column 2: GFP), with pcDNA6/myc-His B/HPGD-GFP (Column 3: HPGD-GFP) or with pIRES2-AcGFP1/HPGD (HPGD-IRES-GFP) respectively. (**A**) The expression of HPGD (28,9 kDa) or HPGD-GFP fusion protein (55,8 kDa) was detected with the HPGD antibody (green bands) on Western Blot. Dilution of the antibody was 1:1.000 (stock solution 0,25 mg/ml). (**B**) As control anti-GFP antibody was applied (red bands) for detection of HPGD-GFP or GFP protein (26,9 kDa). β-actin (black bands; 42 kDa) was used as loading control. One representative experiment out of two is shown.

3.2.9.2 HPGD protein expression in human regulatory T cells

The previous results had shown that relative HPGD mRNA expression is higher in human T_{reg} cells in comparison to T_{conv}. Moreover, HPGD antibody clone 3 had demonstrated specific staining of HPGD in lysates of HPGD-transfected HEK293 cells. Consequently, this antibody was tested for Western blot analysis with T_{reg} and T_{conv} cells to examine whether the differences in HPGD mRNA expression would be also observed on protein level.

For this purpose HPGD expression of freshly isolated human T_{reg} and T_{conv} cells was analyzed by Western blot analysis. HPGD protein expression was significantly higher in T_{reg} than in T_{conv} cells, as shown in Figure 32 A. In Figure 32 B, it is shown that the HPGD antibody detected the expected size of HPGD (28,9 kDa) in T_{reg} cells and that HPGD expression was less intensive in T_{conv} cells. However, a higher antibody concentration (1:200) had to be applied to visualize bands in T cells, than the initial concentration (dilution 1:1.000) that was used for HPGD-GFP-transfected HEK293 cells. Furthermore, more protein had to be subjected to the Western Blot (50 µg of T cell lysates compared to 15 µg of HEK cell lysates) to obtain good results. Taken together the results show that, consistent with the mRNA expression data, T_{reg} cells also display a significantly higher HPGD protein expression compared to T_{conv} cells. Moreover, it was demonstrated that the HPGD antibody specifically detects HPGD protein on Western Blot and can be even used for analysis of primary cells.

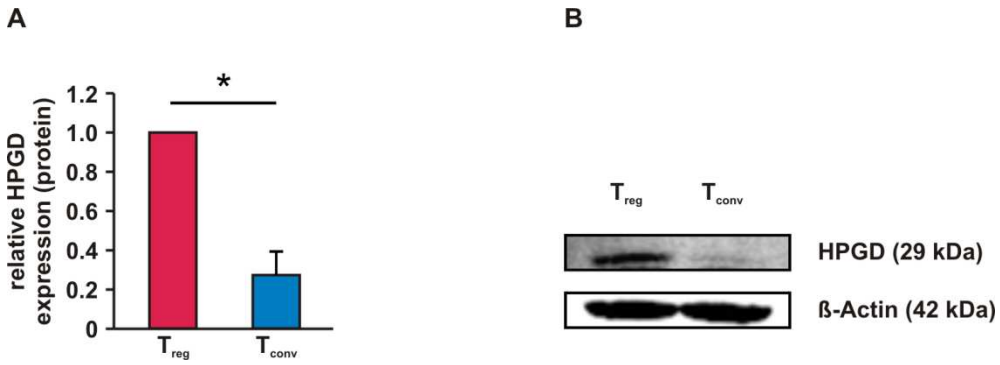

Figure 32: HPGD protein expression is higher in T_{reg} cells than in T_{conv}
Human $CD4^+CD25^+$ T_{reg} cells and $CD4^+CD25^-$ T_{conv} were purified and HPGD protein expression was assessed by Western blot analysis. (**A**) Relative amounts of HPGD were measured densitometrically in comparison to β-actin. Data represent mean values and standard deviations of four independent experiments. Statistically significant differences are marked with an asterisk (* $p < 0.01$) (**B**) One representative Western blot experiment is shown.

3.3 HPGD is expressed specifically in human natural regulatory T cells

3.3.1 HPGD expression in T cell subsets

Human T_{reg} cells were shown to exhibit a higher expression of HPGD on mRNA and protein level than T_{conv}. Following that it was investigated whether HPGD expression was unique for T_{reg} cells or if HPGD would be also expressed in other $CD4^+$ T cell subsets, depending on their activation and differentiation state. The CD45RA surface molecule represents, for instance, a suitable marker to distinguish naïve from activated or memory T cells. The leukocyte specific transmembrane glycoprotein CD45 is a protein tyrosine phosphatase (PTP)[210] and was shown to be required for efficient T and B cell antigen receptor signal transduction [211,212]. Several isoforms of CD45 can be generated by alternative splicing of the exons 4 (A), 5 (B) and 6 (C) and expression of the respective isoforms is dependent on cell type, stage of differentiation and activation state of the cell [212,213]. In humans, the isoform CD45RA is expressed on naïve T lymphocytes (T_{naive}), which represent mature T cells that have not yet encountered antigen. Upon encounter of their cognate antigen T_{naive} cells acquire an activated phenotype, characterized by upregulation of activation markers such as CD25, CD44, and CD69 and down-regulation of CD62L and CD45RA [214-216]. The activated T cells may further differentiate into a memory T cell (T_{memory}), which represents an 'antigen-experienced' T cell that has already encountered and responded to its cognate antigen [216-218]. Besides activated T cells also T_{memory} are $CD45RA^-$ and express the shortest CD45 isoform CD45RO, which lacks RA, RB and RC exons [213,214]. Thus CD45RA represents a suitable marker to distinguish naïve from activated or memory T cells. To address the question whether HPGD expression is enhanced during T cell activation and differentiation, T_{conv} cells

were isolated from human peripheral blood and further separated into $CD4^+CD25^-CD45RA^-$ T_{memory} cells and $CD4^+CD25^-CD45RA^+$ T_{naive} cells. HPGD mRNA expression levels were assessed by qRT-PCR in freshly isolated T_{memory} and T_{naive} cells and compared to T_{reg} cells. HPGD mRNA expression in T_{memory} cells was slightly higher than in T_{naive}, as depicted in Figure 33. However, HPGD expression was constantly lower for memory and naïve T_{conv} in comparison to natural T_{reg} cells (see Figure 33).

The differential HPGD mRNA expression in T_{naive} compared to T_{memory} cells indicates that HPGD expression might be upregulated during T cell differentiation. Furthermore, the results support that an enhanced HPGD expression might be specific for T_{reg} cells.

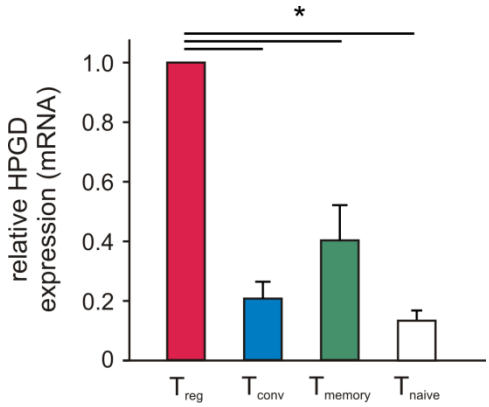

Figure 33: T_{memory} cells reveal a higher HPGD expression than T_{naive} cells
Human natural T_{reg}, T_{conv}, T_{memory} & T_{naive} cells were purified and relative HPGD mRNA expression, compared to B2M expression, was assessed by qRT-PCR. Mean values and standard deviations of three independent experiments are shown. Data are normalized to T_{reg} cells. Statistically significant differences (wilcoxon signed-rank test; $p < 0.05$) are marked with an asterisk.

3.3.2 HPGD expression is not upregulated during T cell differentiation

Human naïve $CD4^+$ T cells can differentiate into a number of different T helper cell subsets with distinct effector cell functions, such as T_H1, T_H2, T_H9 and T_H17 [219,220]. T_H1 cells, for instance, are characterized by production of high levels of IFNγ and are involved in cellular immunity against intracellular microorganisms [219-221]. In contrast, T_H2 cells produce IL-4, IL-5, IL-9 and IL-13 and are required for humoral immunity to protect against parasitic helminthes and other extracellular pathogens [220,222]. T_H9 are characterized by production of IL-9 and IL-10 and are involved in allergic inflammation and defense against extracellular parasites as nematodes [223,224]. T_H17 cells produce IL-17A, IL-17F, IL-21, IL-22, IL-6, TNFα and CCL20 and play an important role in clearance of extracellular bacteria and fungi, mainly at mucosal surfaces [220,225,226]. As higher expression levels of HPGD were detected in T_{memory} cells in comparison to T_{naive}, one could postulate that HPGD expression might increase during T cell differentiation. To test this hypothesis it was investigated whether HPGD expression is

upregulated during differentiation towards different T helper cell subsets such as T_H1, T_H2, T_H9 or T_H17. This question was addressed in the following experiment: $CD4^+CD25^-CD45RA^+$ naïve T cells were purified and differentiated towards the desired T cell subset by stimulation with CD3/CD28/MHC-I-coated beads together with the appropriate cytokines for 5 days. Unstimulated T_{naive} cells (T_{unstim}) as well as T_{naive} cells only stimulated with CD3/CD28/MHC-I-coated beads (T_H0) served as control. To monitor successful differentiation the expression of lineage specific transcription factors, such as T-bet for T_H1 cells, GATA-3 for T_H2, PU.1 for T_H9 and RORγt for T_H17 cells were assessed by qRT-PCR (see Appendix D). HPGD expression was assessed in differentiated T cell subsets, as shown in Figure 34. Relative HPGD expression levels, assessed by qRT-PCR are presented in comparison to freshly isolated T_{conv} and T_{reg} cells (time point 0 h). HPGD expression in T_H0 was equal to freshly isolated T_{conv} and T_{unstim} cells. Differentiation of naïve T cells into T_H1, T_H2, T_H9 or T_H17 cells did not result in the induction of HPGD.

Taken together these results indicate that HPGD expression remains low in T_{conv} cells independent of TCR/CD28 stimulation and their polarization towards different T_H cell lineages. Moreover, the enhanced HPGD expression seems to be specific for T_{reg} cells.

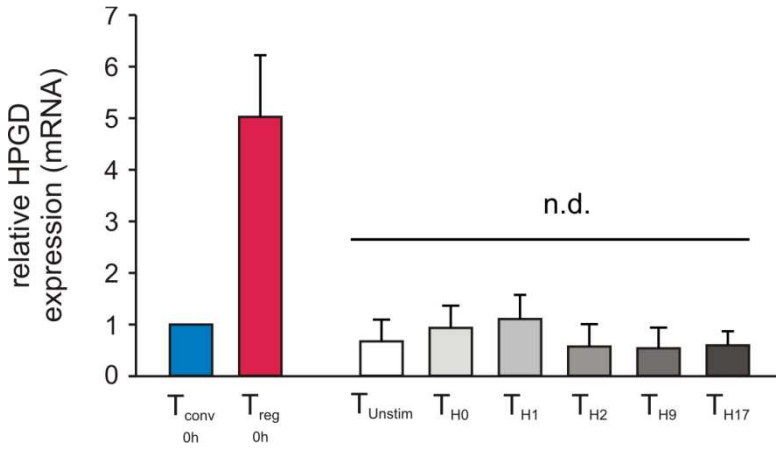

Figure 34: HPGD expression is not upregulated during T cell differentiation
Human T_{naive} cells were purified and differentiated with anti-CD3/CD28/MHC-I-coated beads together with the appropriate cytokines towards T_H1, T_H2, T_H9 and T_H17 cells. Unstimulated T_{naive} cells (T_{unstim}) and T_{naive} only stimulated with CD3/CD28/MHC-I-coated beads without additional cytokines (T_H0) served as control. Freshly isolated T_{reg}, (T_{reg} 0h) and T_{conv} (T_{conv} 0h) served as additional controls. Relative HPGD mRNA expression, compared to B2M expression, was assessed by qRT-PCR. Mean values and standard deviations of three independent experiments are shown. Data were normalized to T_{conv} cells (time point 0 h). n.d.: no statistically significant differences (one-way ANOVA; $p > 0.05$) between the sample groups were observed.

3.3.3 HPGD expression is not upregulated in induced regulatory T cells

Regulatory T cells are generated in the thymus as naturally occurring T_{reg} cells (nT_{reg})[1,16], but there also exist so called induced or adaptive T_{reg} cells (iT_{reg}) that are generated in the periphery [29,30,33]. Similarly to nT_{reg} cells these iT_{reg} display high FOXP3 expression levels, anergy and suppressive function *in vitro* and *in vivo* [30,227]. But on the other hand iT_{reg} cells also differ from nT_{reg} cells. Although they exhibit high FOXP3 expression levels, iT_{reg} cells were shown to lack a part of the gene signature that is specific for nT_{reg} cells [228]. Still differences remain to be elucidated that are specific for nT_{reg} or iT_{reg} cells.

In this context it was investigated whether HPGD expression would be upregulated in iT_{reg} cells or whether HPGD expression is specific for nT_{reg} cells. Therefore, naïve T cells were purified from human peripheral blood and differentiated into iT_{reg} cells by stimulation with CD3/CD28/MHC-I-coated beads together with the appropriate cytokines for 5 days. T_{unstim} and T_H0 cells served as control. To monitor successful induction of adaptive T_{reg} cells the expression of the lineage specific transcription factor FOXP3 was assessed by qRT-PCR (see Appendix D). HPGD mRNA expression was assessed in iT_{reg} cells, as shown in Figure 35. Relative HPGD mRNA expression levels, assessed by qRT-PCR are presented in comparison to freshly isolated T_{conv} and T_{reg} cells (time point 0 h). HPGD expression in T_H0 cells was equal to freshly isolated T_{conv} and T_{unstim} cells. Differentiation of naïve T cells into iT_{reg} cells did not result in the induction of HPGD. Similar observations were made for gene expression profiling (see Figure 72, Appendix D), as T_{conv}, T_{naive} and iT_{reg} cells revealed low HPGD expression levels, whereas T_{reg} cells displayed high HPGD expression levels.

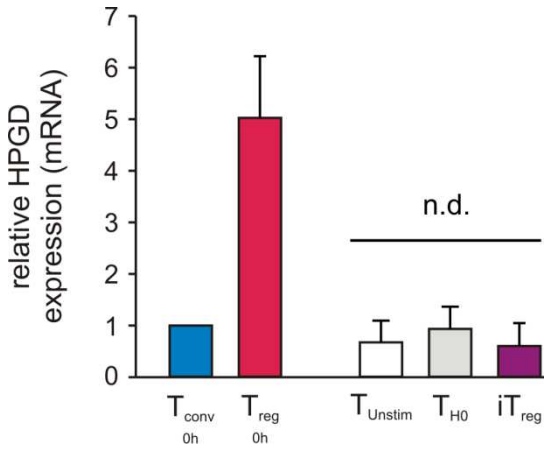

Figure 35: HPGD expression is not upregulated in induced T_{reg} cells
Human T_{naive} cells were purified and differentiated with anti-CD3/CD28/MHC-I-coated beads together with the appropriate cytokines towards iT_{reg} cells. T_{unstim} and T_H0 cells as well as freshly isolated T_{reg}, (T_{reg} 0h) and T_{conv} (T_{conv} 0 h) served as controls. Relative HPGD mRNA expression, compared to B2M, was assessed by qRT-PCR. Mean values and standard deviations of three independent experiments are shown. Data were normalized to T_{conv} cells (time point 0 h). n.d.: no statistically significant differences (one-way ANOVA; $p > 0.05$) between the sample groups were observed.

Taken together, these results indicate that HPGD expression is specific for natural T_{reg} cells and belongs to the nT_{reg} specific gene expression program. HPGD expression levels seem to be settled during T cell maturation and can no longer be induced in T_{naive} cells by extracellular stimulation.

3.4 Influence of PGE_2, TGF-β and IL-10 on HPGD expression in human T_{reg} cells

HPGD plays an important role in the metabolism of prostaglandins and is one of the major prostaglandin E_2 (PGE_2)-metabolizing enzymes [163,167]. Furthermore, PGE_2 is a known potent immunosuppressive, soluble molecule, which is produced by tumor cells [229] and cells of the immune system as for instance monocytes, macrophages or neutrophils [230]. Moreover, tumor-secreted PGE_2 induces FOXP3 expression as well as a regulatory phenotype in T_{conv} cells [231]. Notably, pre-incubation with PGE_2 did also increase FOXP3 expression as well as the suppressive activity of T_{reg} cells [232]. For these reasons, a possible influence of PGE_2 on the HPGD expression in T_{reg} cells was investigated (Figure 35). Human T_{reg} cells were isolated from peripheral blood and incubated for 72 h with PGE_2 or left untreated. After 24, 48 and 72 h cells were harvested. Expression of HPGD on mRNA levels was analyzed by qRT-PCR. Stimulation with PGE_2 did not significantly influence HPGD expression compared to unstimulated T_{reg} cells as depicted in Figure 35, suggesting that HPGD expression in T_{reg} cells is independent of PGE_2 signaling.

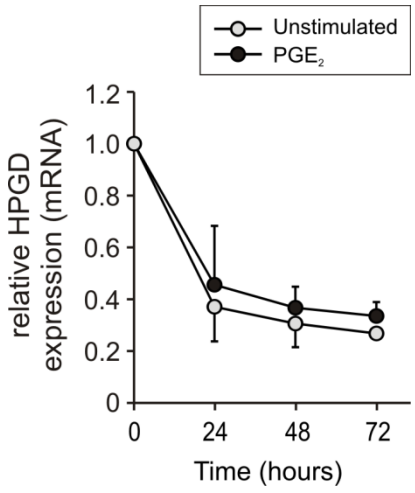

Figure 36: HPGD expression is not influenced by stimulation with PGE_2
Human $CD4^+CD25^+$ T_{reg} cells were purified and left untreated (Unstimulated) or stimulated with 1 µM PGE_2 (PGE_2). Relative HPGD mRNA expression, compared to B2M expression, was assessed by qRT-PCR after 24 h, 48 h and 72 h. Samples are normalized to T_{reg} cells (0 h). Data represent mean values and standard deviations of three independent experiments.

Besides that, tumor cells or cells in the tumor microenvironment can produce TGF-β and IL-10 [229], which were reported to induce T_{reg} cells in the periphery [34,35]. Consequently it was examined whether these factors might have an effect on HPGD expression in T_{reg} cells. Therefore, T_{reg} cells were isolated from human peripheral blood and incubated for 72 h with TGF-β or IL-10, respectively, or left untreated. HPGD mRNA expression was assessed by qRT-PCR after 24, 48 and 72 h. No significant influence could be observed when cells were stimulated with TGF-β, as shown in Figure 36. However, IL-10 stimulation did modulate HPGD expression, as HPGD expression was significantly higher after 24 h in IL-10 stimulated cells compared to unstimulated cells.

This result indicates that IL-10 receptor- signaling modulates HPGD expression, whereas TGF-β signaling has no influence on the HPGD expression in T_{reg} cells.

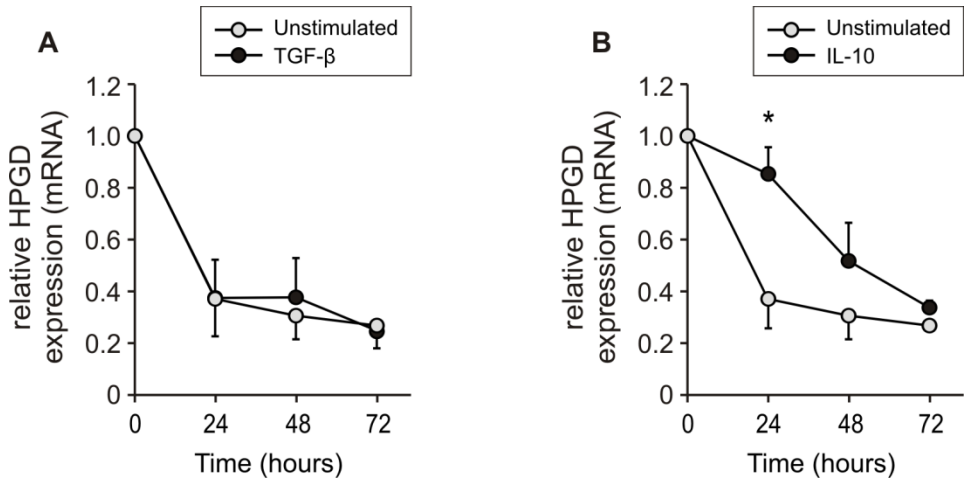

Figure 37: HPGD expression in human T_{reg} cells is influenced by IL-10 but not TGF-β
Human $CD4^+CD25^+$ T_{reg} cells were purified and left untreated (Unstimulated) or stimulated with (**A**) 10 ng/ml TGF-β (TGF-β) or (**B**) 50 ng/ml IL-10 (IL-10). Relative HPGD mRNA expression, compared to B2M expression, was assessed by qRT-PCR after 24 h, 48 h and 72 h. Samples are normalized to T_{reg} cells (0 h). Data represent mean values and standard deviations of at least three independent experiments. Statistically significant differences ($p < 0.05$) are marked with an asterisk.

3.5 Influence of interleukin-2 on HPGD expression in human regulatory T cells

3.5.1 TCR activation in the presence of IL-2 enhances HPGD expression in T_{reg} cells

Regulatory T cells require previous activation for the induction of their suppressor function *in vitro*, as it was shown by Thornton et al. 2004 [233]. Best induction results were achieved when T_{reg} cells were pre-cultured for at least 24 h with anti-CD3-antibody (0.5-1 µg/ml) in the presence of IL-2 (at least 12.5 U/ml) and the absence of T_{conv} cells [233]. Since the previous

results of this study had shown that HPGD expression decreases in unstimulated T_{reg} cells, it was consequently investigated whether this pre-activation with TCR signaling and activation of the IL-2 receptor would influence HPGD expression in T_{reg} cells.

To address this question, human T_{reg} and T_{conv} cells were isolated from peripheral blood and incubated for 24 h in medium supplemented with IL-2 and anti-CD3 antibody. HPGD mRNA expression was assessed by qRT-PCR. TCR stimulation in the presence of IL-2 significantly upregulated HPGD mRNA expression in T_{reg} cells, as shown in Figure 38 A. In contrast, HPGD mRNA expression in T_{conv} cells was unchanged (Figure 38 B). These results show that HPGD expression in T_{reg} cells is differentially regulated than in T_{conv} and can be influenced by TCR/IL-2R activation. Furthermore, these results support that HPGD expression in T_{reg} cells is dependent on extracellular stimuli.

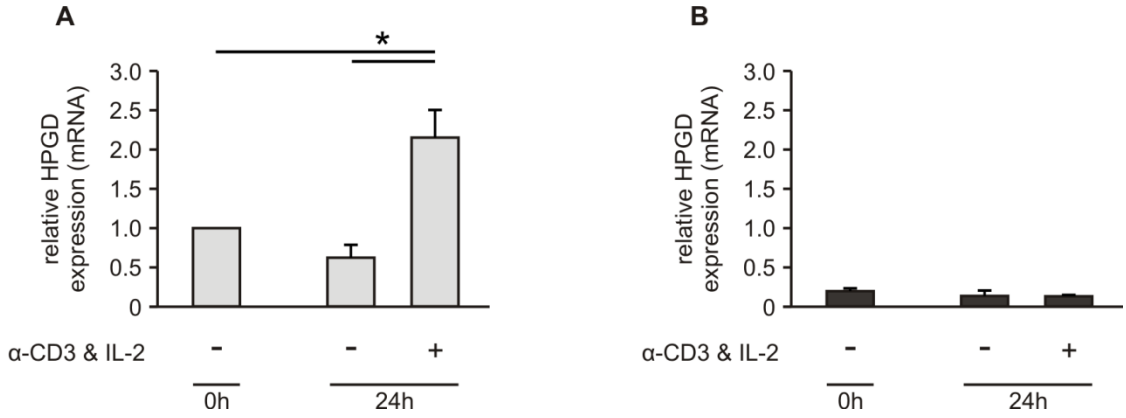

Figure 38: HPGD expression is specifically upregulated in T_{reg} cells upon IL-2/anti-CD3 stimulation.
(**A**) Human T_{reg} (grey columns) and (**B**) T_{conv} cells (black columns) were purified from human peripheral blood and left untreated (-) or stimulated with 1.0 µg/ml anti-CD3 antibody and 20 U/ml IL-2 (IL-2 & α-CD3) for 24 h (+). HPGD mRNA expression, compared to B2M expression, was assessed by qRT-PCR. Samples are normalized to T_{reg} cells (0 h). Data represent mean values and standard deviations of three independent experiments. Statistically significant differences ($p < 0.05$) are marked with an asterisk.

The inducing effects of CD3/IL-2-stimulation on expression of HPGD in T_{reg} cells were further examined over time. Therefore, human T_{reg} and T_{conv} cells were isolated and stimulated for 12 h, 24 h, 48 h and 72 h with IL-2 and anti-CD3. HPGD mRNA expression was assessed by qRT-PCR and it could be established that HPGD is significantly upregulated approximately 2-fold in T_{reg} cells already after 12 h (Figure 39). This upregulation remained relatively stable over a period of 72 h. In contrast, HPGD mRNA expression was not enhanced in T_{conv} cells upon the stimulation with anti-CD3 and IL-2.

This result shows that HPGD expression in T_{reg} cells is differentially regulated than in T_{conv} cells, as TCR activation and IL-2R signaling specifically enhance HPGD mRNA expression in T_{reg} cells. Moreover, these data show that HPGD expression in T_{reg} cells can be modulated by extracellular stimuli.

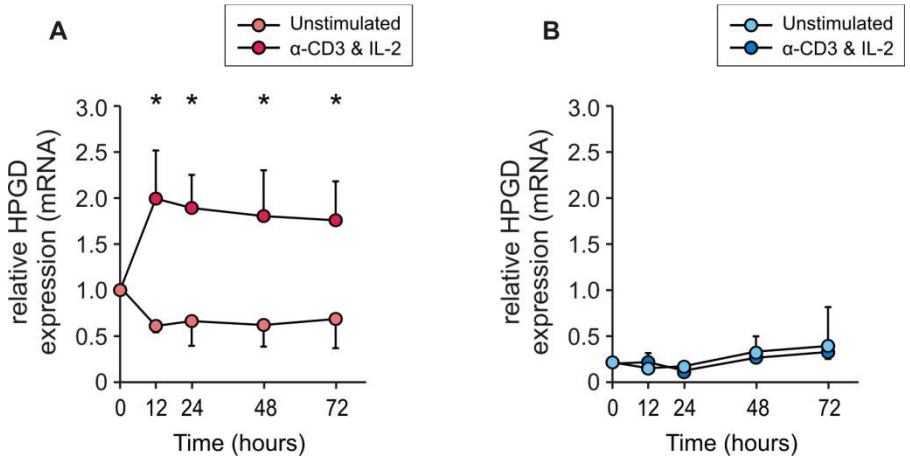

Figure 39: HPGD is specifically upregulated in regulatory T cells upon CD3 & IL-2 stimulation.
(**A**) Human T_{reg} and (**B**)T_{conv} cells were purified from human peripheral blood and left untreated (Unstimulated) or stimulated with 1 µg/ml anti-CD3 antibody and 20 U/ml IL-2 (α-CD3 & IL-2) for 12 h, 24 h, 48 h and 72 h. HPGD mRNA expression, compared to B2M expression, was assessed by qRT-PCR. Samples are normalized to T_{reg} cells (0 h). Mean values and standard deviations represent four independent experiments. Statistically significant differences between unstimulated and α-CD3/IL-2-stimulated samples are marked with an asterisk (* $p < 0.05$).

3.5.2 HPGD upregulation is IL-2 dependent and independent of TCR signaling

Activating pre-culture of T_{reg} cells with anti-CD3-antibody in the presence of IL-2 was shown to specifically induce HPGD expression in T_{reg} cells. However, it might be possible that the observed upregulation of HPGD was induced, for instance, by stimulation with IL-2 alone. This assumption is supported by the observations that the transcription factor activating protein-1 (AP-1) that can be activated by IL-2R signaling via MAPK signaling pathways [136,139], has potential binding sites in the promoter of HPGD [180]. It was therefore investigated whether induction of HPGD expression in T_{reg} cells was a result of TCR or IL-2R activation or due to synergistic effects of both signaling pathways. To assess the relevance of IL-2R signaling for HPGD expression in T_{reg} cells it was investigated whether HPGD expression could be upregulated by IL-2 stimulation alone. Therefore, T_{reg} and T_{conv} cells were isolated from human peripheral blood and stimulated for 12 h, 24 h, 48 h and 72 h with IL-2. The analysis revealed that HPGD was upregulated 2-fold in T_{reg} cells upon stimulation with IL-2 alone after 12 h with a maximum of 2.5-fold expression after 48 h (Figure 40). HPGD

expression in T_{conv} cells on the other hand was not influenced by IL-2 stimulation. This result shows that HPGD expression in T_{reg} cells is dependent on IL-2 signaling and HPGD upregulation can be also mediated by IL-2R signaling alone.

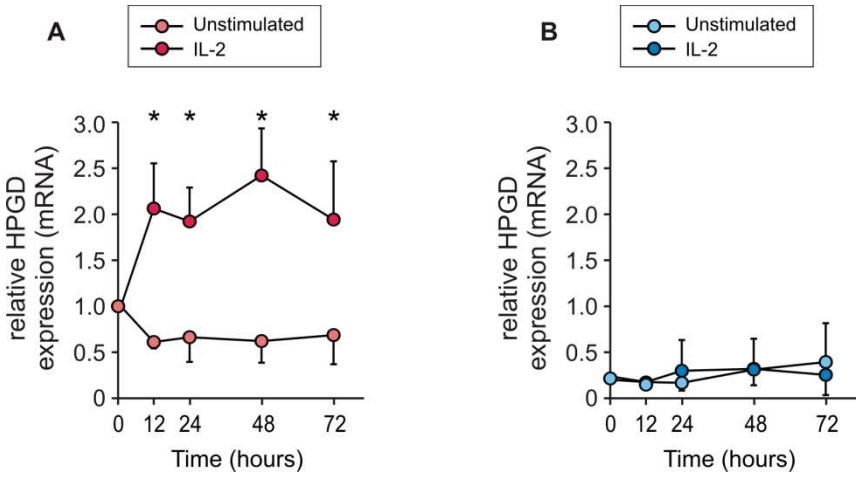

Figure 40: IL-2 stimulation specifically upregulates HPGD expression in regulatory T cells.
(**A**) Human T_{reg} and (**B**) T_{conv} cells were purified from peripheral blood and left untreated (Unstimulated) or stimulated with 20 U/ml IL-2 (IL-2) for 12 h, 24 h, 48 h and 72 h. HPGD mRNA expression, compared to B2M expression, was assessed by qRT-PCR. Samples are normalized to T_{reg} cells (0 h). Data represent mean values and standard deviations of four independent experiments. Statistically significant differences between unstimulated and IL-2 stimulated samples are marked with an asterisk (* $p < 0.05$).

HPGD mRNA expression values of T_{reg} cells, stimulated with IL-2 alone or in the presence of anti-CD3 antibody were compared with each other, but no significant differences between the two different stimulations were observed, as all expression values were relatively similar (Figure 41). This result further supports that IL-2 is important for the induction of HPGD and shows that HPGD upregulation can be also mediated by IL-2 stimulation alone and is not exclusively dependent on the combined effects of TCR and IL-2R signaling.

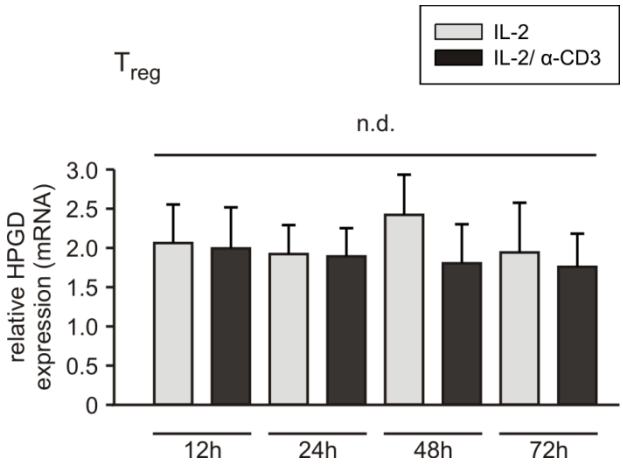

Figure 41: Induction of HPGD mRNA expression is equal after IL-2 or IL-2/ anti-CD3 stimulation.
Human T_{reg} cells were purified from peripheral blood and stimulated with 20 U/ml IL-2 alone (IL-2) or together with1 µg/ml anti-CD3 antibody (IL-2/ α-CD3) for 12 h, 24 h, 48 h and 72 h. HPGD mRNA expression, compared to B2M expression, was assessed by qRT-PCR. Samples are normalized to T_{reg} cells (0 h). Mean values and standard deviations of four independent experiments are shown. n.d.: no statistically significant differences (one-way ANOVA; $p > 0.05$) between sample groups were observed.

In the previous experiments it was shown that IL-2 receptor signaling alone was sufficient to upregulate HPGD expression in T_{reg} cells. In the following part it was therefore tested whether TCR activation alone would be also able to induce HPGD expression in T_{reg} cells. To answer the question whether TCR signaling can induce HPGD mRNA expression, human T_{reg} and T_{conv} cells were isolated from peripheral blood and anti-CD3-antibody was administered over a period of 72 h. Cells were incubated either with soluble anti-CD3-antibody or CD3-conjugated beads, which represents a more physiological way of inducing TCR signaling, as they mimic the contact of T cells with antigen-presenting cells, to determine possible differences between the two stimulation methods. After 12 h, 24 h, 48 h and 72 h cells were harvested and HPGD mRNA expression was assessed by qRT-PCR. As shown in Figure 42, HPGD expression was not upregulated in T_{reg} cells by any stimulation over a period of 72 h. As expected T_{conv} cells showed no enhanced HPGD expression upon TCR stimulation with soluble or bead coupled anti-CD3-antibody. This result suggests that HPGD expression is not influenced by TCR signaling and further supports that HPGD expression in T_{reg} cells is only dependent on IL-2 signaling.

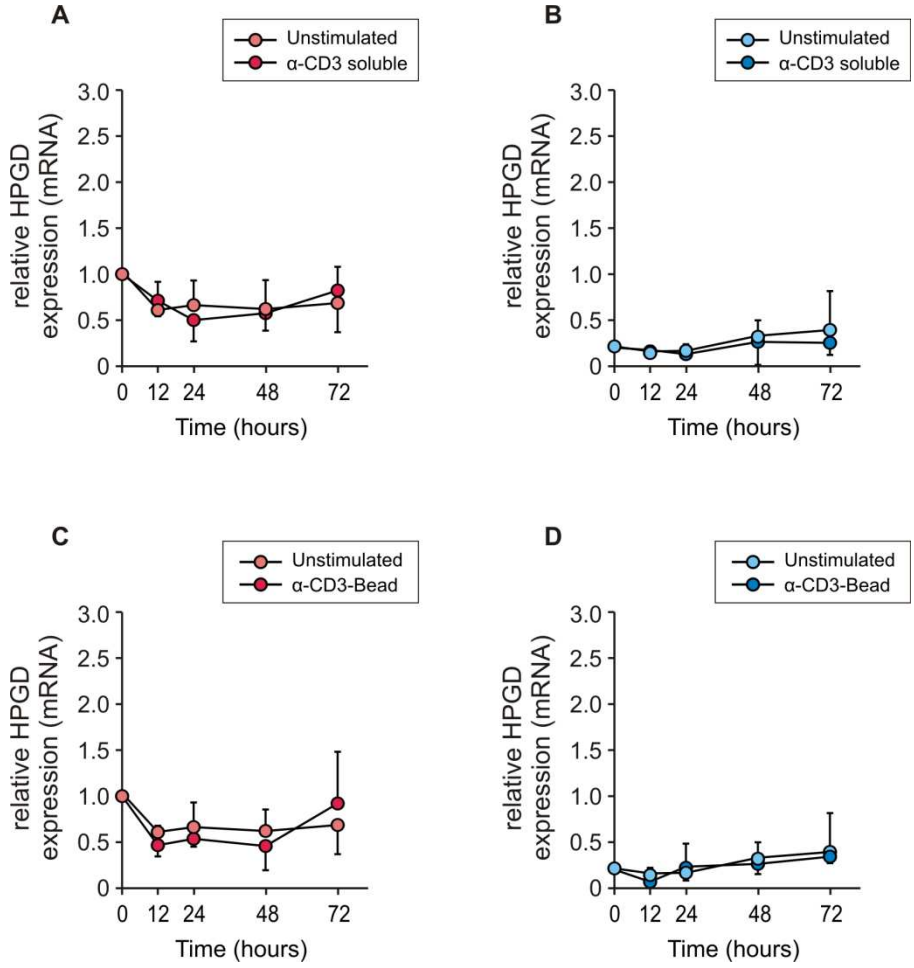

Figure 42: HPGD is not upregulated in T_{reg} or T_{conv} cells upon TCR stimulation.
(**A)** & (**C**) Human T_{reg} and (**B)** & (**D**) T_{conv} cells were purified from peripheral blood and were left untreated (Unstimulated) or stimulated with 1 µg/ml soluble anti-CD3 antibody (α-CD3 soluble) or with bead coupled anti-CD3 antibody (α-CD3-Bead; 2 beads: 1 cell) for 12 h, 24 h, 48 h and 72 h. HPGD mRNA expression, compared to B2M expression, was assessed by qRT-PCR. Samples are normalized to T_{reg} cells (0 h). Data represent mean values and standard deviations of at least three independent experiments.

In addition to TCR activation the influence of costimulation on HPGD expression in T_{reg} and T_{conv} cells was examined. Previous studies had demonstrated that T cell proliferation is differentially regulated in T_{reg} and T_{conv} cells and this could apply likewise to HPGD expression. Thornton et al. 2004 for example had shown that activation of T_{reg} cells was independent of CD80/CD86 costimulation and the additional stimulation with exogenous IL-2 could replace costimulation[233]. However, this observation was different for activation of T_{conv} cells, where IL-2 was not sufficient as a substitute for costimulation, demonstrating that the induction of T cell proliferation, even in the presence of IL-2, is different for T_{reg} and T_{conv} cells [233]. To examine a potential influence of costimulation on HPGD expression, T_{reg} and T_{conv} cells were purified from human peripheral blood and stimulated with anti-CD3/CD28/MHC-I-coated beads for 72 h. Cells were harvested after 12 h, 24 h, 48 h and 72 h and HPGD mRNA expression was assessed by qRT-PCR. Stimulation with

CD3/CD28/MHC-I – coated beads did not enhance HPGD mRNA expression neither in T_{reg} nor in T_{conv} cells, as shown in Figure 43 A and B.

These data suggest that HPGD expression is independent of TCR signaling and costimulation in T_{reg} as well as T_{conv} cells and further support that HPGD expression in T_{reg} cells is only dependent on IL-2R signaling.

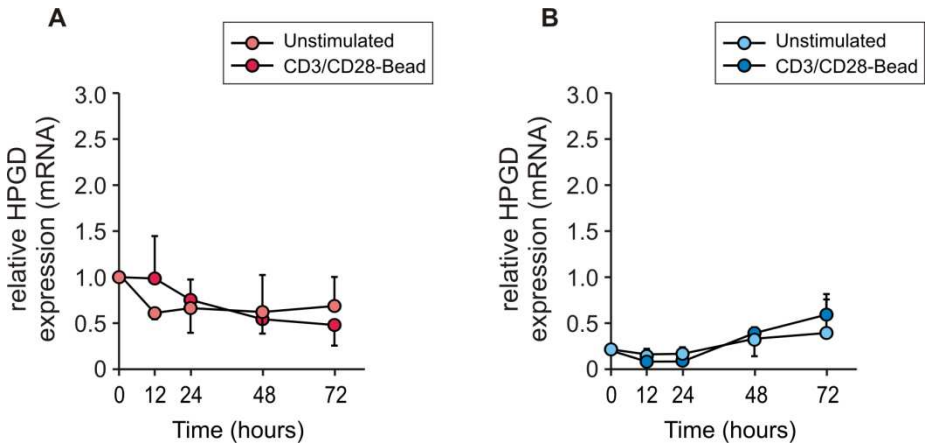

Figure 43: Costimulation via CD28 does not enhance HPGD expression in TCR-stimulated T_{reg} or T_{conv} cells.
(**A)** Human T_{reg} and (**B)** T_{conv} cells were purified from human peripheral blood and left untreated (Unstimulated) or stimulated with CD3/CD28/MHC-I-coated beads (CD3/CD28-Bead; 3 beads: 1 cell) for 12 h, 24 h, 48 h and 72 h. HPGD mRNA expression, compared to B2M expression, was assessed by qRT-PCR. Samples are normalized to T_{reg} cells (0 h). Mean values and standard deviations of at least three independent experiments are shown.

Next, HPGD mRNA expression levels of T_{reg} cells were compared after stimulation for 24 h with the previously mentioned stimuli, to further demonstrate that HPGD mRNA expression in T_{reg} cells is dependent on IL-2 signaling but not TCR signaling with or without costimulation (Figure 44 A). In contrast, HPGD mRNA expression in T_{conv} cells is independent of any of these stimulations, as IL-2 treatment and also TCR ligation with costimulation cannot induce HPGD expression in T_{conv} cells (Figure 44 B).

Taken together these results clearly illustrate that HPGD mRNA expression is differentially regulated in T_{reg} and T_{conv} cells and that IL-2 signaling plays an important role for HPGD expression in T_{reg} cells.

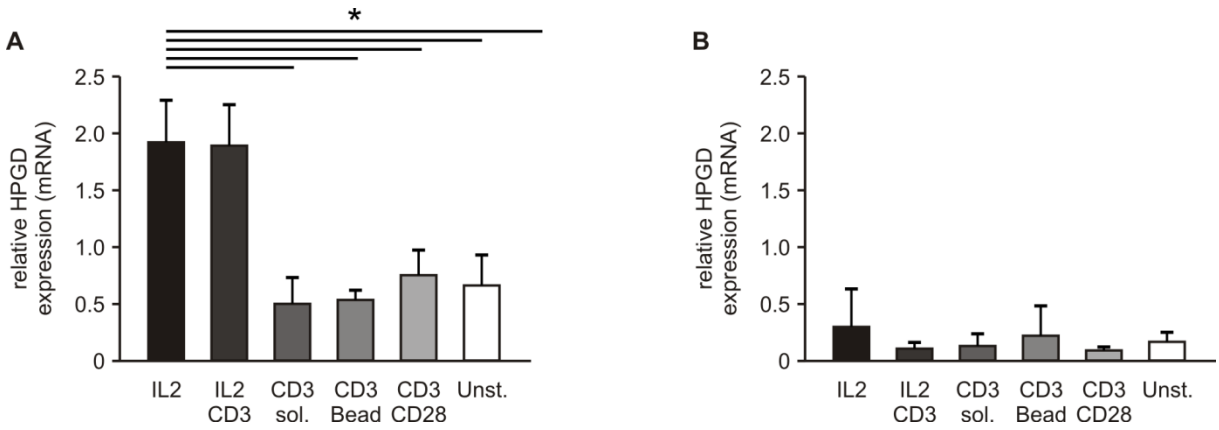

Figure 44: Influence of TCR ligation, costimulation and IL-2 on HPGD expression in T_{reg} and T_{conv} after 24 h stimulation

(**A**) Human T_{reg} and (**B**) T_{conv} cells were purified from peripheral blood and left untreated (Unst.) or stimulated for 24 h with 20 U/ml IL-2 (IL-2) alone or in combination with 1 µg/ml anti-CD3 antibody (IL2/CD3), with 1 µg/ml soluble anti-CD3 antibody (CD3 sol.), with bead bound anti-CD3 antibody (CD3-Bead; 3 beads:1 cell) or with CD3/CD28/MHC-I-coated beads (CD3CD28, 3 beads: 1cell). HPGD mRNA expression, compared to B2M expression, was assessed by qRT-PCR. Samples are normalized to T_{reg} cells (0 h). Data represent mean values and standard deviations of four independent experiments. Statistically significant differences are marked with an asterisk (* $p < 0.05$).

3.5.3 HPGD protein expression after stimulation with IL-2

HPGD mRNA expression was shown to be significantly upregulated upon stimulation with IL-2 in human T_{reg} cells. To determine if the upregulation of HPGD on mRNA level also resulted in an increase of HPGD protein expression, T_{reg} and T_{conv} cells were purified from human peripheral blood and stimulated with IL-2 or left untreated. After 48 h and 72 h cells were harvested and HPGD protein levels were investigated by Western blotting. Assessment of HPGD protein expression in T_{reg} and T_{conv} cells after 48 h and 72 h showed an enhanced HPGD expression upon IL-2 stimulation in T_{reg} whereas this effect could not be observed for T_{conv} cells, depicted in Figure 45.

These results show that HPGD expression in T_{reg} cells is highly dependent of IL-2R signaling, as both HPGD mRNA and protein expression are significantly enhanced after stimulation with IL-2.

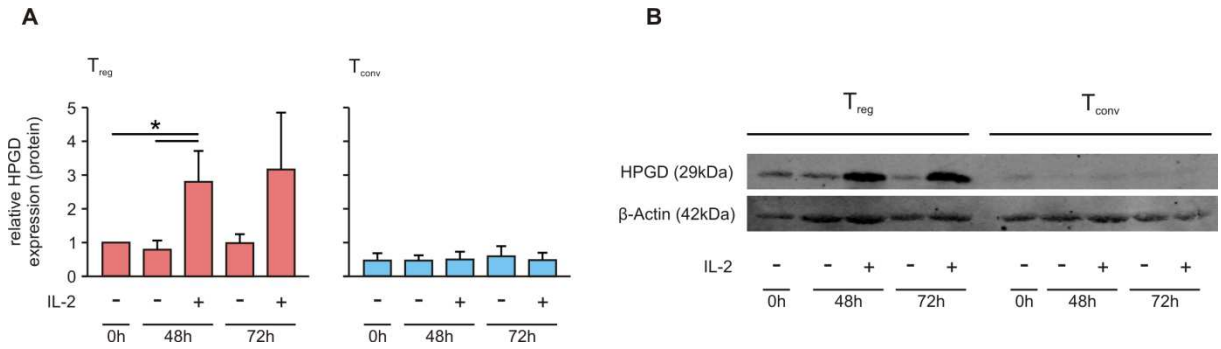

Figure 45: HPGD protein expression is specifically upregulated in T_{reg} cells upon IL-2 stimulation.
Human T_{reg} and T_{conv} cells were purified from peripheral blood and left untreated (-) or stimulated with 20 U/ml IL-2 (+). Cells were harvested after 48 h and 72 h and protein expression of HPGD and β-actin as loading control was analyzed by Western blotting. (**A**) The relative HPGD protein amounts, compared to β-actin, were measured densitometrically. Data represent mean values and standard deviations of at least three independent experiments. Data were normalized to T_{reg} 0 h. Statistically significant differences are marked with an asterisk (* $p < 0.05$). (**B**) One representative Western Blot is shown.

3.5.4 HPGD expression in regulatory T cells is even induced by very low levels of IL-2

The cytokine IL-2 is vitally important for T_{reg} cells because on the one hand they are unable to produce IL-2 themselves [27] and on the other hand they are highly dependable of IL-2, in terms of their development and function [234,235]. Moreover, it was recently shown that also low IL-2 concentrations were sufficient to maintain gene expression of IL-2-dependent target genes in T_{reg} cells [236]. In view of these observations it is of high interest to determine the effects of different IL-2 concentrations on the HPGD expression. To elucidate whether increasing IL-2 concentrations would further enhance HPGD expression and define in addition a minimum IL-2 concentration that would still be able to upregulate HPGD expression, T_{reg} cells were stimulated with different IL-2 concentrations, varying from 1.000 – 0.5 U IL-2/ ml and relative HPGD mRNA expression was analyzed by qRT-PCR after 12 h, 24 h, 48 h and 72 h. Even very low IL-2 concentrations were able to enhance HPGD expression in T_{reg} cells (Figure 46). Notably, maximum HPGD expression was induced using as low as 5-10 U IL-2 per ml while no further increase in HPGD expression was observed when higher IL-2 concentrations were used.

This result suggests that HPGD expression in T_{reg} cells is coupled to a low IL-2R signaling threshold and only low amounts of IL-2 are required to saturate the signaling pathways that lead to HPGD upregulation.

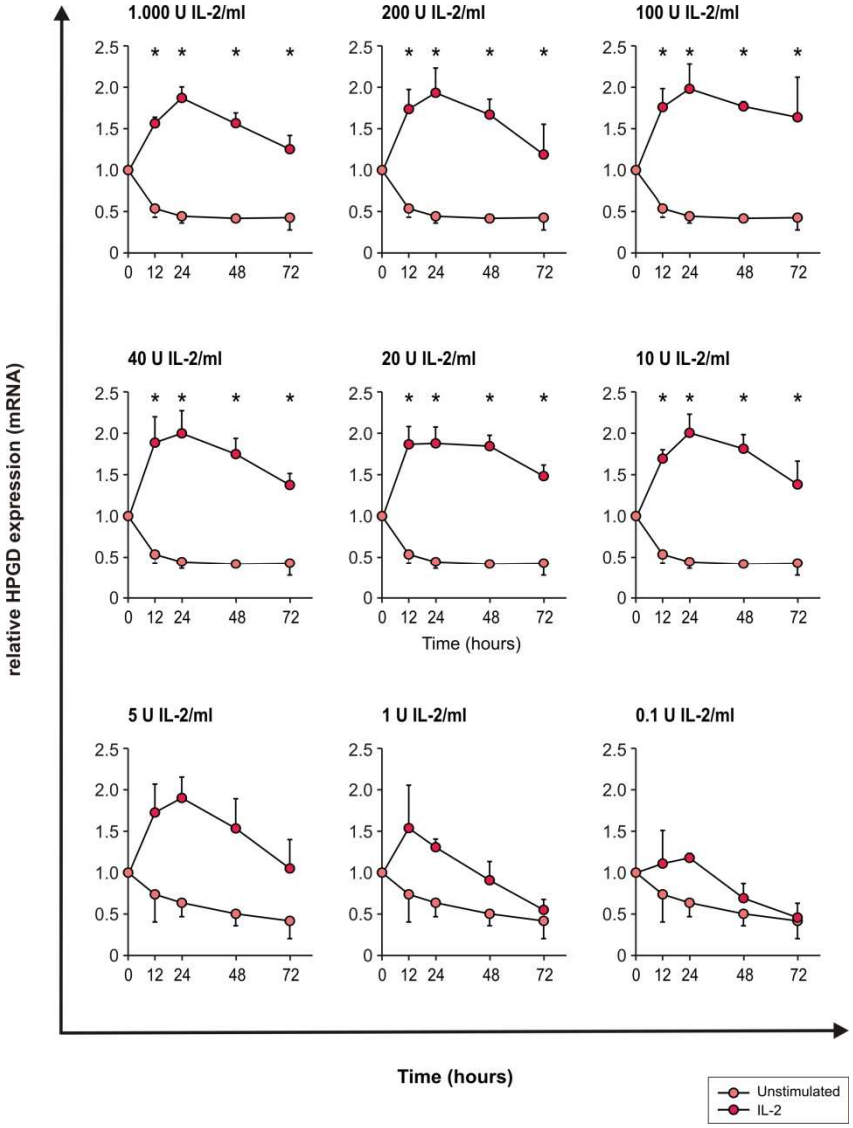

Figure 46: Influence of different IL-2 concentrations on the relative HPGD mRNA expression in T_{reg} cells
Human T_{reg} cells were purified from peripheral blood and left untreated (Unstimulated) or stimulated with different IL-2 concentrations (IL-2). Cells were incubated with concentrations of 1.000, 200, 100, 40, 20, 10, 5, 1 and 0.5 U/ml IL-2. HPGD mRNA expression was assessed by qRT-PCR, compared to B2M expression. Samples are normalized to T_{reg} cells (0 h). Data represent mean values and standard deviations of five independent experiments in row 1-2 and two independent experiments in row 3. Statistically significant differences are marked with an asterisk (* $p < 0.05$).

In addition the HPGD expression at 24 h for all tested IL-2 concentrations is depicted in Figure 47. No further increase in HPGD expression using IL-2 concentrations higher than 5 U/ml could be observed. These data further illustrate that even low IL-2 amounts can enhance HPGD expression in T_{reg} cells and a minimum of 5 U/ml IL-2 is required to induce the maximum of HPGD expression in T_{reg} cells.

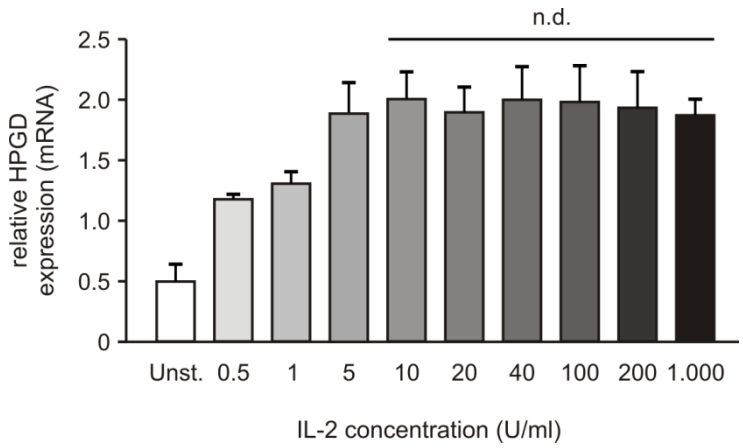

Figure 47: HPGD expression at 24 h in T_{reg} cells stimulated with increasing IL-2 concentrations
Cells were treated and assessed as described for Figure 48 Data represent mean values and standard deviations of five independent experiments for 10 – 1.000 U/ml, and two independent experiments for 0.5-5 U/ml. n.d.: no statistically significant differences (one-way ANOVA; $p > 0.05$) between the sample groups were observed.

3.5.5 IL-2 stimulation does not upregulate HPGD expression in differentiated T cells

Previous results had demonstrated that HPGD expression was not upregulated during T cell differentiation. As HPGD expression in T_{reg} cells was shown to be induced by IL-2R signaling, the question was whether IL-2 stimulation would also have an influence on HPGD in T_H cell subsets. To answer the question whether IL-2R signaling would similarly induce HPGD expression in differentiated T cells, various T_H cell subsets were stimulated with IL-2 to investigate the effect on HPGD expression.

For this purpose T_{naive} cells were differentiated towards T_H1, T_H2, T_H9 and T_H17, as previously described (see section 3.3.2) and then stimulated with IL-2. Relative HPGD mRNA expression was determined by qRT-PCR in the T_H cell subsets after 48 h with or without IL-2 stimulation. Relative HPGD expression levels are presented in comparison to T_{conv} and T_{reg} cells with or without IL-2 stimulation. HPGD expression was not significantly altered upon IL-2 stimulation in the differentiated T cell subsets and HPGD expression levels were comparable to T_{conv} cells, as shown in Figure 48. In contrast, T_{reg} cells displayed a significantly higher HPGD expression upon IL-2 treatment.

Taken together these data show that regulation of HPGD expression is distinct in T_{reg} cells compared to T_H cell lineages and that IL-2R signaling does not enhance HPGD expression in differentiated T cells. Furthermore, the results support the hypothesis that elevated HPGD expression levels are specific for T_{reg} cells.

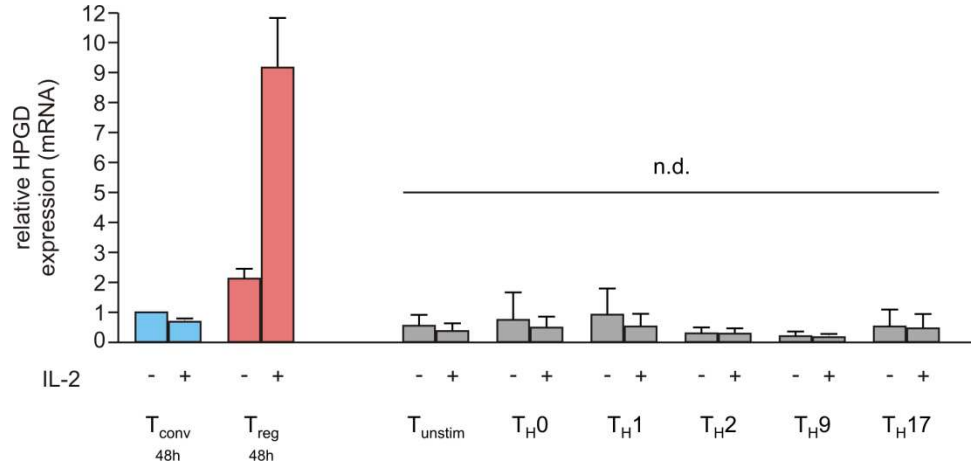

Figure 48: IL-2 stimulation does not enhance HPGD expression in different T helper cell subsets.
Human $CD4^+CD25^-CD45RA^+$ T_{naive} cells were purified and differentiated with CD3/CD28/MHC-I-coated beads together with the appropriate cytokines towards T_H1, T_H2, T_H9 and T_H17 cells. T_{unstim} represent unstimulated T_{naive} and served as control together with T_H0 cells which were only stimulated with CD3/CD28/MHC-I-coated beads without additional cytokines. T_H cells were left untreated (-) or stimulated with 20 U/ml IL-2 (+) for 48 h. Relative HPGD mRNA expression, compared to B2M expression, was assessed by qRT-PCR and data are plotted compared to T_{reg}, (48 h) and T_{conv} (48 h). Mean values and standard deviations of three independent experiments after normalization to unstimulated T_{conv} cells (48 h) are shown. n.d.: no statistically significant differences (one-way ANOVA; $p > 0.05$) between the sample groups were observed.

3.5.6 HPGD expression is not enhanced in iT_{reg} cells upon IL-2R signaling

Similarly to T_H cell subsets also iT_{reg} cells did not displayed an enhanced HPGD expression, comparable to T_{reg} cells. On the one hand iT_{reg} cells were shown to lack a part of the gene signature, which is specific for nT_{reg} cells [228]. On the other hand they display T_{reg} specific characteristics such as high a FOXP3 expression, anergy and suppressive function *in vitro* and *in vivo* [30,227]. Although iT_{reg} cells did not show enhanced HPGD expression they might still upregulate HPGD upon activation with IL-2. To answer the question whether HPGD expression can be induced in iT_{reg} upon IL-2R signaling, T_{naive} were differentiated towards iT_{reg} cells, as previously described (see section 3.3.3) and stimulated with IL-2 for 48 h. Relative HPGD mRNA expression was determined by qRT-PCR after 48 h with or without IL-2 stimulation. Relative HPGD expression levels are presented in comparison to T_{conv} and T_{reg} cells with or without IL-2 stimulation. Notably, stimulation with IL-2 did not result in the induction of HPGD mRNA expression in iT_{reg} cells, as it was observed for T_{reg} cells, shown in Figure 49. In fact HPGD expression levels of iT_{reg} cells, with or without IL-2 stimulation, were comparable with those of T_{unstim}, T_H0 and T_{conv} cells.

Apparently, polarization towards an induced regulatory phenotype was not sufficient to activate the essential gene expression programs, which lead to enhanced HPGD expression in T_{reg} cells and thus IL-2R signaling could also not induce HPGD expression. Obviously,

HPGD expression and regulation in T_{reg} cells are distinct from iT_{reg} cells and HPGD seems to belong to the natural T_{reg}-specific gene signature. Taken together these data indicate that a high HPGD expression is specific for natural T_{reg} cells.

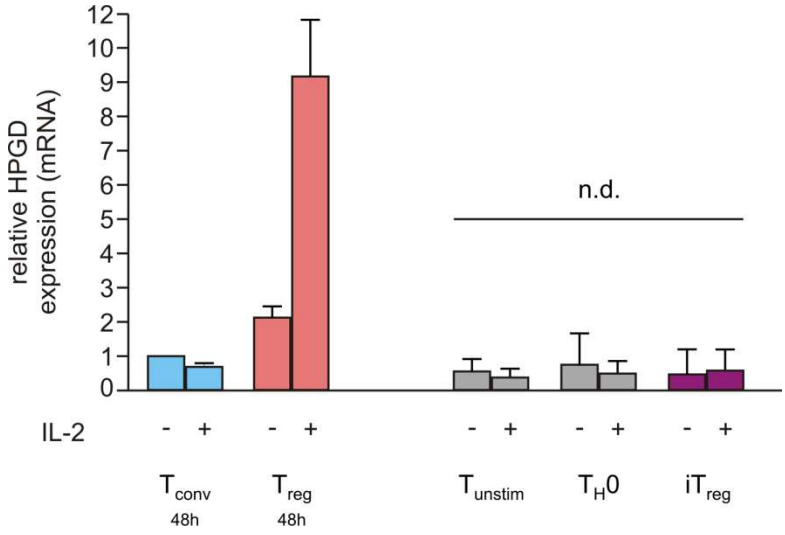

Figure 49: IL-2 stimulation does not enhance HPGD expression in iT_{reg} cells.
Cells were treated and assessed as described for Figure 48. T_{unstim} represent unstimulated T_{naive} and served as control together with T_H0 cells, which were only stimulated with CD3/CD28/MHC-I-coated beads without additional cytokines. HPGD mRNA expression was assessed, compared to B2M, by qRT-PCR. Data are shown compared to T_{reg} (48 h) and T_{conv} (48 h) cells. Mean values and standard deviations of three independent experiments are shown after normalization to unstimulated T_{conv} cells (48 h). n.d.: no statistically significant differences (one-way ANOVA; $p > 0.05$) between the sample groups were observed.

3.6 HPGD is enzymatically active in human regulatory T cells

The HPGD is one of the major enzymes that metabolize prostaglandin E_2 [141,237]. The critical step is thereby the β-oxidation of the 15-hydroxyl group of PGE_2 into a 15-keto group. The conversion into the 15-keto-metabolite thereby represents the first step in the biological inactivation of PGE_2 [141,163]. Enzymatically active HPGD degrades PGE_2, which leads to accumulation of PGE_2-metabolites. However, expression of the HPGD protein does not necessarily result in functional enzymatic activity. To prove that HPGD is functional in T_{reg} cells, the enzymatic activity of HPGD was tested in human T_{reg} and also T_{conv} cells. Therefore, these cells were isolated from human peripheral blood and stimulated with IL-2 for 48 h in order to upregulate HPGD expression in T_{reg} cells prior to further processing. Successful HPGD upregulation was confirmed by qRT-PCR (Figure 50). Enzymatic activity of HPGD was determined in cellular lysates by an radioactive assay, which measures the transfer of tritium from 15(S)-[15-^{3}H]PGE_2 to glutamate by coupling HPGD with glutamate dehydrogenase [178,205]. T_{reg} cells show a high enzymatic activity of HPGD in comparison to T_{conv} cells (Figure 50). The levels of enzymatic activity thereby reflect the differences

between T_{reg} and T_{conv} cells in HPGD mRNA expression, as T_{conv} cells with a low HPGD mRNA expression also display a low enzymatic activity, whereas high HPGD mRNA expression and high enzymatic activity are observed in T_{reg} cells. These data show that human T_{reg} cell express an active and functional enzyme with specific activity.

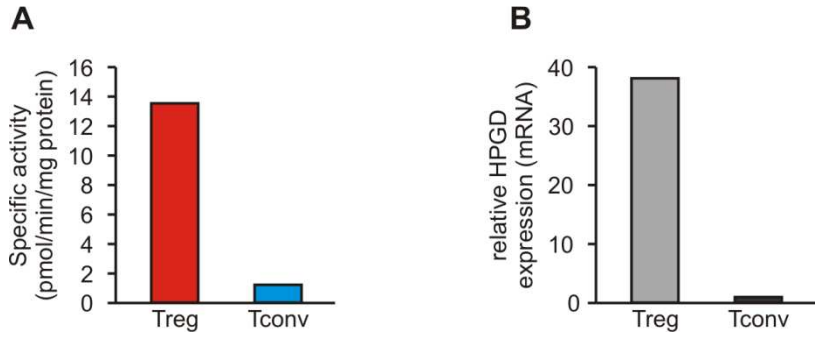

Figure 50: HPGD is enzymatically active in human T_{reg} cells.
Human T_{reg} and T_{conv} cells were purified and stimulated with 20 U/ml IL-2 for 48 h prior to assessment of enzymatic activity. (**A)** Enzymatic activity of HPGD was measured by an radioactive assay that measures the transfer of 15(S)-[15-^{3}H]PGE_2 to glutamate by coupling HPGD with glutamate dehydrogenase. The specific activity of HPGD is depicted as pmol/min/mg protein. (**B)** Relative HPGD expression was assessed by qRT-PCR in T_{reg} and T_{conv} cells and data are normalized to the house keeping control β2M. One representative experiment of two is shown.

3.7 Increased HPGD expression in T_{reg} by IL-2 is dependent on JAK3/STAT5 and PI3K/NF-κB signaling

In the previous experiments it was demonstrated that HPGD expression was significantly enhanced in T_{reg} cells upon stimulation with IL-2. Binding of IL-2 to its receptor leads to activation of different signaling cascades, such as the MAPK and PI3K pathways or JAK/STAT signaling (see also 1.2 Interleukin-2 receptor signaling pathways)[238-242]. The contribution of the above mentioned signaling cascades to upregulation of HPGD in T_{reg} cells was examined by targeting key molecules of the respective pathways with specific inhibitors to elucidate which signaling cascades are in particular involved in IL-2-mediated upregulation of HPGD.

3.7.1 MAPK signaling is not involved in IL-2 mediated HPGD upregulation

To test if signaling events via mitogen-activated protein kinases (MAPK) were involved in IL-2 mediated HPGD upregulation, human T_{reg} cells, were treated with increasing doses of a MEK1 inhibitor (PD98059) with or without additional IL-2 stimulation. T_{reg} cells were pre-

incubated with the inhibitors for 1 h before additional costimulation with IL-2 was initiated. Thus an activation of the IL-2 signaling pathway was avoided before the inhibitor could attain its complete inhibitory effect. HPGD mRNA expression was assessed by qRT-PCR after 24 h. In addition, to exclude effects by the inhibitor on cell death and apoptosis rate, cell viability of human $CD4^+$ T lymphocytes was assessed by measuring incorporation of propidium iodide (PI), after incubation with the inhibitor for of 24 h. Thereby, no toxic effects were observed at the indicated concentrations (see Figure 73, Appendix E). No reduction in the IL-2-mediated upregulation of HPGD was observed upon treatment with the MEK1 inhibitor (Figure 51). Although incubation with the MEK1 inhibitor together with IL-2 slightly enhanced HPGD expression in comparison to DMSO-treated control cells, this increase was not statistically significant. These results therefore suggest that induction of HPGD expression in T_{reg} cells by IL-2 is independent of MAPK signaling.

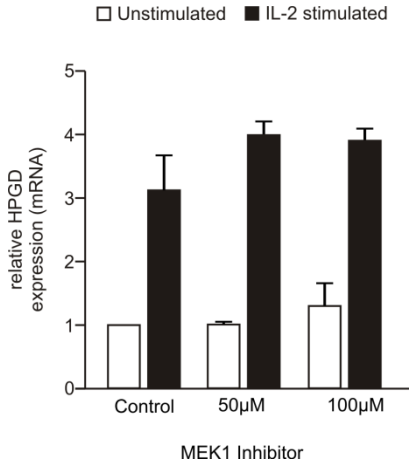

Figure 51: Unchanged upregulation of HPGD in T_{reg} cells after MEK1 inhibition.
Human $CD4^+CD25^+$ T cells were purified from peripheral blood and pre-treated with 50 or 100 µM MEK1 inhibitor (PD98059) or with the respective amount of DMSO (Control) for 1 h. Then 20 U/ml IL-2 (IL-2 stimulated) or medium (Unstimulated) was added. Relative HPGD mRNA expression, compared to B2M expression, was assessed by qRT-PCR 24 h after inhibitor treatment. Mean values and standard deviations of three individual experiments are presented, after normalization to unstimulated control cells.

3.7.2 Inhibition of PI3K and NF-κB decreases IL-2 mediated HPGD upregulation

In the experiments described above it was shown that MAPK signaling was not involved in IL-2-mediated HPGD upregulation. However, upon IL-2R activation besides activation of MAPK also signaling molecules such as the Janus kinase-1 and -3 are activated, which lead to subsequent activation and recruitment of the phosphatidylinositol 3-kinase (PI3K) [126,243]. Therefore, a potential role of the PI3K pathway was investigated. Human T_{reg} cells were treated with increasing doses of a PI3K inhibitor (LY294002) with or without additional IL-2 stimulation. To avoid effects of IL-2 signaling before the inhibitor could mediate its inhibitory effect, T_{reg} cells were pre-incubated with the inhibitor for 1 h before additional costimulation with IL-2 was initiated. HPGD mRNA expression was assessed by qRT-PCR after 24 h of

inhibitor treatment. Moreover, human $CD4^+$ T lymphocytes were stained with PI, after incubation with the inhibitor for 24 h, to test and exclude effects of the inhibitor concerning cell death and apoptosis rate. No toxic effects were observed at the indicated concentrations (see Figure 73, Appendix E). In Figure 52, it is shown that inhibition of PI3K blocks IL-2 mediated HPGD upregulation, as a concentration of 20 µM PI3K inhibitor significantly reduced IL-2-mediated HPGD upregulation. These results indicate a potential role for the PI3K signaling pathway in IL-2-mediated upregulation of HPGD.

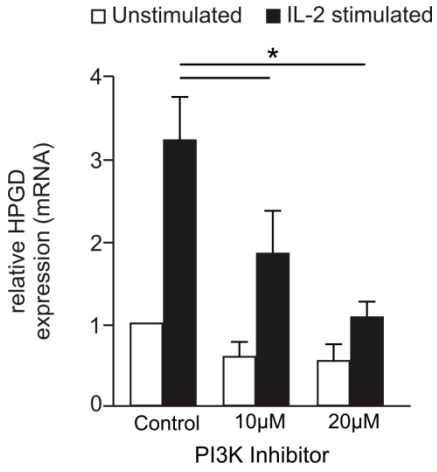

Figure 52: Inhibition of PI3K decreases IL-2 mediated upregulation of HPGD in T_{reg} cells.
Human $CD4^+CD25^+$ T cells were purified from peripheral blood and pre-treated with 10 or 20 µM PI3K inhibitor (LY249002) or with the respective amount of DMSO (Control) for 1 h. Then 20 U/ml IL-2 (IL-2 stimulated) or medium (Unstimulated) were added. Relative HPGD mRNA expression, compared to B2M expression, was assessed by qRT-PCR 24 h after inhibitor treatment. Data are shown as mean values and standard deviations of four individual experiments. Statistical significant differences ($p < 0.01$) are marked with an asterisk.

The activation of PI3K upon IL-2R signaling leads to production of inositol phospholipids PtdIns (3,4,5)P3 and PtdIns(3,4)P2, which attract Akt (also known as Protein Kinase B, PKB) to the plasma membrane where it is phosphorylated[130]. Akt in turn phosphorylates and thus activates IκB kinase (IKK), which is comprised of the catalytic subunits IKK-α and IKK-β and the regulatory subunit IKK-γ (NEMO)[131-133]. IKK phosphorylates the inhibitor of κBα protein (IκBα), which leads to ubiquitination of IκBα, its dissociation from nuclear factor κB (NF-κB, subunits p50 and p65) and eventual degradation of IκBα by the proteasome. The release of NF-κB allows its translocation to the nucleus where it initializes transcription[132-134]. As IL-2-mediated upregulation of HPGD in T_{reg} cells was shown to be dependent of PI3K signaling, the next question was whether NF-κB inhibition would impair the inducing effect of IL-2 on HPGD expression. To answer this question T_{reg} cells were purified from human peripheral blood and treated with increasing doses of NF-κB inhibitor BAY11-7082 or with an alternative NF-κB activation inhibitor. As described above, T_{reg} cells were pre-incubated with the inhibitors for 1 h before additional costimulation with IL-2 was initiated, to avoid activation of the IL-2 signaling pathway before the inhibitor could mediate its inhibitory

effect. HPGD mRNA expression was assessed by qRT-PCR after 24 h. Incubation with 1 µM of NF-κB inhibitor BAY11-7082 did reduce IL-2-mediated upregulation of HPGD, although this effect was not statistically significant. However, incubation with 20 µM of the NF-κB activation inhibitor did significantly reduce the IL-2 induced upregulation of HPGD expression. To exclude toxic effects of the inhibitors with regard to cell death and apoptosis rate, human $CD4^+$ T lymphocytes were incubated with the inhibitor for 24 h and the percentage of dead cells was analyzed by (PI) staining. The inhibitors did not show toxic effects at the indicated concentrations (see Figure 73, Appendix E). Taken together, these results point to a potential role of the PI3K pathway in IL-2 mediated HPGD upregulation, as both blockade of PI3K and NF-κB signaling resulted in a significantly impaired upregulation of HPGD expression after IL-2 administration.

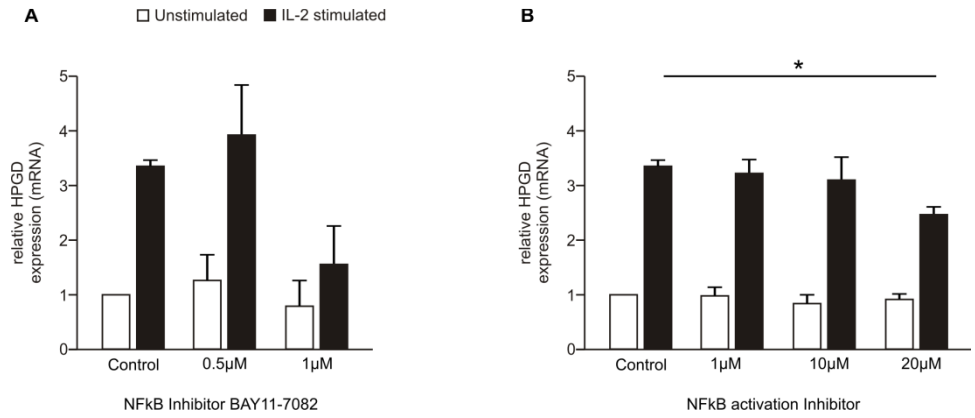

Figure 53: Inhibition of NF-κB blocks IL-2 mediated upregulation of HPGD in T_{reg} cells.
Human $CD4^+CD25^+$ T cells were purified from peripheral blood and pre-treated with different concentrations of one NF-κB inhibitor or with the respective amount of DMSO (Control) for 1 h. Then 20 U/ml IL-2 (IL-2 stimulated) or medium (Unstimulated) was added. Relative HPGD mRNA expression, compared to B2M, was assessed by qRT-PCR 24 h after inhibitor treatment. (**A**) Relative HPGD mRNA expression after treatment with NF-κB inhibitor BAY11-7082. (**B**) Relative HPGD mRNA expression after treatment with NF-κB activation inhibitor. Data represent mean values and standard deviations of four individual experiments. Statistical significant differences ($p < 0.05$) are marked with an asterisk.

3.7.3 JAK3 and STAT5 signaling are involved in IL-2 mediated HPGD upregulation

Besides activation of the PI3K or MAPK pathways, activation of the IL-2 receptor also initiates subsequent activation of JAK3 which in turn activates STAT5. This leads to dimerisation and nuclear translocation of STAT5 where it influences the expression of various genes [129]. To address how JAK3 and STAT5 signaling contributes to the upregulation of HPGD after IL-2 stimulation, T_{reg} cells were treated with specific inhibitors of JAK3 or STAT5 before stimulation with IL-2 was conducted. To exclude toxic effects of the inhibitor,

regarding cell death and apoptosis, human $CD4^+$ T lymphocytes were stained with PI, after incubation with the inhibitor for 24 h. Both inhibitors revealed no toxic effects at the indicated concentrations (see Figure 73, Appendix E). To avoid effects of IL-2 signaling before the inhibitor could mediate its inhibitory effect, T_{reg} cells were pre-incubated with the inhibitor for 1 h before additional costimulation with IL-2 was initiated. HPGD mRNA expression was assessed by qRT-PCR after 24 h of inhibitor treatment.

In Figure 54, it is shown that the stimulating effects of IL-2 on HPGD expression were significantly reduced by inhibition of JAK3 using the selective JAK3 inhibitor Janex-1. HPGD was not upregulated upon IL-2 stimulation when cells were incubated with 100 or 150 µM JAK3 inhibitor.

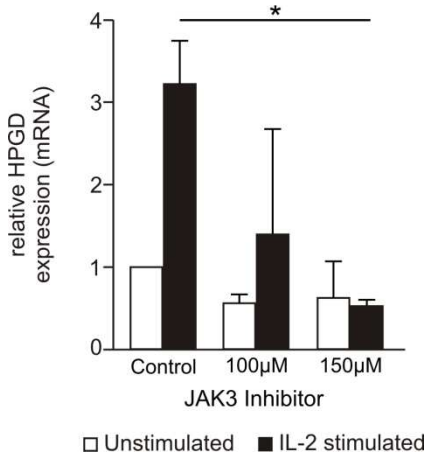

Figure 54: Inhibition of JAK3 decreases IL-2 mediated upregulation of HPGD in T_{reg} cells.
Human $CD4^+CD25^+$ T cells were purified from peripheral blood and pre-treated with 100 or 150 µM JAK3 inhibitor Janex-1 or with the respective amount of DMSO (Control) for 1 h. Then IL-2 (20 U/ml) (IL-2 stimulated) or medium (Unstimulated) was added. Relative HPGD mRNA expression, compared to B2M expression, was assessed by qRT-PCR 24 h after inhibitor treatment. Data are shown as mean values and standard deviations of four individual experiments. Statistical significant differences ($p < 0.01$) are marked with an asterisk.

As JAK3 signaling was shown to be involved in IL-2-mediated HPGD upregulation, we next asked whether inhibition of STAT5 might impair IL-2-induced upregulation of HPGD expression in T_{reg} cells. To answer this question T_{reg} cells were treated with increasing doses of a STAT5-specific inhibitor. T_{reg} cells were pre-incubated with the inhibitors for 1 h before additional costimulation with IL-2 was initiated, to avoid activation of the IL-2 signaling pathway until the inhibitor could mediate its inhibitory effect. HPGD mRNA expression was assessed by qRT-PCR after 24 h.

Similar effects as for experiments with JAK3 inhibitor were obtained when T_{reg} cells were treated with the STAT5 inhibitor. The STAT5 inhibitor blocked IL-2-mediated HPGD upregulation, as cells treated with 300 µM STAT5 inhibitor significantly reduced IL-2-mediated induction of HPGD (Figure 55), while lower concentrations of the inhibitor even resulted in a minor increase of HPGD expression.

These results confirm that JAK3/STAT5 signaling plays a role in IL-2 induced upregulation of HPGD expression in T_{reg} cells. Taken together the experiments addressing the three different signaling pathways for IL-2 signaling could show that the induction of HPGD in T_{reg} cells is dependent upon PI3K/NF-κB and JAK3/STAT5 signaling but MAPK signaling is not involved.

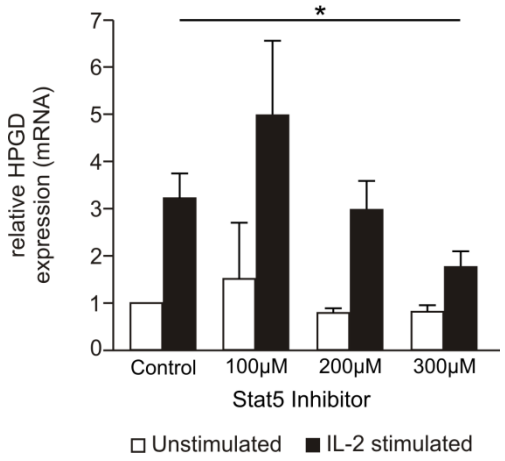

Figure 55: STAT5 inhibition decreases IL-2 mediated upregulation of HPGD in T_{reg} cells.
Human $CD4^+CD25^+$ T cells were purified from peripheral blood and pre-treated with 100, 200 or 300 µM JAK3 inhibitor or with the respective amount of DMSO (Control) for 1 h. Then 20 U/ml IL-2 (IL-2 stimulated) or medium (Unstimulated) was added. Relative HPGD mRNA expression was assessed by qRT-PCR 24 h after inhibitor treatment. Mean and standard deviations of four individual experiments are presented. Statistical significant differences ($p < 0.05$) are marked with an asterisk.

3.8 IL-10 and PGE_2 can augment the IL-2 dependent upregulation of HPGD

It could be demonstrated that IL-2 stimulation enhances HPGD expression. Besides that, also IL-10 stimulation did modulate HPGD expression, as HPGD expression was significantly higher after 24 h in IL-10 stimulated T_{reg} cells compared to unstimulated cells. In contrast, stimulation with PGE_2 or TGF-β did not influence HPGD expression in T_{reg} cells, suggesting that HPGD expression in T_{reg} cells is independent of PGE_2 and TGF-β signaling. In the following it was investigated whether the upregulation of HPGD expression in T_{reg} cells after IL-2 treatment would be influenced by costimulation with IL-10, PGE_2 or TGF-β over time. Human T_{reg} cells were therefore stimulated with IL-2 and incubated with the respective molecules. After 24 h, 48 h and 72 h HPGD mRNA expression was measured by qRT-PCR. Additional stimulation with PGE_2 or IL-10 further enhanced HPGD expression in comparison to T_{reg} cells treated with IL-2 alone, as shown in Figure 56. In contrast, co-stimulation with TGF-β decreased HPGD expression.

These rather unexpected results suggest that IL-10 and PGE_2 in combination with IL-2 costimulation have positive synergistic effects on HPGD mRNA expression in T_{reg} cells, as no or only slight effects were observed when cells are stimulated with IL-10 or PGE_2 alone. On

the contrary, TGF-β revealed a negative effect on IL-2 mediated upregulation of HPGD mRNA expression in T_{reg} cells, despite that no effect was observed when cells were stimulated with TGF-β alone. These data indicate that TGF-β partially blocks IL-2R signaling and thus attenuates the inducing effects of IL-2 on HPGD expression in T_{reg} cells. Furthermore, these results indicate that TGF-β signaling might interfere with HPGD upregulation during the induction of an iT_{reg} cell phenotype and represent a reason for a low HPGD expression in iT_{reg} cells compared to nT_{reg} cells.

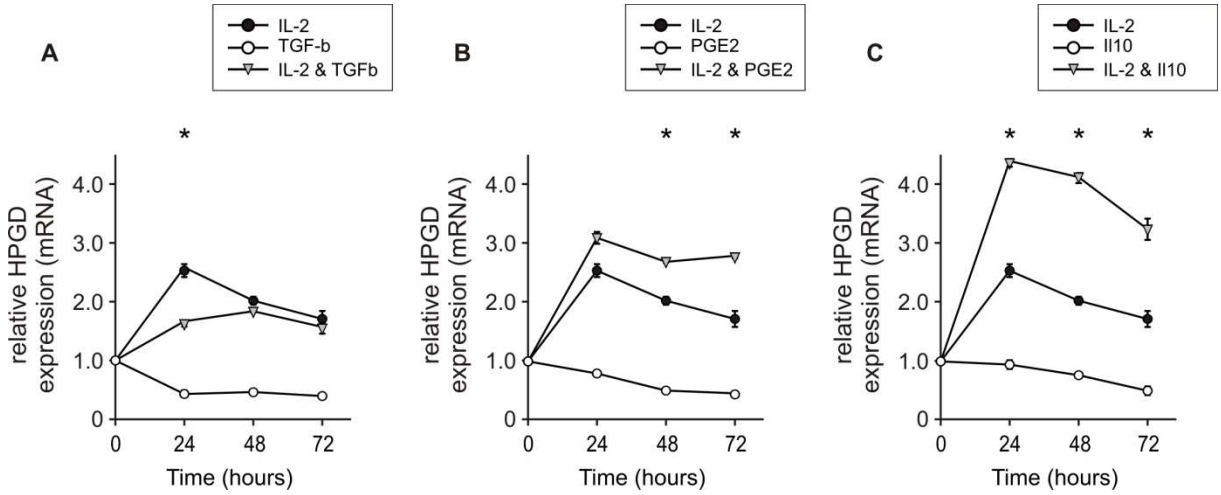

Figure 56: Stimulation with PGE_2 or IL-10 further enhances IL-2 mediated HPGD upregulation
Human $CD4^+CD25^+$ T cells were purified from peripheral blood and incubated with 20 U/ml IL-2 alone or in combination with (**A**) 30 ng/ml TGF-β, (**B**) 1 µM PGE2 or (**C**) 50 ng/ml IL-10 for 24 h, 48 h and 72 h. Relative HPGD mRNA expression, compared to B2M expression, was assessed by qRT-PCR. Mean values and standard deviations of one representative experiment of three are presented, after normalization to T_{reg} cells 0h. Statistical significant differences ($p < 0.05$) between IL-2 stimulated cells and cells treated with IL-2 in combination with TGF-β, PGE2 or IL-10 are marked with an asterisk.

3.9 Murine regulatory T cells show no upregulation of HPGD

3.9.1 HPGD is expressed at similar levels in mouse T_{conv} and T_{reg} cells from C57BL/6 or BALB/c mice

3.9.1.1 Low HPGD expression in T_{reg} cells from C57BL/6 mice compared to T_{conv} cells

After characterizing expression of HPGD in human T_{reg} cells, we wanted to determine its expression in murine T_{reg} cells, to see if the observations made in the human could be transferred to the murine system. Therefore, murine T_{reg} and T_{conv} cells were isolated from spleens of C57BL/6 mice and relative HPGD mRNA expression was assessed by qRT-PCR analysis. Remarkably, murine T_{reg} showed a lower HPGD expression compared to T_{conv} cells (Figure 57). This stands in sharp contrast to previous observations made in the human system,

as human T_{reg} cells showed a significantly higher HPGD mRNA and protein expression than T_{conv} cells. This result therefore suggests that HPGD expression in human T_{reg} cells differs from that in murine cells.

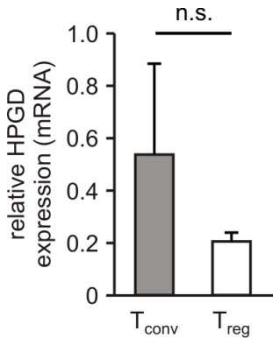

Figure 57: HPGD expression in murine T_{reg} from C57BL/6 mice is lower compared to T_{conv} cells.
Murine T_{reg} (white column) and T_{conv} (grey column) cells were isolated from spleens of C57BL/6 mice. Relative HPGD mRNA expression, compared to B2M expression, was assessed by qRT-PCR. Samples were normalized to T_{conv} cells (0 h). Data represent mean values and standard deviations of four independent experiments. n.s. – not significant.

3.9.1.2 Comparable HPGD expression levels in T_{reg} and T_{conv} cells from BALB/c mice

Next, expression levels of HPGD were investigated in murine T cells from BALB/c mice to exclude that low HPGD expression in T_{reg} cells was due to the genetic background of C57BL/6 mice. Therefore, T_{reg} and T_{conv} cells were isolated from spleens of BALB/c mice and relative HPGD mRNA expression was assessed by qRT-PCR analysis. HPGD mRNA expression was slightly higher in T_{reg} cells compared to T_{conv} cells, as shown in Figure 58. Although this result differs from the observations made in T cells from C57BL/6 mice, the differences in HPGD expression between T_{reg} and T_{conv} cells from BALB/c mice were not statistically significant, but expression levels were rather comparable. These results further support a differential expression of HPGD in murine T_{reg} cells compared to human T_{reg} cells.

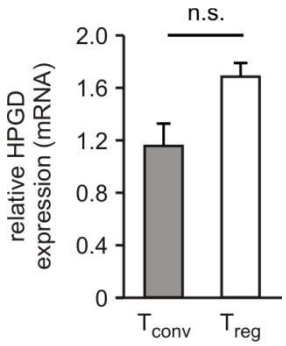

Figure 58: Comparable HPGD expression levels in murine T_{reg} and T_{conv} cells from BALB/c mice
Murine T_{reg} (white column) and T_{conv} (grey column) cells were obtained from spleen of BALB/c mice and relative HPGD mRNA expression, compared to B2M expression, was assessed by qRT-PCR. Samples were normalized to T_{conv} cells (0 h). Data represent mean values and standard deviations of three independent experiments. n.s. – not significant.

3.9.2 Interleukin-2 does not increase HPGD expression in murine T_{reg} cells

3.9.2.1 HPGD expression is not induced upon IL-2R signaling in T_{reg} cells from C57BL/6 mice

In the previous experiments, it could be demonstrated that IL-2 receptor signaling alone was sufficient to upregulate HPGD expression in human T_{reg} cells. Therefore, it was tested whether the same could be observed in murine T_{reg} cells. For this purpose T_{reg} and T_{conv} cells were purified from spleens of C57BL/6 mice and cells were either left untreated or were stimulated with IL-2. After 24 h cells were harvested and HPGD mRNA expression was assessed by qRT-PCR. In Figure 59, it is depicted that IL-2R signaling did not induce HPGD expression in murine T_{reg} cells. IL-2 stimulated T_{reg} cells showed only a slight but not significant increase in HPGD expression, compared to freshly isolated and untreated T_{reg} cells. As expected, IL-2 stimulation did also not upregulate HPGD expression in T_{conv} cells. These results show that IL-2R signaling is insufficient to enhance HPGD expression in murine T cells and further support that expression and regulation of HPGD in murine T_{reg} cells differ from the human system.

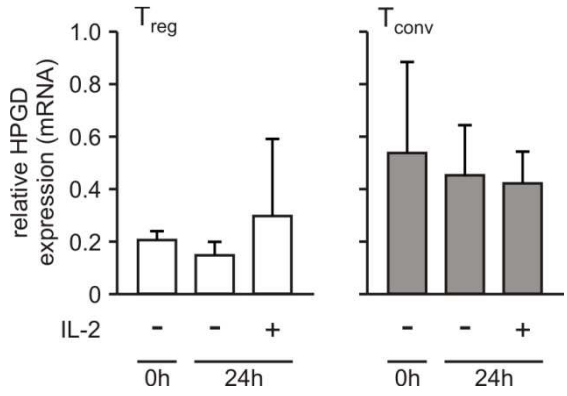

Figure 59: IL-2R signaling does not enhance HPGD expression in murine T_{reg} from C57BL/6 mice.
Murine T_{reg} (white columns) and T_{conv} (grey columns) cells were isolated from spleens of C57BL/6 mice. Cells were either left untreated or stimulated with 20 U/ml IL-2 for 24 h. Relative HPGD mRNA expression, compared to B2M expression, was assessed by qRT-PCR. Samples were normalized to T_{conv} cells (0 h). Data represent mean values and standard deviations of four independent experiments.

3.9.2.2 IL-2R signaling does not enhance HPGD expression in T_{reg} cells from BALB/c mice

In contrast to the observations made for human T_{reg} cells, IL-2 stimulation is insufficient to induce HPGD expression in murine T_{reg} cells. Next, HPGD expression levels of murine T cells from BALB/c mice were investigated after IL-2 treatment to exclude that low HPGD expression and unresponsiveness to IL-2 stimulation were due to the genetic background of C57BL/6 mice. Therefore, T_{reg} and T_{conv} cells were isolated from spleens of BALB/c mice

and cells were either left untreated or were stimulated with IL-2 for 24 h. HPGD expression was not upregulated upon IL-2 treatment neither in T_{reg} nor T_{conv} cells (Figure 60). These results show that the regulation of HPGD expression in murine T_{reg} cells is independent of IL-2 and that the IL-2-mediated upregulation of HPGD, observed in human T_{reg} cells, cannot be confirmed in the murine system.

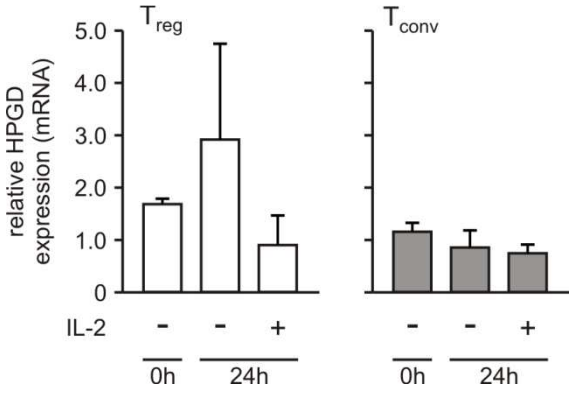

Figure 60: HPGD expression is not enhanced in murine T_{reg} from BALB/c mice upon IL-2 stimulation. Murine T_{reg} (white columns) and T_{conv} (grey columns) cells were isolated from spleen of BALB/c mice. Cells were either left untreated or stimulated with 20 U/ml IL-2 for 24 h. Relative HPGD mRNA expression, compared to B2M expression, was assessed by qRT-PCR. Samples were normalized to T_{conv} cells (0 h). Data represent mean values and standard deviations of three independent experiments.

3.10 Transcriptional regulation of HPGD expression

Regulatory $CD4^+CD25^+$ T cells express the transcription factor FOXP3 (forkhead box P3), a member of the forkhead/winged helix family of transcription factors. FOXP3 not only is a specific marker for T_{reg} cells, but FOXP3 plays an important role as master regulator in the expression of various important T_{reg}-cell associated genes and is crucial for the development and functional phenotype of T_{reg} cells [59-62]. Moreover, FOXP3 is sufficient to induce a T_{reg} phenotype in conventional $CD4^+CD25^-$ T cells [59-61]. FOXP3 modulates the expression of various target genes in T_{reg} cells, as it can repress as well as induce gene expression [244-246]. For this purpose FOXP3 can bind to the promoter and enhancer regions of the respective genes [247], either alone but it can also form a DNA-binding complex together with other transcription factors, for example NFAT (Nuclear Factor of Activated T cells) [248], AML/Runx1 (Runt-related transcription factor 1) [249] or NF-κB (Nuclear Factor κB) [250]. In a complex with NFAT, FOXP3 negatively regulates transcription of *IL-2*, but positively regulates other genes, such as *CD25* and *CTLA4* [251]. Furthermore, FOXP3 can influence gene expression through epigenetic mechanisms, such as chromatin remodeling and histone

deacetylation[247,252]. In the following section the influence of FOXP3 on the expression of HPGD in human T_{reg} cells was investigated and whether FOXP3 can bind to the HPGD locus to modulate gene expression.

3.10.1 Silencing of FOXP3 in human T_{reg} cells enhances HPGD expression

As HPGD expression was shown to be specifically enhanced in human T_{reg} cells compared to T_{conv}, it was of interest to determine whether HPGD is a target gene of FOXP3. To answer the question whether HPGD expression is under the control of FOXP3, it was investigated whether HPGD expression in human T_{reg} cells would be changed after silencing of FOXP3 expression. Therefore, human T_{reg} cells were isolated from peripheral blood and siRNA-mediated knockdown of FOXP3 in T_{reg} cells was performed. Relative HPGD mRNA expression was assessed by qRT-PCR 48 h after the FOXP3 knockdown. The efficiency of the FOXP3 knockdown was assessed by analysis of FOXP3 mRNA expression in qRT-PCR analysis and protein expression in flow cytometry and a reduction of FOXP3 expression could be observed 24 h after knockdown (see Appendix F). In Figure 61, it is shown that HPGD expression is significantly enhanced in T_{reg} cells after silencing of FOXP3 in comparison to T_{reg} cells treated with control siRNA. This result shows that FOXP3 partially blocks HPGD transcription, either by directly or indirectly regulating HPGD expression.

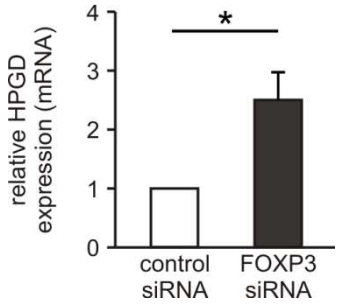

Figure 61: HPGD expression is augmented after silencing of FOXP3 in T_{reg} cells.
Human $CD4^+CD25^+$ T_{reg} cells were isolated from peripheral blood and electroporated with 10 µg control siRNA or FOXP3 siRNA. After 24 h relative HPGD mRNA expression was assessed by qRT-PCR, compared to B2M expression. Data were normalized to control siRNA transfected T_{reg} cells. Mean values and standard deviations of at least three independent experiments are shown. Statistical significant differences ($p < 0.05$) are marked with an asterisk.

3.10.2 FOXP3 can bind to the HPGD promoter

FOXP3 can influence gene expression either by direct interaction with the DNA alone or in a complex with other transcriptional factors [244-247] or by indirect mechanisms, such as chromatin remodeling and histone deacetylation[247,252]. Previous experiments had shown that HPGD expression increases in T_{reg} cells, after silencing of FOXP3, indicating regulation of HPGD by

FOXP3. Therefore, it was tested whether FOXP3 can bind to the HPGD locus and HPGD represents a direct target gene of FOXP3.

To answer the question whether FOXP3 can bind to the HPGD locus, the sequence of the HPGD locus was screened for binding sites of FOXP3 using bioinformatic *in silico* approaches and several potential FOXP3 binding sites were predicted upstream of the transcription start site (TSS) as well as in the genomic locus of HPGD. Five of the predicted binding sites are depicted in an overview of the HPGD locus in Figure 62. In addition, the location of HPGD on chromosome 4, the exon structure of HPGD, a CpG island identified at the HPGD locus, as well as promoter- and enhancer-associated histone modifications are displayed. The promoter of HPGD was identified by the presence of the CpG island and the promoter specific histone modification H3K4Me3 (trimethylation of lysine 4 on histone H3)[253], which was assessed in 9 different cell lines, for example the lymphoblastoid cell line Gm12878, human mammary epithelial cells (HMEC) or normal human epidermal keratinocytes. An enhancer area was identified by the enhancer-associated histone modification H3K3Me1 (Monomethylation of lysine 3 on histone H3)[253], which was also assessed in different cell lines. The above mentioned data were obtained from the UCSC web site. FOXP3 binding to the HPGD locus was assessed by promoter arrays (Prof. Simon C. Barry, unpublished data) and notably four of the predicted FOXP3 binding sites could be verified by FOXP3 ChiP tiling arrays (Figure 62) in human expanded T_{reg} cells, see therefore also Sadlon et al. 2010 [244].

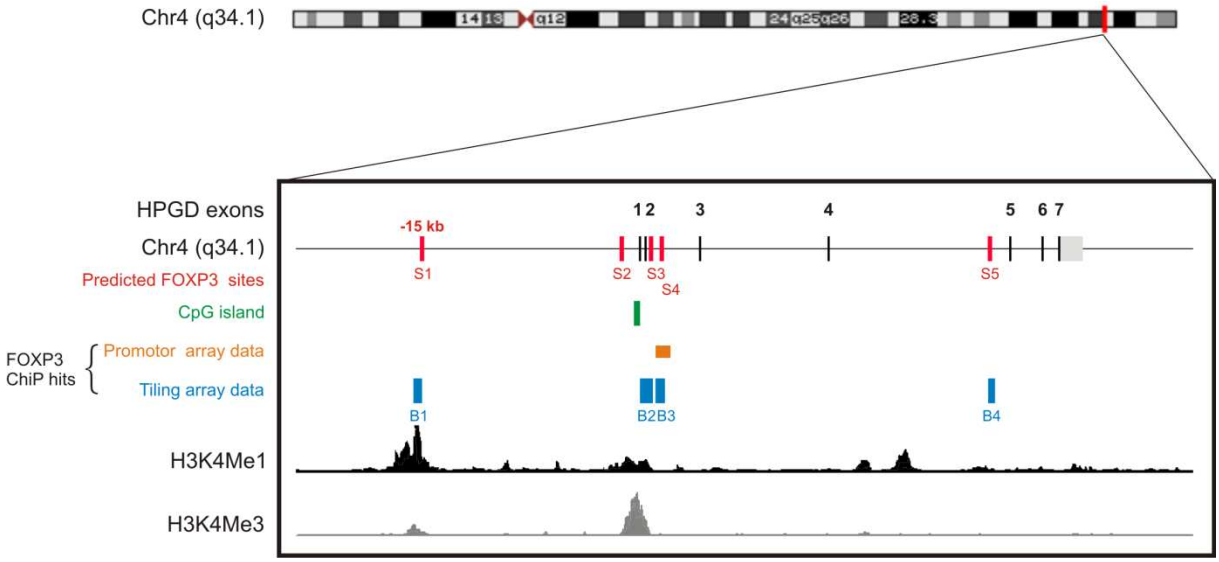

Figure 62: FOXP3 binding sites within the HPGD locus.
The location of the human HPGD gene on chromosome 4 (Chr4 q34.1) is illustrated at the top of the figure. The HPGD gene with exon 1 to 7 was obtained from the University of California Santa Cruz (UCSC) genome assembly web site (http://genome.ucsc.edu), hg18. Visualized are the predicted FOXP3 binding sites S1 to S5 (red bars), the CpG island (green bar), FOXP3 binding sites in the locus of HPGD were obtained from promoter tiling arrays (orange bar) and from FOXP3 ChiP tiling arrays (blue bars B1 to B4) in expanded T_{reg} cells, which confirmed four of the predicted FOXP3 binding sites. Furthermore, histone modifications that are promoter-associated (H3K4Me3) or enhancer-associated (H3K3Me1), assessed in different cell lines (for example Gm12878, HMEC or NHEK cells), are shown. These data were obtained from the UCSC web site.

One of the FOXP3 binding sites was predicted -15kb 5' of the transcription start site in the potential enhancer area. This respective FOXP3 binding site was selected to exemplify that FOXP3 can bind to the HPGD locus, using an electrophoretic mobility shift assay (EMSA). FOXP3 protein bound to the selected FOXP3 binding motif (HPGD) as depicted in Figure 63, illustrated by the shift in fluorescence intensity in lane 2. To test if the binding is specific a mutated HPGD (mut-HPGD) oligonucleotide was used and no binding of this oligonucleotide to FOXP3 could be detected (lane 6). Furthermore, the signal intensity was reduced in the presence of an oligonucleotide with a known FOXP3 binding motif (FKH), which was used as a competitor (lane 3). In the presence of the mut-HPGD oligonucleotide, however, signal intensity was not reduced (lane 4). As further control to proof specific FOXP3 binding, an histidin-specific antibody was included in the binding reaction of HPGD oligonucleotide and FOXP3 protein (Figure 76, lane 2 Appendix H). Binding of the histidin antibody to the His-tag within the recombinant FOXP3 protein, resulted into a second, supershifted band, which indicated specific binding of FOXP3 to the HPGD oligonucleotide. Taken together the results show that the binding of FOXP3 to the HPGD oligonucleotide was specific. Moreover, this analysis shows that FOXP3 can bind to the HPGD locus and thus might influence the expression of HPGD.

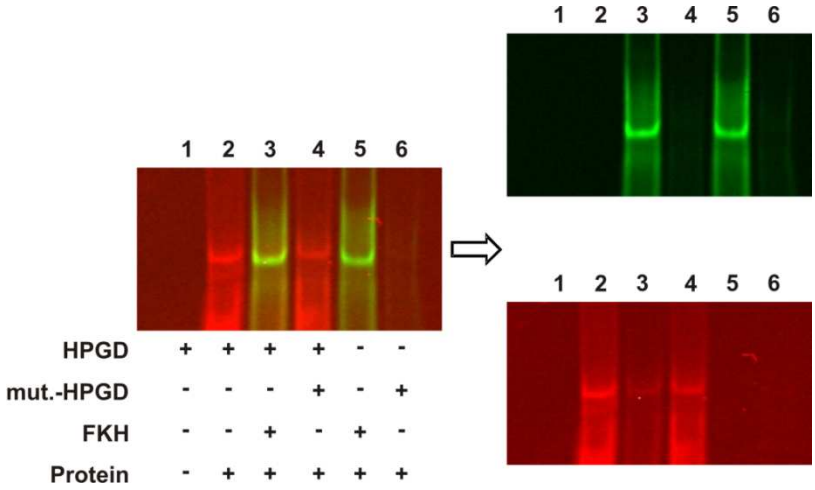

Figure 63: Specific binding of FOXP3 to the HPGD gene.
An EMSA was performed with recombinant FOXP3 protein (Protein) and the following oligonucleotides: (HPGD): a dimer of the HPGD gene with a FOXP3 binding motif, labeled with the infrared dye DY-681 (shown in red, lanes 1-3 & 4). (mut.-HPGD): a dimer of the HPGD gene with the mutated FOXP3 binding motif, labeled with infrared dye DY-781 (shown in green, lanes 4 & 6). (FKH): a dimer of the forkhead FKH binding motif in the GM-CSF enhancer, labeled with the infrared dye DY-781 (shown in green, lanes 3 & 5). One representative experiment out of three is shown.

3.11 HPGD plays no role for the expression of FOXP3 or the suppressive function of human T_{reg} cells

3.11.1 FOXP3 expression in T_{reg} cells is not influenced by silencing of HPGD

The role of HPGD for the T_{reg} cell function was examined in the following section, as significantly higher HPGD expression was found in human T_{reg} cells compared to T_{conv}, T_H cell subsets and iT_{reg} cells, which indicated a specific function in the T_{reg} cell. Although FOXP3 was shown to partially block HPGD expression in T_{reg} cells and FOXP3 binding to the HPGD locus was demonstrated, we examined the possibility that HPGD could regulate the expression of FOXP3. To answer this question, FOXP3 expression levels in human T_{reg} cells were examined after silencing of HPGD. Therefore, human T_{reg} cells were isolated from peripheral blood and siRNA-mediated knockdown of HPGD in T_{reg} cells was performed. Relative FOXP3 mRNA expression was assessed by qRT-PCR and FOXP3 protein expression was examined by flow cytometric analysis of intracellular FOXP3 staining, 24 h after the knockdown of HPGD. The efficiency of the HPGD knockdown was assessed by analysis of HPGD mRNA expression and a significant reduction of HPGD expression could be observed 24 h after knockdown (Figure 64).

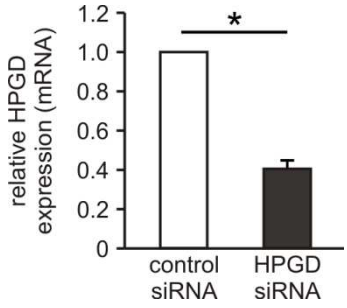

Figure 64: Efficiency of the HPGD knockdown in human T_{reg} cells.
Human $CD4^+CD25^+$ T cells were purified from peripheral blood and treated with control siRNA or HPGD siRNA. Knockdown efficiency was assessed by qRT-PCR in comparison to B2M expression 24 h after knockdown. Mean values and standard deviations of seven individual experiments are presented. Data were normalized to T_{reg} cells treated with control siRNA. Statistical significant differences are marked with an asterisk (* $p < 0.05$).

Silencing of HPGD did not significantly influence FOXP3 expression on mRNA and protein level, as T_{reg} cells displayed comparable FOXP3 expression levels after the HPGD knockdown compared to T_{reg} cells treated with control siRNA, shown in Figure 65.

These results suggest that HPGD has no influence on FOXP3 expression in human T_{reg} cells.

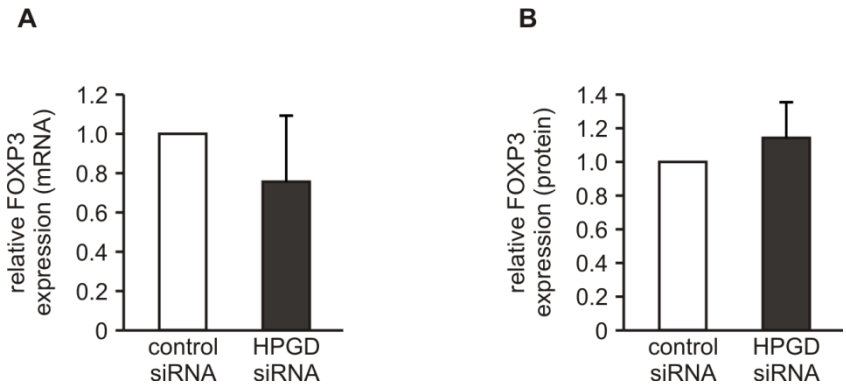

Figure 65: Relative FOXP3 mRNA and protein expression after HPGD knockdown in human T_{reg} cells.
Human $CD4^+CD25^+$ T cells were purified from peripheral blood and treated with control siRNA or HPGD siRNA. (**A**) Relative FOXP3 mRNA expression, compared to B2M expression, was assessed by qRT-PCR 24 h after knockdown. (**B**) Relative FOXP3 protein expression was assessed by intracellular FOXP3 flow cytometric staining 24 h after HPGD knockdown. Data are shown as mean and standard deviations of seven individual experiments.

3.11.2 Silencing of HPGD does not influence the suppressive function of T_{reg} cells

One characteristic of regulatory T cells is their suppressive function *in vitro* and *in vivo* [18,79,80]. Thus, a possible role of HPGD for T_{reg} cells might be that HPGD expression is critical for their suppressive function. To answer the question whether HPGD is crucial for the suppressive function of T_{reg} cells, the suppressive activity was examined after silencing HPGD by siRNA-mediated knockdown in T_{reg} cells. The suppressive activity of T_{reg} cells was examined in a suppression assay, which represents a method to determine their functional status. In brief, human T_{reg} cells were purified from peripheral blood, treated with HPGD

siRNA or control siRNA, respectively, and 24 h after the knockdown these T_{reg} cells were further used for a suppression assay. Therefore, CFSE-labeled T_{conv} cells were stimulated with anti-CD3/CD28/MHC-I-coated beads (3 beads per 1 cell) and siRNA-treated T_{reg} cells were titrated to the T_{conv} cells in different ratios. Proliferation of T_{conv} cells was assessed by flow cytometry after 72 h. Silencing of HPGD in T_{reg} cells did not influence their suppressive capacity, as T_{reg} cells displayed a similar suppressive capacity after treatment with control siRNA as well as HPGD siRNA (Figure 66). This result indicates that HPGD plays no important role for the suppressive function of T_{reg} cells at least *in vitro*.

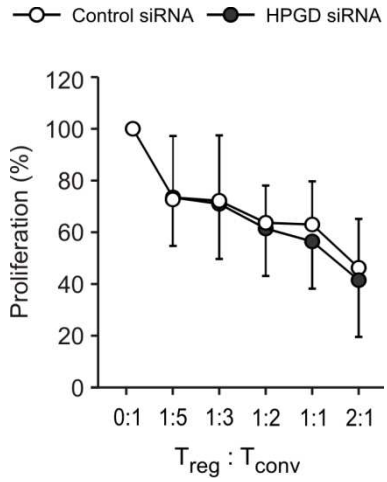

Figure 66: Knockdown of HPGD in human T_{reg} cells does not influence their suppressive capacity.
Human $CD4^+CD25^+$ T cells were purified from peripheral blood and a siRNA-mediated HPGD or control knockdown was performed. Suppressive function of human T_{reg} was assessed 24 h after knockdown in a suppression assay. Therefore, siRNA-treated T_{reg} cells were titrated in different ratios to CFSE-labeled T_{conv} cells, which were stimulated with anti-CD3/CD28/MHC-I coated beads (3 beads: 1 T cell). Proliferation of T_{conv} cells was assessed after 72 h by flow cytometry. Data are presented after normalization to T_{conv} cells, which were incubated with beads but without T_{reg} cells. Data are shown as mean values and standard deviations of at least three individual experiments.

3.11.3 Chemical inhibition of HPGD has no significant effect on HPGD mRNA expression in T_{reg} cells

The role of HPGD for the regulatory phenotype of T_{reg} cells was further investigated when HPGD was chemically inhibited. Chemical inhibition of HPGD was tested as an alternative approach to the siRNA mediated knockdown of HPGD. Therefore, the inhibitor CK47A (5-[[4-(ethoxycyrbonyl)phenyl]azo]-2-hydroxy-benzeneacetic acid; CAY10397) was used. CK47A is a potent, selective inhibitor of HPGD with an IC_{50} of approximately 10 µM. The inhibitor was pretested on $CD4^+$ T cells to define an optimal concentration, which results in no unspecific side effects. 20 µM was found to be a suitable concentration that did not have toxic effects on $CD4^+$ T cells, as shown in Figure 67, and was used as appropriate working concentrations for the following experiments.

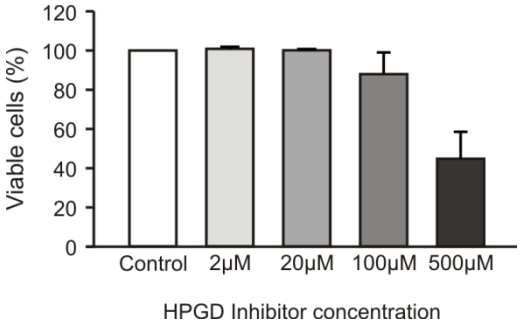

Figure 67: An HPGD inhibitor concentration of 20 µM represents a suitable working concentration.
Human $CD4^+$ T cells were purified from peripheral blood and treated with different HPGD inhibitor concentrations for 24 h or DMSO (control). Consequently cell viability was measured by propidium iodide incorporation in flow cytometry. Data are shown as mean values and standard deviations of three individual experiments after normalization to DMSO treated control cells.

Next, it was examined whether chemical inhibition of HPGD in human T_{reg} cells would influence HPGD expression. The inhibition of HPGD did not significantly change HPGD mRNA expression in T_{reg} cells, compared to DMSO treated control cells (Figure 68). HPGD mRNA expression showed a slight positive tendency after HPGD inhibitor treatment, which might indicate that HPGD expression is regulated via a feedback loop in human T_{reg} cells. However, further experiments would be necessary to address this in more detail.

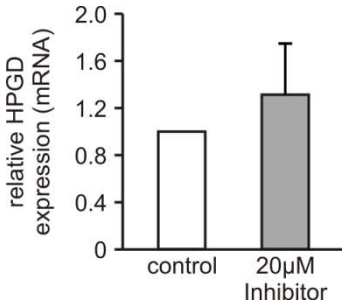

Figure 68: HPGD expression is enhanced upon chemical inhibition of HPGD in human T_{reg} cells.
Human $CD4^+CD25^+$ T cells were purified from peripheral blood and treated with 20 µM HPGD inhibitor CK47A (20 µM inhibitor) or with the respective amount of DMSO (Control) for 24 h. Relative HPGD mRNA expression, compared to B2M expression, was assessed by qRT-PCR. Data are normalized to DMSO treated T_{reg} cells. Standard deviations and mean values of three individual experiments are shown.

3.11.3.1 FOXP3 expression in T_{reg} cells is not influenced by chemical inhibition of HPGD

The previous results had demonstrated that FOXP3 expression was not influenced by silencing of HPGD. As an alternative approach to the siRNA mediated knockdown, HPGD was chemically inhibited to determine a potential influence on FOXP3 expression in T_{reg} cells. Human T_{reg} cells were isolated from peripheral blood and incubated with 20 µM HPGD inhibitor or the respective amount of DMSO for 24 h. Relative FOXP3 mRNA expression was assessed by qRT-PCR and FOXP3 protein expression was examined by flow cytometric analysis of intracellular FOXP3 staining, after chemical inhibition of HPGD. In Figure 69 it is shown that FOXP3 mRNA and protein expression were unchanged in T_{reg} cells after inhibition of HPGD.

This result indicates that HPGD has no influence on FOXP3 expression in human T_{reg} cells.

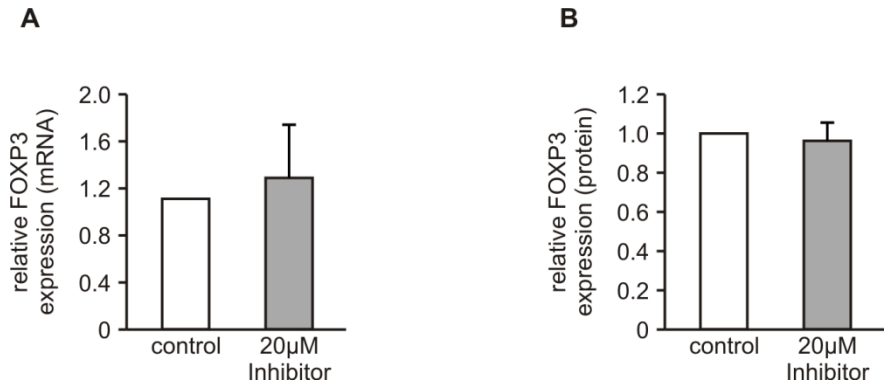

Figure 69: FOXP3 expression is not influenced by chemical inhibition of HPGD in T_{reg} cells.
Human $CD4^+CD25^+$ T cells were purified from peripheral blood and treated with 20 µM HPGD inhibitor CK47A (20 µM inhibitor) or with the respective amount of DMSO (Control). (**A**) Relative FOXP3 mRNA expression, compared to B2M expression, was assessed by qRT-PCR 24 h after inhibitor treatment. (**B**) Relative FOXP3 protein expression was assessed by intracellular FOXP3 staining 24 h after inhibitor treatment. Data are normalized to control cells and are shown as mean values and standard deviations of three individual experiments.

3.11.3.2 No change in suppressive function of T_{reg} after chemical inhibition of HPGD

Although the former results had shown that silencing of HPGD in T_{reg} cells does not influence their suppressive function, the suppressive activity of T_{reg} cells was also examined after chemical inhibition of HPGD, to answer the question whether the enzymatic function of HPGD is crucial for the suppressive activity of T_{reg} cells. Chemical inhibition should guarantee the complete blockade of the enzymatic function of HPGD. In brief, human T_{reg} cells were isolated from peripheral blood and treated with 20 µM HPGD inhibitor CK47A (20 µM inhibitor) or with the respective amount of DMSO (control) for 24 h. Following this treatment the suppressive activity of these T_{reg} cells was examined in a suppression assay, in which these T_{reg} cells were titrated in different ratios to CFSE-labeled T_{conv} cells, stimulated with anti-CD3/CD28/MHC-I coated beads (3 beads per 1 cell). The proliferation of T_{conv} cells was assessed after 72 h by flow cytometry. In Figure 71, it is shown that chemical inhibition of HPGD in T_{reg} cells did only slightly enhance their suppressive activity compared to DMSO treated control T_{reg} cells. These results therefore indicate that the suppressive capacity of T_{reg} cells is not dependent of the enzymatic activity of HPGD. This result is further supported by the observations of the previous siRNA-mediated silencing of HPGD in T_{reg} cells, which did not significantly affect their suppressive activity.

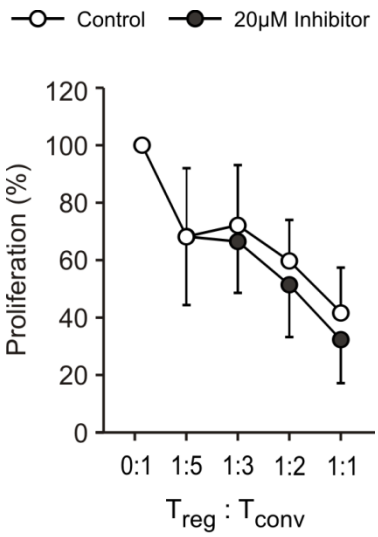

Figure 70: Chemical inhibition of HPGD in human T_{reg} cells does not significantly change their suppressive capacity.
Human $CD4^+CD25^+$ T cells were purified from peripheral blood and were treated with 20 µM HPGD inhibitor CK47A (20 µM inhibitor) or with the respective amount of DMSO (Control) for 24 h. Subsequently the suppressive activity of T_{reg} was assessed in a suppression assay. Data were analyzed and processed as described in Figure 66. The presented data are mean values and standard deviations of three individual experiments.

Taken together, the experiments addressing the role of HPGD for the T_{reg} cell illustrate that HPGD and its enzymatic activity seem to be neither necessary for the FOXP3 expression in T_{reg} cells nor for their suppressive function at least *in vitro*. However, the enzymatic activity of HPGD may still mediate other important functions within the cell or might be required for the suppressive activity of T_{reg} cells *in vivo* and could not yet be elucidated with the present experiments.

4 Discussion

4.1 Specific expression of HPGD in human regulatory T cells

The characteristics and functions of $CD4^+CD25^+$ regulatory T cells have been extensively studied – yet further investigation is required to completely determine how T_{reg} cells mediate their suppressive activity especially *in vivo* and which molecules are actually involved. Up to now various molecules have been identified to be crucial for the function and development of T_{reg} cells and to serve as marker molecules [254]. Among these is the lineage specific transcription factor FOXP3 that influences as a master regulator the transcription of many target genes in humans and mice [244-246]. However, there are still unknown genes that are required for a complete phenotype of T_{reg} cells with full regulatory function.

In order to identify novel target molecules involved in the development and function of human regulatory T cells, global gene expression profiling was carried out. Therefore, T_{reg} and T_{conv} cells from healthy individuals as well as patients suffering from chronic lymphocytic leukemia (CLL), under resting as well as cells under activating or inhibiting conditions, were integrated. This approach should designate novel genes specifically expressed in T_{reg} cells in comparison to T_{conv} cells. In contrast to previous approaches from other groups [206,207], the use of T_{conv} cells, kept under a wide variety of different conditions, should exclude genes that are unspecifically regulated in T_{conv} and T_{reg} cells. In this context HPGD was identified as a gene that was highly expressed in T_{reg} cells in comparison to T_{conv} cells. HPGD represents a key enzyme in the metabolism of prostaglandins and is one of the major PGE_2-metabolizing enzymes [163,167]. Remarkably, the expression pattern of HPGD was similar to that of the transcription factor FOXP3, with a high expression specifically in T_{reg} cells and a low expression in T_{conv} cells (Figure 5). This stands in contrast to other molecules such as CTLA4 and CD127, which are commonly used to describe and distinguish T_{reg} from T_{conv} cells. In fact, CTLA4 and CD127 displayed even high expression levels for T_{conv} cells and did not reveal the same T_{reg}- or T_{conv}-restricted expression pattern, as it was the case for HPGD (Figure 6). Moreover, these molecules are not strictly T_{reg}-specifically expressed, as CTLA4 is transiently upregulated on $CD4^+$ and $CD8^+$ T cells, 2-3 days following activation[68,255] and CD127 was recently shown to be downregulated on $CD4^+$ T cells in general upon activation[68,256]. For these reasons CTLA4 and CD127 are insufficient in their qualities as T_{reg}-specific marker molecules.

Consistent with the gene expression data relative HPGD mRNA expression was shown to be significantly higher expressed in human T_{reg} cells than in human T_{conv} cells (Figure 7). The differential expression of HPGD in T_{reg} cells compared to T_{conv} cells was also validated on protein level by Western blot analysis (Figure 32). With these results it was demonstrated that T_{reg} cells express the enzyme HPGD, which might maintain specific functions within the T_{reg} cell.

Since no monoclonal antibody for detection of HPGD protein was commercially available at the time the thesis was conducted, a monoclonal antibody specific for human HPGD was generated in cooperation with Ravi Hingorani and Robert Balderas, both Becton Dickinson Biosciences. Within this context several antibody clones were tested, concerning their binding specificity and staining performance in flow cytometry, Western blot analysis and immunofluorescence staining. For all three methods, best results were achieved with HPGD antibody clone 3 that demonstrated specific and efficient staining of cells transfected with HPGD or a HPGD-GFP fusion protein. However, the HPGD antibody appeared to be not suitable for flow cytometric and immunofluorescence stainings of primary cells, because T_{reg} and T_{conv} cells did not appear to be differentially stained by the antibody and HPGD staining was either absent or equally distributed in all cells. One reason we might not have detected staining of HPGD in primary cells, could be that the primary cells do not express HPGD protein. This hypothesis, however, stands in contrast to the results of Western blot analysis, which detected HPGD protein in T_{reg} cell lysates (Figure 32). Furthermore, enzymatic activity of HPGD was demonstrated in T_{reg} cells during this study which also nicely reflected the differences between T_{reg} and T_{conv} cells, concerning their relative HPGD mRNA expression (Figure 50). High enzymatic activity in T_{reg} cells was accompanied by high HPGD mRNA expression and vice versa in T_{conv} cells. Another reason for the absence of HPGD staining might be low affinity of the HPGD antibody. This would be supported by the fact that only highly transfected HEK293 cells, overexpressing HPGD protein, were sufficiently stained. In addition, high protein amounts of T_{reg} cell lysates had to be subjected to Western blotting in order to efficiently detect HPGD on Western Blot. Although, HPGD expression in untransfected HEK293 cells could be detected by qRT-PCR data (Figure 16) and in addition these cells were slightly stained in flow cytometry with high HPGD antibody concentrations (dilution 1:100, Figures 13-15), this staining cannot be considered as evidence for endogenous staining of HPGD in these cells. One argument against this is the 100.000 fold higher HPGD mRNA expression in HPGD-GFP transfected cells compared to untransfected cells. It is rather unlikely that these differences might be also observed on protein level. Even more so as

highly HPGD-GFP transfected cells, visualized by GFP signal intensity, were only appropriately stained with the HPGD antibody. Another argument is that HPGD was likewise undetectable in untransfected HEK293 cells on Western Blot. These results, therefore, indicate that the observed slight background staining, observed in flow cytometry, was rather caused by unspecific staining due to an oversaturated antibody solution and support the hypothesis of a low affinity of the HPGD antibody. Similarly, the results obtained from immunofluorescence support a low affinity of the HPGD antibody, as FOXP3 positive $CD4^+$ T cells showed no differential HPGD staining compared to FOXP3 negative $CD4^+$ T cells. A third reason for the unsatisfying HPGD staining results of primary cells in flow cytometry and immunofluorescence might be the differential treatment of the cells. For Western blot analysis the protein is treated with SDS, which leads to irreversible denaturation of the protein structure. This may alter the structure and availability of the epitope and thus its ability to interact with the HPGD antibody, consequently changing the staining result. On the contrary, in flow cytometry and immunofluorescence the three-dimensional protein structure is conserved by the treatment for instance with formaldehyde. Potential epitopes might thereby be covered or less accessible, which impairs the interaction with the HPGD antibody and in turn the staining result. Supporting this hypothesis is the fact that HPGD protein expression in T_{reg} cells was only detected by Western blotting. The epitopes might have become better accessible for the HPGD antibody on Western Blot, resulting in an improved detection. In conclusion, the analysis frame of the HPGD protein expression was very limited due to a low affinity of the HPGD antibody. The antibody was used in Western blot analysis for the detection of HPGD in primary cells. For flow cytometric or immunofluorescence staining, however, it was uneligible, because only HPGD-overexpressing cells were appropriately stained.

Although HPGD expression was shown to be higher in T_{reg} cells on mRNA as well as protein level than in T_{conv} cells, we wanted to determine whether HPGD expression was specific for T_{reg} cells or could be also found in other $CD4^+$ T cell subsets, with regard to their activation state and differentiation stage. Therefore HPGD mRNA expression was assessed in T_{memory} and T_{naive} cells, which were distinguished during this study by their differential expression of the leukocyte specific transmembrane glycoprotein CD45. The isoform CD45RA allows the discrimination of naïve from activated or memory T cells [210], as the isoform CD45RA is expressed on human naïve T lymphocytes. Upon encounter of their cognate antigen T_{naive} cells acquire an activated phenotype. They upregulate activation markers such as CD25, CD44, and CD69 but down-regulate CD62L and CD45RA [214-216]. These activated, ‘antigen-

experienced' T cells can further differentiate into a memory T cell [216-218], which is also $CD45RA^-$ and expresses the shortest CD45 isoform CD45RO [213,214]. First examinations had revealed a higher HPGD expression level in T_{memory} cells than in T_{naive} cells, indicating that HPGD expression might be upregulated during T cell activation and differentiation. However, when the assumption was tested whether HPGD expression would be upregulated during T cell activation or differentiation, enhanced HPGD expression was neither detected in activated T cells (T_H0 cells, Figure 34) nor in the different T helper cell subsets, T_H1, T_H2, T_H9 as well as T_H17 cells (Figure 34). Instead, HPGD expression levels did not increase but remained constantly lower compared to T_{reg} cells. This result indicated a T_{reg} cell specific HPGD expression, which seems to be fixated already during early thymic differentiation and establishment of the T_{reg} cell phenotype. The polarization of the T_{conv} cells seemed to be already so strong and established that even the culture conditions that induce an iT_{reg} cell phenotype were not sufficient to induce HPGD expression *in vitro*.

Remarkably, also induced T_{reg} cells did not upregulate HPGD expression, as shown by gene expression profiling and qRT-PCR data (Figure 35 and 72). This is of special interest as on the one hand induced T_{reg} and naturally occurring T_{reg} cells have certain characteristics in common, such as a high FOXP3 expression and suppressive function *in vitro* and *in vivo* [30,227]. On the other hand iT_{reg} cells also strongly differ from nT_{reg} and differences in gene expression between iT_{reg} and nT_{reg} still remain to be elucidated. A study by Hill et al. 2007 demonstrated for instance that iT_{reg} cells lack a part of the gene signature, specific for nT_{reg} cells, despite their high FOXP3 expression [228]. Thus, the specific HPGD expression in nT_{reg} cells indicates that HPGD represents a novel marker molecule for nT_{reg} cells. Over the last years several molecules were proposed as potential marker molecules to differentiate nT_{reg} from iT_{reg} cells and different marker molecules for human and murine nT_{reg} cells were summarized by Yi et al. [257]. However, these potential markers failed as real nT_{reg} cell markers, as they were either upregulated on activated T_{conv} cells or expressed by naïve or other regulatory T cell subsets [257]. Nonetheless, it is of high interest to distinguish between nT_{reg} from iT_{reg} cells, to designate the origin of the enhanced T_{reg} numbers that are found, for instance, in the tumor microenvironment [109,112,113](see also Introduction 1.1.5). Up to now it remains unclear whether these T_{reg} cells are induced from non-T_{reg} cells, promoted by tumor-secreted cytokines, or if pre-existing T_{reg} cells migrate into the tumor tissue and eventually proliferate there. Besides that, a specific marker for nT_{reg} cells would be beneficial for their detection in various disease models. Moreover, a marker molecule specific for nT_{reg} cells could help to define a cell population with a stable regulatory phenotype that is not lost during

the following T_{reg} cell expansion, because large cell amounts of a pure T_{reg} cell population are required in clinical trials for cell-based tolerogenic therapy of autoimmune diseases, graft rejection or graft versus host disease [258,259]. Although, highly purified human T_{reg} cell populations (greater than 90% $CD4^+FOXP3^+$ cells) can be obtained by fluorescence-activated cells sorting on $CD25^{high}$, the percentage of $FOXP3^+$ cells decreases already after 2 weeks of expansion to 50% [260]. Moreover, FOXP3 expression can be induced in $FOXP3^+$ T_{conv} cells by stimulation of the TCR in the presence of TGF-β, without inducing suppressive activity in these cells [261]. Thus even highly purified $FOXP3^+$ cell populations may represent a mixture of T_{reg} and non-T_{reg} cells. For these reasons a nT_{reg} cell specific molecule could help to define a pure T_{reg} cell population with a stable regulatory phenotype. Recently, the transcription factor Helios was identified as specifically expressed in thymic derived T_{reg} cells and was therefore proposed to be a nT_{reg} specific marker [206,262]. Notably, Helios expression was absent in induced T_{reg} cells and was shown to influence FOXP3 expression and suppressive activity in T_{reg} cells [262,263]. However, this statement was soon challenged by another study, which demonstrated coexpression of Helios in induced T_{reg} cells and claimed that Helios expression is dependent on the method of activation and not on the origin of the cell [264]. Therefore, a true nT_{reg} cell specific marker still remains to be identified. Although HPGD expression in thymic-derived T_{reg} cells needs to be examined, we might have identified such a novel molecule that is specific for nT_{reg} cells, as the present study demonstrates an high HPGD expression in nT_{reg} cells but low expression in iT_{reg}, activated T_{conv} and T helper cell subsets.

4.2 Regulatory function of T_{reg} cells *in vitro* is independent of HPGD

Since HPGD was specifically expressed in nT_{reg} cells, compared to iT_{reg}, T_{conv} and T_H cell subsets, various questions arose from these findings, for instance, what function HPGD fulfills in T_{reg} cells. As pre-incubation with PGE_2 upregulates FOXP3 expression and even enhances the suppressive function of T_{reg} cells [232], the high expression levels of a PGE_2 metabolizing enzymes [141] in T_{reg} cells seem to be contradictory. However, the enzymatic activity of HPGD might be involved in the regulation of various signaling pathways, which in turn might influence FOXP3 expression. For this reason FOXP3 expression was examined after silencing HPGD in human T_{reg} cells by siRNA knockdown. Alternatively, the enzymatic function of HPGD was chemically inhibited by the specific HPGD inhibitor CK47A, which is a potent, selective inhibitor of HPGD. First we observed that HPGD knockdown did not influence FOXP3 mRNA and protein expression in comparison to control knockdown

(Figure 65). Also chemical inhibition of HPGD did not alter FOXP3 mRNA or protein expression in comparison to DMSO treated control cells (Figure 69). Hence, FOXP3 expression in T_{reg} cells seemed to be independent of the enzymatic function of HPGD. Yet, the enzymatic function of HPGD might still be required for the regulatory phenotype of the T_{reg} cell. Baratelli et al. 2005 reported PGE_2 pre-treated T_{reg} cells could still suppress proliferation of T_{conv} cells, which were separated by trans-well inserts. Notably, neither anti-IL-10 nor anti-TGF-β neutralizing antibodies did reverse these effects, suggesting the contribution of additional soluble factors other than IL-10 or TGF-β [232]. As PGE_2 can be metabolized by HPGD, these soluble factors might represent metabolites of PGE_2 that might be secreted and also have immunosuppressive properties. Moreover, PGE_2 secretion was suggested to be a suppressive mechanism used by T_{reg} cells [265,266] and PGE_2 inhibits the proliferation of $CD4^+$ T cells [267,268]. Thus HPGD might repel the suppressive effects of PGE_2 in the T_{reg} cell, while at the same time an effective suppression of T_{conv} is guaranteed. For these reasons we sought to investigate the contribution of HPGD to the suppressive phenotype of T_{reg} cells *in vitro*. However, silencing of HPGD by siRNA knockdown in T_{reg} cells did not affect their suppressive activity (Figure 66), as T_{reg} cells treated with control siRNA equally inhibited proliferation of T_{conv} cells. Similar results were obtained for chemical inhibition of HPGD, which did not significantly change the suppressive function of T_{reg} cells (Figure 70). Although these observations suggest that suppression by T_{reg} cells is independent of the enzymatic activity of HPGD, it might be still required for an *in vivo* function. Moreover, the *in vitro* measurement of suppressive activity might not represent the optimal read-out, to determine a potential role of HPGD for the regulatory function of T_{reg} cells. For instance, cell-contact dependency was postulated for T_{reg} cells, as indicated by *in vitro* assays [19,72], but at the same time several cell-contact-independent suppression mechanisms have been described to be used by T_{reg} cells *in vivo* (see Introduction 1.1.4). Besides, blocking one of these mechanisms might not necessarily increase or impair the complete suppressive capacity and so the contribution of HPGD to the regulatory phenotype of T_{reg} cells remains to be elucidated.

4.3 Influence of extracellular stimuli on the HPGD expression in human T_{reg} cells

Regulatory T cells can be influenced by various stimuli, for example by TCR stimulation and additional signals via costimulatory and cytokine receptors are also involved [19]. Especially the cytokine IL-2 was shown to be important for the development and function of T_{reg} cells. Mice

deficient in IL-2, IL-2Rα or IL-2Rβ have strongly reduced numbers of T_{reg} cells and die prematurely from a severe lymphoproliferative and autoimmune syndrome [234,235] Furthermore, it was shown that blocking the IL-2R on T_{reg} cells leads to a loss of their regulatory activity, suggesting a possible role of IL-2 for suppressor function [91]. T_{reg} cells were further shown to require previous activation for the induction of their suppressor function *in vitro* [233]. Pre-cultured for at least 24 h with anti-CD3-antibody (0.5-1 µg/ml) in the presence of IL-2 (at least 12.5 U/ml) and the absence of T_{conv} cells guaranteed best induction results [233]. Since unstimulated human T_{reg} cells in the present study downregulated HPGD mRNA expression already after 12 h, indicating a dependency on extracellular stimuli, the influence of TCR ligation in the presence of IL-2 or CD28 costimulation on HPGD expression were consequently examined. Notably, TCR ligation in the presence of IL-2 did significantly upregulate HPGD expression in T_{reg} but not in T_{conv} cells (Figures 38 & 39). Moreover, the enzymatic activity of HPGD was also enhanced by IL-2 stimulation and a high enzymatic activity in T_{reg} cells was accompanied by a high HPGD mRNA expression in comparison to the low activity and HPGD mRNA expression in T_{conv} cells (Figure 50). As the suppressive function and FOXP3 expression of T_{reg} cells can be also induced upon TCR/ IL-2 stimulation [233], these findings indicate a potential role of HPGD for the T_{reg} cell function, despite the previous negative results from the *in vitro* suppression assays. Soon it became evident that HPGD upregulation was due to IL-2 but not TCR stimulation. Notably, the inducing effect of IL-2 on HPGD expression seemed to be restricted to T_{reg} cells as T_H1, T_H2, T_H9 or T_H17 did not upregulate HPGD expression upon IL-2 stimulation (Figure 48). Even induced T_{reg} cells did not enhance HPGD expression upon IL-2R signaling, as it was observed for nT_{reg} cells (Figure 49). These results show that IL-2R signaling in T_{reg} cells is differentially regulated than in other T cell subsets. Moreover, these results once more demonstrate that HPGD expression seems to be specific for naturally occurring T_{reg} cells, in comparison to other $CD4^+$ T cell subsets and further indicate a T_{reg} cell specific function for HPGD.

Remarkably the effects of IL-2 on HPGD expression were even observed at low IL-2 concentrations (10 U IL-2/ml) (Figure 46). This result corresponds to earlier studies, which demonstrated that IL-2-dependent targets in T_{reg} cells are coupled to a low IL-2R signaling threshold [236]. As T_{reg} cells are unable to secrete IL-2 [27] and only few IL-2 producing cells are in the thymus and these cells are furthermore not abundant in the periphery [269-271], T_{reg} cells need to utilize IL-2 effectively in an environment where this essential cytokine is only transiently and minimally expressed. Additionally, the grade of IL-2R signaling is associated

with different functional activities of nT_{reg} cells, as for instance low IL-2R signaling supports thymic development or the induction of FoxP3, whereas high IL-2R signaling is required for T_{reg} cell growth [272]. These observations explain why even low IL-2 concentrations did upregulate HPGD expression. Moreover, no correlation between the HPGD expression level and the amount of IL-2 was observed, as increasing concentrations of IL-2 (10 U – 1.000 U/ml) led to similar HPGD expression levels in T_{reg} cells. This indicates that only low amounts of IL-2 are required to saturate signaling pathways that lead to an upregulation of the HPGD expression and no further HPGD increase can be achieved by increasing amounts of IL-2.

Besides TCR/IL-2R activation the influence of costimulation on HPGD expression in T_{reg} and T_{conv} cells was examined, as T cell proliferation was shown to be differentially regulated in T_{reg} and T_{conv} cells and this could be likewise for the HPGD expression. The activation of T_{reg} cells was shown to be independent of CD80/CD86 costimulation, as stimulation with exogenous IL-2 could replace costimulation[233]. However, this observation was different for the activation of T_{conv} cells, where IL-2 was not sufficient as a substitute for costimulation, to induce T cell proliferation [233]. Thus, HPGD expression in T_{conv} cells might be influenced by TCR/CD28 activation. However, stimulation with anti-CD3/CD28/MHC-I-coated beads did not affect HPGD mRNA expression in T_{conv} cells (Figure 43). T_{reg} cells did also not enhance HPGD expression upon this stimulation. This result was expected and is in line with the observation that T_{reg} cells are unable to produce IL-2 even after TCR/CD28 activation [27].

Investigations into the underlying pathways of IL-2R signaling revealed a crucial role of PI3K and NF-κB signaling for the IL-2 mediated upregulation of HPGD (Figures 52 & 53). This was demonstrated by incubation with inhibitors specifically targeting these signaling molecules, which in turn impaired IL-2 mediated HPGD upregulation in T_{reg} cells. However, this observation is in contrast to a study by Bensinger et al. 2004 demonstrating that $CD4^+CD25^+$ T_{reg} cells stimulated with exogenous IL-2 failed to activate the PI3K-Akt pathway and exclusively activated STAT5, because activation (phosphorylation) was not observed for Akt and only for STAT5 [273]. In addition, the same study also shows that proximal IL-2R signaling in $CD4^+CD25^+$ T_{reg} cells is sufficient to activate PI3K and that the negative regulation lies downstream of PI3K and is due to the lipid phosphatases PTEN and Src homology 2-containing inositol polyphosphate 5-phosphatase (SHIP)-1 [273]. Therefore, it can be speculated that PI3K could still activate other targets than Akt, thus leading to the observed effects. Another explanation for the observed results could be that other signaling

molecules than PI3K were inhibited by the PI3K inhibitor. Although the PI3K inhibitor LY294002 used in this study is reported to be a highly selective one that does not inhibit other lipid and protein kinases such as PI4 kinase, PKC, MAP kinase or c-Src, it cannot be excluded that the observed results with the PI3K inhibitor are caused by inhibition of signaling molecules other than PI3K. Similar events can be assumed for NF-κB. On the one hand NF-κB could be activated by other IL-2-dependent signaling events and inhibition of NF-κB downmodulated IL-2-dependent HPGD expression. On the other hand inhibition of NF-κB might also have targeted other signaling events connected with IL-2-mediated HPGD upregulation.

Nonetheless, in accordance with the study of Bensinger et al. 2004 is the observation that inhibition of JAK3 and STAT5-signaling did down-modulate IL-2 mediated HPGD upregulation (Figures 54 & 55). This result indicates an important role of STAT5 in the regulation of HPGD expression. Potential binding sites for STAT5 were predicted in the HPGD promoter area and future experiments should investigate whether STAT5 binds to these sites in the HPGD promoter and directly acts on HPGD expression. In contrast to these findings, MAPK signaling was not required for the IL-2 dependent induction of HPGD in T_{reg} cells. As expected, chemical inhibition of MEK1 did not significantly change the IL-2 influenced HPGD expression (Figure 51). This result is in line with the above mentioned observation of Bensinger and colleagues [273] that IL-2 stimulation does not activate the MAPK- pathway in T_{reg} cells.

In addition to IL-2 the influence of PGE_2 on HPGD expression in T_{reg} cells was investigated. Prostaglandin E_2 is a soluble, immune suppressive molecule that is produced by many different cell types including cells of the immune system, such as monocytes, macrophages and neutrophils [230], but also by tumor cells [229]. PGE_2 plays thereby an important role in carcinogenesis as it inhibits for instance tumor cell apoptosis, induces tumor-cell proliferation and increases tumor progression [274,275]. Furthermore, PGE_2 inhibits the proliferation of $CD4^+$ T cells [267,268] and notably, pre-incubation with PGE_2 did increase FOXP3 expression as well as the suppressive activity of T_{reg} cells [232]. In addition, tumor-secreted PGE_2 was shown to induce FOXP3 expression as well as a regulatory phenotype in $CD4^+CD25^-$T cells [231,232]. Human $CD4^+CD25^+$ adaptive T_{reg} cells that were induced by PGE_2 *in vitro,* did express cyclooxygenase 2 (COX-2) and FOXP3 and produced PGE_2 to suppress effector T cell responses [266]. For these reasons the enhanced expression of the PGE_2-metabolizing enzyme HPGD in T_{reg} cells seems to be counterintuitive. It could be hypothesized that HPGD is

required to protect the T_{reg} cell from T cell inhibitory effects of PGE_2 by inactivating PGE_2, while at the same time this would enable the activation of T_{reg} specific functions. PGE_2 signaling occurs through 4 classes of receptors, the E prostanoid receptors EP1 to EP4, which have been reported to be expressed on T cells [276,277]. It was shown that EP2 and EP4 were required for PGE_2-mediated induction of T_{reg} cell FOXP3 gene expression [231]. Furthermore, EP3 and EP4 were recently identified in the nuclear envelope of porcine cerebral microvascular endothelial cells, suggesting the presence of functional nuclear receptors for PGE_2 [278], although these receptors have not yet been shown on the nuclear envelope in T_{reg} cells to my knowledge. For these reasons it could be speculated that PGE_2 signaling might influence HPGD expression in the T_{reg} cell. Therefore, we investigated whether incubation with PGE_2 would influence HPGD expression in T_{reg} cells. However, the treatment of human T_{reg} cells with PGE_2 alone did not significantly modulate the HPGD mRNA expression in T_{reg} cells in comparison to unstimulated T_{reg} cells, as HPGD expression decreased under both conditions to 40 – 30 % over a period of 72 h (Figure 36). In addition to the EP receptors also prostaglandin specific transporters (PGT) have been described [279-281], however, PGT have not been specifically shown on T_{reg} cells. Assuming that PGE_2 could enter the T_{reg} cell via PGT the present HPGD expression level seems to be sufficient to prevent suppressive effects of PGE_2 on the T_{reg} cell.

Other immune suppressive molecules such as TGF-β [282,283] or IL-10 [284-286] have also been detected in several tumors or tumor cell lines and were reported to induce T_{reg} cells in the periphery [34,35]. In addition, IL-10 was shown to maintain FOXP3 expression and suppressive capacity of regulatory T cells[287] and is produced by T_{reg} cells and Tr1 cells[35]. Similarly, TGF-β was also shown to induce FOXP3 expression and the conversion of $CD4^+CD25^-$ T cells into regulatory $CD4^+CD25^+$ T cells (T_H3) [34,104]. Furthermore, secretion of TGF-β [45] and membrane-tethered TGF-β on T_{reg} cells were shown to be involved in suppression of T_{conv} cells [54,89]. Therefore, an influence of TGF-β and IL-10 on the HPGD expression in T_{reg} cells cannot be excluded and the importance of these molecules for the HPGD expression in T_{reg} cells was consequently investigated. Similar to the results obtained by PGE_2 stimulation, TGF-β alone did not reveal a significant influence on HPGD expression in T_{reg} cells compared to unstimulated cells (Figure 37). However, IL-10 stimulation positively influenced HPGD expression, as the HPGD expression was still significantly higher after 24 h with IL-10 stimulation in comparison to unstimulated cells (Figure 37). These results indicate that HPGD in T_{reg} cells is responsive to IL-10 signaling. Positive effects of IL-10 were also previously demonstrated with villous trophoblasts that showed decreased HPGD expression in the

presence of IL-1β but effects were antagonized by IL-10 stimulation[176]. IL-10 receptor signaling activates the Janus tyrosine kinases JAK1 and Tyk2 that lead to an activation of the transcription factor STAT3 [288], and in mice it was shown that selective deletion of STAT3 in T_{reg} cells led to spontaneous intestinal inflammation, which was associated with T_H17 cell increase [289]. Therefore, it is possible that IL-10 acts on HPGD expression via STAT3. With specific inhibition of STAT3 in T_{reg} cells this issue could be investigated. Moreover, EMSA and ChiP assays could provide further evidence for direct binding of STAT3 to the HPGD promoter.

In addition to these experiments, it was examined whether stimulation with TGF-β, IL-10 or PGE_2 would impair or reverse the inducing effects of IL-2 on HPGD expression in T_{reg} cells. TGF-β thereby significantly reduced IL-2-mediated HPGD upregulation after 24 h, suggesting a negative regulatory role of TGF-β (Figure 56). Besides that TGF-β plays an important role in the induction of regulatory T cells and participates in the suppression of T_{conv} cells (as mentioned before), it was also reported that TGF-β together with IL-2 enhances the suppressive effects of nT_{reg} cells [290,291]. The observation that TGF-β impairs the IL-2-mediated upregulation of HPGD expression might therefore indicate that HPGD is not necessary for the suppressive capacity of T_{reg} cells but maintains another function. Otherwise HPGD expression would be further enhanced, due to the activation of the respective suppression programs. In contrast to TGF-β, the presence of PGE_2 and especially IL-10 did further increase IL-2-induced HPGD expression (Figure 56), compared to cells stimulated with IL-2 only (Figure 40). These rather unexpected results suggested that IL-10 and PGE_2 in combination with IL-2 costimulation have positive synergistic effects on HPGD mRNA expression in T_{reg} cells, as no effect on HPGD expression was observed when cells were stimulated with IL-10 or PGE_2 alone and also IL-2 stimulation alone resulted in lower HPGD expression levels than in combination with IL-10 or PGE_2. One explanation for this phenomenon could be that negative signaling pathways, which partially block HPGD expression, are compensated by IL-10 or PGE_2 signaling and consequently HPGD expression is further enhanced. Moreover, IL-10 signaling alone had already demonstrated positive effects on HPGD expression. As mentioned above, HPGD expression might be regulated by IL-10R signaling via for example STAT3. Assuming that both, the induction of STAT5 by IL-2 and STAT3 by IL-10R signaling, lead to upregulation of HPGD expression, the inducing effects of these two signaling pathways might potentiate.

Besides that STAT5 and STAT3 could directly bind to HPGD, IL-2R and IL-10R signaling might alternatively activate the same target genes, distinct from HPGD, which in turn upregulate HPGD expression. AP-1 represents such a candidate, for which potential binding sites were identified and validated in the promoter of HPGD [180]. Notably, AP-1 can be activated not only by IL-2R signaling [136-138] but JunB, a potential AP-1 component [292], was shown to be also a target gene of STAT3 [293].

In conclusion these results demonstrate that HPGD expression is dependent on extracellular stimuli and further indicate that HPGD expression in T_{reg} cells is adapted to the present microenvironment in which the cells remain. Thus, HPGD might be necessary for tissue-specific or disease-associated functions of the T_{reg} cell (see therefore Discussion 4.6).

4.4 Transcriptional regulation of HPGD expression in T_{reg} cells

In context with the above mentioned studies we also sought to investigate the influence of FOXP3 on HPGD expression in human T_{reg} cells. With FOXP3 being the lineage marker of T_{reg} cells and controlling their development and function via regulating the expression of many target genes [59-62], FOXP3 might similarly control the expression of HPGD. Silencing of FOXP3 by siRNA- knockdown in T_{reg} cells resulted in significantly enhanced HPGD expression levels, indicating that HPGD expression is partially blocked by FOXP3 (Figure 61). These results were rather unexpected, as HPGD expression was significantly higher in T_{reg} than in T_{conv}, similarly to FOXP3 expression. Therefore, it could be assumed that the knockdown of FOXP3 should lead to the down-modulation of HPGD, in case that HPGD would be a direct target of FOXP3. However, we observed the contrary as HPGD expression was upregulated upon FOXP3 knockdown. Furthermore, the fact that HPGD is upregulated after a FOXP3 knockdown would rather indicate that FOXP3 negatively regulates HPGD expression. But this does not explain the significantly higher HPGD expression in T_{reg} compared to T_{conv}, which show a low FOXP3 and HPGD expression. A possible explanation for the observed effects could be that FOXP3 has no direct influence on HPGD in T_{reg} cells but regulates other factors, which in turn influence HPGD expression. Knockdown of FOXP3 might lead to an imbalance in the expression of these other factors and consequently HPGD is upregulated. IL-2 expression in T_{reg} cells, for instance, is repressed by a complex of FOXP3 and NFAT [248]. Upon silencing of FOXP3, this blockade is abandoned and IL-2 can now be activated by a newly formed complex, consisting of NFAT-AP1 [248]. IL-2 is transcribed and

consequently induces upregulation of HPGD expression, as demonstrated above. Moreover, it cannot be excluded that the siRNA-mediated FOXP3 knockdown did also affect other genes than FOXP3 and thus HPGD expression was enhanced. A further reason could be that FOXP3 keeps the HPGD expression on a fine regulated optimal expression level, which is disturbed by the loss of FOXP3 and thus leads to enhanced HPGD expression.

To further elucidate the observed effects we investigated whether FOXP3 can bind to the HPGD locus and thus directly influence HPGD expression. Transcription factor binding site prediction identified several potential FOXP3 binding sites upstream of the transcription start site (TSS) as well as in the genomic locus of HPGD (Figure 62). We could confirm binding of FOXP3 to a potential enhancer area at the HPGD locus. In addition to EMSA (Figure 63), further FOXP3 binding sites were confirmed in the HPGD locus by FOXP3 ChiP tiling arrays (Figure 62). Taken together, these findings indicate that FOXP3 can bind to the HPGD locus and could thus influence HPGD expression by direct interaction. The data obtained from the FOXP3 ChiP tiling arrays were, however, generated on basis of expanded T_{reg} cells and therefore differences to naturally occurring T_{reg} cells cannot be excluded. Although it was demonstrated that FOXP3 can bind to the HPGD locus further experiments are required to clarify whether binding of FOXP3 to HPGD consequently leads to gene transcription or not. Thus a luciferase reporter assay should be performed for the identified FOXP3 binding regions to prove functional consequences of FOXP3 binding to the HPGD locus.

Besides the regulation of gene expression by FOXP3 also other transcription factors and control mechanisms should be closer examined to gain further insight into the differential HPGD expression between T_{reg} and T_{conv} cells. Gene expression in eukaryotic cells is a well-regulated process and can be controlled on different levels, such as transcription, RNA splicing, translation and post-translational modification of the protein. The transcriptional processes are thereby highly dependent of the interactions of transcription factors with their cognate regulatory sequences but also epigenetic mechanisms influence gene expression. For instance, Baron et al. 2007 had demonstrated that CpG islands were specifically demethylated in T_{reg} cells within the gene locus of the human FOXP3 gene, in particular in an evolutionary conserved element in the 5' untranslated region, which they named 'T_{reg}-specific demethylated region' (TSDR), while this region was methylated in naïve $CD4^+$ T cells. Notably, when the authors analyzed the methylation status of the FOXP3 TSDR of activated T_{conv} and TGF-β-induced T_{reg} cells, the selected CpG motif remained completely methylated, despite that cells upregulated CD25 and displayed high FOXP3 expression levels [294]. In

addition, they could further demonstrate that the DNA methylation status in TSDR not only regulated *FOXP3* gene transcription but was also critical for a stable FOXP3 expression [295]. Similarly, a methylation-specific PCR with bisulfite-treated DNA could be performed to examine the methylation status of the HPGD locus of T_{reg} cells and compared it with those of T_{conv} and iT_{reg} cells. Demethylated CpG islands in the HPGD body of nT_{reg} cells in comparison to methylated regions of iT_{reg} or T_{conv} cells would provide an explanation for the lower HPGD expression in these cells.

Moreover remodeling of the chromatin structure for instance by modification of histone tails plays an important role in gene expression [296]. Trimethylation of lysine 4 on histone H3 (H3K4me3) thereby represents a permissive histone modification, which marks active promoters [253]. The same can be observed for acetylation of histone H4 (H4Ac), which was shown to enhance transcription factor binding to nucleosomal DNA [297]. In contrast di- and trimethylation of lysine 27 or 9 on histone H3 (H3K27Me2/3 or H3K9Me2/3) and trimethylation of lysine 20 on histone 4 (H4K20Me3), however, are associated with gene silencing [298,299]. Permissive and repressive histone modifications at the HPGD locus should be compared between T_{reg} and T_{conv}, as this could provide further explanations for differences in gene expression. Therefore, a chromatin immunoprecipitation with specific antibodies for the respective histone modifications could be conducted, combined with a subsequent qPCR (ChIP-qPCR) which overspans the promoter area with specific primer pairs. Alternatively to the qPCR, the immunoprecipitated DNA fragments could be sequenced (ChIP-Seq) [299,300]. Preliminary ChIP-Seq data generated by our group point towards no significant differences between T_{reg} and T_{conv} concerning the permissive histone modifications H3K4me3 and H4Ac and the repressive modification H3K27me3. However, differences in histone modifications can only give an indication for a possible regulatory scenario. A permissive histone modification does not necessarily correlate with the level of gene expression [296]. Both cell types may show the same permissive histone modification, regardless of their differences in gene expression [296]. Further insight into the regulation of HPGD gene transcription could be provided by another approach, combining chromatin immunoprecipitation with an antibody specific for RNA polymerase II (RNAPII) with following ChIP-Seq. RNAPII is essential for DNA transcription as it catalyzes the synthesis of mRNA precursors [301]. Interestingly, stalled RNAPII at the promoter region of many genes was observed and it was suggested that this served to facilitate rapid gene expression [302]. Notably, the level of RNAPII occupancy at the promoter region could be correlated with the activity of the respective gene. Genes that either lack RNAPII binding or show an high enrichment of RNAPII at the transcription site, were

found to be silent or weakly expressed [303]. In contrast, genes that show a distribution of RNAPII throughout the transcription unit are highly expressed [303]. RNAPII occupancy at the HPGD promoter region could therefore provide further insight into transcriptional regulation of HPGD. Regulatory T cells might show RNAPII occupancy throughout the transcriptional unit whereas no RNAPII binding or only occupancy at the transcription start site of HPGD would be expected for T_{conv} or iT_{reg} cells. Additionally, DNase I hypersensitive sites could be examined at the HPGD locus of T_{reg} and T_{conv}, as these sites also indicate active gene loci, similar to DNA methylation and histone modifications [296].

In conclusion the following model of HPGD regulation in T_{reg} could be proposed: Constant IL-2 signaling, which is essential for the T_{reg} cell, is required for an enhanced HPGD expression in T_{reg}. Thereby, FOXP3 maintains HPGD expression in a fine-regulated balance. Upon silencing of FOXP3, however, this balance is irritated. Other transcription factors that were previously blocked by FOXP3 may now have a stimulating effect on HPGD expression, with the consequence that HPGD expression is upregulated. Moreover, IL-2 expression that was previously repressed by the FOXP3-NFAT complex can now be activated by the newly formed NFAT-AP1 complex [248], resulting into enhanced IL-2 expression levels and possibly IL-2 secretion. Extracellular IL-2 increases until a critical level of 5 to 10 U/ml is reached, which is sufficient for upregulation of HPGD. The enhanced IL-2 concentration activates signaling cascades, such as JAK3/STAT5 signaling, which in turn overrule the influence of FOXP3 and activate gene transcription. HPGD expression is consequently upregulated.

Further studies, however, are required to completely elucidate, which transcription factors and signaling events are actually involved in the regulation of the HPGD expression in T_{reg} cells under resting as well as activating conditions.

4.5 Differences of HPGD expression between human and murine T_{reg} cells

After characterizing expression of HPGD in human T_{reg} cells, HPGD expression was also assessed in murine T_{reg} cells in comparison to T_{conv} cells, to see if the observations made in the human could be transferred to the murine system. Remarkably, a lower HPGD expression was found in murine T_{reg} cells in comparison to T_{conv} isolated from C57BL/6 mice (Figure 57). Although T_{reg} cells from BALB/c mice displayed a slightly higher HPGD expression compared to T_{conv}, the expression levels were not significantly higher (Figure 58). Furthermore, HPGD expression in murine T cells was not specifically upregulated in T_{reg} cells

upon IL-2 stimulation, independent of C57BL/6 or a BALB/c genetic background (Figures 59 & 60). On the one hand these results demonstrate that gene expression in murine and human T_{reg} cells is not necessarily congruent and that species specific differences may exist. This was already observed for other molecules, which showed specific and constitutive expression in murine or human T_{reg} cells, but were not expressed at all or only in a subset of human or murine T_{reg} cells. Expression of neuropilin-1 (Nrp-1) was shown, for instance, to be specifically and constitutively expressed on murine nT_{reg} cells, independent of their activation status [304], whereas human T_{reg} cells did not express Nrp-1, regardless of their origins [305]. Another example is the ectoenzyme CD39 that is uniformly expressed on murine T_{reg} cells, but is only expressed by a subset of human T_{reg} cells with an effector/memory-like phenotype [51].

On the other hand murine cells for the present study were isolated from spleen, whereas human cells were isolated from peripheral blood. Therefore, one could hypothesize that HPGD expression in T_{reg} cells is dependent on the tissue and its particular microenvironment. This assumption is supported by a study of Feuerer et al. 2009, which demonstrated that murine fat tissue-derived T_{reg} cells displayed a distinct and specific gene expression profile, which clearly differed from the expression pattern of T_{reg} cells derived from spleen or lymph nodes, with HPGD being one of the transcripts that was specifically enhanced in fat-derived T_{reg} cells [306]. Future experiments should focus on HPGD expression of murine and human T_{reg} cells derived from various tissues to answer the question of a tissue-specific HPGD expression in T_{reg} cells. Moreover, the results obtained from these studies would elucidate differences between murine T_{reg} and human T_{reg} cells concerning their HPGD expression levels. Assuming that T_{reg} cells exhibit a tissue-specific expression pattern for HPGD, the contribution of HPGD to a potential tissue-specific and also disease-associated role of T_{reg} cells needs to be investigated (see therefore also next section 4.6).

4.6 Role of HPGD for tissue specific functions of T_{reg} cells

Taken together, in the present study it was shown that HPGD represents a novel gene, which is specific for human naturally occurring T_{reg} cells. Although the relevance of HPGD for the T_{reg} cell function remains to be elucidated, the present study indicates a tissue-specific expression and thus a potential tissue-specific role of HPGD for T_{reg} cells. Tissue-specific expression was indicated by the observation that spleen derived murine T_{reg} cells did not show

a higher HPGD expression compared to murine T_{conv} cells as it was observed for human T cells, which were purified from peripheral blood. Moreover, it was clearly demonstrated that HPGD mRNA expression of human T_{reg} cells can be modulated by various extracellular stimuli, such as the cytokines IL-2 and IL-10 or PGE_2 in combination with IL-2, while HPGD mRNA expression levels decreased in the absence of any stimulus. HPGD expression may be adapted *in vivo*, depending on the particular microenvironment of each tissue in which the T_{reg} cell resides. To elucidate whether HPGD expression in T_{reg} cells is tissue-dependent and facilitates a tissue-specific role of the T_{reg} cells, different questions have to be answered: First the expression levels of T_{reg} cells derived from different tissues need to be assessed. As mentioned earlier, differences in HPGD expression between the murine and human system could thereby be investigated, to determine potential species specific differences. In this context HPGD expression levels of thymus derived T_{reg} cells would throw further light on whether HPGD expression is indeed specific for thymic derived nT_{reg} cells.

Depending on these results, the next step should be to examine whether HPGD expression in T_{reg} cells is modified in certain disease models. Differential expression of a PGE_2 metabolizing enzyme in T_{reg} cells might be of interest especially in the tumor microenvironment, as on the one hand increased colonic mucosal levels of PGE_2 were reported in patients with adenomatous polyps and colorectal carcinomas [307,308] and on the other hand increased numbers of T_{reg} cells were observed in various tumors (see also introduction 1.1.5) [109,112,113]. Notably, HPGD seems to play an important role in cancer as a tumor suppressor, because a loss of HPGD expression in various tissues was associated with the progression of the particular tumor, whereas over-expression of HPGD in these cells could reverse tumor progression [183-187] (see also introduction 1.3.5).

Besides, PGE_2 was reported to inhibit the proliferation of $CD4^+$ T cells [267,268]. Hence, in a microenvironment enriched with PGE_2, HPGD might protect the T_{reg} cell from the negative effects of PGE_2. Moreover, T_{reg} cells were suggested to exert their suppressive function also by PGE_2 secretion [265,266]. Thus, the protective effect of HPGD might be a prerequisite for efficient suppression of T cell proliferation by the T_{reg} cell. In addition to that, the enzymatic activity of HPGD might play a role for the suppressive function of T_{reg} cells *in vivo*, despite the negative results in the present *in vitro* experiments. As HPGD was shown to be functional in T_{reg} cells it could be investigated whether PGE_2 metabolites are generated in T_{reg} cells and whether these metabolites maintain certain functions for the cell itself. These PGE_2 metabolites, for instance, might be secreted and exhibit immunosuppressive characteristics or

maintain other functions. Preliminary data generated from our group with 13,14-dihydro-15-keto PGE_2 indicated that this PGE_2 metabolite also inhibits proliferation of T_{conv} cells similarly to PGE_2. Since PGE_2 is rapidly converted *in vivo* into 13,14-dihydro-15-keto PGE_2 [309,310], secretion of PGE_2 metabolites might represent a further mechanism that T_{reg} cells might use to suppress the proliferation of T_{conv} cells. Unfortunately, the metabolite 13,14-dihydro-15-keto PGE_2 is not very stable and a variable amount of non-enzymatic degradation is observed resulting into 13,14-dihydro-15-keto PGA_2 [311,312]. Thus, it is rather unlikely that the metabolite 13,14-dihydro-15-keto PGE_2 maintains an immunosuppressive function, but that other, more stable metabolites might be involved.

Besides various prostaglandins, such as PGE_1, PGE_2, $PGF_{1\alpha}$, $PGF_{2\alpha}$, PGI_2 and 6-keto-$PGF_{1\alpha}$, HPGD can also use other molecules as substrates, such as lipoxin A_4 or unsaturated fatty acids, for instance 12-HHT or 15-HETE (see also Introduction 1.3.3) [168-170]. The metabolites of these lipid mediators might be also important for the T_{reg} cell itself or be involved in tissue-specific functions. Furthermore, HPGD expression might be also important for a potential role of T_{reg} cells in the adipose tissue and in obesity. Adipose tissue of lean individuals was found to be highly enriched with T_{reg} cells with a specific gene expression profile and HPGD being one of the transcripts that were specifically enhanced [306]. However, an altered constitution of T cells, resident in the adipose tissue, was observed during obesity, with reduced T_{reg} cell numbers [306], whereas enhanced numbers of T_H1 cells and $CD8^+$ T cells were reported [313]. Notably, obesity and metabolic dysfunction are associated with a low-grade chronic inflammation. Thereby, evidence is accumulating, that lipid mediators (mentioned above) play an important role in the induction of low-grade inflammation [314]. This assumption is supported by the observation of high levels of arachidonate in adipose tissue of obese human individuals [315,316]. Moreover, lipid mediators can activate immune receptors, such as G-protein-coupled receptors and Toll-like receptors (TLR) and might induce low-grade inflammation [317]. Thus, HPGD expression might be required for T_{reg} cells to control and suppress inflammatory reactions in the adipose tissue and thus prevent adipocyte and metabolic dysfunction, which causes obesity and diabetes. In addition, lipid mediators are also involved in other human diseases, including rheumatoid arthritis, multiple sclerosis and various chronic inflammatory diseases [317] and HPGD might similarly play a role for the maintenance of immune homeostasis in the respective tissues.

Finally, to gain further insight into the function of HPGD for the T_{reg} cell and its relevance for the regulatory phenotype, T_{conv} cells could be transduced lentivirally with HPGD. Due to

over-expression of HPGD, T_{conv} cells might gain T_{reg}-associated features, such as an anergic and suppressive phenotype or the upregulation of characteristic marker molecules.

In summary the results of the present study provide a basis for future experiments to examine the role of HPGD for a potential tissue-specific function of T_{reg} cells and moreover could help to determine their function in the tumor microenvironment and in other diseases.

5 Zusammenfassung

Fokus dieser Studie war die Charakterisierung der Hydroxyprostaglandin dehydrogenase 15-(NAD) (HPGD) in $CD4^+CD25^+$ regulatorischen T-Zellen (T_{reg}) im Hinblick auf die Regulation von HPGD und seine Rolle für die suppressive Funktion von T_{regs}. Auf der einen Seite übernimmt HPGD eine essentielle Funktion im Prostaglandin-Metabolismus und ist dabei eines der Hauptenzyme, die Prostaglandin E_2 (PGE_2) verstoffwechseln. Auf der anderen Seite wurde gezeigt, dass HPGD ein Tumor Suppressor ist. Die Expression von HPGD in regulatorischen T Zellen ist von speziellem Interesse, da erhöhte Mengen von T_{regs} im Tumorgewebe gefunden werden können und PGE_2 diese Zellen aktiviert und zudem zur Karzinogenese beiträgt.

Die vorliegende Studie zeigt, dass HPGD signifikant höher in T_{regs} exprimiert wird als im Vergleich in $CD4^+CD25^-$ T-Zellen (T_{conv}). Insbesondere war die HPGD Expression spezifisch für natürlich vorkommenden T_{regs} (nT_{regs}), da HPGD während der T-Zelldifferenzierung nicht hochreguliert wurde und auch induzierte regulatorische T-Zellen (iT_{reg}) bemerkenswerterweise keine erhöhte HPGD Expression zeigten. Des Weiteren konnte die HPGD Expression ausschließlich in nT_{regs} durch verschiedene extrazelluläre Stimuli spezifisch moduliert werden. Sogar kleinste Mengen an Interleukin 2 (IL-2) waren ausreichend die HPGD Expression stark zu erhöhen. Diese Daten weisen daraufhin, dass HPGD zum spezifischen Genrepertoire von nT_{regs} gehört, da eine niedrige IL-2 Rezeptor-Signaltransduktion auch die Entwicklung von T_{regs} im Thymus fördert. HPGD stellt daher ein neues T_{reg}-spezifisches Molekül dar, das zur Unterscheidung zwischen nT_{regs} und iT_{regs} verwendet werden kann. Zusätzlich weist die Abhängigkeit der HPGD Expression vom extrazellulären Mikromilieu auch auf eine Gewebe-spezifische Expression und potentielle Funktion von HPGD in der T_{reg} Zelle hin.

Zusammengefasst zeigen die Ergebnisse dieser Studie, dass HPGD ein neues Gen repräsentiert, das spezifisch in natürlich vorkommenden regulatorischen Zellen exprimiert wird. Obwohl die Bedeutung von HPGD für die Funktion von T_{regs} noch unklar ist, liefert die vorliegende Studie eine Basis für nachfolgende Experimente, die eine Gewebe-spezifische Funktion von T_{regs} als auch deren Rolle im Tumormikromilieu aufklären kann.

6 References

1. Asano, M., Toda, M., Sakaguchi, N. & Sakaguchi, S. Autoimmune disease as a consequence of developmental abnormality of a T cell subpopulation. *J Exp Med* **184**, 387-396 (1996).
2. Gershon, R.K. & Kondo, K. Cell interactions in the induction of tolerance: the role of thymic lymphocytes. *Immunology* **18**, 723-737 (1970).
3. Gershon, R.K. & Kondo, K. Infectious immunological tolerance. *Immunology* **21**, 903-914 (1971).
4. Okumura, K. & Tada, T. Regulation of homocytotropic antibody formation in the rat. VI. Inhibitory effect of thymocytes on the homocytotropic antibody response. *J Immunol* **107**, 1682-1689 (1971).
5. Droege, W. Amplifying and suppressive effect of thymus cells. *Nature* **234**, 549-551 (1971).
6. Kerbel, R.S. & Eidinger, D. Enhanced immune responsiveness to a thymus-independent antigen early after adult thymectomy: evidence for short-lived inhibitory thymus-derived cells. *Eur J Immunol* **2**, 114-118 (1972).
7. Cantor, H., Shen, F.W. & Boyse, E.A. Separation of helper T cells from suppressor T cells expressing different Ly components. II. Activation by antigen: after immunization, antigen-specific suppressor and helper activities are mediated by distinct T-cell subclasses. *J Exp Med* **143**, 1391-1340 (1976).
8. Jandinski, J., Cantor, H., Tadakuma, T., Peavy, D.L. & Pierce, C.W. Separation of helper T cells from suppressor T cells expressing different Ly components. I. Polyclonal activation: suppressor and helper activities are inherent properties of distinct T-cell subclasses. *J Exp Med* **143**, 1382-1390 (1976).
9. Kronenberg, M.*, et al.* RNA transcripts for I-J polypeptides are apparently not encoded between the I-A and I-E subregions of the murine major histocompatibility complex. *Proc Natl Acad Sci U S A* **80**, 5704-5708 (1983).
10. Steinmetz, M.*, et al.* A molecular map of the immune response region from the major histocompatibility complex of the mouse. *Nature* **300**, 35-42 (1982).
11. Green, D.R., Flood, P.M. & Gershon, R.K. Immunoregulatory T-cell pathways. *Annu Rev Immunol* **1**, 439-463 (1983).
12. Sakaguchi, S., Sakaguchi, N., Asano, M., Itoh, M. & Toda, M. Immunologic self-tolerance maintained by activated T cells expressing IL-2 receptor alpha-chains (CD25). Breakdown of a single mechanism of self-tolerance causes various autoimmune diseases. *J Immunol* **155**, 1151-1164 (1995).
13. Papiernik, M., de Moraes, M.L., Pontoux, C., Vasseur, F. & Penit, C. Regulatory CD4 T cells: expression of IL-2R alpha chain, resistance to clonal deletion and IL-2 dependency. *Int Immunol* **10**, 371-378 (1998).
14. Taams, L.S.*, et al.* Human anergic/suppressive CD4(+)CD25(+) T cells: a highly differentiated and apoptosis-prone population. *Eur J Immunol* **31**, 1122-1131 (2001).
15. Stephens, L.A., Mottet, C., Mason, D. & Powrie, F. Human CD4(+)CD25(+) thymocytes and peripheral T cells have immune suppressive activity in vitro. *Eur J Immunol* **31**, 1247-1254 (2001).
16. Itoh, M.*, et al.* Thymus and autoimmunity: production of CD25+CD4+ naturally anergic and suppressive T cells as a key function of the thymus in maintaining immunologic self-tolerance. *J Immunol* **162**, 5317-5326 (1999).
17. Fisson, S.*, et al.* Continuous activation of autoreactive CD4+ CD25+ regulatory T cells in the steady state. *J Exp Med* **198**, 737-746 (2003).
18. Takahashi, T.*, et al.* Immunologic self-tolerance maintained by CD25+CD4+ naturally anergic and suppressive T cells: induction of autoimmune disease by breaking their anergic/suppressive state. *Int Immunol* **10**, 1969-1980 (1998).
19. Thornton, A.M. & Shevach, E.M. CD4+CD25+ immunoregulatory T cells suppress polyclonal T cell activation in vitro by inhibiting interleukin 2 production. *J Exp Med* **188**, 287-296 (1998).

20. Apostolou, I., Sarukhan, A., Klein, L. & von Boehmer, H. Origin of regulatory T cells with known specificity for antigen. *Nat Immunol* **3**, 756-763 (2002).
21. Jordan, M.S.*, et al.* Thymic selection of CD4+CD25+ regulatory T cells induced by an agonist self-peptide. *Nat Immunol* **2**, 301-306 (2001).
22. Bettini, M.L. & Vignali, D.A. Development of thymically derived natural regulatory T cells. *Ann N Y Acad Sci* **1183**, 1-12 (2010).
23. van Santen, H.M., Benoist, C. & Mathis, D. Number of T reg cells that differentiate does not increase upon encounter of agonist ligand on thymic epithelial cells. *J Exp Med* **200**, 1221-1230 (2004).
24. Tang, Q.*, et al.* Cutting edge: CD28 controls peripheral homeostasis of CD4+CD25+ regulatory T cells. *J Immunol* **171**, 3348-3352 (2003).
25. Salomon, B.*, et al.* B7/CD28 costimulation is essential for the homeostasis of the CD4+CD25+ immunoregulatory T cells that control autoimmune diabetes. *Immunity* **12**, 431-440 (2000).
26. Malek, T.R., Yu, A., Vincek, V., Scibelli, P. & Kong, L. CD4 regulatory T cells prevent lethal autoimmunity in IL-2Rbeta-deficient mice. Implications for the nonredundant function of IL-2. *Immunity* **17**, 167-178 (2002).
27. Fehervari, Z. & Sakaguchi, S. Development and function of CD25+CD4+ regulatory T cells. *Curr Opin Immunol* **16**, 203-208 (2004).
28. Gregg, R.*, et al.* The number of human peripheral blood CD4+ CD25high regulatory T cells increases with age. *Clin Exp Immunol* **140**, 540-546 (2005).
29. Thorstenson, K.M. & Khoruts, A. Generation of anergic and potentially immunoregulatory CD25+CD4 T cells in vivo after induction of peripheral tolerance with intravenous or oral antigen. *J Immunol* **167**, 188-195 (2001).
30. Apostolou, I. & von Boehmer, H. In vivo instruction of suppressor commitment in naive T cells. *J Exp Med* **199**, 1401-1408 (2004).
31. Hawiger, D.*, et al.* Dendritic cells induce peripheral T cell unresponsiveness under steady state conditions in vivo. *J Exp Med* **194**, 769-779 (2001).
32. Hawiger, D., Masilamani, R.F., Bettelli, E., Kuchroo, V.K. & Nussenzweig, M.C. Immunological unresponsiveness characterized by increased expression of CD5 on peripheral T cells induced by dendritic cells in vivo. *Immunity* **20**, 695-705 (2004).
33. Kretschmer, K.*, et al.* Inducing and expanding regulatory T cell populations by foreign antigen. *Nat Immunol* **6**, 1219-1227 (2005).
34. Jordan, M.A. & Baxter, A.G. The genetics of immunoregulatory T cells. *J Autoimmun* **31**, 237-244 (2008).
35. Roncarolo, M.G.*, et al.* Interleukin-10-secreting type 1 regulatory T cells in rodents and humans. *Immunol Rev* **212**, 28-50 (2006).
36. Collison, L.W.*, et al.* IL-35-mediated induction of a potent regulatory T cell population. *Nat Immunol* **11**, 1093-1101 (2010).
37. Gandhi, R.*, et al.* Cutting edge: human latency-associated peptide+ T cells: a novel regulatory T cell subset. *J Immunol* **184**, 4620-4624 (2010).
38. Malone, F., Carper, K., Reyes, J. & Li, W. gammadeltaT cells are involved in liver transplant tolerance. *Transplant Proc* **41**, 233-235 (2009).
39. Seino, K.I.*, et al.* Requirement for natural killer T (NKT) cells in the induction of allograft tolerance. *Proc Natl Acad Sci U S A* **98**, 2577-2581 (2001).
40. Zhou, J., Carr, R.I., Liwski, R.S., Stadnyk, A.W. & Lee, T.D. Oral exposure to alloantigen generates intragraft CD8+ regulatory cells. *J Immunol* **167**, 107-113 (2001).
41. Zhang, Z.X., Yang, L., Young, K.J., DuTemple, B. & Zhang, L. Identification of a previously unknown antigen-specific regulatory T cell and its mechanism of suppression. *Nat Med* **6**, 782-789 (2000).
42. Curotto de Lafaille, M.A. & Lafaille, J.J. Natural and adaptive foxp3+ regulatory T cells: more of the same or a division of labor? *Immunity* **30**, 626-635 (2009).
43. Minami, Y., Kono, T., Miyazaki, T. & Taniguchi, T. The IL-2 receptor complex: its structure, function, and target genes. *Annu Rev Immunol* **11**, 245-268 (1993).

44. Sakaguchi, S. Naturally arising CD4+ regulatory t cells for immunologic self-tolerance and negative control of immune responses. *Annu Rev Immunol* **22**, 531-562 (2004).
45. Read, S., Malmstrom, V. & Powrie, F. Cytotoxic T lymphocyte-associated antigen 4 plays an essential role in the function of CD25(+)CD4(+) regulatory cells that control intestinal inflammation. *J Exp Med* **192**, 295-302 (2000).
46. Seddiki, N*., et al.* Expression of interleukin (IL)-2 and IL-7 receptors discriminates between human regulatory and activated T cells. *J Exp Med* **203**, 1693-1700 (2006).
47. Liu, W*., et al.* CD127 expression inversely correlates with FoxP3 and suppressive function of human CD4+ T reg cells. *J Exp Med* **203**, 1701-1711 (2006).
48. Shimizu, J., Yamazaki, S., Takahashi, T., Ishida, Y. & Sakaguchi, S. Stimulation of CD25(+)CD4(+) regulatory T cells through GITR breaks immunological self-tolerance. *Nat Immunol* **3**, 135-142 (2002).
49. McHugh, R.S*., et al.* CD4(+)CD25(+) immunoregulatory T cells: gene expression analysis reveals a functional role for the glucocorticoid-induced TNF receptor. *Immunity* **16**, 311-323 (2002).
50. Huang, C.T*., et al.* Role of LAG-3 in regulatory T cells. *Immunity* **21**, 503-513 (2004).
51. Borsellino, G*., et al.* Expression of ectonucleotidase CD39 by Foxp3+ Treg cells: hydrolysis of extracellular ATP and immune suppression. *Blood* **110**, 1225-1232 (2007).
52. Tran, D.Q*., et al.* Selective expression of latency-associated peptide (LAP) and IL-1 receptor type I/II (CD121a/CD121b) on activated human FOXP3+ regulatory T cells allows for their purification from expansion cultures. *Blood* **113**, 5125-5133 (2009).
53. Chen, M.L., Yan, B.S., Bando, Y., Kuchroo, V.K. & Weiner, H.L. Latency-associated peptide identifies a novel CD4+CD25+ regulatory T cell subset with TGFbeta-mediated function and enhanced suppression of experimental autoimmune encephalomyelitis. *J Immunol* **180**, 7327-7337 (2008).
54. Nakamura, K., Kitani, A. & Strober, W. Cell contact-dependent immunosuppression by CD4(+)CD25(+) regulatory T cells is mediated by cell surface-bound transforming growth factor beta. *J Exp Med* **194**, 629-644 (2001).
55. Vu, M.D*., et al.* OX40 costimulation turns off Foxp3+ Tregs. *Blood* **110**, 2501-2510 (2007).
56. Choi, B.K*., et al.* 4-1BB-dependent inhibition of immunosuppression by activated CD4+CD25+ T cells. *J Leukoc Biol* **75**, 785-791 (2004).
57. Kwon, B.S*., et al.* Immune responses in 4-1BB (CD137)-deficient mice. *J Immunol* **168**, 5483-5490 (2002).
58. Wang, R., Wan, Q., Kozhaya, L., Fujii, H. & Unutmaz, D. Identification of a regulatory T cell specific cell surface molecule that mediates suppressive signals and induces Foxp3 expression. *PLoS One* **3**, e2705 (2008).
59. Fontenot, J.D., Gavin, M.A. & Rudensky, A.Y. Foxp3 programs the development and function of CD4+CD25+ regulatory T cells. *Nat Immunol* **4**, 330-336 (2003).
60. Hori, S., Nomura, T. & Sakaguchi, S. Control of regulatory T cell development by the transcription factor Foxp3. *Science* **299**, 1057-1061 (2003).
61. Khattri, R., Cox, T., Yasayko, S.A. & Ramsdell, F. An essential role for Scurfin in CD4+CD25+ T regulatory cells. *Nat Immunol* **4**, 337-342 (2003).
62. Sakaguchi, S., Yamaguchi, T., Nomura, T. & Ono, M. Regulatory T cells and immune tolerance. *Cell* **133**, 775-787 (2008).
63. Brunkow, M.E*., et al.* Disruption of a new forkhead/winged-helix protein, scurfin, results in the fatal lymphoproliferative disorder of the scurfy mouse. *Nat Genet* **27**, 68-73 (2001).
64. Chatila, T.A*., et al.* JM2, encoding a fork head-related protein, is mutated in X-linked autoimmunity-allergic disregulation syndrome. *J Clin Invest* **106**, R75-81 (2000).
65. Bennett, C.L*., et al.* The immune dysregulation, polyendocrinopathy, enteropathy, X-linked syndrome (IPEX) is caused by mutations of FOXP3. *Nat Genet* **27**, 20-21 (2001).
66. Wildin, R.S*., et al.* X-linked neonatal diabetes mellitus, enteropathy and endocrinopathy syndrome is the human equivalent of mouse scurfy. *Nat Genet* **27**, 18-20 (2001).

67. Roncador, G*., et al.* Analysis of FOXP3 protein expression in human CD4+CD25+ regulatory T cells at the single-cell level. *Eur J Immunol* **35**, 1681-1691 (2005).
68. Allan, S.E*., et al.* Activation-induced FOXP3 in human T effector cells does not suppress proliferation or cytokine production. *Int Immunol* **19**, 345-354 (2007).
69. Passerini, L*., et al.* STAT5-signaling cytokines regulate the expression of FOXP3 in CD4+CD25+ regulatory T cells and CD4+CD25- effector T cells. *Int Immunol* **20**, 421-431 (2008).
70. Walker, M.R., Carson, B.D., Nepom, G.T., Ziegler, S.F. & Buckner, J.H. De novo generation of antigen-specific CD4+CD25+ regulatory T cells from human CD4+CD25- cells. *Proc Natl Acad Sci U S A* **102**, 4103-4108 (2005).
71. Walker, M.R*., et al.* Induction of FoxP3 and acquisition of T regulatory activity by stimulated human CD4+CD25- T cells. *J Clin Invest* **112**, 1437-1443 (2003).
72. Shevach, E.M. CD4+ CD25+ suppressor T cells: more questions than answers. *Nat Rev Immunol* **2**, 389-400 (2002).
73. Su, L*., et al.* Murine CD4+CD25+ regulatory T cells fail to undergo chromatin remodeling across the proximal promoter region of the IL-2 gene. *J Immunol* **173**, 4994-5001 (2004).
74. Tang, Q*., et al.* In vitro-expanded antigen-specific regulatory T cells suppress autoimmune diabetes. *J Exp Med* **199**, 1455-1465 (2004).
75. Klein, L., Khazaie, K. & von Boehmer, H. In vivo dynamics of antigen-specific regulatory T cells not predicted from behavior in vitro. *Proc Natl Acad Sci U S A* **100**, 8886-8891 (2003).
76. Walker, L.S., Chodos, A., Eggena, M., Dooms, H. & Abbas, A.K. Antigen-dependent proliferation of CD4+ CD25+ regulatory T cells in vivo. *J Exp Med* **198**, 249-258 (2003).
77. Takahashi, T. & Sakaguchi, S. Naturally arising CD25+CD4+ regulatory T cells in maintaining immunologic self-tolerance and preventing autoimmune disease. *Curr Mol Med* **3**, 693-706 (2003).
78. Thornton, A.M. & Shevach, E.M. Suppressor effector function of CD4+CD25+ immunoregulatory T cells is antigen nonspecific. *J Immunol* **164**, 183-190 (2000).
79. Shevach, E.M., McHugh, R.S., Piccirillo, C.A. & Thornton, A.M. Control of T-cell activation by CD4+ CD25+ suppressor T cells. *Immunol Rev* **182**, 58-67 (2001).
80. Piccirillo, C.A. & Shevach, E.M. Cutting edge: control of CD8+ T cell activation by CD4+CD25+ immunoregulatory cells. *J Immunol* **167**, 1137-1140 (2001).
81. Paust, S., Lu, L., McCarty, N. & Cantor, H. Engagement of B7 on effector T cells by regulatory T cells prevents autoimmune disease. *Proc Natl Acad Sci U S A* **101**, 10398-10403 (2004).
82. Grossman, W.J*., et al.* Differential expression of granzymes A and B in human cytotoxic lymphocyte subsets and T regulatory cells. *Blood* **104**, 2840-2848 (2004).
83. Gondek, D.C., Lu, L.F., Quezada, S.A., Sakaguchi, S. & Noelle, R.J. Cutting edge: contact-mediated suppression by CD4+CD25+ regulatory cells involves a granzyme B-dependent, perforin-independent mechanism. *J Immunol* **174**, 1783-1786 (2005).
84. Zhao, D.M., Thornton, A.M., DiPaolo, R.J. & Shevach, E.M. Activated CD4+CD25+ T cells selectively kill B lymphocytes. *Blood* **107**, 3925-3932 (2006).
85. Cao, X*., et al.* Granzyme B and perforin are important for regulatory T cell-mediated suppression of tumor clearance. *Immunity* **27**, 635-646 (2007).
86. Ren, X*., et al.* Involvement of cellular death in TRAIL/DR5-dependent suppression induced by CD4(+)CD25(+) regulatory T cells. *Cell Death Differ* **14**, 2076-2084 (2007).
87. Garin, M.I*., et al.* Galectin-1: a key effector of regulation mediated by CD4+CD25+ T cells. *Blood* **109**, 2058-2065 (2007).
88. Asseman, C., Mauze, S., Leach, M.W., Coffman, R.L. & Powrie, F. An essential role for interleukin 10 in the function of regulatory T cells that inhibit intestinal inflammation. *J Exp Med* **190**, 995-1004 (1999).
89. Green, E.A., Gorelik, L., McGregor, C.M., Tran, E.H. & Flavell, R.A. CD4+CD25+ T regulatory cells control anti-islet CD8+ T cells through TGF-beta-TGF-beta receptor interactions in type 1 diabetes. *Proc Natl Acad Sci U S A* **100**, 10878-10883 (2003).
90. Collison, L.W*., et al.* The inhibitory cytokine IL-35 contributes to regulatory T-cell function. *Nature* **450**, 566-569 (2007).

91. de la Rosa, M., Rutz, S., Dorninger, H. & Scheffold, A. Interleukin-2 is essential for CD4+CD25+ regulatory T cell function. *Eur J Immunol* **34**, 2480-2488 (2004).
92. Pandiyan, P., Zheng, L., Ishihara, S., Reed, J. & Lenardo, M.J. CD4+CD25+Foxp3+ regulatory T cells induce cytokine deprivation-mediated apoptosis of effector CD4+ T cells. *Nat Immunol* **8**, 1353-1362 (2007).
93. Duthoit, C.T., Mekala, D.J., Alli, R.S. & Geiger, T.L. Uncoupling of IL-2 signaling from cell cycle progression in naive CD4+ T cells by regulatory CD4+CD25+ T lymphocytes. *J Immunol* **174**, 155-163 (2005).
94. Bopp, T*., et al.* Cyclic adenosine monophosphate is a key component of regulatory T cell-mediated suppression. *J Exp Med* **204**, 1303-1310 (2007).
95. Deaglio, S*., et al.* Adenosine generation catalyzed by CD39 and CD73 expressed on regulatory T cells mediates immune suppression. *J Exp Med* **204**, 1257-1265 (2007).
96. Tang, Q*., et al.* Visualizing regulatory T cell control of autoimmune responses in nonobese diabetic mice. *Nat Immunol* **7**, 83-92 (2006).
97. Tadokoro, C.E*., et al.* Regulatory T cells inhibit stable contacts between CD4+ T cells and dendritic cells in vivo. *J Exp Med* **203**, 505-511 (2006).
98. Oderup, C., Cederbom, L., Makowska, A., Cilio, C.M. & Ivars, F. Cytotoxic T lymphocyte antigen-4-dependent down-modulation of costimulatory molecules on dendritic cells in CD4+ CD25+ regulatory T-cell-mediated suppression. *Immunology* **118**, 240-249 (2006).
99. Serra, P*., et al.* CD40 ligation releases immature dendritic cells from the control of regulatory CD4+CD25+ T cells. *Immunity* **19**, 877-889 (2003).
100. Fallarino, F*., et al.* Modulation of tryptophan catabolism by regulatory T cells. *Nat Immunol* **4**, 1206-1212 (2003).
101. Mellor, A.L. & Munn, D.H. IDO expression by dendritic cells: tolerance and tryptophan catabolism. *Nat Rev Immunol* **4**, 762-774 (2004).
102. Liang, B*., et al.* Regulatory T cells inhibit dendritic cells by lymphocyte activation gene-3 engagement of MHC class II. *J Immunol* **180**, 5916-5926 (2008).
103. Sarris, M., Andersen, K.G., Randow, F., Mayr, L. & Betz, A.G. Neuropilin-1 expression on regulatory T cells enhances their interactions with dendritic cells during antigen recognition. *Immunity* **28**, 402-413 (2008).
104. Chen, W*., et al.* Conversion of peripheral CD4+CD25- naive T cells to CD4+CD25+ regulatory T cells by TGF-beta induction of transcription factor Foxp3. *J Exp Med* **198**, 1875-1886 (2003).
105. Groux, H*., et al.* A CD4+ T-cell subset inhibits antigen-specific T-cell responses and prevents colitis. *Nature* **389**, 737-742 (1997).
106. Schaefer, C*., et al.* Characteristics of CD4+CD25+ regulatory T cells in the peripheral circulation of patients with head and neck cancer. *Br J Cancer* **92**, 913-920 (2005).
107. Wolf, A.M*., et al.* Increase of regulatory T cells in the peripheral blood of cancer patients. *Clin Cancer Res* **9**, 606-612 (2003).
108. Ormandy, L.A*., et al.* Increased populations of regulatory T cells in peripheral blood of patients with hepatocellular carcinoma. *Cancer Res* **65**, 2457-2464 (2005).
109. Sasada, T., Kimura, M., Yoshida, Y., Kanai, M. & Takabayashi, A. CD4+CD25+ regulatory T cells in patients with gastrointestinal malignancies: possible involvement of regulatory T cells in disease progression. *Cancer* **98**, 1089-1099 (2003).
110. Hiraoka, N., Onozato, K., Kosuge, T. & Hirohashi, S. Prevalence of FOXP3+ regulatory T cells increases during the progression of pancreatic ductal adenocarcinoma and its premalignant lesions. *Clin Cancer Res* **12**, 5423-5434 (2006).
111. Liyanage, U.K*., et al.* Prevalence of regulatory T cells is increased in peripheral blood and tumor microenvironment of patients with pancreas or breast adenocarcinoma. *J Immunol* **169**, 2756-2761 (2002).
112. Curiel, T.J*., et al.* Specific recruitment of regulatory T cells in ovarian carcinoma fosters immune privilege and predicts reduced survival. *Nat Med* **10**, 942-949 (2004).
113. Bates, G.J*., et al.* Quantification of regulatory T cells enables the identification of high-risk breast cancer patients and those at risk of late relapse. *J Clin Oncol* **24**, 5373-5380 (2006).

114. Pardoll, D. Does the immune system see tumors as foreign or self? *Annu Rev Immunol* **21**, 807-839 (2003).
115. Ishida, T.*, et al.* Specific recruitment of CC chemokine receptor 4-positive regulatory T cells in Hodgkin lymphoma fosters immune privilege. *Cancer Res* **66**, 5716-5722 (2006).
116. Liu, V.C.*, et al.* Tumor evasion of the immune system by converting CD4+CD25- T cells into CD4+CD25+ T regulatory cells: role of tumor-derived TGF-beta. *J Immunol* **178**, 2883-2892 (2007).
117. Valzasina, B., Piconese, S., Guiducci, C. & Colombo, M.P. Tumor-induced expansion of regulatory T cells by conversion of CD4+CD25- lymphocytes is thymus and proliferation independent. *Cancer Res* **66**, 4488-4495 (2006).
118. Bazan, J.F. Structural design and molecular evolution of a cytokine receptor superfamily. *Proc Natl Acad Sci U S A* **87**, 6934-6938 (1990).
119. Lenardo, M.*, et al.* Mature T lymphocyte apoptosis--immune regulation in a dynamic and unpredictable antigenic environment. *Annu Rev Immunol* **17**, 221-253 (1999).
120. Paliard, X.*, et al.* Simultaneous production of IL-2, IL-4, and IFN-gamma by activated human CD4+ and CD8+ T cell clones. *J Immunol* **141**, 849-855 (1988).
121. Seder, R.A. & Paul, W.E. Acquisition of lymphokine-producing phenotype by CD4+ T cells. *Annu Rev Immunol* **12**, 635-673 (1994).
122. Waldmann, T.A.*, et al.* Expression of interleukin 2 receptors on activated human B cells. *J Exp Med* **160**, 1450-1466 (1984).
123. Grimm, E.A., Mazumder, A., Zhang, H.Z. & Rosenberg, S.A. Lymphokine-activated killer cell phenomenon. Lysis of natural killer-resistant fresh solid tumor cells by interleukin 2-activated autologous human peripheral blood lymphocytes. *J Exp Med* **155**, 1823-1841 (1982).
124. Henney, C.S., Kuribayashi, K., Kern, D.E. & Gillis, S. Interleukin-2 augments natural killer cell activity. *Nature* **291**, 335-338 (1981).
125. Benveniste, E.N. & Merrill, J.E. Stimulation of oligodendroglial proliferation and maturation by interleukin-2. *Nature* **321**, 610-613 (1986).
126. Gaffen, S.L. Signaling domains of the interleukin 2 receptor. *Cytokine* **14**, 63-77 (2001).
127. Liu, K.D., Gaffen, S.L., Goldsmith, M.A. & Greene, W.C. Janus kinases in interleukin-2-mediated signaling: JAK1 and JAK3 are differentially regulated by tyrosine phosphorylation. *Curr Biol* **7**, 817-826 (1997).
128. Zhu, M.H., Berry, J.A., Russell, S.M. & Leonard, W.J. Delineation of the regions of interleukin-2 (IL-2) receptor beta chain important for association of Jak1 and Jak3. Jak1-independent functional recruitment of Jak3 to Il-2Rbeta. *J Biol Chem* **273**, 10719-10725 (1998).
129. Ihle, J.N. STATs: signal transducers and activators of transcription. *Cell* **84**, 331-334 (1996).
130. Steelman, L.S.*, et al.* Roles of the Raf/MEK/ERK and PI3K/PTEN/Akt/mTOR pathways in controlling growth and sensitivity to therapy-implications for cancer and aging. *Aging (Albany NY)* **3**, 192-222 (2011).
131. Israel, A. The IKK complex: an integrator of all signals that activate NF-kappaB? *Trends Cell Biol* **10**, 129-133 (2000).
132. Bonizzi, G. & Karin, M. The two NF-kappaB activation pathways and their role in innate and adaptive immunity. *Trends Immunol* **25**, 280-288 (2004).
133. Hayden, M.S. & Ghosh, S. Signaling to NF-kappaB. *Genes Dev* **18**, 2195-2224 (2004).
134. Dolcet, X., Llobet, D., Pallares, J. & Matias-Guiu, X. NF-kB in development and progression of human cancer. *Virchows Arch* **446**, 475-482 (2005).
135. Zhou, Y.J.*, et al.* Hierarchy of protein tyrosine kinases in interleukin-2 (IL-2) signaling: activation of syk depends on Jak3; however, neither Syk nor Lck is required for IL-2-mediated STAT activation. *Mol Cell Biol* **20**, 4371-4380 (2000).
136. Mortellaro, A.*, et al.* New immunosuppressive drug PNU156804 blocks IL-2-dependent proliferation and NF-kappa B and AP-1 activation. *J Immunol* **162**, 7102-7109 (1999).
137. Cianferoni, A.*, et al.* Defective nuclear translocation of nuclear factor of activated T cells and extracellular signal-regulated kinase underlies deficient IL-2 gene expression in Wiskott-Aldrich syndrome. *J Allergy Clin Immunol* **116**, 1364-1371 (2005).

138. Kim, H.P., Imbert, J. & Leonard, W.J. Both integrated and differential regulation of components of the IL-2/IL-2 receptor system. *Cytokine Growth Factor Rev* **17**, 349-366 (2006).
139. Miyazaki, T.*, et al.* Three distinct IL-2 signaling pathways mediated by bcl-2, c-myc, and lck cooperate in hematopoietic cell proliferation. *Cell* **81**, 223-231 (1995).
140. Anggard, E. & Samuelsson, B. Prostaglandins and Related Factors.28.Metabolism of prostaglandin E1 in guinea pig lung: the structures of two metabolites. *J Biol Chem* **12**, 4097-4102 (1964).
141. Ensor, C.M. & Tai, H.H. 15-Hydroxyprostaglandin dehydrogenase. *J Lipid Mediat Cell Signal* **12**, 313-319 (1995).
142. Anggard, E. The biological activities of three metabolites of prostaglandin E 1. *Acta Physiol Scand* **66**, 509-510 (1966).
143. Braithwaite, S.S. & Jarabak, J. Studies on a 15-hydroxyprostaglandin dehydrogenase from human placenta. Purification and partial characterization. *J Biol Chem* **250**, 2315-2318 (1975).
144. Schlegel, W. & Greep, R.O. Prostaglandin 15-hydroxy dehydrogenase from human placenta. *Eur J Biochem* **56**, 245-252 (1975).
145. Bergholte, J.M. & Okita, R.T. Isolation and properties of lung 15-hydroxyprostaglandin dehydrogenase from pregnant rabbits. *Arch Biochem Biophys* **245**, 308-315 (1986).
146. Chang, W.C., Wu, H.L., Hsu, S.Y. & Chen, F.S. Isolation of rat renal NAD(+)-dependent 15-hydroxyprostaglandin dehydrogenase. *Prostaglandins Leukot Essent Fatty Acids* **41**, 19-25 (1990).
147. Lee, S.C. & Levine, L. Prostaglandin metabolism. II. Identification of two 15-hydroxyprostaglandin dehydrogenase types. *J Biol Chem* **250**, 548-552 (1975).
148. Krook, M., Marekov, L. & Jornvall, H. Purification and structural characterization of placental NAD(+)-linked 15-hydroxyprostaglandin dehydrogenase. The primary structure reveals the enzyme to belong to the short-chain alcohol dehydrogenase family. *Biochemistry* **29**, 738-743 (1990).
149. Pichaud, F., Delage-Mourroux, R., Pidoux, E., Jullienne, A. & Rousseau-Merck, M.F. Chromosomal localization of the type-I 15-PGDH gene to 4q34-q35. *Hum Genet* **99**, 279-281 (1997).
150. Nandy, A.*, et al.* Genomic structure and transcriptional regulation of the human NAD+-dependent 15-hydroxyprostaglandin dehydrogenase gene. *J Mol Endocrinol* **31**, 105-121 (2003).
151. Ensor, C.M., Yang, J.Y., Okita, R.T. & Tai, H.H. Cloning and sequence analysis of the cDNA for human placental NAD(+)-dependent 15-hydroxyprostaglandin dehydrogenase. *J Biol Chem* **265**, 14888-14891 (1990).
152. Ensor, C.M., Zhang, H. & Tai, H.H. Purification, cDNA cloning and expression of 15-oxoprostaglandin 13-reductase from pig lung. *Biochem J* **330 (Pt 1)**, 103-108 (1998).
153. Pichaud, F.*, et al.* Sequence of a novel mRNA coding for a C-terminal-truncated form of human NAD(+)-dependent 15-hydroxyprostaglandin dehydrogenase. *Gene* **162**, 319-322 (1995).
154. Delage-Mourroux, R.*, et al.* Cloning and sequencing of a new 15-hydroxyprostaglandin dehydrogenase related mRNA. *Gene* **188**, 143-148 (1997).
155. Ensor, C.M. & Tai, H.H. Site-directed mutagenesis of the conserved tyrosine 151 of human placental NAD(+)-dependent 15-hydroxyprostaglandin dehydrogenase yields a catalytically inactive enzyme. *Biochem Biophys Res Commun* **176**, 840-845 (1991).
156. Ensor, C.M. & Tai, H.H. Bacterial expression and site-directed mutagenesis of two critical residues (tyrosine-151 and lysine-155) of human placental NAD(+)-dependent 15-hydroxyprostaglandin dehydrogenase. *Biochim Biophys Acta* **1208**, 151-156 (1994).
157. Matsuo, M., Ensor, C.M. & Tai, H.H. Cloning and expression of the cDNA for mouse NAD(+)-dependent 15-hydroxyprostaglandin dehydrogenase. *Biochim Biophys Acta* **1309**, 21-24 (1996).

158. Bracken, K.E., Elger, W., Jantke, I., Nanninga, A. & Gellersen, B. Cloning of guinea pig cyclooxygenase-2 and 15-hydroxyprostaglandin dehydrogenase complementary deoxyribonucleic acids: steroid-modulated gene expression correlates to prostaglandin F2 alpha secretion in cultured endometrial cells. *Endocrinology* **138**, 237-247 (1997).
159. Jornvall, H*., et al.* Short-chain dehydrogenases/reductases (SDR). *Biochemistry* **34**, 6003-6013 (1995).
160. Zhou, H. & Tai, H.H. Threonine 188 is critical for interaction with NAD+ in human NAD+-dependent 15-hydroxyprostaglandin dehydrogenase. *Biochem Biophys Res Commun* **257**, 414-417 (1999).
161. Cho, H. & Tai, H.H. Threonine 11 of human NAD(+)-dependent 15-hydroxyprostaglandin dehydrogenase may interact with NAD(+) during catalysis. *Prostaglandins Leukot Essent Fatty Acids* **66**, 505-509 (2002).
162. Mak, O.T., Jornvall, H. & Jeffery, J. The primary prostaglandin-inactivating enzyme of human placenta is a dimeric short-chain dehydrogenase. *Biosci Rep* **2**, 503-508 (1982).
163. Okita, R.T. & Okita, J.R. Prostaglandin-metabolizing enzymes during pregnancy: characterization of NAD(+)-dependent prostaglandin dehydrogenase, carbonyl reductase, and cytochrome P450-dependent prostaglandin omega-hydroxylase. *Crit Rev Biochem Mol Biol* **31**, 101-126 (1996).
164. Kankofer, M. The enzymes responsible for the metabolism of prostaglandins in bovine placenta. *Prostaglandins Leukot Essent Fatty Acids* **61**, 359-362 (1999).
165. Wermuth, B. NADP-dependent 15-hydroxyprostaglandin dehydrogenase is homologous to NAD-dependent 15-hydroxyprostaglandin dehydrogenase and other short-chain alcohol dehydrogenases. *Prostaglandins* **44**, 5-9 (1992).
166. Krook, M., Ghosh, D., Stromberg, R., Carlquist, M. & Jornvall, H. Carboxyethyllysine in a protein: native carbonyl reductase/NADP(+)-dependent prostaglandin dehydrogenase. *Proc Natl Acad Sci U S A* **90**, 502-506 (1993).
167. Tai, H.H., Ensor, C.M., Tong, M., Zhou, H. & Yan, F. Prostaglandin catabolizing enzymes. *Prostaglandins Other Lipid Mediat* **68-69**, 483-493 (2002).
168. Serhan, C.N., Fiore, S., Brezinski, D.A. & Lynch, S. Lipoxin A4 metabolism by differentiated HL-60 cells and human monocytes: conversion to novel 15-oxo and dihydro products. *Biochemistry* **32**, 6313-6319 (1993).
169. Bergholte, J.M., Soberman, R.J., Hayes, R., Murphy, R.C. & Okita, R.T. Oxidation of 15-hydroxyeicosatetraenoic acid and other hydroxy fatty acids by lung prostaglandin dehydrogenase. *Arch Biochem Biophys* **257**, 444-450 (1987).
170. Liu, Y., Yoden, K., Shen, R.F. & Tai, H.H. 12-L-hydroxy-5,8,10-heptadecatrienoic acid (HHT) is an excellent substrate for NAD+-dependent 15-hydroxyprostaglandin dehydrogenase. *Biochem Biophys Res Commun* **129**, 268-274 (1985).
171. Agins, A.P., Thomas, M.J., Edmonds, C.G. & McCloskey, J.A. Identification of 12-keto-5,8,10-heptadecatrienoic acid as an arachidonic acid metabolite produced by human HL-60 leukemia cells. *Biochem Pharmacol* **36**, 1799-1805 (1987).
172. Xun, C.Q., Ensor, C.M. & Tai, H.H. Regulation of synthesis and activity of NAD(+)-dependent 15-hydroxy-prostaglandin dehydrogenase (15-PGDH) by dexamethasone and phorbol ester in human erythroleukemia (HEL) cells. *Biochem Biophys Res Commun* **177**, 1258-1265 (1991).
173. Xun, C.Q., Tian, Z.G. & Tai, H.H. Stimulation of synthesis de novo of NAD(+)-dependent 15-hydroxyprostaglandin dehydrogenase in human promyelocytic leukaemia (HL-60) cells by phorbol ester. *Biochem J* **279 (Pt 2)**, 553-558 (1991).
174. Frenkian, M., Pidoux, E., Baudoin, C., Segond, N. & Jullienne, A. Indomethacin increases 15-PGDH mRNA expression in HL60 cells differentiated by PMA. *Prostaglandins Leukot Essent Fatty Acids* **64**, 87-93 (2001).
175. Patel, F.A., Clifton, V.L., Chwalisz, K. & Challis, J.R. Steroid regulation of prostaglandin dehydrogenase activity and expression in human term placenta and chorio-decidua in relation to labor. *J Clin Endocrinol Metab* **84**, 291-299 (1999).

176. Pomini, F., Caruso, A. & Challis, J.R. Interleukin-10 modifies the effects of interleukin-1beta and tumor necrosis factor-alpha on the activity and expression of prostaglandin H synthase-2 and the NAD+-dependent 15-hydroxyprostaglandin dehydrogenase in cultured term human villous trophoblast and chorion trophoblast cells. *J Clin Endocrinol Metab* **84**, 4645-4651 (1999).
177. Chi, X. & Tai, H.H. Interleukin-4 up-regulates 15-hydroxyprostaglandin dehydrogenase (15-PGDH) in human lung cancer cells. *Exp Cell Res* **316**, 2251-2259 (2010).
178. Miyaki, A., Yang, P., Tai, H.H., Subbaramaiah, K. & Dannenberg, A.J. Bile acids inhibit NAD+-dependent 15-hydroxyprostaglandin dehydrogenase transcription in colonocytes. *Am J Physiol Gastrointest Liver Physiol* **297**, G559-566 (2009).
179. Matsuo, M., Ensor, C.M. & Tai, H.H. Characterization of the genomic structure and promoter of the mouse NAD+-dependent 15-hydroxyprostaglandin dehydrogenase gene. *Biochem Biophys Res Commun* **235**, 582-586 (1997).
180. Greenland, K.J*., et al.* The human NAD+-dependent 15-hydroxyprostaglandin dehydrogenase gene promoter is controlled by Ets and activating protein-1 transcription factors and progesterone. *Endocrinology* **141**, 581-597 (2000).
181. Huang, G*., et al.* 15-Hydroxyprostaglandin dehydrogenase is a target of hepatocyte nuclear factor 3beta and a tumor suppressor in lung cancer. *Cancer Res* **68**, 5040-5048 (2008).
182. Coggins, K.G*., et al.* Metabolism of PGE2 by prostaglandin dehydrogenase is essential for remodeling the ductus arteriosus. *Nat Med* **8**, 91-92 (2002).
183. Celis, J.E*., et al.* Loss of adipocyte-type fatty acid binding protein and other protein biomarkers is associated with progression of human bladder transitional cell carcinomas. *Cancer Res* **56**, 4782-4790 (1996).
184. Yan, M*., et al.* 15-Hydroxyprostaglandin dehydrogenase, a COX-2 oncogene antagonist, is a TGF-beta-induced suppressor of human gastrointestinal cancers. *Proc Natl Acad Sci U S A* **101**, 17468-17473 (2004).
185. Wolf, I*., et al.* 15-hydroxyprostaglandin dehydrogenase is a tumor suppressor of human breast cancer. *Cancer Res* **66**, 7818-7823 (2006).
186. Heighway, J*., et al.* Expression profiling of primary non-small cell lung cancer for target identification. *Oncogene* **21**, 7749-7763 (2002).
187. Li, M*., et al.* Suppression of invasive properties of colorectal carcinoma SW480 cells by 15-hydroxyprostaglandin dehydrogenase gene. *Cancer Invest* **26**, 905-912 (2008).
188. Nelson, P.N*., et al.* Monoclonal antibodies. *Mol Pathol* **53**, 111-117 (2000).
189. Haurum, J.S. Recombinant polyclonal antibodies: the next generation of antibody therapeutics? *Drug Discov Today* **11**, 655-660 (2006).
190. Kohler, G. & Milstein, C. Continuous cultures of fused cells secreting antibody of predefined specificity. *Nature* **256**, 495-497 (1975).
191. Ward, E.S., Gussow, D., Griffiths, A.D., Jones, P.T. & Winter, G. Binding activities of a repertoire of single immunoglobulin variable domains secreted from Escherichia coli. *Nature* **341**, 544-546 (1989).
192. Smith, G.P. Filamentous fusion phage: novel expression vectors that display cloned antigens on the virion surface. *Science* **228**, 1315-1317 (1985).
193. McCafferty, J., Griffiths, A.D., Winter, G. & Chiswell, D.J. Phage antibodies: filamentous phage displaying antibody variable domains. *Nature* **348**, 552-554 (1990).
194. Hoogenboom, H.R. & Winter, G. By-passing immunisation. Human antibodies from synthetic repertoires of germline VH gene segments rearranged in vitro. *J Mol Biol* **227**, 381-388 (1992).
195. Kruisbeek, A.M. Isolation of mouse mononuclear cells. *Curr Protoc Immunol* **Chapter 3**, Unit 3 1 (2001).
196. Chemnitz, J.M*., et al.* RNA fingerprints provide direct evidence for the inhibitory role of TGFbeta and PD-1 on CD4+ T cells in Hodgkin lymphoma. *Blood* **110**, 3226-3233 (2007).

197. Assenmacher, M., Schmitz, J. & Radbruch, A. Flow cytometric determination of cytokines in activated murine T helper lymphocytes: expression of interleukin-10 in interferon-gamma and in interleukin-4-expressing cells. *Eur J Immunol* **24**, 1097-1101 (1994).
198. Popma, S.H.*, et al.* Immune monitoring in xenotransplantation: the multiparameter flow cytometric mixed lymphocyte culture assay. *Cytometry* **42**, 277-283 (2000).
199. Albertine, K.H. & Gee, M.H. In vivo labeling of neutrophils using a fluorescent cell linker. *J Leukoc Biol* **59**, 631-638 (1996).
200. Elbashir, S.M.*, et al.* Duplexes of 21-nucleotide RNAs mediate RNA interference in cultured mammalian cells. *Nature* **411**, 494-498 (2001).
201. Hamilton, A.J. & Baulcombe, D.C. A species of small antisense RNA in posttranscriptional gene silencing in plants. *Science* **286**, 950-952 (1999).
202. Chomczynski, P. & Sacchi, N. Single-step method of RNA isolation by acid guanidinium thiocyanate-phenol-chloroform extraction. *Anal Biochem* **162**, 156-159 (1987).
203. Laemmli, U.K. Cleavage of structural proteins during the assembly of the head of bacteriophage T4. *Nature* **227**, 680-685 (1970).
204. Tong, M. & Tai, H.H. Induction of NAD(+)-linked 15-hydroxyprostaglandin dehydrogenase expression by androgens in human prostate cancer cells. *Biochem Biophys Res Commun* **276**, 77-81 (2000).
205. Otani, T.*, et al.* Levels of NAD(+)-dependent 15-hydroxyprostaglandin dehydrogenase are reduced in inflammatory bowel disease: evidence for involvement of TNF-alpha. *Am J Physiol Gastrointest Liver Physiol* **290**, G361-368 (2006).
206. Sugimoto, N.*, et al.* Foxp3-dependent and -independent molecules specific for CD25+CD4+ natural regulatory T cells revealed by DNA microarray analysis. *Int Immunol* **18**, 1197-1209 (2006).
207. Pfoertner, S.*, et al.* Signatures of human regulatory T cells: an encounter with old friends and new players. *Genome Biol* **7**, R54 (2006).
208. Li, C. & Wong, W.H. Model-based analysis of oligonucleotide arrays: expression index computation and outlier detection. *Proc Natl Acad Sci U S A* **98**, 31-36 (2001).
209. Mizuguchi, H., Xu, Z., Ishii-Watabe, A., Uchida, E. & Hayakawa, T. IRES-dependent second gene expression is significantly lower than cap-dependent first gene expression in a bicistronic vector. *Mol Ther* **1**, 376-382 (2000).
210. Saunders, A.E. & Johnson, P. Modulation of immune cell signalling by the leukocyte common tyrosine phosphatase, CD45. *Cell Signal* **22**, 339-348 (2010).
211. Hermiston, M.L., Xu, Z. & Weiss, A. CD45: a critical regulator of signaling thresholds in immune cells. *Annu Rev Immunol* **21**, 107-137 (2003).
212. Penninger, J.M., Irie-Sasaki, J., Sasaki, T. & Oliveira-dos-Santos, A.J. CD45: new jobs for an old acquaintance. *Nat Immunol* **2**, 389-396 (2001).
213. Tchilian, E.Z. & Beverley, P.C. CD45 in memory and disease. *Arch Immunol Ther Exp (Warsz)* **50**, 85-93 (2002).
214. Boyman, O., Letourneau, S., Krieg, C. & Sprent, J. Homeostatic proliferation and survival of naive and memory T cells. *Eur J Immunol* **39**, 2088-2094 (2009).
215. De Rosa, S.C., Herzenberg, L.A. & Roederer, M. 11-color, 13-parameter flow cytometry: identification of human naive T cells by phenotype, function, and T-cell receptor diversity. *Nat Med* **7**, 245-248 (2001).
216. Dutton, R.W., Bradley, L.M. & Swain, S.L. T cell memory. *Annu Rev Immunol* **16**, 201-223 (1998).
217. Okada, R., Kondo, T., Matsuki, F., Takata, H. & Takiguchi, M. Phenotypic classification of human CD4+ T cell subsets and their differentiation. *Int Immunol* **20**, 1189-1199 (2008).
218. Leitenberg, D. & Bottomly, K. Regulation of naive T cell differentiation by varying the potency of TCR signal transduction. *Semin Immunol* **11**, 283-292 (1999).
219. Zhou, L., Chong, M.M. & Littman, D.R. Plasticity of CD4+ T cell lineage differentiation. *Immunity* **30**, 646-655 (2009).

220. Annunziato, F. & Romagnani, S. Heterogeneity of human effector CD4+ T cells. *Arthritis Res Ther* **11**, 257 (2009).
221. Szabo, S.J*., et al.* A novel transcription factor, T-bet, directs Th1 lineage commitment. *Cell* **100**, 655-669 (2000).
222. Zheng, W. & Flavell, R.A. The transcription factor GATA-3 is necessary and sufficient for Th2 cytokine gene expression in CD4 T cells. *Cell* **89**, 587-596 (1997).
223. Veldhoen, M*., et al.* Transforming growth factor-beta 'reprograms' the differentiation of T helper 2 cells and promotes an interleukin 9-producing subset. *Nat Immunol* **9**, 1341-1346 (2008).
224. Dardalhon, V*., et al.* IL-4 inhibits TGF-beta-induced Foxp3+ T cells and, together with TGF-beta, generates IL-9+ IL-10+ Foxp3(-) effector T cells. *Nat Immunol* **9**, 1347-1355 (2008).
225. Crome, S.Q., Wang, A.Y. & Levings, M.K. Translational mini-review series on Th17 cells: function and regulation of human T helper 17 cells in health and disease. *Clin Exp Immunol* **159**, 109-119 (2010).
226. Wilson, N.J*., et al.* Development, cytokine profile and function of human interleukin 17-producing helper T cells. *Nat Immunol* **8**, 950-957 (2007).
227. Aricha, R., Feferman, T., Fuchs, S. & Souroujon, M.C. Ex vivo generated regulatory T cells modulate experimental autoimmune myasthenia gravis. *J Immunol* **180**, 2132-2139 (2008).
228. Hill, J.A*., et al.* Foxp3 transcription-factor-dependent and -independent regulation of the regulatory T cell transcriptional signature. *Immunity* **27**, 786-800 (2007).
229. Alleva, D.G., Burger, C.J. & Elgert, K.D. Tumor-induced regulation of suppressor macrophage nitric oxide and TNF-alpha production. Role of tumor-derived IL-10, TGF-beta, and prostaglandin E2. *J Immunol* **153**, 1674-1686 (1994).
230. Simmons, D.L., Botting, R.M. & Hla, T. Cyclooxygenase isozymes: the biology of prostaglandin synthesis and inhibition. *Pharmacol Rev* **56**, 387-437 (2004).
231. Sharma, S*., et al.* Tumor cyclooxygenase-2/prostaglandin E2-dependent promotion of FOXP3 expression and CD4+ CD25+ T regulatory cell activities in lung cancer. *Cancer Res* **65**, 5211-5220 (2005).
232. Baratelli, F*., et al.* Prostaglandin E2 induces FOXP3 gene expression and T regulatory cell function in human CD4+ T cells. *J Immunol* **175**, 1483-1490 (2005).
233. Thornton, A.M., Piccirillo, C.A. & Shevach, E.M. Activation requirements for the induction of CD4+CD25+ T cell suppressor function. *Eur J Immunol* **34**, 366-376 (2004).
234. Schimpl, A*., et al.* IL-2 and autoimmune disease. *Cytokine Growth Factor Rev* **13**, 369-378 (2002).
235. Nelson, B.H. IL-2, regulatory T cells, and tolerance. *J Immunol* **172**, 3983-3988 (2004).
236. Yu, A., Zhu, L., Altman, N.H. & Malek, T.R. A low interleukin-2 receptor signaling threshold supports the development and homeostasis of T regulatory cells. *Immunity* **30**, 204-217 (2009).
237. Tai, H.H., Tong, M. & Ding, Y. 15-hydroxyprostaglandin dehydrogenase (15-PGDH) and lung cancer. *Prostaglandins Other Lipid Mediat* **83**, 203-208 (2007).
238. Malek, T.R. & Castro, I. Interleukin-2 receptor signaling: at the interface between tolerance and immunity. *Immunity* **33**, 153-165 (2010).
239. Gomez, J., Garcia-Domingo, D., Martinez, A.C. & Rebollo, A. Role of NF-kappaB in the control of apoptotic and proliferative responses in IL-2-responsive T cells. *Front Biosci* **2**, d49-60 (1997).
240. Cacalano, N.A. & Johnston, J.A. Interleukin-2 signaling and inherited immunodeficiency. *Am J Hum Genet* **65**, 287-293 (1999).
241. Iwashima, M*., et al.* Genetic evidence for Shc requirement in TCR-induced c-Rel nuclear translocation and IL-2 expression. *Proc Natl Acad Sci U S A* **99**, 4544-4549 (2002).
242. Lindemann, M.J., Benczik, M. & Gaffen, S.L. Anti-apoptotic signaling by the interleukin-2 receptor reveals a function for cytoplasmic tyrosine residues within the common gamma (gamma c) receptor subunit. *J Biol Chem* **278**, 10239-10249 (2003).

243. Waldmann, T.A., Dubois, S. & Tagaya, Y. Contrasting roles of IL-2 and IL-15 in the life and death of lymphocytes: implications for immunotherapy. *Immunity* **14**, 105-110 (2001).
244. Sadlon, T.J*., et al.* Genome-wide identification of human FOXP3 target genes in natural regulatory T cells. *J Immunol* **185**, 1071-1081 (2010).
245. Zheng, Y*., et al.* Genome-wide analysis of Foxp3 target genes in developing and mature regulatory T cells. *Nature* **445**, 936-940 (2007).
246. Marson, A*., et al.* Foxp3 occupancy and regulation of key target genes during T-cell stimulation. *Nature* **445**, 931-935 (2007).
247. Chen, C., Rowell, E.A., Thomas, R.M., Hancock, W.W. & Wells, A.D. Transcriptional regulation by Foxp3 is associated with direct promoter occupancy and modulation of histone acetylation. *J Biol Chem* **281**, 36828-36834 (2006).
248. Wu, Y*., et al.* FOXP3 controls regulatory T cell function through cooperation with NFAT. *Cell* **126**, 375-387 (2006).
249. Ono, M*., et al.* Foxp3 controls regulatory T-cell function by interacting with AML1/Runx1. *Nature* **446**, 685-689 (2007).
250. Bettelli, E., Dastrange, M. & Oukka, M. Foxp3 interacts with nuclear factor of activated T cells and NF-kappa B to repress cytokine gene expression and effector functions of T helper cells. *Proc Natl Acad Sci U S A* **102**, 5138-5143 (2005).
251. Hu, H., Djuretic, I., Sundrud, M.S. & Rao, A. Transcriptional partners in regulatory T cells: Foxp3, Runx and NFAT. *Trends Immunol* **28**, 329-332 (2007).
252. Li, B*., et al.* FOXP3 interactions with histone acetyltransferase and class II histone deacetylases are required for repression. *Proc Natl Acad Sci U S A* **104**, 4571-4576 (2007).
253. Heintzman, N.D*., et al.* Distinct and predictive chromatin signatures of transcriptional promoters and enhancers in the human genome. *Nat Genet* **39**, 311-318 (2007).
254. Sakaguchi, S., Miyara, M., Costantino, C.M. & Hafler, D.A. FOXP3+ regulatory T cells in the human immune system. *Nat Rev Immunol* **10**, 490-500 (2010).
255. Walunas, T.L*., et al.* CTLA-4 can function as a negative regulator of T cell activation. *Immunity* **1**, 405-413 (1994).
256. Aerts, N.E*., et al.* Activated T cells complicate the identification of regulatory T cells in rheumatoid arthritis. *Cell Immunol* **251**, 109-115 (2008).
257. Yi, H., Zhen, Y., Jiang, L., Zheng, J. & Zhao, Y. The phenotypic characterization of naturally occurring regulatory CD4+CD25+ T cells. *Cell Mol Immunol* **3**, 189-195 (2006).
258. Bluestone, J.A., Thomson, A.W., Shevach, E.M. & Weiner, H.L. What does the future hold for cell-based tolerogenic therapy? *Nat Rev Immunol* **7**, 650-654 (2007).
259. Roncarolo, M.G. & Battaglia, M. Regulatory T-cell immunotherapy for tolerance to self antigens and alloantigens in humans. *Nat Rev Immunol* **7**, 585-598 (2007).
260. Hoffmann, P*., et al.* Only the CD45RA+ subpopulation of CD4+CD25high T cells gives rise to homogeneous regulatory T-cell lines upon in vitro expansion. *Blood* **108**, 4260-4267 (2006).
261. Tran, D.Q., Ramsey, H. & Shevach, E.M. Induction of FOXP3 expression in naive human CD4+FOXP3 T cells by T-cell receptor stimulation is transforming growth factor-beta dependent but does not confer a regulatory phenotype. *Blood* **110**, 2983-2990 (2007).
262. Thornton, A.M*., et al.* Expression of Helios, an Ikaros transcription factor family member, differentiates thymic-derived from peripherally induced Foxp3+ T regulatory cells. *J Immunol* **184**, 3433-3441 (2010).
263. Getnet, D*., et al.* A role for the transcription factor Helios in human CD4(+)CD25(+) regulatory T cells. *Mol Immunol* **47**, 1595-1600 (2010).
264. Verhagen, J. & Wraith, D.C. Comment on "Expression of Helios, an Ikaros transcription factor family member, differentiates thymic-derived from peripherally induced Foxp3+ T regulatory cells". *J Immunol* **185**, 7129; author reply 7130 (2010).
265. Yaqub, S*., et al.* Regulatory T cells in colorectal cancer patients suppress anti-tumor immune activity in a COX-2 dependent manner. *Cancer Immunol Immunother* **57**, 813-821 (2008).

266. Mahic, M., Yaqub, S., Johansson, C.C., Tasken, K. & Aandahl, E.M. FOXP3+CD4+CD25+ adaptive regulatory T cells express cyclooxygenase-2 and suppress effector T cells by a prostaglandin E2-dependent mechanism. *J Immunol* **177**, 246-254 (2006).
267. Ruggeri, P.*, et al.* Polyamine metabolism in prostaglandin E2-treated human T lymphocytes. *Immunopharmacol Immunotoxicol* **22**, 117-129 (2000).
268. Chemnitz, J.M.*, et al.* Prostaglandin E2 impairs CD4+ T cell activation by inhibition of lck: implications in Hodgkin's lymphoma. *Cancer Res* **66**, 1114-1122 (2006).
269. D'Souza, W.N. & Lefrancois, L. Frontline: An in-depth evaluation of the production of IL-2 by antigen-specific CD8 T cells in vivo. *Eur J Immunol* **34**, 2977-2985 (2004).
270. Sojka, D.K., Bruniquel, D., Schwartz, R.H. & Singh, N.J. IL-2 secretion by CD4+ T cells in vivo is rapid, transient, and influenced by TCR-specific competition. *J Immunol* **172**, 6136-6143 (2004).
271. Yang-Snyder, J.A. & Rothenberg, E.V. Spontaneous expression of interleukin-2 in vivo in specific tissues of young mice. *Dev Immunol* **5**, 223-245 (1998).
272. Cheng, G., Yu, A. & Malek, T.R. T-cell tolerance and the multi-functional role of IL-2R signaling in T-regulatory cells. *Immunol Rev* **241**, 63-76 (2011).
273. Bensinger, S.J.*, et al.* Distinct IL-2 receptor signaling pattern in CD4+CD25+ regulatory T cells. *J Immunol* **172**, 5287-5296 (2004).
274. Sumitani, K.*, et al.* Specific inhibition of cyclooxygenase-2 results in inhibition of proliferation of oral cancer cell lines via suppression of prostaglandin E2 production. *J Oral Pathol Med* **30**, 41-47 (2001).
275. Gately, S. The contributions of cyclooxygenase-2 to tumor angiogenesis. *Cancer Metastasis Rev* **19**, 19-27 (2000).
276. Hata, A.N. & Breyer, R.M. Pharmacology and signaling of prostaglandin receptors: multiple roles in inflammation and immune modulation. *Pharmacol Ther* **103**, 147-166 (2004).
277. Tilley, S.L., Coffman, T.M. & Koller, B.H. Mixed messages: modulation of inflammation and immune responses by prostaglandins and thromboxanes. *J Clin Invest* **108**, 15-23 (2001).
278. Bhattacharya, M.*, et al.* Localization of functional prostaglandin E2 receptors EP3 and EP4 in the nuclear envelope. *J Biol Chem* **274**, 15719-15724 (1999).
279. Schuster, V.L. Prostaglandin transport. *Prostaglandins Other Lipid Mediat* **68-69**, 633-647 (2002).
280. Bao, Y.*, et al.* Prostaglandin transporter PGT is expressed in cell types that synthesize and release prostanoids. *Am J Physiol Renal Physiol* **282**, F1103-1110 (2002).
281. Shiraya, K.*, et al.* A novel transporter of SLC22 family specifically transports prostaglandins and co-localizes with 15-hydroxyprostaglandin dehydrogenase in renal proximal tubules. *J Biol Chem* **285**, 22141-22151 (2010).
282. Shirai, Y.*, et al.* Plasma transforming growth factor-beta 1 in patients with hepatocellular carcinoma. Comparison with chronic liver diseases. *Cancer* **73**, 2275-2279 (1994).
283. Toomey, D.*, et al.* TGF-beta1 is elevated in breast cancer tissue and regulates nitric oxide production from a number of cellular sources during hypoxia re-oxygenation injury. *Br J Biomed Sci* **58**, 177-183 (2001).
284. Blay, J.Y.*, et al.* Serum interleukin-10 in non-Hodgkin's lymphoma: a prognostic factor. *Blood* **82**, 2169-2174 (1993).
285. Gastl, G.A.*, et al.* Interleukin-10 production by human carcinoma cell lines and its relationship to interleukin-6 expression. *Int J Cancer* **55**, 96-101 (1993).
286. Masood, R.*, et al.* Interleukin-10 is an autocrine growth factor for acquired immunodeficiency syndrome-related B-cell lymphoma. *Blood* **85**, 3423-3430 (1995).
287. Murai, M.*, et al.* Interleukin 10 acts on regulatory T cells to maintain expression of the transcription factor Foxp3 and suppressive function in mice with colitis. *Nat Immunol* **10**, 1178-1184 (2009).
288. Donnelly, R.P., Dickensheets, H. & Finbloom, D.S. The interleukin-10 signal transduction pathway and regulation of gene expression in mononuclear phagocytes. *J Interferon Cytokine Res* **19**, 563-573 (1999).

289. Chaudhry, A.*, et al.* CD4+ regulatory T cells control TH17 responses in a Stat3-dependent manner. *Science* **326**, 986-991 (2009).
290. Horwitz, D.A., Zheng, S.G. & Gray, J.D. The role of the combination of IL-2 and TGF-beta or IL-10 in the generation and function of CD4+ CD25+ and CD8+ regulatory T cell subsets. *J Leukoc Biol* **74**, 471-478 (2003).
291. Taylor, P.A., Lees, C.J. & Blazar, B.R. The infusion of ex vivo activated and expanded CD4(+)CD25(+) immune regulatory cells inhibits graft-versus-host disease lethality. *Blood* **99**, 3493-3499 (2002).
292. Vaiopoulos, A.G., Papachroni, K.K. & Papavassiliou, A.G. Colon carcinogenesis: Learning from NF-kappaB and AP-1. *Int J Biochem Cell Biol* **42**, 1061-1065 (2010).
293. Alvarez, J.V.*, et al.* Identification of a genetic signature of activated signal transducer and activator of transcription 3 in human tumors. *Cancer Res* **65**, 5054-5062 (2005).
294. Baron, U.*, et al.* DNA demethylation in the human FOXP3 locus discriminates regulatory T cells from activated FOXP3(+) conventional T cells. *Eur J Immunol* **37**, 2378-2389 (2007).
295. Polansky, J.K.*, et al.* DNA methylation controls Foxp3 gene expression. *Eur J Immunol* **38**, 1654-1663 (2008).
296. Cuddapah, S., Barski, A. & Zhao, K. Epigenomics of T cell activation, differentiation, and memory. *Curr Opin Immunol* **22**, 341-347 (2010).
297. Vettese-Dadey, M.*, et al.* Acetylation of histone H4 plays a primary role in enhancing transcription factor binding to nucleosomal DNA in vitro. *Embo J* **15**, 2508-2518 (1996).
298. Wang, Z.*, et al.* Combinatorial patterns of histone acetylations and methylations in the human genome. *Nat Genet* **40**, 897-903 (2008).
299. Barski, A.*, et al.* High-resolution profiling of histone methylations in the human genome. *Cell* **129**, 823-837 (2007).
300. Johnson, D.S., Mortazavi, A., Myers, R.M. & Wold, B. Genome-wide mapping of in vivo protein-DNA interactions. *Science* **316**, 1497-1502 (2007).
301. Sims, R.J., 3rd, Belotserkovskaya, R. & Reinberg, D. Elongation by RNA polymerase II: the short and long of it. *Genes Dev* **18**, 2437-2468 (2004).
302. Muse, G.W.*, et al.* RNA polymerase is poised for activation across the genome. *Nat Genet* **39**, 1507-1511 (2007).
303. Zeitlinger, J.*, et al.* RNA polymerase stalling at developmental control genes in the Drosophila melanogaster embryo. *Nat Genet* **39**, 1512-1516 (2007).
304. Bruder, D.*, et al.* Neuropilin-1: a surface marker of regulatory T cells. *Eur J Immunol* **34**, 623-630 (2004).
305. Milpied, P.*, et al.* Neuropilin-1 is not a marker of human Foxp3+ Treg. *Eur J Immunol* **39**, 1466-1471 (2009).
306. Feuerer, M.*, et al.* Lean, but not obese, fat is enriched for a unique population of regulatory T cells that affect metabolic parameters. *Nat Med* **15**, 930-939 (2009).
307. Rigas, B., Goldman, I.S. & Levine, L. Altered eicosanoid levels in human colon cancer. *J Lab Clin Med* **122**, 518-523 (1993).
308. Pugh, S. & Thomas, G.A. Patients with adenomatous polyps and carcinomas have increased colonic mucosal prostaglandin E2. *Gut* **35**, 675-678 (1994).
309. Metz, S.A., Rice, M.G. & Robertson, R.P. Applications and limitations of measurement of 15-keto,13,14-dihydro prostaglandin E2 in human blood by radioimmunoassay. *Prostaglandins* **17**, 839-861 (1979).
310. Hamberg, M. & Samuelsson, B. On the metabolism of prostaglandins E 1 and E 2 in man. *J Biol Chem* **246**, 6713-6721 (1971).
311. Granstrom, E., Hamberg, M., Hansson, G. & Kindahl, H. Chemical instability of 15-keto-13,14-dihydro-PGE2: the reason for low assay reliability. *Prostaglandins* **19**, 933-957 (1980).
312. Fitzpatrick, F.A., Aguirre, R., Pike, J.E. & Lincoln, F.H. The stability of 13,14-dihydro-15 keto-PGE2. *Prostaglandins* **19**, 917-931 (1980).
313. Nishimura, S.*, et al.* CD8+ effector T cells contribute to macrophage recruitment and adipose tissue inflammation in obesity. *Nat Med* **15**, 914-920 (2009).

314. Iyer, A., Fairlie, D.P., Prins, J.B., Hammock, B.D. & Brown, L. Inflammatory lipid mediators in adipocyte function and obesity. *Nat Rev Endocrinol* **6**, 71-82 (2010).
315. Williams, E.S., Baylin, A. & Campos, H. Adipose tissue arachidonic acid and the metabolic syndrome in Costa Rican adults. *Clin Nutr* **26**, 474-482 (2007).
316. Savva, S.C*., et al.* Association of adipose tissue arachidonic acid content with BMI and overweight status in children from Cyprus and Crete. *Br J Nutr* **91**, 643-649 (2004).
317. Shimizu, T. Lipid mediators in health and disease: enzymes and receptors as therapeutic targets for the regulation of immunity and inflammation. *Annu Rev Pharmacol Toxicol* **49**, 123-150 (2009).

Appendix

A. Vector charts

Vector charts of plasmids that were used and generated during this work are listed in Table 6 and 7.

Table 6: Vector charts of plasmids used during the present study

1. pcDNA6/V5-His B (Invitrogen Life Technologies, Karlsruhe (DE))	**2. pENTR4 GFP 3' (Invitrogen Life Technologies, Karlsruhe (DE))**
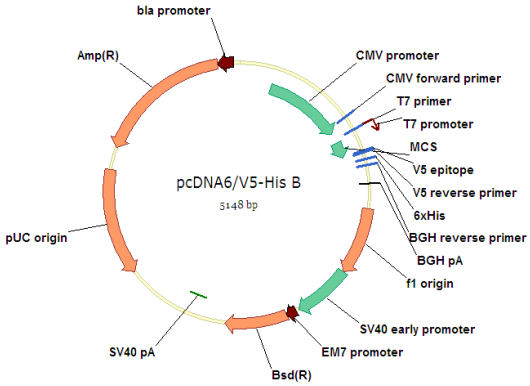	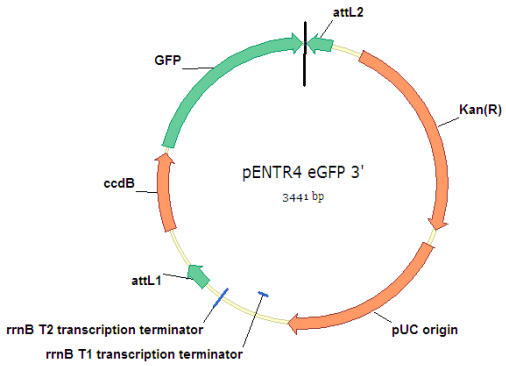
3. pLenti6.2/V5-Dest EF1α (Invitrogen Life Technologies, Karlsruhe (DE))	**4. pIRES2-AcGFP1 (Clontech Laboratories, US)**
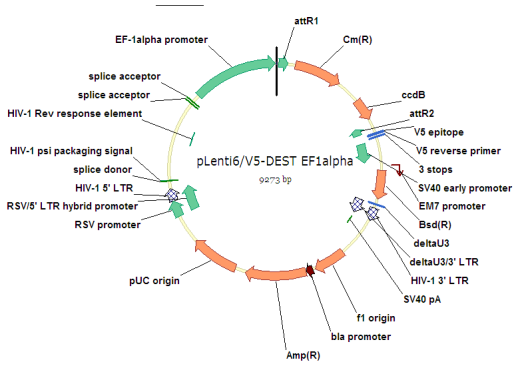	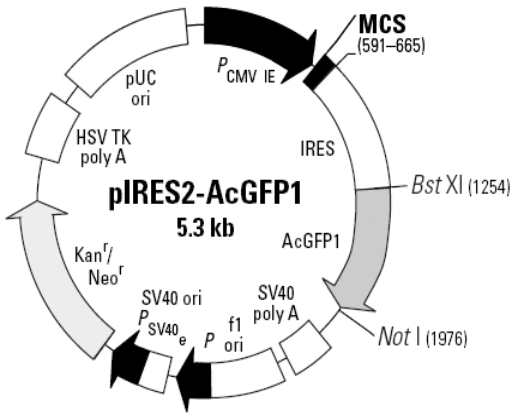

Table 7: Vector charts of plasmids generated during the present study

5. pLenti6.2/V5-Dest EF1α/HPGD-GFP (generated during the present study)	**6. pcDNA6/V5-His B/HPGD (generated during the present study)**
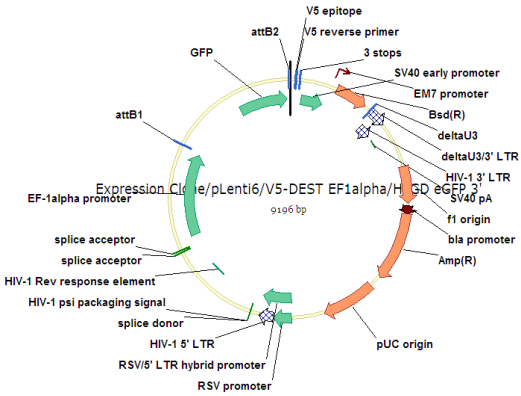	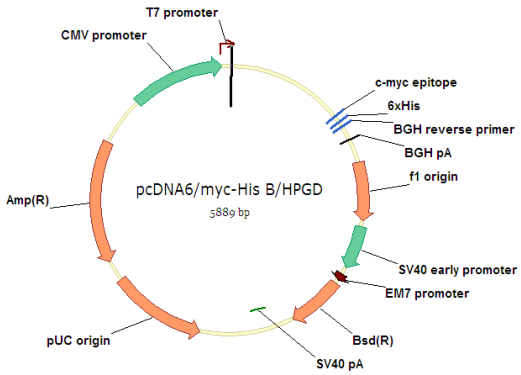
7. pcDNA6/V5-His B/HPGD-GFP (generated during the present study)	**8. pcDNA6/V5-His B/eGFP**
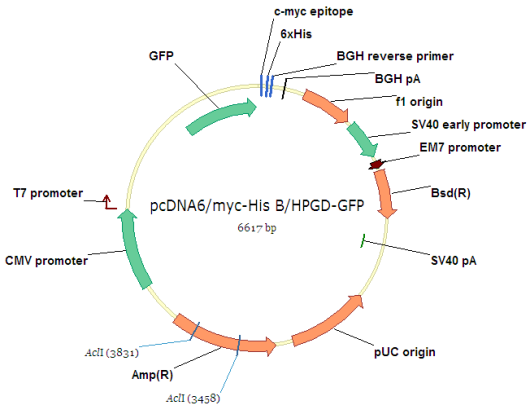	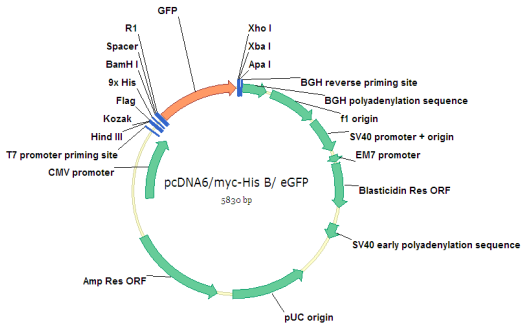

B. Experimental conditions for the gene expression profiling approach

$CD4^+$ T cells were isolated from human peripheral blood of healthy individuals or cancer patients (CLL). The cells were either left untreated (resting) or were incubated with different stimuli up to 24 h. The experimental conditions are listed in Table 8. Details concerning stimulation, coating and generation of the beads (also aAPCs) can be found under 2.2.2.8. In general the beads were used at a ratio of 3 beads: 1 T cell.

Table 8: Different experimental conditions for gene expression profiling

Condition	Abbreviation	Cell type	Treatment	Donor
1	Teff-H-0h-unstim	$CD4^+$ T cell	Rested for 0 h	Healthy
2	Teff-H-8h-unstim	$CD4^+$ T cell	Rested for 8 h	Healthy
3	Teff-H-12h-unstim	$CD4^+$ T cell	Rested for 12 h	Healthy
4	Teff-H-18h-unstim	$CD4^+$ T cell	Rested for 18 h	Healthy
5	Teff-H-19h-unstim	$CD4^+$ T cell	Rested for 19 h	Healthy
6	Teff-H-20h-unstim	$CD4^+$ T cell	Rested for 20 h	Healthy
7	Teff-H-26h-unstim	$CD4^+$ T cell	Rested for 26 h	Healthy
8	Teff-H-8h-CD3	$CD4^+$ T cell	CD3/MHC-I-beads for 8 h	Healthy
9	Teff-H-8h-CD3/CD28	$CD4^+$ T cell	CD3/CD28/MHC-I-beads for 8 h	Healthy
10	Teff-H-20h-CD3/CD28	$CD4^+$ T cell	CD3/CD28/MHC-I-beads for 20 h	Healthy
11	Teff-H-8h-CD3/CD28/PD1	$CD4^+$ T cell	CD3/CD28/PD1-beads for 8 h	Healthy
12	Teff-H-8h-CD3/CD28/CTLA4	$CD4^+$ T cell	CD3/CD28/CTLA4-beads for 8 h	Healthy
13	Teff-H-8h-CD3/CD28+TGF-β	$CD4^+$ T cell	CD3/CD28/MHC-I-beads + TGF-β (30 ng/ml) for 8 h	Healthy
14	Teff-H-8h-CD3/CD28+PGE2	$CD4^+$ T cell	CD3/CD28/MHC-I-beads + PGE_2 (1 µM) for 8 h	Healthy
15	Teff-H-8h-CD3/CD28+IL10	$CD4^+$ T cell	CD3/CD28/MHC-I-beads + IL-10 (50 ng/ml) for 8 h	Healthy
16	Teff-H-A-0h-unstim	$CD4^+CD25^{low}$T cell	Rested for 0 h	Healthy
17	Teff-H-B-0h-unstim	$CD4^+CD25^{int}$ T cell	Rested for 0 h	Healthy
18	Teff-H-C-0h-unstim	$CD4^+CD25^{low-int}$ T cell	Rested for 0 h	Healthy
19	Teff-H-D-0h-unstim	$CD4^+CD25^-$ T cell	Rested for 0 h	Healthy
20	Teff-CLL-D-0h-unstim	$CD4^+CD25^-$ T cell	Rested for 0 h	CLL
21	Teff-H-D-24h-unstim	$CD4^+CD25^-$ T cell	Rested for 24 h	Healthy
22	Teff-H-D-24h-CD3+IL2	$CD4^+CD25^-$ T cell	CD3(1µg/ml) + IL2(20U/ml) for 24 h	Healthy
23	Teff-CLL-D-24h-CD3+IL2	$CD4^+CD25^-$ T cell	CD3(1µg/ml) + IL2(20U/ml) for 24 h	CLL
24	Teff-H-D-24h-	$CD4^+CD25^-$ T cell	CD3(1µg/ml) + IL2(20U/ml) for 24 h	Healthy

	CD3+IL2			
25	Treg-H-0h-unstim	$CD4^+CD25^+$T cell	Rested for 0 h	Healthy
26	Treg-H-6h-unstim	$CD4^+CD25^+$T cell	Rested for 6 h	Healthy
27	Treg-H-0h-unstim	$CD4^+CD25^+$T cell	Rested for 0 h	Healthy
28	Treg-CLL-0h-unstim	$CD4^+CD25^+$T cell	Rested for 0 h	CLL
29	Treg-H-24h-CD3+IL2	$CD4^+CD25^+$T cell	CD3(1µg/ml) + IL2(20U/ml) for 24 h	Healthy
30	Treg-CLL-24h-CD3+IL2	$CD4^+CD25^+$T cell	CD3(1µg/ml) + IL2(20U/ml) for 24 h	CLL
31	Treg-H-24h-unstim	$CD4^+CD25^+$T cell	Rested for 24 h	Healthy
32	Treg-H-exp	$CD4^+CD25^+$T cell	T_{reg} expanded (CD3/CD28/MHC-I-beads + IL2(300U/ml))	Healthy
33	Treg-H-exp-Rapa	$CD4^+CD25^+$T cell	T_{reg} expanded with Rapamycin (CD3/CD28/MHC-I-beads + IL2(300U/ml) + Rapamycin (100ng/ml))	Healthy
34	Treg-H-exp-24h-CD3/CD28	$CD4^+CD25^+$T cell	T_{reg} expanded (CD3/CD28/MHC-I-beads + IL2(300U/ml)) and additionally stimulated with CD3/CD28/MHC-I-beads for 24 h	Healthy

C. HPGD gene expression in T_{reg} cells is higher compared to other PBMC subpopulations

HPGD expression levels in $CD14^+$ monocytes, $CD19^+$ B lymphocytes, $CD3^+$ T lymphocytes and $CD56^+$ NK cells were examined to answer the question whether these PBMC subsets show HPGD expression and on account of this the observed HPGD staining in flow cytometry might be due to intracellular staining of HPGD. In addition, HPGD expression levels in the PBMC subsets were compared with those of T_{reg} and T_{conv} cells. PBMC were isolated from human peripheral blood as described in 2.2.2.3 and separated into $CD14^+$ monocytes, $CD19^+$ B lymphocytes, $CD3^+$ T lymphocytes and $CD56^+$ NK cells. Furthermore, $CD4^+$ T cells were isolated as described in 2.2.2.4 and separated into $CD4^+CD25^+$ T_{reg} and $CD4^+CD25^-$ T_{conv} as described in 2.2.2.5. In Figure 71, it is shown that the mean HPGD expression values in the different cell populations were below or near the background level (dotted line) compared to the high expression levels of T_{reg} cells. Only NK cells showed a slightly enhanced HPGD expression. This result indicates that the observed HPGD signals in flow cytometry were unspecific and due to binding of the HPGD antibodies to unblocked Fc receptors.

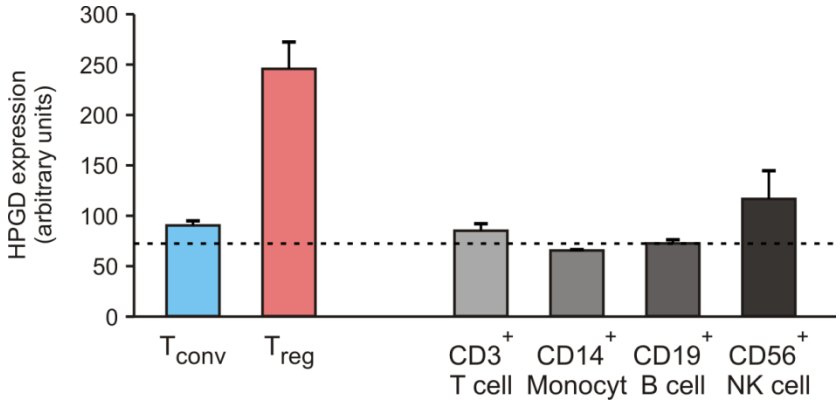

Figure 71: Differential HPGD expression in different PBMC populations
The average gene expression of HPGD in different PBMC populations was obtained by DNA microarray experiments. Therefore, $CD4^+$ T cells and PBMC were isolated from human peripheral blood. $CD4^+$ T cells were separated into $CD4^+CD25^+$ T_{reg} and $CD4^+CD25^-$ T_{conv} cells, PBMC into $CD14^+$ monocytes, $CD19^+$ B lymphocytes, $CD3^+$ T lymphocytes and $CD56^+$ NK cells. The graphic was created with pre-analyzed data, which was normalized with the quantile method. Mean values and standard deviations of three individual experiments are shown. The dotted line indicates the background level of 72.56 arbitrary units, which was calculated with the R statistical software package, using the quantile normalized data.

D. HPGD gene expression is not upregulated during iT_{reg} cell differentiation

HPGD expression levels of induced regulatory T cells were compared with those of different $CD4^+$ T cell subsets. Therefore $CD4^+$ T cells were isolated as described in 2.2.2.4 and were left untreated (T_{unstim}) or stimulated with anti-CD3/CD28/MHC-I coated beads (T_{stim}). $CD4^+$ T cells were further separated into $CD4^+CD25^+$ T_{reg}, $CD4^+CD25^-$ T_{conv}, $CD4^+CD25^-CD45RA^+$ T_{naive} and $CD4^+CD25^-CD45RA^-$ T_{memory} cells as described in 2.2.2.5 and T_{naive} were differentiated towards iT_{reg} cells as described in 2.2.2.6. In Figure 72, it is shown that the mean HPGD expression values in the various cell populations was below or near the background level compared to high expression levels of T_{reg} cells. This result further supports the assumption that HPGD expression is specific for T_{reg} cells.

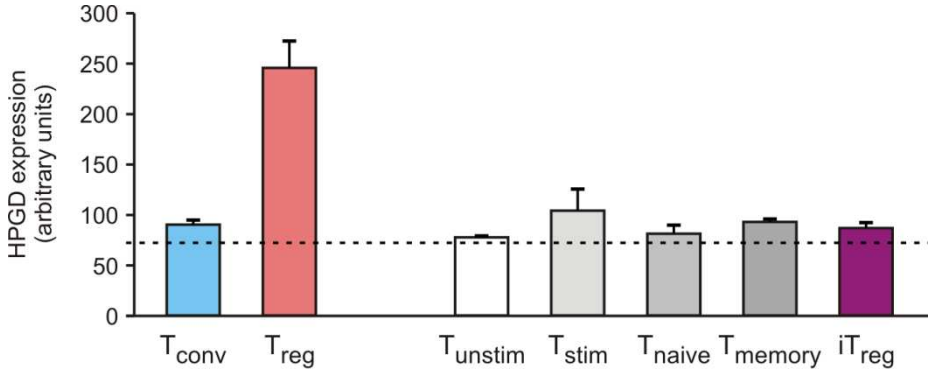

Figure 72: HPGD expression is not upregulated during differentiation towards iT_{reg} cells
The average gene expression of HPGD in different PBMC populations was obtained by DNA microarray experiments. Therefore $CD4^+$ T cells were isolated from human peripheral blood and left untreated (T_{unstim}), stimulated with anti-CD3/CD28/MHC-I coated beads (T_{stim}) or separated into $CD4^+CD25^+$ T_{reg}, $CD4^+CD25^-$ T_{conv}, $CD4^+CD25^-CD45RA^+$ T_{naive} and $CD4^+CD25^-CD45RA^-$ T_{memory} cells. T_{naive} were differentiated into iT_{reg} cells. The graphic was created with pre-analyzed data, which was normalized with the quantile method. Mean values and standard deviations of three individual experiments are shown. The dotted line indicates the background level of 72.56 arbitrary units, which was calculated with the R statistical software package, using the quantile normalized data.
.

E. Expression of lineage specific transcription factors as read out for successful T-cell differentiation

Successful differentiation towards different T helper cell subsets was controlled by upregulation of lineage specific transcription factors, depicted in Figure 73.

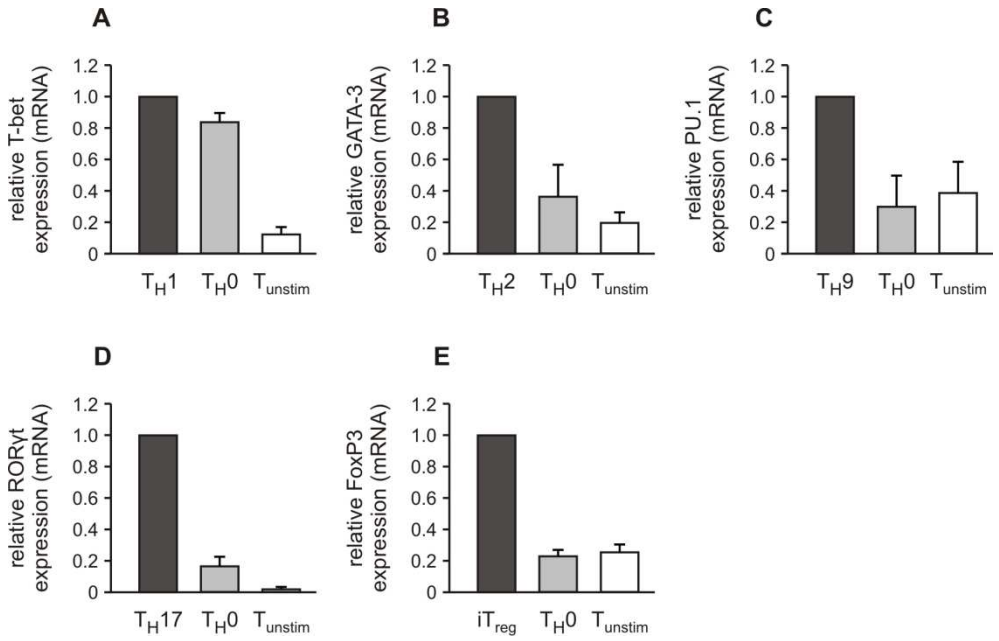

Figure 73: Upregulated expression of lineage specific transcription factors as read out for successful T cell differentiation towards a T_H1, T_H2, T_H9, T_H17 and iT_{reg} cell phenotype
Human $CD4^+CD25^-CD45RA^+$ T_{naive} cells were purified and stimulated with anti-CD3/CD28/MHC-I-coated beads and the appropriate cytokines to induce differentiation towards T_H1, T_H2, T_H9, T_H17 or iT_{reg} cells. T_H0 cells represent control cells that were only stimulated with anti-CD3/CD28/MHC-I-coated beads. T_{unstim} represent unstimulated control cells. Relative mRNA expression was assessed by qRT-PCR after 7 days of T cell differentiation in comparison to B2M expression. (**A**) Relative T-bet mRNA expression in T_H1, T_H0 and T_{unstim} cells. (**B**) Relative GATA-3 mRNA expression in T_H2, T_H0 and T_{unstim} cells. (**C**) Relative PU.1 mRNA expression in T_H9, T_H0 and T_{unstim} cells. (**D**) Relative RORγt mRNA expression in T_H17, T_H0 and T_{unstim} cells. (**E**) Relative FOXP3 mRNA expression in iT_{reg}, T_H0 and T_{unstim} cells. Mean values and standard deviations of three independent experiments are shown. Data were normalized to the respective T cell subset.

F. Test of toxic effects of different inhibitors on $CD4^+$ T lymphocytes

In the previous experiments it was shown that HPGD expression was significantly enhanced in T_{reg} cells upon stimulation with IL-2. Binding of IL-2 to the IL-2 receptor leads to activation of different signaling cascades, such as the MAPK and PI3K pathways or JAK/STAT signaling. The contribution of the above mentioned signaling cascades to upregulation of HPGD in T_{reg} cells was examined by targeting key molecules of the respective pathways with specific inhibitors to elucidate which signaling molecules are involved in IL-2-mediated HPGD upregulation. To exclude effects by the respective inhibitors on cell death and apoptosis rate, the different inhibitors were tested on cell toxicity by assessment of cell viability of $CD4^+$ T lymphocytes. Therefore, $CD4^+$ T cells were purified from human peripheral blood and incubated for 24 h with the different inhibitors in increasing concentrations (see Figure 74). After 24 h cell viability was measured by means of propidium iodide incorporation in flow cytometry. The inhibitors showed no toxic effects at the indicated concentrations, as shown in Figure 74.

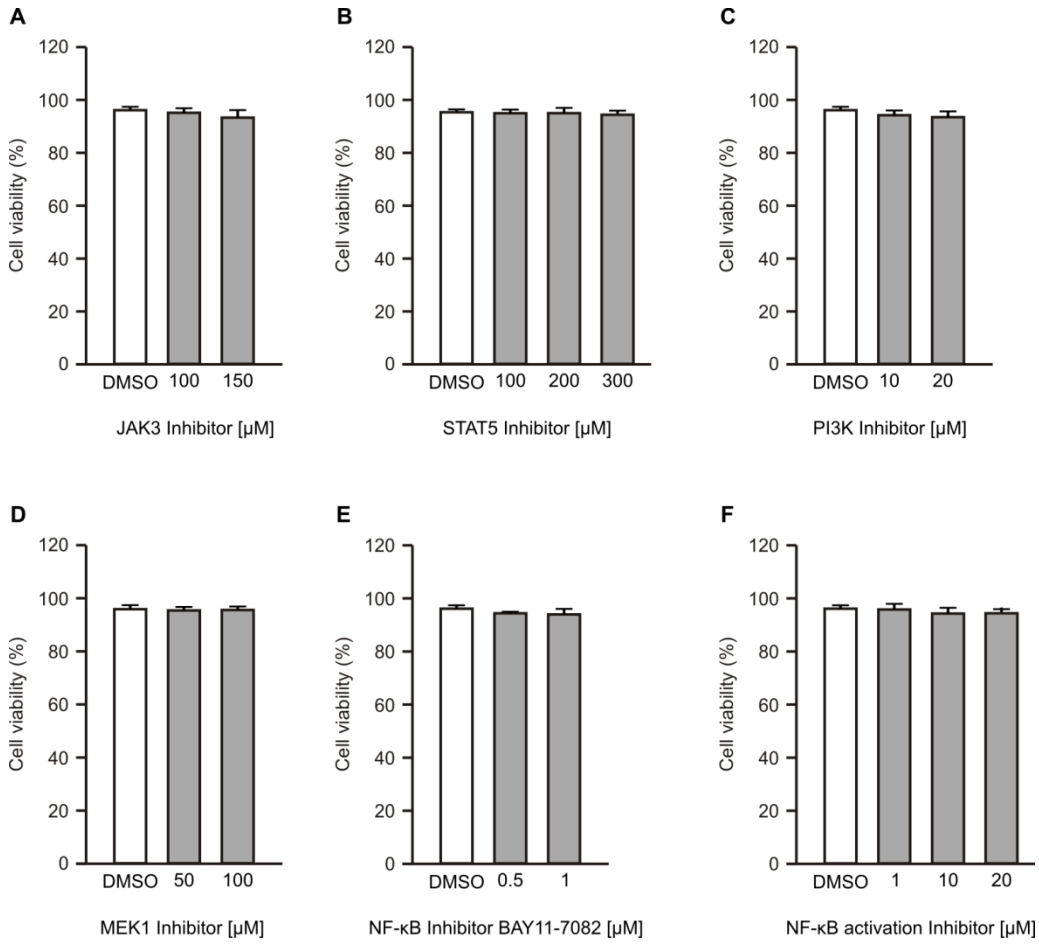

Figure 74: Cell viability of CD4$^+$ T cells after treatment with different inhibitors in different concentrations

Human CD4$^+$ T cells were purified and stimulated for 24 h with different inhibitors or the respective amount of DMSO. Following inhibitors were used: (**A**) JAK3 inhibitor (Janex-1) as 100 & 150µM, (**B**) STAT5 inhibitor as 100, 200 & 300µM, (**C**) PI3K inhibitor (LY249002) as 10 & 20µM, (**D**) MEK1 inhibitor (PD98059) as 50 & 100µM, (**E**) NF-κB inhibitor BAY11-7082 as 0.5 & 1µM and (**F**) NF-κB activation inhibitor as 1, 10 & 20µM. The percentage of dead cells was analyzed by propidium iodide (PI) staining. Data represent mean values and standard deviations of three experiments.

G. Control of the siRNA mediated FOXP3 knockdown in human regulatory T cells

The transcription factor FOXP3 can influence the expression of various target genes in T_{reg} cells, as it can repress as well as induce gene expression.[244-246] As HPGD expression was shown to be specifically enhanced in human T_{reg} cells compared to T_{conv}, it was of interest to determine whether HPGD is a target gene of FOXP3. To answer the question whether HPGD expression is under the control of FOXP3, it was tested whether HPGD expression in human T_{reg} cells would be changed after silencing FOXP3 by a siRNA knockdown. Therefore, human T_{reg} cells were isolated from peripheral blood and siRNA-mediated knockdown of FOXP3 or a control knockdown in T_{reg} cells was performed. FOXP3 mRNA expression was assessed by qRT-PCR analysis and protein expression by intracellular flow cytometric

staining 48 h after the knockdown, to examine the efficiency of the knockdown. A reduction of FOXP3 expression could be observed on mRNA as well as protein level after knockdown, as shown in Figure 75 A and B, indicating efficient knockdown of FOXP3.

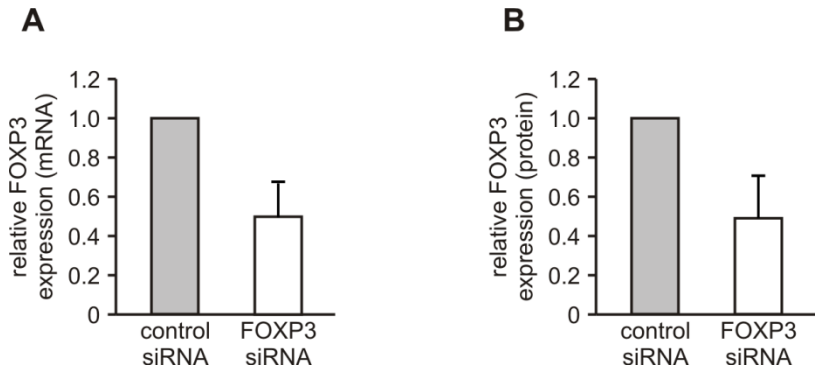

Figure 75: Efficiency of siRNA-mediated FOXP3 knockdown in T_{reg} cells
Human $CD4^+CD25^+$ T cells were purified from peripheral blood and treated with control siRNA or FOXP3 siRNA. (**A**) Relative FOXP3 mRNA expression was assessed by qRT-PCR in comparison to B2M expression 48 h after the control or FOXP3 knockdown. (**B**). Relative FOXP3 protein expression was assessed by intracellular FOXP3 staining 48 h after the control or FOXP3 knockdown. Data were normalized to control siRNA transfected cells and are shown as mean and standard deviations of at least three individual experiments.

H. Electrophoretic mobility shift Assay – Supershift

Previous experiments had shown that HPGD expression increases in T_{reg} cells, after silencing of FOXP3, indicating regulation of HPGD by FOXP3. Therefore, it was tested whether FOXP3 can bind to the HPGD locus and HPGD represents a direct target gene of FOXP3. To answer the question whether FOXP3 can bind to the HPGD locus, the sequence of the HPGD locus was screened for binding sites of FOXP3 using bioinformatic *in silico* approaches and several potential FOXP3 binding sites were predicted upstream of the transcription start site (TSS) as well as in the genomic locus of HPGD. One of the FOXP3 binding sites, which was predicted -15kb 5' of the transcription start site in a potential enhancer area, was selected to exemplify that FOXP3 can bind to the HPGD locus, using an electrophoretic mobility shift assay (EMSA). FOXP3 protein bound to the selected FOXP3 binding motif (HPGD), as depicted above in Figure 63. The binding was specific as a mutated HPGD (mut-HPGD) oligonucleotide showed no binding to FOXP3 and moreover the signal intensity was reduced in the presence of an oligonucleotide with a known FOXP3 binding motif (FKH), which was used as a competitor. The recombinant FOXP3 protein used for these experiments has a histidin tag. As a further control experiment an anti-histidin antibody was therefore added to the reaction mix. As control an isotype control antibody was used. Incubation with the anti-

histidin antibody led to a shift in fluorescence intensity of a part of the band, as shown in Figure 76 (lane 2), which was not observed for incubation with isotype control antibody (lane 3) or when no histidin-antibody was added (lane 1). This result further shows that FOXP3 bound specifically to the HPGD oligonucleotide and that FOXP3 can bind to the HPGD locus.

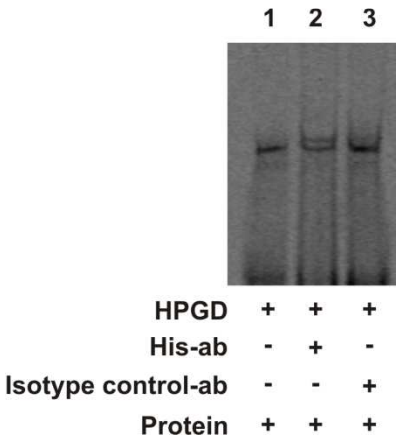

Figure 76: Specific binding of FOXP3 to the HPGD gene.
An EMSA was performed with recombinant FOXP3 protein (Protein) and a dimer of the HPGD gene with a FOXP3 binding motif (HPGD), labeled with the infrared dye DY-681 (Lane 1). An anti-histidin antibody (His-ab, Lane 2) or isotype control antibody (Isotype control-ab, Lane 3) were added to the reaction mix. One representative experiment out of two is shown.

List of publications

Beyer M, Thabet Y, Müller RU, Sadlon T, Classen S, Lahl K, Basu S, Zhou X, Bailey-Bucktrout SL, Krebs W, **Schönfeld EA**, Böttcher J, Golovina T, Mayer CT, Hofmann A, Sommer D, Debey-Pascher S, Endl E, Limmer A, Hippen KL, Blazar BR, Balderas R, Quast T, Waha A, Mayer G, Famulok M, Knolle PA, Wickenhauser C, Kolanus W, Schermer B, Bluestone JA, Barry SC, Sparwasser T, Riley JL, Schultze JL.

"Repression of the genome organizer SATB1 in regulatory T cells is required for suppressive function and inhibition of effector differentiation."

Nat Immunol. 2011 Aug 14; 12 (9):898-907

Danksagung

Mein besonderer Dank gilt Herrn Professor Dr. Joachim L. Schultze, der mir die Möglichkeit gab in seiner Arbeitsgruppe zu diesem interessanten Thema meine Doktorarbeit anzufertigen. Seine gute Betreuung, sein Enthusiasmus und seine konstruktive Kritik haben wesentlich zum Entstehen diese Arbeit beigetragen.

Mein großer Dank gilt insbesondere Herrn Dr. Marc Beyer für die intensive Betreuung während meiner Dissertation. Er hat mir während der gesamten Zeit mit fachlichen und experimentellen Ratschlägen zur Seite gestanden.

Des Weiteren möchte ich mich bei Herrn Professor Dr. Waldemar Kolanus, meinem Zweitgutachter, bedanken.

Ich bedanke mich auch sehr bei Herrn Professor Dr. Andrew J. Dannenberg und Dr. Kotha Subbaramaiah für die schnelle und unkomplizierte Bestimmung der enzymatischen Aktivität der Hydroxyprostaglandin Dehydrogenase 15-(NAD) in regulatorischen T Zellen.

Zudem möchte ich Dr. Thomas Quast aus der AG Kolanus für die Einführung am LSM danken.

Mein weiterer Dank gilt Andrea Hofmann, Fatima Kreusch und Dr. Svenja Debey-Pascher die mich mit Rat und Tat in Sachen Statistik und Bioinformatik unterstützt haben. Des Weiteren möchte ich mich bei meinen Laborkollegen Daniel Sommer, Wolfgang Krebs, Stefanie Riesenberg, Andrea Ninocastro und Yasser Thabet bedanken für die angeregten Diskussionen, hilfreichen Tipps, das gute Laborklima und die lustige Zeit die wir gemeinsam hatten, bedanken.

Ich möchte mich auch bei meinen Freunden insbesondere Anna Buck, Darius Madjidi, Friedericke Ehrmann, Nicole Russ und Christina Hambach für die schöne Zeit bedanken die wir hatten und dass sie immer an mich geglaubt haben.

Mein herzlichster Dank gilt jedoch meinen Eltern Gabriele und Bernd Schönfeld, meinen Großmüttern Helene Mielke und Sogi Schönfeld und meinem Freund Alexander Süßmann für Ihre grenzenlose Geduld und Liebe und dass sie mich während der gesamten Zeit meiner Dissertation immer unterstützt, motiviert und an mich geglaubt haben.